2005

Theoretical investigation of dynamic properties of magnetic molecule systems as probed by NMR and pulsed fields experiments

Ioannis Rousochatzakis
Iowa State University

Theoretical investigation of dynamic properties of magnetic molecule systems as probed by NMR and pulsed fields experiments

by

Ioannis Rousochatzakis

A dissertation submitted to the graduate faculty

in partial fulfillment of the requirements for the degree of

DOCTOR OF PHILOSOPHY

Major: Condensed Matter Physics

Program of Study Committee:
Marshall Luban, Major Professor
David Vaknin
Joerg Schmalian
David Carter-Lewis
James Evans

Iowa State University

Ames, Iowa

2005

Graduate College
Iowa State University

This is to certify that the doctoral dissertation of

Ioannis Rousochatzakis

has met the dissertation requirements of Iowa State University

Signature was redacted for privacy.

Committee Member

Signature was redacted for privacy.

Committee Member

Signature was redacted for privacy.

Committee Member

Signature was redacted for privacy.

Committee Member

Signature was redacted for privacy.

Major Professor

Signature was redacted for privacy.

For the Major Program

"When setting out upon your way to Ithaca,
wish always that your course be long,
full of adventure, full of discovery."

ITHAKA
Constantine P. Cavafis (1911)

TABLE OF CONTENTS

CHAPTER 1. Introduction: Overview and Thesis Organization 1

1.1 General introduction 1

1.2 Thesis Organization 3

References 5

CHAPTER 2. Theory and Experiment in Magnetic Molecules 9

2.1 Introduction 9

2.2 Hamiltonian terms in magnetic molecules 10

2.2.1 Exchange interactions 11

2.2.2 Single-ion effects 12

2.2.3 Spin-phonon (magnetoelastic) interactions 13

2.3 Hilbert space and diagonalization problem 16

2.4 Probing magnetic molecules: Static and dynamic properties 17

2.4.1 Static properties: Magnetization, Susceptibility and Specific Heat 18

2.4.2 Dynamic properties: Correlation functions and why they are important 22

References 25

CHAPTER 3. Theoretical aspects of Open Systems 29

3.1 Introduction 29

3.2 Closed systems 30

3.2.1 Pure initial state 31

3.2.2 Mixed initial state 32

3.3 Open systems 34

3.3.1 The reduced density matrix 36

3.4 Derivation of the master equations in the Markovian limit 37

3.4.1 Application: Non-degenerate spectra with non-equidistant levels 40

3.5 Correlation functions of open systems: The quantum regression theorem 41

3.5.1 Application: Non-degenerate spectra with non-equidistant levels 44

References 48

CHAPTER 4. Nuclear Magnetic Resonance as a probe of spin dynamics of magnetic molecules 50

4.1 Introduction 50

4.2 General aspects of NMR in the context of magnetic molecule systems 52

4.3 Nuclear spin-lattice relaxation rate $1/T_1$ 55

4.4 Spectral functions of magnetic molecules regarded as open systems 59

4.4.1 Away from level-crossings 60

4.4.2 Level-crossing effects 65

4.5 Summary and open issues 66

References 67

CHAPTER 5. Magnetic susceptibility and spin dynamics of polyoxovanadate cluster V12: a proton NMR study of a model spin tetramer 69

5.1 Introduction 70

5.2 Experimental details 71

5.3 Experimental Results 72

5.4 Analysis of experimental results 73

5.4.1 Magnetic susceptibility 73

5.4.2 ^{1}H NMR line width (FWHM) vs T 74

5.4.3 ^{1}H spin-lattice relaxation rate T_1^{-1} 76

5.5 Summary and conclusions 82

Acknowledgements 83

References 83

CHAPTER 6. Pulsed Fields measurements: The Landau-Zener-Stückelberg model without dissipation 85

6.1 Introduction 85

6.2 The LZS model without dissipation 87

6.3 Order of magnitude considerations in actual magnetic molecule systems 92

References 93

CHAPTER 7. Hysteresis Loops and Adiabatic Landau-Zener-Stückelberg transitions in the Magnetic Molecule $\{V_6\}$ 95

References 103

CHAPTER 8. Master Equations for pulsed magnetic fields: Application to magnetic molecules 104

8.1 Introduction 105

8.2 Master equations for spin S 107

8.3 Master equations for the general isotropic Heisenberg model 113

8.4 Dissipative LZS model in the adiabatic regime 116

8.4.1 General theory 116

8.4.2 Qualitative analysis 120

8.5 Summary 124

Acknowledgements 126

References 126

CHAPTER 9. Summary and open issues 129

References 134

APPENDIX A. Single-ion anisotropy and the $g-$tensor in transition-metal ions . . . 136

References 138

APPENDIX B. Van Vleck formula for the susceptibility 140

B.1 Isotropic Heisenberg model and fluctuation formula 141

B.2 Magnetic ion with a non-degenerate ground state and total spin 1/2 142

B.3 Remark: Differential susceptibility 143

APPENDIX C. Pauli Master equations from Fermi's Golden rule 144

C.1 General treatment 144

C.2 Order of magnitude considerations: Applicability of Fermi's Golden rule 147

References 149

APPENDIX D. Decay of coherences: The element $R_{nm,nm}$ 151

APPENDIX E. Some physical constants, and the CGS system of units 153

ACKNOWLEDGEMENTS 156

1. Introduction: Overview and Thesis Organization

1.1 General introduction

The field of molecular magnetism[1–6] has become a subject of intense theoretical and experimental interest and has rapidly evolved during the last years. This inter-disciplinary field concerns magnetic systems at the molecular or "nanoscopic" level, whose realization has become feasible due to recent advances in the field of chemical synthesis.

These "nanomagnetic" systems crystallize in regular 3-dimensional structures with large identical molecular units placed at each unit cell. Each molecule incorporates a finite number N of exchange coupled magnetic ions, which, in most cases, belong to the Fe (3d) group, e.g., Fe^{3+} and Mn^{2+} ($s = 5/2$), Mn^{3+} ($s = 2$), Cr^{3+} and Mn^{4+} ($s = 3/2$), Cu^{2+} and V^{4+} (s=1/2). Their mutual magnetic interactions are of the super-exchange type, i.e., they are mediated by non-magnetic ions or by a group of non-magnetic ions (organic "bridges" or "ligands"). Moreover, it is very often the case that these interactions can be adequately described by the isotropic Heisenberg model with the corresponding exchange constants being typically of the order of a few tens of Kelvin.

Importantly, the number of non-magnetic ions within each molecular cluster (a few hundred) is much larger than the number of magnetic ions: N varies from 2 (e.g., the $\{Fe_2\}$ dimer,[11, 12]) up to 30 (e.g., the giant keplerate $\{Mo_{72}Fe_{30}\}$[13]). As a result, magnetic ions belonging to adjacent molecules within a crystal sample are "shielded" from each other. Typically then, the inter-molecular magnetic interactions are of dipolar origin only and are therefore negligible[1] as compared to the strong intra-molecular exchange interactions. In other words, a macroscopic measurement on a crystalline sample reflects the physical properties of one isolated molecular unit. Hence, magnetic molecules provide practical realizations of model, zero-dimensional magnetic systems, and therefore may show properties which are intermediate between those of single-ion paramagnets and conventional bulk magnets. Of particular theoretical interest is also the possibility of exploring the transition from classical (high T, high

[1] Nevertheless, the dipolar interactions may become important at very low T for molecules with a large spin ground state. In particular, they can give rise to dipolar ordering.[7–10]

intrinsic spins s) towards quantum behavior (low T, small intrinsic spins s). The zero-dimensionality, in conjunction with the relatively small number of spins within each molecule makes these systems a convenient platform for studying fundamental problems in magnetism, but also exploring fundamental issues connected to the observation of pure quantum-mechanical effects at the macroscopic level.[14–25]

The possibility of chemically combining different magnetic ions with ligands in a diverse way allows one to tune the physical properties of these systems either from pure theoretical motivation or for obtaining a magnetic behavior suitable for potential applications.[2] For a given magnetic molecule system, the specific details of its discrete energy spectrum and, accordingly, its specific magnetic properties vary according to a number of factors. The most noteworthy are: (i) the number of magnetic ions N, (ii) the relative magnitude and the sign of the various exchange constants J, (iii) the spin value s of each ion, (iv) the spin topology of the molecule (i.e., the arrangements of the magnetic ions and the exchange pathways) and (iv) the existence or absence of various anisotropic energy terms in the spin Hamiltonian such as single-ion anisotropy and anisotropic exchange. In addition one should add the microscopic interactions with the local deformations of the host lattice (spin-phonon or magnetoelastic interaction), which play an important role in the spin dynamics and, in particular, the decay of spin fluctuations. Also, the hyperfine interaction with the nuclear spins (nuclear spin bath[34]) becomes important at very low T, where the role of phonons as a heat bath is suppressed.

One can loosely divide the magnetic molecules into two large categories according to the spin value S_G of their ground state. The first category includes the ones with a large S_G and are termed Single Molecule Magnets (SMMs). The most famous of this type are the clusters $\{Mn_{12}ac\}$[35], and $\{Fe_8\}$[36] both of which have $S_G = 10$. The large S_G value arises from the dominance of the ferromagnetic (FM) exchange interactions within the molecule. Molecules of the second category have a small S_G value (e.g., $S_G = 0$ or $1/2$) which typically arises from antiferromagnetic (AFM) exchange. The AFM ring systems[11, 12, 42–45] have $S_G = 0$, and are the most well known members of this type. The spin $1/2$ tetramer $\{V_{12}\}$ studied in chapter 5 has also $S_G = 0$. On the other hand, for the magnetic molecule $\{V_6\}$ studied in chapter 7, which can be pictured as two nearly independent spin $1/2$ triangles, the AFM coupling within each spin triangle leads to a frustrated $S_G = 1/2$ ground state.

The difference in the values of S_G between these two categories of molecules plays a dramatic role both in the order of magnitude of the corresponding spin-lattice relaxation times τ_s and the so-called tunneling effect (see below). Specifically, the large S_G value in SMMs is responsible for both the formation of an energy barrier for the relaxation of the magnetization and the appearance of extremely

[2]To our knowledge these include quantum computing,[26–29] magnetic memory units,[30] low–T refrigerants using the magnetocaloric effect,[31, 32] and finally the use of magnetic molecules as imaging contrast agents in Biomedicine.[33]

small energy gaps or "tunnel-splittings" δ (δ can be of order $\sim 10^{-7}$ K in $\{Mn_{12}ac\}$) between avoided level-crossings.

In particular, the energy barrier in SMMs originates from single-ion uniaxial anisotropy (of the form DS_z^2, where D is a constant) together with the large value of S_G. The height of the barrier (which can be a few tens of K) increases with increasing S_G and D, which in turn gives rise to extremely long spin-lattice relaxation times τ_s (τ_s can be of the order of several months).[37, 38] Such a barrier is absent in molecules of the second type and the corresponding relaxation times are much shorter ($\tau_s \sim 1$ ms at low T).

On the other hand, the tunneling effect,[3] which is manifested in both categories of molecules (but with a different overall amplitude), is nothing else than a manifestation of the so-called Landau-Zener-Stückelberg (LZS) effect (see chapter 6).[4] The overall effect of the LZS transitions depends on the energy gap δ at the level-anticrossing point as well as the sweep rate of the external magnetic field. Now, as we explain in chapter 6, in SMMs the extremely small δ results in nonadiabatic LZS transitions whereas in molecules with low S_G (where typically $\delta \sim 0.1$ K) we are always in the extreme adiabatic regime of the LZS effect.

1.2 Thesis Organization

During the course of our research efforts, we have theoretically investigated a number of issues pertinent to both static and dynamical properties of magnetic molecule systems. Our main efforts, in particular, have been devoted to the study of their dynamical properties, as probed by the nuclear spin-lattice relaxation rate $1/T_1$, as well as pulsed field measurements of the dynamical magnetization $M(t)$. For this reason, we have divided the body of this dissertation into three major parts.

The first part, which consists of chapters 2 and 3, sets the stage for the analysis undertaken in subsequent chapters. In particular, we start in chapter 2, by providing a detailed description and the background on the various interactions present in magnetic molecule systems, and also define the physical quantities of both theoretical and experimental interest. In chapter 3, we give a general account of the physics of open systems in general. We define the reduced density matrix and provide the derivation, in the Markovian limit, of its equation of motion (generalized master equation). Then, using the so-called quantum regression theorem, we arrive at a general first-principles expression for the

[3] See for example Refs. [39, 40] and Ref. [41] for $\{Mn_{12}ac\}$ and $\{Fe_8\}$, respectively, and chapter 7 and references therein for the corresponding effect in molecules with low S_G.

[4] The effect of LZS transitions in SMMs is termed "tunneling" because the LZS effect involves two states from opposite sides of the barrier.

spectral density functions, which takes into account the effect of the coupling to environmental degrees of freedom. The results of chapter 3 are to be employed both in the second and the third part of this dissertation, as we explain below.

The second part consists of chapters 4 and 5, and is devoted to the theoretical interpretation of a number of experimental findings obtained from NMR. In particular, in chapter 4, which is the basis of a future publication, provides a general theoretical account for $1/T_1$. To this end, we first apply the master equations developed in chapter 3 with the nuclear spin being the central system of interest and taking the hyperfine interaction with the nearby electronic moments, to be the dominant source of nuclear relaxation. In this way, we define $1/T_1$ and express it in terms of the various spectral functions of the magnetic molecule, evaluated at the nuclear Larmor frequency ω_L. To accurately account for the equilibrium electronic spin fluctuations we use the results of chapter 3, with the magnetic molecule being the central system of interest and the phonons playing the role of the heat bath. Using the obtained, "broadened" form of the electronic spectral functions, and employing a number of simplifying symmetry arguments, we arrive at a convenient expression based on which one can analyze and interpret the temperature and field dependence of $1/T_1$.

Chapter 5, which appears in Phys. Rev. B **69**, 094436 (2004), consists of a detailed theoretical and experimental study of a model spin 1/2 tetramer, namely the magnetic molecule $\{V_{12}\}$. This study includes the interpretation of (i) magnetic susceptibility data, (ii) NMR linewidth data, and (iii) $1/T_1$ data.

The third part of the dissertation is devoted to pulsed field studies of magnetic molecules. To this end, we first provide, in chapter 6, the analytical derivation of the well-known, 2-level, LZS transition probability. We only deal with the pure quantum-mechanical LZS model, i.e., we neglect the effect of thermal transitions (dissipative LZS effect). The appropriate generalization to the study of the combined effects of quantum-mechanical and thermal transitions is given in chapter 8.

In chapter 7, which appears in Phys. Rev. Lett. **94**, 147204 (2005), we present a theoretical analysis of the low temperature pulsed field experiments performed on the magnetic molecule $\{V_6\}$. The striking feature about this system, is that at low enough temperatures ($T \ll 60$ K) it behaves as a spin 1/2 entity. The experimental data of $M(t)$ in the presence of a variety of closed field sweeps, show both hysteresis loops and almost exact reversals of $M(t)$ at $B \approx 0$. The hysteresis effects are reproduced by using a generalization of the standard Bloch equation for the relaxation of the magnetization. The first-principles derivation of this equation is given in chapter 8. The fit to the experimental data reveals that the dominant contribution to the relaxation originates from one-phonon processes, and an

estimate of the spin-phonon coupling energy is also provided. On the other hand, the almost exact magnetization reversals at $B \approx 0$ are associated to LZS transitions, originating from the existence of a small intra-molecular anisotropic exchange, not observed in static experiments. The small deviation from the quantum-mechanical prediction of exact magnetization reversal is attributed to the role of thermal dissipation.

The work described in chapter 7 motivated us to undertake a first-principles analytical study of all the various phenomena manifested in pulsed field experiments. This is described in chapter 8, which appears in Phys. Rev. B **72**, 134424 (2005). Our analysis consists of a generalization of the master equation approach to time-dependent fields and is devoted to the large class of magnetic molecules with a low spin ground state S_G. The main underlying assumption of our study will be that the phonons are in equilibrium at all experimental times. This restricts the applicability of the theory to typically $T \gtrsim 1$ K, since for lower T the phonon bottleneck effect[46, 47] takes place.

More specifically, the analysis described in chapter 8 accounts for the following phenomena manifested in pulsed field measurements of $M(t)$. (i) Magnetization hysteresis effects: These originate from the fact that the experimental time scale τ_e, determined by the field sweep rate, is in the regime of the spin-lattice relaxation times τ_s. Equivalently, these effects are manifestations of a "slowing-down" of the spin dynamics occurring at low T. (ii) Magnetization steps: These occur at specific values of the magnetic field, where a level anti-crossing takes place in the magnetic energy spectrum. They are accordingly manifestations of LZS transitions. For molecules with a low spin ground state these transitions correspond to the extreme adiabatic regime of the LZS effect, in contrast to the magnetization tunneling that occurs in SMMs, where one is in the non-adiabatic regime. (iii) Magnetic Foehn effect: This concerns the appearance of magnetization plateaus following the LZS steps. As we discuss in chapter 8, this effect is closely related to the occurrence of the LZS effect. Finally, although our analysis is restricted to typically $T \gtrsim 1$ K, we nevertheless indicate how the phonon bottleneck effect occurring at lower T can give rise to an enhanced Foehn effect.

References

[1] O. Kahn, *Molecular Magnetism* (VCH publishers, New York, 1993)

[2] D. Gatteschi, Phil. Trans. R. Soc. Lond. A **357**, 3079-3097 (1999), and references therein.

[3] A. Caneschi, D. Gatteschi, C. Sangregorio, R. Sessoli, L. Sorace, A. Cornia, M. A. Novak, C. Paulsen, and W. Wernsdorfer, J. Mag. Mag. Mat. **200**, 182-201 (1999), and references therein.

[4] *Magnetism, Molecules to Materials: Nanosized magnetic materials*, vol. 3, edited by J. S. Miller, and M. Drillon (Wiley-VCH, Weinheim, 2002), and references therein.

[5] D. Gatteschi, and R. Sessoli, Angew. Chem. Int. Ed. **42**, 268-297 (2003), and references therein.

[6] D. Gatteschi, and R. Sessoli, J. Mag. Mag. Mat. **272-276**, 1030-1036 (2004), and references therein.

[7] J. F. Fernández, and J. J. Alonso, Phys. Rev. B **62**, 53 (2000).

[8] J. F. Fernández, Phys. Rev. B **66**, 064423 (2002).

[9] A. Morello, F. L. Mettes, F. Luis, J. F. Fernández, J. Krzystek, G. Aromi, G. Christou, and L. J. de Jongh, Phys. Rev. Lett. **90**, 017206 (2003).

[10] A. Morello, F. L. Mettes, O. N. Bakharev, H. B. Brom, L. J. de Jongh, F. Luis, J. F. Fernández, and G. Aromí, cond-mat/0509261.

[11] F. Le Gall, F. F. de Biani, A. Caneschi, P. Cinelli, A. Cornia, A. C. Fabretti, and D. Gatteschi, Inorg. Chim. Acta **262**, 123-132, 1997.

[12] M. Gerloch, and F. E. Mabbs, J. Chem. Soc. A, 1900-1906, (1967).

[13] A. Müller, M. Luban, C. Schröder, R. Modler, P. Kögerler, M. Axenovich, J. Schnack, P. Kanfield, S. Bud'ko, and N. Harisson, ChemPhysChem **2**, 517-521 (2001).

[14] E. Schrödinger, Naturwissenschaften **23**, 807 (1935).

[15] A. O. Caldeira, A. Leggett, Phys. Rev. Lett. **46** 211 (1981).

[16] E. M. Chudnovsky, and L. Gunther, Phys. Rev. Lett. **60**, 661 (1988).

[17] E. M. Chudnovsky, and J. Tejada, *Macroscopic Quantum Tunneling of the Magnetic Moment*, Cambridge Studies in Magnetism, vol. 4 (Cambridge University Press, Cambridge, 1998), and references therein.

[18] B. Barbara, and L. Gunther, Phys. World **12**(3), 35 (1999).

[19] P. C. E. Stamp, Nature **383**, 125 (1996).

[20] E. M. Chudnovsky, Science **274**, 838 (1996).

[21] B. Barbara, and E. M. Chudnovsky, Phys. Lett. A **145**, 205 (1990).

[22] I. V. Krive, and O. B. Zaslawskii, J. Phys. Cond. Matt. **2**, 9457 (1990).

[23] D. Loss, D. P. DiVincenzo, and G. Grinstein, Phys. Rev. Lett. **69**, 3232(1992).

[24] A. Honecker, F. Meier, D. Loss, and B. Normand, Eur. Phys. J. B **27**, 487 (2002).

[25] A. Chiolero, and D. Loss, Phys. Rev. Lett. **80**, 169 (1998).

[26] D. Deutsch, and R. Jozsa, Proc. R. Soc. Lond. A **439**, 553 (1992).

[27] J. A. Jones, Science **280**, 229 (1998).

[28] M. N. Leuenberger, and D. Loss, Nature **410**, 789 (2001).

[29] *Quantum Computing and Quantum Bits in Mesoscopic Systems*, edited by A. Leggett, B. Ruggiero, and P. Silvestrini (Kluwer Academic, New York, 2004).

[30] C. Joachim, J. K. Gimzewski, and A. Aviram, Nature **408**, 541 (2000).

[31] F. Torres, J. M. Hernández, X. Bohigas, and J. Tejada, Appl. Phys. Lett. **77**, 3248 (2000).

[32] J. Tejada, Polyhedron **20**, 1751 (2001).

[33] E. Rodríguez, A. Roig, E. Molins, C. Arús, M. R. Quintero, M. E. Cabañas, S. Cerdán, P. Lopez-Larrubia, C. Sanfeliu, NMR in Biomedicine, **18**, 300-307 (2005).

[34] N. V. Prokof'ev, and P. C. E. Stamp, Rep. Prog. Phys. **63**, 669-726 (2000).

[35] T. Lis, Acta Cryst. B **36**, 2042 (1980).

[36] K. Wieghardt, K. Pohl, I. Jibril, and G. Huttner, Angew. Chem. Int. Ed. Engl. **23**, 77 (1984).

[37] R. Sessoli, D. Gatteschi, A. Caneschi, and M. A. Novak, Nature **365**, 141 (1993).

[38] A.-L. Bara, P. Debrunner, D. Gatteschi, Ch. E. Schulz, and R. Sessoli, Europhys. Lett. **35**, 133 (1996).

[39] J. R. Friedman, M. P. Sarachik, J. Tejada, and R. Zolio, Phys. Rev. Lett. **76**, 3830 (1996).

[40] L. Thomas, F. Lionti, R. Ballou, D. Gatteschi, R. Sessoli, and B. Barbara, Nature **383**, 145 (1996).

[41] W. Wernsdorfer, and R. Sessoli, Science **284**, 133 (1999).

[42] A. Caneschi, A. Cornia, A. C. Fabretti, S. Foner, D. Gatteschi, R. Grandi, L. Schenetti, Chem. Eur. J. **2**, 1379 (1996); A. Cornia, A. G. M. Jansen, M. Affronte, G. L. Abbati, and D. Gatteschi, Angew. Chem. Int. Ed. **38**, 2264 (1999).

[43] K. L. Taft, C. D. Delfs, G. C. Papaefthymiou, S. Foner, D. Gatteschi, and S. J. Lippard, J. Am. Chem. Soc. **116**, 823 (1994).

[44] A. Caneschi, A. Cornia, A. C. Fabretti, and D. Gatteschi, Angew. Chem. Int. Ed. Engl. **38**, 1295 (1999).

[45] J. van Slageren, R. Sessoli, D. Gatteschi, A. A. Smith, M. Helliwell, R. E. P. Winpenny, A. Cornia, A. L. Barra, A. G. M. Jansen, E. Rentschler, and G. A. Timco, Chem. Eur. J. **8**, 277 (2001).

[46] A. Abragam and B. Bleaney, *Electron Paramagnetic Resonance of Transition Ions* (Clarendon Press, Oxford, 1970), Chap. 10.

[47] K. W. H. Stevens, Rep. Prog. Phys. **30**, 189 (1967).

2. Theory and Experiment in Magnetic Molecules

2.1 Introduction

A first step towards understanding the physics of a particular magnetic molecule system, is an analysis based on chemical structure arguments, which mainly gives the type (intrinsic spins s) and the number of N interacting ions within each molecular unit. Furthermore, the existence or not of an exchange interaction between two adjacent magnetic ions can be inferred by carefully looking at the geometry and the positioning of certain bridging ligands. In addition, point symmetry arguments justify or exclude the existence of various anisotropic energy terms. Based on such an analysis, an "approximant" spin Hamiltonian H is first written down. However, this is still a model Hamiltonian with a set of unknown parameters such as the various exchange constants, single-ion anisotropy parameters, etc. It is the experiment that eventually will affirm whether this model Hamiltonian is good enough and also, when compared to the predictions of the theory, give numerical values for the various parameters. Static macroscopic probes suitable for giving such information, are of course the measurement of equilibrium magnetization versus temperature and magnetic field, the zero-field magnetic susceptibility versus temperature, and more infrequently the specific heat (Refs. [1–3]) and torque magnetometry (Refs. [3–6]). On the other hand, dynamic probes such as the ones considered in this dissertation, i.e., Nuclear Magnetic Resonance (NMR) and pulsed field techniques can in principle give more detailed and rich microscopic information about these systems. It is essential then to understand what these experiments actually probe and how they are related to certain quantities that one can calculate from an adjustable model Hamiltonian.

In this chapter, we provide a general background on the various energy terms of the spin Hamiltonian, the essential model parameters and the physical quantities that are of both theoretical and experimental interest. In particular, in Sec. 2.2 we discuss the exchange interactions (both isotropic and anisotropic), single-ion effects as well as the coupling of the electronic moments to the local deformations of the host lattice, i.e., phonons. In Sec. 2.3, we comment on the dimensionality of the Hilbert space and the diagonalization problem. In Sec. 2.4, we define the experimental quantities of interest and specifically

we separate them into two categories, namely the static and the dynamic ones. In the first category, we include the zero-field magnetic susceptibility, the equilibrium magnetization as a function of temperature and field, and the specific heat. On the other hand, the second category concerns what every dynamical experiment in condensed matter really probes, namely correlation functions. In particular, we will be concerned with the various spin-spin correlation functions both in time and frequency domain. To this end, we discuss the general properties of these quantities with the molecule first considered as a thermally isolated (closed) system, i.e., by neglecting interactions with environmental degrees of freedom. We leave the extension to open systems in chapter 3. The relevance of the spin-spin correlation functions in the particular case of NMR is discussed in chapter 4.

2.2 Hamiltonian terms in magnetic molecules

The magnetic interactions inside a typical magnetic molecule vary both in their magnitude and their specific origin. In addition, they become manifest depending on the experiment at hand, and the external conditions such as temperature and field. Specifically, the dominant magnetic energy terms are the strong intra-molecular superexchange interactions between neighboring magnetic ions within each molecular unit. These mainly determine the temperature and field dependence of static, macroscopic quantities such as the equilibrium magnetization and the zero-field susceptibility. Anisotropic exchange terms, arising from the combined effect of exchange and spin-orbit (LS) coupling, are also present but their effect is not noticeable in static measurements since they are usually very small ($\lesssim 0.1$ K). However, they can be manifested in dynamic type of experiments such as the pulsed field magnetization measurements (discussed in chapters 6,7, and 8) by giving rise to abrupt magnetization steps.

On the other hand, single-ion effects, such as the anisotropy of the $g-$factor as well as single-ion spin anisotropy (which gives rise to small energy splittings, even at zero field), can be seen at relatively low temperatures, when, for example, only a low energy subspace of the magnetic spectrum is populated. In particular, a dramatic manifestation of such single-ion effects occurs in SMMs. These systems, as explained in chapter 1, have a ground state with a large total spin S_G (e.g., $S_G = 10$ for Mn_{12} and Fe_8). The $(2S_G + 1)-$fold spin degeneracy is split at zero field, due to an axial anisotropy term of the form DS_z^2 (which stems from single-ion terms $\sum_i d_i\, s_{iz}^2$). As a result, an energy barrier against thermal relaxation is formed which is responsible for relaxation times of "macroscopic" order $10^3 - 10^5$ s. In addition, small transverse anisotropic terms can give rise to an admixture of two states at opposite sides of the barrier giving rise to a tunneling of the magnetization. This observation has been one of the most exciting ones in magnetic molecule systems.

Other magnetic energy terms are for example the intra- and inter-molecular dipolar interactions as well as the hyperfine coupling with nuclear spins. The latter are of importance in NMR, since they provide the means of probing the electronic spin fluctuations (see chapter 4).

In addition to the above, there are interactions with the environmental degrees of freedom, collectively called lattice or bath. Such terms are for example the spin-phonon interactions which provide the dominant source of spin-lattice relaxation and are also of great interest in dynamic experiments. In fact, as shown in subsequent chapters (4,6,7, and 8), information about these interactions can be obtained from both NMR and pulsed fields. In the first case, a measurement of the so-called nuclear spin-lattice relaxation rate $1/T_1$ gives the thermal broadening of the zero frequency portion of the spin-spin correlation functions. In pulsed field experiments, at low T, the measured dynamical magnetization shows pronounced hysteresis, which gives information about the thermal relaxation rate and therefore the spin-phonon interactions.

In what follows, we will consider the various exchange interactions, the single-ion terms and the origin of the spin-phonon coupling.

2.2.1 Exchange interactions

The dominant energy terms of the Hamiltonian of a magnetic molecule system consist of the isotropic superexchange[7–9] coupling between neighboring magnetic ions. These can be described by the isotropic Heisenberg model

$$H_{iso} = \sum_{i<j}^{N} J_{ij}\ \mathbf{s}_i \cdot \mathbf{s}_j\ , \tag{2.1}$$

where the sum extends over all spin sites i and j, and $\{J_{ij}\}$ denotes the set of exchange parameters. According to our convention, if J is positive the energy is minimized for anti-parallel or anti-ferromagnetic (AFM) alignment. On the other hand, a negative J favors parallel or ferromagnetic (FM) alignment. For a highly symmetrical magnetic molecule structure (such as the AFM rings), a single J parameter is often adequate.

The isotropic Heisenberg interaction as written in Eq. (2.1) is very common in insulating magnetic systems. The nature and values of the exchange parameters depend on the system at hand. Generally though, it is essential to examine the electronic structure and the detailed positioning of the various magnetic as well as non-magnetic ions comprising the crystal. To this end, qualitative rules have been first developed by Goodenough[8], and extended by Kanamori[9]. On the basis of electonic structure considerations, Anderson[10] has laid a theoretical foundation for describing the above bilinear isotropic spin exchange interactions. Nevertheless, in some cases, certain phenomena cannot be explained in terms

of the above isotropic exchange terms. To explain these effects, Moriya[11] has introduced antisymmetric and anisotropic energy couplings between spins. Such terms are present in magnetic molecules as well. Thus, the isotropic Heisenberg superexchange interactions need to be supplemented by various anisotropic terms, which are generally much smaller. Hence, the interaction between two adjacent ions at sites i and j, including the isotropic exchange of Eq. (2.1), can be compactly written in terms of a second rank tensor $\mathbf{E}$ (see below), as

$$(H_{ex})_{ij} = \mathbf{s}_i \cdot \mathbf{E}_{ij} \cdot \mathbf{s}_j \equiv \sum_{\mu\nu} E_{ij}^{\mu\nu} s_i^{\mu} s_j^{\nu} \ , \tag{2.2}$$

where $\{\mu,\nu\}$ denote cartesian coordinates. Like any second rank tensor, one can split $\mathbf{E}_{ij}$ in a zero-th rank scalar J_{ij}, a first rank vector $\mathbf{A}_{ij}$, and finally a traceless, second rank, tensor $\mathbf{\Sigma}_{ij}$. This gives

$$(H_{ex})_{ij} = J_{ij}\ \mathbf{s}_i \cdot \mathbf{s}_j + \mathbf{A}_{ij} \cdot (\mathbf{s}_i \times \mathbf{s}_j) + \mathbf{s}_i \cdot \mathbf{\Sigma}_{ij} \cdot \mathbf{s}_j \ , \tag{2.3}$$

where

$$\begin{aligned} J_{ij} &\equiv Tr(\mathbf{E}_{ij})/3 \ , \\ A_{ij}^{\tau} &\equiv \varepsilon^{\mu\nu\tau} E_{ij}^{\mu\nu}/2 \ , \\ \Sigma_{ij}^{\mu\nu} &\equiv (E_{ij}^{\mu\nu} + E_{ij}^{\nu\mu})/2 - Tr(\mathbf{E}_{ij})\delta^{\mu\nu}/3 \ . \end{aligned} \tag{2.4}$$

and $\varepsilon^{\mu\nu\tau}$ denotes the usual Levi-Civita symbol.[48] The first term of Eq. (2.3) accounts for the isotropic interactions already present in Eq. (2.1). The second term is the so-called Dzyaloshinskii-Moriya interaction. It is anisotropic and anti-symmetric in $i \leftrightarrow j$. Such terms are present in magnetic molecule systems and can be manifested in pulsed field experiments (see chapters 7,8). The third term is also anisotropic, but symmetric in $i \leftrightarrow j$. A very general account of isotopic and anisotropic (both symmetric and anti-symmetric) energy terms has been given by Erdös.[12]

2.2.2 Single-ion effects

In the magnetic Hamiltonian of exchanged coupled spins there are also contributions that are already present in single, paramagnetic ions. Generally, the Hamiltonian of a single ion placed in a crystal consists of three terms, namely the free ion energy (including the inter-electronic coulomb repulsion and spin-orbit energies), the interaction with the electric field (see for example Ref. [13], and references therein) created by the neighboring ions (called crystal or ligand field) and finally the orbital and spin part of the Zeeman interaction with the external magnetic field.

Typically, the ions comprising a magnetic molecule belong to the ($3d$) Fe group. For these ions, the crystal field is large compared to the LS-coupling and the Zeeman energies. Thus, the crystal field

must be taken into account before the spin-orbit and the Zeeman energies in the perturbation scheme. In the first stage of neglecting the spin-orbit and the Zeeman energies, the orbital degeneracy of the lowest spectroscopic energy term is split by the crystal field, typically (in magnetic molecules) giving rise to an orbitally non-degenerate ground state $|A>$, i.e., a spin-only multiplet with total spin s, being $(2s+1)-$fold degenerate. A significant consequence is that the orbital angular momentum is quenched inside this manifold and therefore it does not directly contribute to the magnetic properties, e.g., the susceptibility. However, the inclusion of the remaining LS-coupling and Zeeman terms in the second stage of perturbation theory, results in a small admixture of higher orbital states back in to the ground state, and a splitting of the $(2s+1)-$fold degeneracy, which in turn gives rise to various noticeable single-ion effects. These, when expressed in the language of an effective spin Hamiltonian (inside the ground manifold), consist of a spin anisotropy term, an anisotropy in the $g-$factor and finally the Van Vleck paramagnetic term (see Appendix A). The last term is second order in the external field, as it is the case for the typical Larmor (orbital) diamagnetic term, always present in magnetic ions. Since both are spin independent, they give rise to two temperature independent contributions to the magnetic susceptibility of opposite sign; for more details see Appendix A (see also [14, 15]). Here we will consider only the spin anisotropy term $(H_{ani})_i$, and the modification of the $g-$factor of the Zeeman energy $(H_Z)_i$ for a given ion at site i. According to Appendix A, one can generally write these two effects as

$$(H_z)_i = \mu_B \mathbf{B} \cdot \mathbf{g}_i \cdot \mathbf{s}_i \ , \tag{2.5}$$

and

$$(H_{ani})_i = \mathbf{s}_i \cdot \mathbf{D}_i \cdot \mathbf{s}_i \ , \tag{2.6}$$

where $\mathbf{D}_i$ is a second-rank, symmetric and traceless tensor, and $\mathbf{g}_i$ is a symmetric second-rank tensor; the departure of the $\mathbf{g}_i$ from its isotropic, spin-only value of $g^{\mu\nu} = 2\delta^{\mu\nu}$, is proportional to the LS-coupling energy. Generally, spin anisotropy is present in ions with $s > 1/2$ and for crystal field symmetry lower than cubic.

2.2.3 Spin-phonon (magnetoelastic) interactions

As we are going to show in subsequent chapters, the existence of spin-phonon interactions becomes manifest in dynamical type of experiments such as NMR and pulsed field measurements. In the first case (see chapter 4), the so-called nuclear spin-lattice relaxation rate $1/T_1$ gives information about the decay of the spin fluctuations which arise from the coupling to phonons. In the second case (see chapters 6,7, and 8) we shall see that the dynamical relaxation of the instantaneous magnetization, in

the presence of fast varying magnetic fields, is determined again by the interaction with phonons. In fact, for the pulsed field measurements in the magnetic molecule $\{V_6\}$ (chapter 7), we have been able to confirm that the dominant contribution to the relaxation stems from one-phonon processes.

Regardless of the particular experiment at hand, there is one, very significant reason why the phonons should be the source of the spin fluctuations in magnetic molecule systems, and this is energy conservation. As we have repeatedly mentioned, the energy excitations in these nanomagnetic spin systems are of the order of the exchange constants J, which in turn are typically of order of a few tens of K. Thus, in order to make a transition from one state to another, the system must exchange the corresponding energy difference with a reservoir. Clearly, the only heat bath that can provide this energy is the one corresponding to the phonon excitations. Moreover, as the temperature decreases below J, the number of available, *resonant*, phonon modes being excited drops rapidly and, accordingly, the characteristic rates describing the spin fluctuations slow down. This is confirmed by NMR measurements of the nuclear spin lattice relaxation rate $1/T_1$ (see chapter 4).

Let us first denote the position of a given ion i, as $\mathbf{r}_i = \mathbf{r}_i^0 + \delta\mathbf{r}_i$, where $\delta\mathbf{r}_i$ accounts for the small displacements from its equilibrium position $\mathbf{r}_i^0$. Then for two adjacent ions i and j, we can write

$$\mathbf{r}_{ij} \equiv \mathbf{r}_i - \mathbf{r}_j = (\mathbf{r}_i^0 - \mathbf{r}_j^0) + \delta\mathbf{r}_i - \delta\mathbf{r}_j \equiv \mathbf{r}_{ij}^0 + \delta\mathbf{r}_{ij} \ . \tag{2.7}$$

In order to include the phonon dynamics one should express the displacement vectors $\delta\mathbf{r}_{ij} \equiv \delta\mathbf{r}_i - \delta\mathbf{r}_j$, in terms of the phonon creation and destruction operators. For our purposes we shall work with the operators $\delta\mathbf{r}_{ij}$.

Now, one can classify the spin-phonon interactions appearing in magnetic molecule systems into two general categories. In the first, the origin of the coupling lies in the modulation of the various exchange constants $J_{ij}(\mathbf{r}_{ij})$ due to the fluctuation of $\mathbf{r}_{ij}$ around their mean values $\mathbf{r}_{ij}^0$. To arrive at the corresponding spin-phonon coupling one usually performs an expansion of the exchange constants as

$$J(\mathbf{r}_{ij}) \simeq J(\mathbf{r}_{ij}^0) + \frac{\partial J}{\partial \delta\mathbf{r}_{ij}} \cdot \delta\mathbf{r}_{ij} + \text{ higher order terms} \ , \tag{2.8}$$

where the various derivatives are taken at $\delta\mathbf{r}_{ij} = 0$. The second term of this expansion, being of first order in $\delta\mathbf{r}_{ij}$, is adequate for describing one-phonon processes (see for example Ref. [13]); to account for higher order processes (such as Raman two-phonon processes) one generally needs to keep the higher order terms in Eq. (2.8). Placing Eq. (2.8) into the isotropic Heisenberg Hamiltonian, one obtains extra terms that operate in both spin and phonon space, which are of the form

$$V_{s-ph} = \sum_{i<j} \Big(\frac{\partial J_{ij}}{\partial \delta\mathbf{r}_{ij}} \cdot \delta\mathbf{r}_{ij} \ + \ \text{higher order terms} \Big) \ \mathbf{s}_i \cdot \mathbf{s}_j \ . \tag{2.9}$$

This coupling is still isotropic, i.e., it conserves both $\mathbf{S}^2$ and S_z of the whole molecule. Nevertheless, in can generally break the spatial symmetries (e.g., spin permutation symmetries). Anisotropic spin-phonon couplings can arise in a similar way by taking into account the modulation, due to phonons, of the anisotropic exchange terms (if present), or the intra-molecular dipolar interactions.

The second general category of spin-phonon interactions concerns energy terms that are already present in single paramagnetic ions. Let us discuss this type of interaction in some detail. Consider again a single magnetic ion i of the Fe (3d) group with spin s, and collectively denote the positions of its neighboring non-magnetic ions with an index n and their positions by $\mathbf{r}_n \equiv \mathbf{r}_n^0 + \delta\mathbf{r}_n$, as before. As we explained above and in Appendix A, the large crystal field present in the Fe group ions splits the free ion ground state degeneracy and gives rise[1] to an orbitally non-degenerate ground manifold $|A>$ (the higher orbital states are denoted by $|A'>$). The inclusion of the LS-coupling gives rise to a second order split of the remaining $(2s+1)$-fold spin degeneracy even at zero field. This effect can be accounted for by giving an effective spin Hamiltonian with a spin anisotropy term e.g., $d\ s_z^2$. The value of the parameter d depends on the crystal field splitting and the magnitude of the LS-coupling. This value is a constant since the crystal field $V_c = V_c(\mathbf{r}_{i,n}^0)$ is considered to be static, i.e., the actual relative motions of the neighboring ions have been neglected. Let us consider now what happens when we include the modulation of the crystal field due to phonons. In this case, one again performs an expansion of the crystal field, similar to Eq. (2.8), i.e.,

$$V_c(\mathbf{r}_{i,n}) = V_c(\mathbf{r}_{i,n}^0) + \sum_n \frac{\partial V_c}{\partial \delta\mathbf{r}_{i,n}} \cdot \delta\mathbf{r}_{i,n} + \text{ higher order terms }, \tag{2.10}$$

with the various derivatives in the second and higher terms of the r.h.s. taken at the mean positions $\mathbf{r}_{i,n} = \mathbf{r}_{i,n}^0$. The first static term has already taken into account and gives the single-ion anisotropy effects. The second and higher terms contain the various displacement operators $\delta\mathbf{r}_{i,n}$, whose dynamics is determined by the phonon Hamiltonian. Clearly, one needs to add this small energy in the perturbation scheme described in Appendix A, together with the LS-coupling and the Zeeman energies. As a result, in the effective Hamiltonian (within the ground manifold $|A>$) there will be additional terms (apart from those described in Appendix A) operating in both spin and phonon space. Details of such an analysis can be found for instance in Refs. [16–19].

For both categories of spin-phonon interaction discussed above, one can further express the various deformations $\delta\mathbf{r}_{ij}$ and $\delta\mathbf{r}_{i,n}$, in terms of appropriate (displacement) normal modes of the given molecular unit in order to utilize its symmetry properties. Moreover, for long-wavelength (acoustic) lattice deformations one can even think in terms of the elasticity theory approach[20–23] and replace the mod-

[1]This is not generally true, but is typically the case for ions comprising a magnetic molecule.

ulations $\delta\mathbf{r}_{ij} \equiv \delta\mathbf{r}_i - \delta\mathbf{r}_j$, by the spatial derivatives of the displacement vector field $\mathbf{u}(\mathbf{r})$ (multiplied by the appropriate lattice constants), i.e., $\partial\mathbf{u}(\mathbf{r})/\partial\mathbf{r}$ (with elements $\partial u_\alpha/\partial r_{\alpha'}$), known as the deformation tensor. This in turn can be split into its symmetric part,

$$\varepsilon_{\alpha\alpha'} \equiv \frac{1}{2}\left(\partial u_\alpha/\partial r_{\alpha'} + \partial u_{\alpha'}/\partial r_\alpha\right) , \tag{2.11}$$

known as the strain, and the antisymmetric part

$$\omega_{\alpha\alpha'} \equiv \frac{1}{2}\left(\partial u_\alpha/\partial r_{\alpha'} - \partial u_{\alpha'}/\partial r_\alpha\right) , \tag{2.12}$$

known as the rotation tensor. One can further split the strain $\varepsilon_{\alpha\alpha'}$ as

$$\varepsilon_{\alpha\alpha'} = \frac{1}{3}\left(\nabla\cdot\mathbf{u}\right)\,\delta_{\alpha\alpha'} + [\frac{1}{2}\left(\partial u_\alpha/\partial r_{\alpha'} + \partial u_{\alpha'}/\partial r_\alpha\right) - \frac{1}{3}\left(\nabla\cdot\mathbf{u}\right)\,\delta_{\alpha\alpha'}] , \tag{2.13}$$

where the first term, $\nabla\cdot\mathbf{u}/3$, is a zero-rank tensor (scalar) related to changes of volume without deformation, whereas the second term corresponds to a traceless, second-rank tensor. On the other hand, the rotation tensor, $\omega_{\alpha\alpha'}$, is a first-rank, "pseudovector" and its elements are related to $\nabla\times\mathbf{u}$, since, for example,

$$\omega_{xy} = \frac{1}{2}\left(\partial u_x/\partial y - \partial u_y/\partial x\right) = -\frac{1}{2}\left(\nabla\times\mathbf{u}\right)_z . \tag{2.14}$$

Eventually, Eqs. (2.9) and (2.10) can be thought of as expansions in the strain $\varepsilon_{\alpha\alpha'}$ and the rotation tensor $\omega_{\alpha\alpha'}$. For further details see Ref. [24]. In particular, the coupling of spin (or magnetization) degrees of freedom with local rotations of the host lattice was first obsreved and utilized in the famous Einstein-de Haas experiment.[25] Of particular interest is also the importance of time-reversal symmetry implications on the question of the existence of spin-phonon coupling terms that are linear with respect to spin.[16, 26, 27]

2.3 Hilbert space and diagonalization problem

Consider a magnetic molecule comprising N equivalent ions with spin s, each. The dimension of the corresponding Hilbert space is therefore

$$D \equiv \dim\{H\} = (2s+1)^N . \tag{2.15}$$

This grows very rapidly (exponentially) with the number of spins. For instance, for the $\{Fe_{12}\}$ AFM ring system, which consists of 12 Fe^{3+} ($s = 5/2$) ions, $D = 6^{12} \simeq 2.177\times 10^9$.

The difficulty of finding the complete set of eigenvalues and eigenstates of the spin Hamiltonian varies accordingly. For example, in molecules with a small N the diagonalization can be done even

analytically, whereas for higher N one must resort to numerical techniques, such as Quantum Monte Carlo,[28] exact diagonalization,[2] etc. In addition, classical calculations, both analytical,[30–35] and numerical (i.e., classical Monte Carlo, see e.g., Ref. [36, 37]) provide good approximations especially for large intrinsic spins s and high enough temperatures. For a general account on theoretical and numerical techniques for diagonalizing the spin Hamiltonian, as well as a discussion on the various symmetries and some systematic features of the energy spectra of magnetic molecules can be found in the review article by J. Schnack,[38] and references therein. We also refer, in particular, to Ref. [39] for a discussion on the appearance of the so-called rotational band levels.

2.4 Probing magnetic molecules: Static and dynamic properties

Consider a magnetic molecule system at thermal equilibrium with a bath (e.g., phonons) at temperature T. This stationary state can be described by the density matrix

$$\rho(T) = e^{-\beta H}/Z \ , \tag{2.16}$$

where $\beta = 1/k_B T$ is the inverse temperature, k_B denoting the Boltzmann's constant and $Z = Tr(\rho)$ the partition function. Given this state, one in principle can evaluate all quantities of interest by e.g., diagonalizing H and obtaining the complete set of energy eigenstates $\{|n>\}$ and eigenvalues $\{E_n\}$. In what follows we discuss both static quantities of interest as well as correlation functions in both time and frequency domain. However, as we explain later on, the stationary state given by Eq. (2.16) does not provide sufficient information in order to adequately account for the actual correlations, since these functions generally decay due to small interactions with the surrounding degrees of freedom, not included in H. The specifics of these interactions, such as the explicit functional form of the decay of the correlations, or even how fast this decay proceeds, are not included in Eq. (2.16). The necessary extension to this case (in the Markovian limit) is given in the following chapter. In the present chapter, these interactions will be ignored, i.e., we treat the magnetic molecule as a closed, thermally isolated system.

[2] For instance, there exist numerical diagonalization codes designed specifically for finite clusters of spins, which utilize the so-called Irreducible Tensor Operator (ITO) technique. See, in particular, the so-called MAGPACK (Magnetic Properties Analysis Package for Spin Clusters) code developed by J.J.Borras-Almenar *et al.*, of the Univ. of Valencia, Spain.[29]

2.4.1 Static properties: Magnetization, Susceptibility and Specific Heat

2.4.1.1 Magnetization

Here, we will denote by M the magnetic moment along the z-axis (axis of the external field), unless otherwise specified. In particular, for a system with N spins, the total magnetic moment per mole M_{mole} is

$$M_{mole} = -N_A \sum_{i=1}^{N} g_i \mu_B < s_{iz} > \ , \tag{2.17}$$

where $N_A = 6.023 \times 10^{23}$ is the Avogadro's number (i.e., the number of magnetic molecules contained in one mole of substance), g_i denotes the spectroscopic g-factor of the $i-$th ion (assumed to be isotropic), μ_B the Bohr magneton, and $< s_{iz} >$ denotes the thermal average of the $i-$th spin along the z-axis, i.e.,

$$< s_{iz} >= Tr(\rho(T) s_{iz}) = \frac{1}{Z} \sum_{n} e^{-\beta E_n} < n|s_{iz}|n > \ . \tag{2.18}$$

The minus sign in Eq. (2.17) arises from the fact that the individual magnetic moment operator μ_i is antiparallel to the spin $\mathbf{s}_i$, since the electron's charge is negative, i.e., $\mu_i = -g_i \mu_B \mathbf{s}_i$. If all ions are equivalent (same spin s_i and g_i) then $M_{mole} = -N_A g \mu_B < S_z >$, where $< S_z >$ refers to the total spin of the molecule. This will be implicitly assumed from now on.

In addition to the temperature dependence of M, a measurement of the magnetization as a function of field is also of interest, in particular for studying level crossing effects. These are described as follows. As one varies the external magnetic field, one modifies the energies of the spin Hamiltonian, and consequently several successive intersections between different (usually a pair of) energy levels occur. In particular, if the two lowest energy levels intersect at a specified field value B_c, then this will give rise to a magnetization step at low temperatures; the height of the step corresponds to the difference between the magnetic moments of the two levels. In addition B_c depends on the zero-field energy difference of the two levels which is of the same order as that of the exchange constants J's. For instance, for the AFM ring systems (see the corresponding Figures in chapter 4) the lowest level crossing occurs at $B_c = J/(g\mu_B)$. Experimentally then one can determine the exchange parameter by inspection of the crossing field B_c.

2.4.1.2 Susceptibility

The zero-field magnetic susceptibility denoted by χ_0 is defined as the limit of M/B or $\partial M/\partial B$ when the external field B goes to zero. These two definitions are equivalent since at small fields M is linear in B. Experimental data of $\chi_0(T)$ are usually taken from the ratio M/B, with M measured at a chosen,

small finite field ($\sim$ 500 Gauss). As long as this field is small enough the measured χ_0 should be field independent. However, in cases[3] where there are low energy excitations that are comparable with this small measuring field, then at low T, the measured M/B shows a field dependence. In such cases M/B and $\partial M/\partial B$ are two different quantities.

Generally, an analytical evaluation of χ_0 from a model Hamiltonian takes place in two steps. First, one determines the energy spectrum $\{E_n(B)\}$ up to second order in the field e.g., by treating the Zeeman term as a small perturbation. This allows one to evaluate the thermal average of M up to first order in B. The proportionality constant is then, according to the above, the zero-field magnetic susceptibility. A general analysis along this lines is given in Appendix B which results in a very general and convenient expression (the so-called Van Vleck formula). For the isotropic Heisenberg Hamiltonian this reduces to the well-known fluctuation formula for the susceptibility

$$(\chi_0 T)_{mole} = N_A \frac{(g\mu_B)^2}{3k_B} < \mathbf{S}^{\,2} >_0 = N_A \frac{(g\mu_B)^2}{3k_B} \sum_{i,j=1}^{N} < \mathbf{s}_i \cdot \mathbf{s}_j >_0 \ , \tag{2.19}$$

where the symbol $<>_0$ stands for the thermal average in the absence of the field. According to this expression, the intrinsic (i.e., before the application of the small external field) spin fluctuations are a measure of how susceptible the system is in becoming magnetized.

The fluctuation formula is very useful (even when an analytical evaluation of χ_0 is impossible, e.g., for systems with a large Hilbert space) since it allows for several conclusions to be drawn, based on solely physical considerations. First, Eq. (2.19) gives the limiting behavior of $\chi_0 T$ both at the low$-T$ and the high$-T$ regimes, as follows. Assuming that the magnetic molecule has a spin $S_G = 0$ ground state that is well separated (i.e., by E_g, the lowest energy excitation) from the excited levels, then as $T \to 0$,

$$(\chi_0 T)_{mole} \to N_A \frac{(g\mu_B)^2}{3k_B} S_G(S_G+1) = 0 \ . \tag{2.20}$$

This is the case of AFM rings. More importantly, $\chi_0 T$ approaches this limit exponentially ($\sim e^{-\beta E_g}$), thus revealing the existence of the first energy gap. On the other hand, in the high temperature regime ($k_B T \gg J$), correlations between different ionic spins are expected to vanish, i.e., for $i \neq j$

$$\lim_{k_B T \gg J} < \mathbf{s}_i \cdot \mathbf{s}_j >= 0 \ . \tag{2.21}$$

Hence, at high T

$$< \mathbf{S}^2 > \ \to \sum_{i=1}^{N} < \mathbf{s}_i^2 >= Ns(s+1), \tag{2.22}$$

[3]This is usually the case for SMM's, due to the existence of small single-ion anisotropic terms.

and therefore

$$(\chi_0 T)_{mole} \rightarrow N N_A \frac{(g\mu_B)^2}{3k_B} s(s+1) \ , \quad T \gg J/k_B \ . \tag{2.23}$$

Secondly, in lowering the temperature starting from this high-T or "saturation" regime, correlations between different ions start building up due to the exchange interactions. In particular, for two such ions at sites i and j, $< \mathbf{s}_i \cdot \mathbf{s}_j >$ will be positive or negative according to whether these interactions favor parallel (ferromagnetic) or anti-parallel (anti-ferromagnetic) alignments. Generally then, at high T, one approaches the saturation regime from below (above) for AFM (FM) interactions. Of course, in the case of competing FM and AFM interactions a more careful analysis is required. To this end, one can obtain a high temperature expansion of $\chi_0 T$ by evaluating traces of spin operators and without solving for the exact eigenvalues.[4] Such an expansion has been very useful in experimentally determining the values of the exchange parameters. More details can be found in Ref. [42].

Finally, although the fluctuation formula is valid for isotropic Hamiltonians, it serves also as a good approximation at high T, for systems with small anisotropic terms, since their effect manifests only at low T. On the other hand, to account for the low$-T$ behavior of $\chi_0 T$ one can use a parametric form for the various anisotropic terms and then employ the Van Vleck formula (Appendix B).

An important remark, regarding experimental data of χ_0 in actual magnetic molecule samples, is appropriate here. This concerns additional contributions to the susceptibility that manifest at specific temperature regimes. Such terms are, for example, the single-ion diamagnetic and Van Vleck paramagnetic contributions (see Appendix B), as well as spin impurity contributions (e.g., from detached ions). The first two are temperature independent and thus can be seen in experimental plots of $\chi_0 T$ vs T, at high enough T, where the dominant contribution from the exchange energies saturates to the value given by Eq. (2.23). On the other hand, impurity contributions usually become manifest at the low$-T$ regime, where they contribute to χ_0 like $\sim 1/T$.[5] This contribution is proportional to the concentration of the impurities. In any case, such terms should be carefully identified and subsequently substracted from the measured data.

2.4.1.3 Specific Heat

The measurement of the specific heat of magnetic molecule samples requires special care. The reason is that, unlike the previous primarily magnetic probes, there is a large contribution of non-magnetic origin, the dominant one being that of phonons. To obtain then the contribution from the exchanged

[4] This is analogous to Van Vleck's derivation of the NMR spectrum moments.[40, 41]

[5] This is true as long as $g\mu_B B$ remains much smaller than $k_B T$ where $M \propto B$; as T keeps decreasing one approaches the saturation regime where the impurity contribution to χ_0 becomes field dependent.

coupled ions only, one needs to identify and substract from the measured data the contribution of the phonons. Unfortunately, the specific heat of phonons in these molecular systems does not have a clear analytical temperature dependence. One is then inclined to look at the field dependence for a fixed T, since such a field dependence should arise solely from the magnetic degrees of freedom.

The magnetic contribution to the specific heat C^s_{mole} per mole is given by

$$C^s_{mole} = N_A \frac{\partial U}{\partial T} = N_A \frac{1}{k_B T^2} \frac{\partial^2}{\partial \beta^2} \ln Z \ , \tag{2.24}$$

which, after some straightforward algebra, can be written in the well known energy fluctuation form

$$C^s_{mole}/(N_A k_B) = (\delta U)^2/(k_B T)^2 \equiv (< H_s^2 > - < H_s >^2)/(k_B T)^2 \ . \tag{2.25}$$

In a completely analogous manner with that of the spin fluctuation formula (Eq. (2.19)) for the magnetic susceptibility, the above expression says that the intrinsic energy fluctuations give a measure of how "susceptible" the system can be in exchanging thermal energy with the bath degrees of freedom.

An important remark for spin systems in general is that the magnetic energy spectrum is bounded from above, unlike systems with spatial degrees of freedom.[6] As a result the energy fluctuations term $(\delta U)^2$ saturates to a constant value in the high temperature regime. Then, according to Eq. (2.25), the magnetic portion of the specific heat drops like $1/T^2$, at high T. On the other hand, and for the previous example of AFM rings, at low temperatures, C^s usually drops like $\sim e^{-\beta E_g}/T^2$ due to the finite energy excitation gap.

A typical signature of a magnetic contribution to the specific heat is the so-called Shottky anomaly usually seen in gapped energy systems. This "anomaly" refers to an enhancement of the observed specific heat whenever the thermal energy $k_B T$ happens to be close to an energy excitation; it is then a "thermal resonance" effect, according to the above energy fluctuation formula. For magnetic molecule systems this has been nicely used to probe level crossing effects.[1–3] Consider for example, a magnetic system at low enough temperatures so that only the two lowest energy levels are populated. The specific heat of this gapped system is, according to the above energy fluctuation formula, given by

$$C^s_{mole}/(N_A k_B) = x^2 \mathrm{sech}^2 x \ , \tag{2.26}$$

where $x \equiv \Delta/(2k_B T)$, and Δ denotes the energy difference of the two levels. This function has a peak at $x \sim 1$. Now, if Δ is a function of the field B then one can fix T and measure the magnetic

[6] In fact, this is the reason why spin systems can attain negative temperatures. For instance, when energy is continuously being supplied to a two-level spin system then eventually the population of the upper level becomes higher than that of the lower level, a state which can only be described by assigning a negative temperature in the associated Boltzmann's factors.

contribution C^s to the specific heat as a function of B. At very low T this will provide the position of the level crossing. Remarkably, under certain conditions, it can also provide information on whether this crossing is a true level crossing or a level anticrossing.[1–3]

2.4.2 Dynamic properties: Correlation functions and why they are important

In addition to the experimental relevance of the above static thermodynamic quantities, there exist several types of dynamic quantities, such as time correlation functions, generalized susceptibilities, response and relaxation functions, etc. All these quantities are interrelated and thus contain the same amount of information. Their significance stems from the fact that they are actually what one probes in a vast variety of dynamical experimental techniques, such as spectroscopic ones (frequency domain e.g., Inelastic Neutron Scattering, Nuclear or Electron Magnetic Resonance, etc) or response and relaxation type of experiments (time domain).[7] These dynamic quantities provide yet another link between experiments and theoretical models, in addition to static quantities. However, the correlation functions contain also information about the small interactions with the surrounding degrees of freedom. For the moment, we will concentrate on the general definition and properties of time correlation functions of magnetic molecules, considered as thermally isolated (or closed). The necessary extension in order to include the small interactions with a thermal bath, is given in the following chapter.

Consider a given pair of hermitian operators O^q and $O^{q'}$, such as, for instance, the spin operators s_i^x and s_j^z of two ions at cites i and j, respectively. The time correlation function $J_{qq'}(t+\tau,t)$ is defined as

$$J_{qq'}(t+\tau,t) \equiv < O^q(t+\tau)O^{q'}(t) >= Tr(\rho(T)O^q(t+\tau)O^{q'}(t)), \tag{2.27}$$

where $O^q(t+\tau) \equiv e^{iH(t+\tau)/\hbar}O^q e^{-iH(t+\tau)/\hbar}$ and similarly for $O^{q'}(t)$.

From the stationarity of $\rho(T)$, one easily obtains that $J_{qq'}(t+\tau,t)$ is invariant under a simultaneous time translation of both time arguments, e.g., in particular,

$$J_{qq'}(t+\tau,t) = J_{qq'}(\tau,0)\ . \tag{2.28}$$

For this reason, in what follows, we will drop the second time variable and also write $J_{qq'}(t)$ instead of $J_{qq'}(\tau,0)$.

Physically, for a stationary state, one expects that at large enough times the correlations between O^q and $O^{q'}$ vanish (i.e., $J_{qq'}(t)$ tends to $< O^q >< O^{q'} >$ as $t \to \infty$).[8] In the above statement, the

[7] Basic properties of these functions such as symmetry and dispersion relations, sum rules, as well as their relevance with various experimental probes, can be found in several excellent books (see for example Refs. [43–47]).

[8] It is then sometimes more convenient to work with the fluctuation operators $\delta O^q \equiv O^q - < O^q >$ instead of O^q.

notion of large enough times actually means $t >> \tau_c$, where τ_c denotes a characteristic time scale of the system over which all correlations vanish and for this reason is known as the "correlation time". In the next chapter, we shall speak of the bath correlation time τ_B, a significant quantity in the general context of the theory of open systems.

Another property of $J_{qq'}(t)$, following from its definition, is

$$(J_{qq'}(t))^* = J_{q'q}(-t) \ , \tag{2.29}$$

since both O^q and $O^{q'}$ are hermitian.

Now, assuming that the exact energy spectrum of the Hamiltonian H of the magnetic molecule system (considered as "closed"), is known, one can explicitly write $J_{qq'}(t)$ as

$$J_{qq'}(t) = \frac{1}{Z}\sum_{n,m} e^{-\beta E_n} e^{i\omega_{nm}t} O^q_{nm} O^{q'}_{mn} \ , \tag{2.30}$$

where $\hbar\omega_{mn} \equiv E_m - E_n$ denote are the characteristic Bohr frequencies of H. In the above expression, the frequencies ω_{nm} that correspond to vanishing matrix elements O^q_{nm} and/or $O^{q'}_{mn}$, do not appear. To this end, an a priori knowledge of certain symmetries of the Hamiltonian and the resulting selection rules is of particular importance. For instance, as we are going to see in the next chapter, based on this general consideration and for the isotropic Heisenberg model, one can separate the spin-spin correlation functions appearing in the expression for the nuclear spin-lattice relaxation rate $1/T_1$, into two groups: The longitudinal correlation functions (O^q, $O^{q'}$ being one of $\{s^z_i\}$, with $i = 1, \ldots, N$) and the transverse ones (O^q, $O^{q'}$ being one of $\{s^x_i,\ s^y_i\}$).

Experiments in frequency domain probe the Fourier transform of $J_{qq'}(t)$, usually called "the spectral density" and denoted by $J_{qq'}(\omega)$. This can be written, according to the above, as

$$J_{qq'}(\omega) \equiv \int_{-\infty}^{+\infty} dt\ e^{i\omega t} J_{qq'}(t) = \frac{2\pi}{Z}\sum_{n,m} e^{-\beta E_n} O^q_{nm} O^{q'}_{mn} \delta(\omega + \omega_{nm}) \ . \tag{2.31}$$

An important property of the spectral density, which also arises from the stationarity of $\rho(T)$, is the so-called detailed-balance relation

$$J_{qq'}(-\omega) = e^{-\beta\omega} J_{q'q}(\omega) \ . \tag{2.32}$$

As explained in the following chapter, Eq. (2.32) merely expresses the fact that since the populations of two levels, $|n>$ and $|m>$ differ according to

$$P_n/P_m = e^{-\beta\omega_{nm}} \ , \tag{2.33}$$

the overall absorption or emission of energy with $\omega = \omega_{nm}$, should also carry this factor. A second property of the spectral density is

$$\left(J_{qq'}(\omega)\right)^* = J_{q'q}(\omega) \ , \tag{2.34}$$

following from Eq. (2.29), above.

Several comments related to the discreteness of the magnetic molecule spectrum are in order here. First, the appearance of the $\delta-$functions in the r.h.s. of Eq. (2.31) is a consequence of the fact that we started with the Hamiltonian of a closed system, and hence they are merely an expression of energy conservation: An external probe (ω) can exchange energy with the spin system (ω_{nm}) only if a resonance condition is satisfied. For instance, the proton spin-lattice relaxation rate $1/T_1$, probes electronic spin-spin correlations at the proton Larmor frequency (ω_L) as determined by its gyromagnetic ratio and the external magnetic field. This frequency is extremely small as compared with typical excitations (ω_{nm}) in a magnetic molecule, a first essential ingredient in understanding and analyzing $1/T_1$ data (see chapter 4).

On the other hand, no real system exists that is completely isolated from its "environment". In fact, it is the tiny interactions with these "environmental" degrees of freedom that provide the means of relaxation to the equilibrium state. Although such small coupling terms do not really affect static properties, they become significant in affecting the equilibrium fluctuations in a system with a discrete energy spectrum, such as a magnetic molecule crystal. As shown in chapter 3, a correct description of these thermal fluctuations begins by considering the molecule together with the bath as a closed system. The large heat capacity of the reservoir results in an irreversible dynamics of the system's degrees of freedom. These irreversibility effects will show up in the spectral densities $J_{qq'}(\omega)$, as measured in an experiment, as a broadening of the above discrete $\delta-$lines. As we explain in the next chapter, it is exactly these thermal broadening effects that have been probed by the $1/T_1$ measurements in NMR experiments.

From the above general considerations alone, we see that the time correlation functions or equivalently the spectral densities, as measured in dynamic experiments, contain significant information about the spectrum of H. Depending on the experiment at hand, one can probe a variety of different correlation functions (different O^q and $O^{q'}$) and more importantly, different frequency or time scales. In addition, they carry information about the spin-bath interactions, not seen in static experiments.

In addition to the spectral density $J_{qq'}(\omega)$, the one-sided Fourier transform $J^{(1)}_{qq'}(\omega)$ is often of practical use. This is defined as

$$J^{(1)}_{qq'}(\omega) \equiv \int_0^{+\infty} dt\ e^{i(\omega+i0^+)t} J_{qq'}(t)\ , \tag{2.35}$$

By making use of the identity

$$\int_0^{\infty} ds\ e^{i(\omega+i0^+)s} = \frac{i}{\omega+i0^+} = \pi\delta(\omega) + i\mathcal{P}\frac{1}{\omega}\ , \tag{2.36}$$

with $\mathcal{P}$ denoting the Cauchy principal value,[48] we can obtain the following convenient expression for $J^{(1)}_{qq'}(\omega)$

$$J^{(1)}_{qq'}(\omega) = \frac{1}{Z}\sum_{nm} e^{-\beta E_n} O^q_{nm} O^{q'}_{mn} [\pi\delta(\omega+\omega_{nm}) + i\mathcal{P}\frac{1}{\omega+\omega_{nm}}]$$
$$= \frac{1}{2} J_{qq'}(\omega) + i\Pi_{qq'}(\omega) \ , \tag{2.37}$$

where we have used Eq. (2.31) and defined the quantity $\Pi_{qq'}(\omega)$ as

$$\Pi_{qq'}(\omega) = \mathcal{P}\sum_{nm} \frac{e^{-\beta E_n}}{Z} \frac{O^q_{nm} O^{q'}_{mn}}{\omega+\omega_{nm}} \ . \tag{2.38}$$

This quantity has the property

$$\left(\Pi_{qq'}(\omega)\right)^* = \Pi_{q'q}(\omega) \ , \tag{2.39}$$

which is similar to Eq. (2.34) for $J_{qq'}(\omega)$. Combining the above expressions, one obtains, in particular, the relation

$$J_{qq'}(\omega) = J^{(1)}_{qq'}(\omega) + \left(J^{(1)}_{q'q}(\omega)\right)^* \ . \tag{2.40}$$

We shall make use of these expressions in the following chapter, when discussing the generalized master equations for open systems.

References

[1] M. Affronte, J. C. Lasjaunias, A. Cornia, and A. Caneschi, Phys. Rev. B **60**, 1161 (1999).

[2] M. Affronte, T. Guidi, R. Caciuffo, S. Carretta, G. Amoretti, J. Hinderer, I. Sheikin, A. A. Smith, R. E. P. Winpenny, J. van Slageren, and D. Gatteschi, J. Mag. Mag. Mat. **272-276**, 1050 (2004).

[3] M. Affronte, A. Cornia, A. Lascialfari, F. Borsa, D. Gatteschi, J. Hinderer, M. Horvatić, A. Jansen, and M.-H. Julien, Phys. Rev. Lett. **88**, 167202 (2002).

[4] A. Cornia, A. G. M. Jansen, and M. Affronte, Phys. Rev. B **60**, 12177 (1999).

[5] O. Waldmann, J. Schülein, R. Koch, P. Müller, I. Bernt, R. W. Saalfrank, H. P. Andres, H. U. Güdel, and P. Allenspach, Inorg. Chem. **38**, 5879 (1999).

[6] O. Waldmann, R. Koch, S. Schromm, J. Schülein, P. Müller, I. Bernt, R. W. Saalfrank, F. Hampel, E. Balthes, Inorg. Chem. **40**, 2986 (2001).

[7] R. M. White, *Quantum Theory of Magnetism* (Springer-Verlag, Berlin, 1983).

[8] J. B. Goodenough, Phys. Rev. B **100** 564(1955); J. Phys. Chem. Solids **6**, 287 (1958). See also J. B. Goodenough, *Magnetism and the Chemical Bond* (Interscience, New York, 1963).

[9] J. Kanamori, J. Phys. Chem. Solids **10**, 87 (1959).

[10] P. W. Anderson, Phys. Rev. **115**, 2 (1959); Solid State Phys. **14**, 99 (1963).

[11] T. Moriya, Phys. Rev. **120**, 91 (1960); Phys. Rev. Lett. **4**, 228 (1960).

[12] P. Erdös, J. Phys. Chem. Solids **27**, 1705 (1966).

[13] A. Abragam, and B. Bleaney, *Electron Paramagnetic Resonance of Transition Metal Ions* (Dover Publications Inc., New York, 1986).

[14] A. Bencini, and D. Gatteschi, *EPR of Exchange Coupled Systems* (Springer, Berlin 1990).

[15] D. Dai, and M. H. Whangbo, J. Chem. Phys. **118**, 29 (2003).

[16] K. W. H. Stevens, Rep. Prog. Phys. **30**, 189-226 (1967).

[17] R. D. Mattuck, and M. W. P. Strandberg, Phys. Rev. **119**, 1204 (1960).

[18] J. W. Culvahouse, W. P. Unruh, and D. K. Brice, Phys. Rev. **129**, 2430 (1963).

[19] D. K. Ray, T. Ray, and P. Rudra, Proc. Phys. Soc. **87**, 485 (1966).

[20] L. D. Landau, and E. M. Lifshitz, *Theory of Elasticity* (Pergamon Press Inc., New York, 1959).

[21] D. C. Wallace, *Thermodynamics of Crystals* (Wiley, New York, 1972).

[22] N. W. Ashcroft, and N. D. Mermin, *Solid state Physics* (Brooks/Cole, Thomson Learning Inc., Singapure, 1976) Ch. 22.

[23] R. P. Feynman, R. B. Leighton, and M. Sands, *The Feynman lectures on Physics*, Vol. II (Addison-Wesley, New York, 1964), Ch. 38.

[24] B. Lüthi, in *Dynamical Properties of Solids*, vol. 3, edited by G. K. Horton, and A. A. Maradudin (North-Holland Publishing Company, Amsterdam, 1980).

[25] A. Einstein, and W. J. de Haas, Verh. d. D. Phys. Ges. **17**, 152 (1915).

[26] F. Hartmann-Boutron, P. Politi, and J. Villain, International Journal of Modern Physics B **10**, No. 21, 2577-2637 (1996).

[27] E. M. Chudnowsky, Phys. Rev. Lett. **72**, 3433 (1994).

[28] L. Engelhardt, Ph. D. thesis, Iowa State University, in preparation.

[29] J. J. Borras-Almenar, J. M. Clemente-Juan, E. Coronado, and B. S. Tsukerblat, Inorg. Chem. **1999**, 38, 6081-6088; see also *Journal of Computational Chemistry*, Vol. 22, No. 9 (John Wiley & Sons, Inc., 2001), pg. 985-991.

[30] J. H. Luscombe, M. Luban, and F. Borsa, J. Chem. Phys. **108**, 7266 (1998).

[31] M. Luban, and J. Luscombe, Am. J. Phys. **67**, 1161 (1999).

[32] D. Mentrup, J. Schnack, and M. Luban, Physica A **272**, 153 (1999).

[33] O. Ciftja, M. Luban, M. Auslender, and J. H. Luscombe, Phys. Rev. B **60**, 10122 (1999).

[34] D. Mentrup, H.-J. Schmidt, J. Schnack, and M. Luban, Physica A **278**, 214 (2000).

[35] R. A. Klemm, and M. Luban, Phys. Rev. B **64**, 104424 (2001).

[36] C. Schröder, H.-J. Schmidt, J. Schnack, and M. Luban, Phys. Rev. Lett. **94**, 207203 (2005).

[37] C. Schröder, H. Nojiri, J. Schnack, P. Hage, M. Luban, and P. Kögerler, Phys. Rev. Lett. **94**, 017205 (2005).

[38] J. Schnack, in *Quantum Magnetism*, Lect. Notes Phys. **645**, 155-194 (2004); cond-mat/0501625 (2005).

[39] J. Schnack, and M. Luban, Phys. Rev. B **63**, 014418 (2000).

[40] C. P. Slichter, *Principles of Magnetic Resonance* (Springer Verlag, Berlin, 1989).

[41] A. Abragam, *Principles of Nuclear Magnetism* (Clarendon Press, Oxford, 1961).

[42] H.-J. Schmidt, J. Schnack, and M. Luban, Phys. Rev. B **64**, 224415 (2001).

[43] R. Kubo, M. Toda, and N. Hashitsume, *Statistical Physics II, Nonequilibrium Statistical Mechanics* (Springer-Verlag, Second Edition, 1991).

[44] E. Fick, and G. Sauermann, *The Quantum Statistics of Dynamic Processes* (Springer-Verlag, 1990).

[45] J. Dupuy, and A. J. Dianoux (Editors), *Microscopic Structure and Dynamics of Liquids* (Plenum Press, New York, 1978).

[46] S. Dattagupta, *Relaxational Phenomena in Condensed Matter Physics* (Academic Press, Inc., 1987).

[47] D. Forster, *Hydrodynamic Fluctuations, Broken symmetry, and Correlation Functions* (W. A. Benjamin, Inc., 1975).

[48] G. B. Arfken, and H. J. Weber, *Mathematical Methods for Physicists* (Academic Press, New York, 1995), 4th International edition.

3. Theoretical aspects of Open Systems

3.1 Introduction

Every physical system $\mathcal{A}$ is "open", in the sense that it, even slightly, interacts with the degrees of freedom of its surroundings, collectively termed the "bath" or the "lattice" $\mathcal{B}$. This is usually a large reservoir at temperature T, with much larger heat capacity than that of the system $\mathcal{A}$ under study. As a result, when $\mathcal{A}$ is externally perturbed (or probed), the state of $\mathcal{B}$ is not altered.[1] On the other hand, the small coupling of $\mathcal{A}$ to $\mathcal{B}$ does alter the state of A. In fact, it provides the only means of relaxation to its equilibrium state with the temperature T, of the bath.

In this chapter, we will first show how the quantum-mechanical transition rates among states of $\mathcal{A}$ are given in terms of certain spectral densities of the bath $\mathcal{B}$. This connection is two-fold, since apart from studying the dynamical behavior of a system $\mathcal{A}$ approaching equilibrium (e.g., after it has been perturbed slightly out of its equilibrium), it also provides an indirect means of studying the equilibrium properties of $\mathcal{B}$. Let us consider, for example, what information is obtained by a measurement of the nuclear spin-lattice relaxation rate $1/T_1$ in magnetic molecules, discussed in the following chapter. This rate first of all describes how fast the nuclear system ($\mathcal{A}$) relaxes back to its equilibrium state after it has been perturbed by a series of radiofrequency (rf) pulses in a typical NMR experiment. In addition however, it provides a means of studying the spectral density of its surroundings $\mathcal{B}$, which in the case of a magnetic molecule are the electronic moments comprising the molecule. Hence, by probing the nuclear spin one indirectly "measures" certain spectral densities of the magnetic molecule system. Moreover, since the magnetic molecule is itself an open system (but in thermal equilibrium) interacting mainly with phonons, its spectral densities, as probed by $1/T_1$, contain physical information about the spin-phonon interactions.

In Appendix C we derive the so-called Pauli Master equations governing the evolution of the populations of the various states of $\mathcal{A}$, starting from Fermi's Golden rule. However, there are certain

[1] More accurately, the resulting bath excitations decay much faster than the relevant experimental time scale (see below).

aspects of the general problem of the physics of open systems, which cannot be taken into account by such an approach. On the other hand, a very general and suitable tool for formulating the physics of open systems and their several associated effects (such as relaxation and decoherence) is that of the density matrix and its governing equation of motion. Furthermore, the conditions under which certain approximations (such as the Markovian approximation) can be employed, are more transparently understood within this approach. In addition, by using the so-called quantum regression theorem,[1–4] we will show how one can calculate, in principle, various out-of-equilibrium but also equilibrium time correlation functions. The latter ones are of special interest in the NMR study of magnetic molecules, discussed in the next chapter. Finally, as we show in chapter 7, our present analysis, which is based on the condition of static external fields, can be generalized to dynamic fields as well. But first, we shall need to set the theoretical basis for discussing the physics of open systems.

The organization of this chapter is the following. In Sec. 3.2, we define the density matrix of a system neglecting any interactions with environmental degrees of freedom. This is done for both a pure and a mixed initial state. In Sec. 3.3 we include the small interactions with a large reservoir and define the quantity of most interest, namely the reduced density matrix. Then, in Sec. 3.4, following the standard perturbation approach, we provide the derivation of the equation of motion of the reduced density matrix in the Markovian limit (defined below). We also show that the evolution of the diagonal matrix elements of the reduced density matrix can be decoupled from the nondiagonal ones for spectra with non-degenerate and non-equidistant energy levels. In Sec. 3.5 we apply the so-called quantum-regression theorem in order to arrive, starting from the generalized master equation, at expressions for the various spectral densities. We shall then demonstrate that the Markovian limit corresponds to Lorentzian broadened spectra lines, and we shall also make the correspondence between (i) the linewidth of the elastic peak with the eigenvalues of the relaxation matrix $\mathbf{\Lambda}$ (defined below), and (ii) the linewidths of the remaining, inelastic peaks of the spectrum with the corresponding decoherence rates.

3.2 Closed systems

We consider first a closed system $\mathcal{E}$ with Hamiltonian H, and we denote its eigenenergies and eigenstates by E_n and $|n>$, respectively. We will distinguish two different cases regarding the initial preparation, and more specifically the amount of information that one has at $t = 0$: (i) the "pure" state and (ii) the "mixed" state. Take, for instance, a beam of neutrons entering, at $t = 0$, a region with a uniform magnetic field along the $z-$axis. This system is said to be (thermally) closed if one

can neglect any thermal effects i.e., the coupling to environmental degrees of freedom. But its state at $t = 0$ depends on the amount of information known about the spin polarization of the neutrons. In particular, if the beam is initially unpolarized, with $p_{-1/2}$ and $p_{1/2}$ being the percentages of spin-up ($|+1/2>$) and spin-down ($|-1/2>$) states, respectively, then this generally corresponds to a mixed state. A pure state corresponds to, for example $\{p_{1/2} = 1,\ p_{-1/2} = 0\}$, or $\{p_{1/2} = 0,\ p_{-1/2} = 1\}$. [2]

3.2.1 Pure initial state

In this first case, one assumes that our system $\mathcal{E}$ is prepared in a given quantum-mechanical state $|\psi(0)>$. Generally, this state can be written as a linear superposition of the energy eigenstates $|n>$, i.e.,

$$|\psi(0)>=\sum_n c_n|n> \ , \tag{3.1}$$

where $c_n \equiv< n|\psi(0)>$. The time evolution of $|\psi(t)>$ is governed by H, according to

$$|\psi(t)>= e^{-iHt/\hbar}|\psi(0)>=\sum_n e^{-iE_nt/\hbar}c_n|n> \ . \tag{3.2}$$

By definition, the density matrix ρ for such a system is given by

$$\rho(t) = |\psi(t)>< \psi(t)| = \sum_{nn'} e^{-i\omega_{nn'}t}c_nc^*_{n'}|n>< n'| \ , \tag{3.3}$$

(where $\omega_{nn'} \equiv (E_n - E_{n'})/\hbar$), and it satisfies the so-called Liouville-von Neumann equation

$$i\hbar\dot{\rho}(t) = [H, \rho(t)] \ , \tag{3.4}$$

being equivalent to the time-dependent Schrödinger equation for $|\psi(t)>$. Similarly with the wavefunction $|\psi(t)>$, the density matrix gives the complete information about the system $\mathcal{E}$. For instance, the expectation value of any given operator X can be expressed as

$$< X(t) >=< \psi(t)|X|\psi(t)>=\sum_{nn'} \rho_{nn'}(t)\ X_{n'n} = Tr(\rho(t)\ X) \ , \tag{3.5}$$

with

$$\rho_{nn'}(t) = e^{-i\omega_{nn'}t}c_nc^*_{n'} \ , \tag{3.6}$$

being the representation of $\rho(t)$ in the $\{|n>\}$ basis. One should remark that the diagonal elements of ρ ("populations") do not change in time, whereas the non-diagonal ones ("coherences") vary harmonically

[2] For our previous example, such an initial state can be prepared by taking an unpolarized beam through a region with a non-uniform or gradient magnetic field. The two spin components are then separated into two beams each being described by a pure state.

in time with the characteristic Bohr frequencies of $\mathcal{E}$. This stems from the fact that $\mathcal{E}$ is considered to be an ideally closed system.

Often, one introduces the density matrix in the Heisenberg picture, $\widetilde{\rho} \equiv e^{iHt/\hbar}\ \rho\ e^{-iHt/\hbar}$, for which

$$\widetilde{\rho}_{nn'}(t) = e^{i\omega_{nn'}t}\rho_{nn'}(t) = \sum_{nn'} c_n c_{n'}^* = \widetilde{\rho}_{nn'}(0) = \rho_{nn'}(0)\ , \tag{3.7}$$

i.e., $d\widetilde{\rho}/dt = 0$, similarly with the Heisenberg picture of a wavefunction.

3.2.2 Mixed initial state

The case of a mixed initial state corresponds to situations where we do not have the complete knowledge about the quantum-mechanical state of the system at $t = 0$. This lack of information at $t = 0$ is accounted for by assigning a probability p_s for the system to be in any given (pure) state $|\psi_s(0) >$ (the states $\{|\psi_s(0) >\}$ are assumed to be normalized, i.e., $< \psi_s(0)|\psi_s(0) >= 1$, but they are not necessarily mutually orthogonal). Equivalently, one thinks of an ensemble of $\mathcal{N}$ identical systems $\{\mathcal{E}_1, \mathcal{E}_2, \ldots, \mathcal{E}_{\mathcal{N}}\}$, each one being prepared in a pure state $|\psi_s(0) >$, with a certain probability p_s. Thus, p_s denotes the ratio of the number $\mathcal{N}_s$ of systems that have all been prepared in the same $|\psi_s(0) >$ state, divided by the total number of systems $\mathcal{N}$.

Clearly, such an initial state cannot be expressed by just a wavefunction, as in the previous case. There is a certain uncertainty of statistical character in addition to the quantum-mechanical one. Now, it is important to realize that this is merely a statement about the initial condition: Each member of the ensemble (of the $\mathcal{N}$ identical closed systems) still evolves according to Schrödinger's equation, and the probabilities p_s do not change with time.

The above ensemble can be described by generalizing Eq. (3.3) to

$$\rho(0) \equiv \sum_s p_s |\psi_s(0) >< \psi_s(0)| \equiv \overline{|\psi(0) >< \psi(0)|}\ , \tag{3.8}$$

which represents a statistical average over all members of the ensemble. Clearly, this density matrix contains both a statistical and a pure quantum-mechanical type of probability. Denoting by c_n^s the projections $< n|\psi_s(0) >$, i.e.,

$$|\psi_s(0) >= \sum_n c_n^s |n >\ , \tag{3.9}$$

one obtains the more explicit form

$$\rho(0) = \sum_{s,n,n'} p_s c_n^s c_{n'}^{s*} |n >< n'| \equiv \sum_{n,n'} \overline{c_n c_{n'}^*}\ |n >< n'|\ . \tag{3.10}$$

Furthermore, since each member of the ensemble evolves independently according to Schrödinger's equation, the density matrix evolves again according to Eq. (3.4), and

$$\rho(t) = \sum_s p_s |\psi_s(t)><\psi_s(t)| = \sum_{n,n'} e^{-i\omega_{nn'}t}\ \overline{c_n c_{n'}^*}\ |n><n'| \ , \tag{3.11}$$

or, equivalently

$$\rho_{nn'}(t) = e^{-i\omega_{nn'}t}\ \overline{c_n c_{n'}^*} \ . \tag{3.12}$$

Similarly, the elements of the density matrix $\widetilde{\rho}$ in the Heisenberg picture are again time independent and are given by

$$\widetilde{\rho}_{nn'}(t) = e^{i\omega_{nn'}t}\rho_{nn'}(t) = \ \overline{c_n c_{n'}^*} = \widetilde{\rho}_{nn'}(0) = \rho_{nn'}(0) \ . \tag{3.13}$$

In addition, the expectation value of a physical quantity X involves a statistical and a quantum-mechanical average, i.e.,

$$< X(t) >= \sum_s p_s < \psi_s(t)|X|\psi_s(t) > \ \ , \tag{3.14}$$

which in turn gives

$$< X(t) >= Tr(\rho(t)\ X) \ , \tag{3.15}$$

i.e., the same general expression with Eq. (3.5) of the pure case.

According to the above, for a closed system and for both a pure and a mixed initial state, the subsequent time evolution does not involve any transfer of populations ("relaxation") or a decay of the non-diagonal elements ("decoherence"). This is related to the fact that the various probabilities p_s, once determined from the initial condition, do not change in time. Effects such as relaxation and decoherence are clearly associated with the physics of open systems and will be discussed below.

Finally let us make the following remarks. By definition, and for both a pure and a mixed state the density matrix obeys the completeness relation

$$Tr(\rho) = \sum_n \rho_{nn} = 1 \ . \tag{3.16}$$

since $Tr\rho = \sum_s p_s \sum_n |c_n^s|^2 = \sum_s p_s = 1$. Nonetheless, although $Tr(\rho^2) = 1$ for a pure state, the same is not generally true for a mixed state, but the general inequality

$$Tr(\rho^2) \leq 1 \ , \tag{3.17}$$

holds instead. This can be shown by invoking the Schwarz inequality for all pairs of $|\psi_s(0)>$ and $|\psi_k(0)>$

$$|<\psi_s(0)|\psi_k(0)>|^2 \ \leq \ <\psi_s(0)|\psi_s(0)><\psi_k(0)|\psi_k(0)> \ \ , \tag{3.18}$$

which reduces to

$$\sum_{nm}(c_n^{s*}c_m^s)(c_n^k c_m^{k*}) \leq \sum_{nm}(c_n^s c_n^{s*})(c_m^k c_m^{k*}) \ , \tag{3.19}$$

inasmuch as $0 \leq p_s \leq 1$, for all s. Then the inequality (3.17) follows straightforwardly. The equal sign follows from the Schwarz inequality when the set of states $\psi_s(0)$ are all "parallel" to one given state. Equivalently the sum in Eq. (3.8) reduces to one term only, i.e., a pure state. Generally then, the quantity $Tr(\rho^2)$ gives a criterion for whether a given density matrix corresponds to a pure or a mixed state. Further details regarding the density matrix can be found in Refs.[4, 5].

3.3 Open systems

All physical systems are in essence open, since they interact, even slightly with external degrees of freedom. Consider an open system $\mathcal{A}$ which is in thermal contact with a bath $\mathcal{B}$ (see Fig. 3.1). We will assume that we only observe (or probe) $\mathcal{A}$, with the bath being a large reservoir at temperature T. Clearly, one can regard the combined system of $\mathcal{A} \oplus \mathcal{B}$ as a closed system $\mathcal{E}$ and therefore we can apply the previous general results for ideally closed systems. One then should begin with the total Hamiltonian of $\mathcal{E}$

$$H_{tot} = H_A + H_B + V \ . \tag{3.20}$$

Here H_A, H_B stand for the energies of the two subsystems $\mathcal{A}$ and $\mathcal{B}$, respectively, when isolated, and V denotes their coupling energy (Fig. 3.1). This can always be written in the general form

$$V = \hbar \sum_q A^q \otimes B^q \ , \tag{3.21}$$

where A^q (B^q) are operators of the system $\mathcal{A}$ ($\mathcal{B}$). The results of the previous section apply here for the density matrix of the whole system $\rho_{tot}(t)$. On the other hand, the mere fact that we only observe the subsystem $\mathcal{A}$, and not the whole dynamics of $\mathcal{E}$, introduces certain dynamical effects such as decoherence and relaxation. Thus, contrary to the dynamical behavior of ρ_{tot}, the populations of the relevant density matrix of $\mathcal{A}$ only (the "reduced" density matrix ρ_A, defined below), do change in time, and this is associated with energy exchange with $\mathcal{B}$ ("relaxation"). In addition, the coupling to $\mathcal{B}$ usually gives rise to a decay of the non-diagonal elements of the ρ_A (loss of coherence or "decoherence"). Consider, in particular, the case when $\mathcal{A}$ has reached thermal equilibrium with the bath at temperature T. We know from quantum statistical mechanics that this stationary state case can be described by the mixed density matrix, given by

$$\rho_A(T) = e^{-\beta H_A}/Z_A = \sum_n \frac{e^{-\beta E_n}}{Z_A} \ |n><n| \ . \tag{3.22}$$

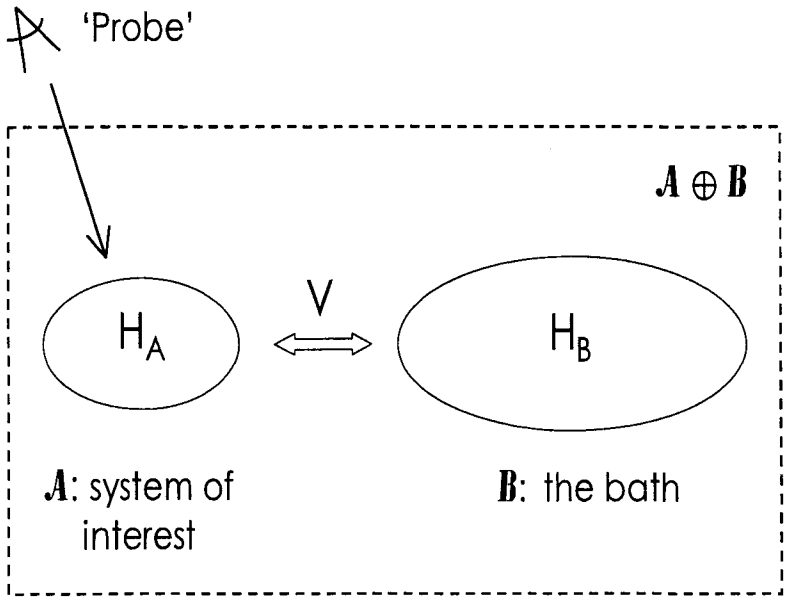

Figure 3.1 Schematic representation of the typical situation when probing an open system $\mathcal{A}$. The system $\mathcal{B}$ is considered to be a large reservoir at temperature T. In thermal equilibrium, $\mathcal{A}$ and $\mathcal{B}$ have the same temperature. Their mutual interaction V is usually so small (compared to k_BT) that cannot be "seen" by static experiments. However, the effect of V can be manifested in a dynamic experiment. For instance, if $\mathcal{A}$ is slightly perturbed out of equilibrium (e.g., by an external field), then V is the source of the recovery back to its equilibrium state. This recovery takes place with a set of characteristic times, collectively denoted by τ_A. These times characterize the recovery to equilibrium of all physical quantities of system $\mathcal{A}$, including the (out-of-equilibrium) correlation functions. The interaction energy V manifests also in the decay of equilibrium fluctuations, in cases where the experiment directly probes a correlation function of $\mathcal{A}$, without perturbing its state. As an example for the latter case consider the measurement of $1/T_1$ (see chapter 4): The probe is the nuclear spin, $\mathcal{A}$ is the magnetic molecule, $\mathcal{B}$ corresponds to the phonon system.

where $Z_A = \sum_n e^{-\beta E_n}$, where now $\{E_n\}$ and $\{|n>\}$ denote the set of eigenvalues and eigenstates of H_A. The probability of being in a given microscopic energy state $|n>$[3] is given by the Boltzmann factor

$$p_n = e^{-\beta E_n}/Z_A. \tag{3.23}$$

The above density matrix describes only the equilibrium of $\mathcal{A}$ and says nothing about its dynamical behavior towards this state. In addition, it does not provide any information about the coupling with $\mathcal{B}$ and the resulting quantum-mechanical transition rates between states of $\mathcal{A}$. In particular, this coupling modifies the behavior of equilibrium time correlation functions. In what follows we will deal with the formulation of such more general questions and in particular we shall derive the so-called generalized master equation in the limit of very short bath correlation times. In this way, we will arrive at the Pauli master equations for the populations, shown in Appendix C starting from Fermi's Golden rule. Our approach, will shed some light not only on the approximations involved but also provide equations for the non-diagonal elements of the density matrix as well. Finally, we shall discuss and make use of the quantum regression theorem for describing the time correlation functions and fluctuations. But first, we shall need to define the reduced density matrix.

3.3.1 The reduced density matrix

Let us begin with the equation of motion for the density matrix ρ_{tot} of the combined system $\mathcal{E}$. This is given by the Liouville-von Neumann equation

$$i\hbar\dot{\rho}_{tot}(t) = [H_{tot}, \rho_{tot}(t)] = [H_A + H_B + V, \rho_{tot}(t)] \ . \tag{3.24}$$

Given this general equation, the next goal is to devise a means for obtaining information for the dynamics of $\mathcal{A}$ only. To see how this can be done, let us consider an operator X pertaining to the subsystem $\mathcal{A}$, only. Its thermal average is given by

$$< X(t) >= Tr(X\rho_{tot}(t)) = Tr_{\mathcal{A}}Tr_{\mathcal{B}}(X\rho_{tot}(t)) \ , \tag{3.25}$$

where we have split the trace operation to one ($Tr_{\mathcal{A}}$) over the system's degrees of freedom and another ($Tr_{\mathcal{B}}$) over the bath degrees of freedom. Since X refers to system $\mathcal{A}$ only, the above relation gives

$$< X(t) >= Tr_{\mathcal{A}}[X \ Tr_{\mathcal{B}}(\rho_{tot}(t))] \equiv Tr_{\mathcal{A}}[X \ \rho_A(t))] \ , \tag{3.26}$$

where we have defined the so-called reduced density matrix $\rho_A(t) \equiv Tr_{\mathcal{B}}(\rho_{tot}(t))$. This quantity is of central interest; by taking a partial trace over the bath degrees of freedom one obtains all relevant

[3]The index s used in our previous conventions, here corresponds to the quantum numbers $\{n\}$ of the eigenstates of H_A.

thermal averages of $\mathcal{A}$.[4] The main goal is then to derive an equation of motion of the reduced density matrix only, starting from

$$i\hbar\dot{\rho}_A(t) = Tr_B[H_A + H_B + V, \rho_{tot}(t)] \ . \tag{3.27}$$

3.4 Derivation of the master equations in the Markovian limit

The effect of the bath on the system $\mathcal{A}$, apart from depending on the strength of V (usually assumed very small), varies significantly depending on the competition of the various time scales of the problem. Let us then start by considering these time scales. First, there are the intrinsic times of $\mathcal{A}$ and $\mathcal{B}$. In particular, the transition rates between the states of $\mathcal{A}$ as a result of the coupling to $\mathcal{B}$ set one, such time scale. This is usually called the relaxation time denoted by τ_A. A similar time scale, usually called the bath correlation time τ_B, can be assigned to the bath: this arises either from intra-bath interactions (e.g., phonon-phonon interactions if the bath consists of the phonon degrees of freedom) or from interactions between the bath $\mathcal{B}$ and a third system $\mathcal{C}$.[5] The above times τ_A and τ_B are the characteristic time scales of the decay of physical quantities, such as correlation functions (This is why, in particular, τ_B is called correlation time, since it gives the decay rate of the various fluctuations within the bath). Furthermore, one also has additional time scales such as for example $1/\omega_A$, set by the characteristic Bohr frequencies ω_A of $\mathcal{A}$. Finally, to observe certain dynamical thermal effects one should be able to measure in the appropriate time scale, denoted by τ_e. Specifically, this experimental time scale should be at the regime of τ_A. In chapters 6,7, and 8 where we discuss the response of the magnetic molecule systems to pulsed magnetic fields, such an experimental time scale enters explicitly in the Hamiltonian and is determined by the magnetic field's sweep rate. Here we consider only static external fields. The appropriate generalization of the present analysis of master equations to the case of pulsed fields is given in chapter 8.

Here, in accordance with Appendix C, we shall derive an equation of motion for ρ_A (generalized master equation) in the weak coupling limit and assuming that the correlation time of the bath τ_B is much shorter than the typical relaxation times τ_A of $\mathcal{A}$ (Markovian limit). This allows one to employ second order perturbation theory in V (Born approximation), and neglect certain memory effects (Markov approximation). In addition we will assume that $\omega_A \gg 1/\tau_e$ (rotating wave approximation (RWA)). These approximations give rise to a set of equations of motion for the populations and the

[4] As shown later on, to express dynamical quantities of $\mathcal{A}$, such as time correlation functions, in terms of the reduced density matrix is a little more complicated than expressing one-time thermal averages.

[5] This is for example the case of NMR in magnetic molecules, where one probes the nuclear spins ($\mathcal{A}$), which mainly interact with the electronic magnetic moments ($\mathcal{B}$), and which in turn are affected by interactions with phonons ($\mathcal{C}$).

coherences with time independent coefficients. In particular, the equations for the populations will be identical to those derived from Fermi's Golden rule, shown in Appendix C.

For clarity, in what follows, we shall denote ρ_A by ρ. In performing a perturbation expansion in V, it is very convenient to switch to the interaction picture density matrix $\widetilde{\rho}_{tot}$ defined by

$$\widetilde{\rho}_{tot}(t) \equiv e^{i(H_A+H_B)t/\hbar}\rho_{tot}(t)e^{-i(H_A+H_B)t/\hbar} \ . \tag{3.28}$$

It follows from Eq. (3.24) that $\widetilde{\rho}_{tot}(t)$ obeys the equation of motion

$$i\hbar\frac{d\widetilde{\rho}_{tot}}{dt} = [\widetilde{V}(t), \widetilde{\rho}_{tot}(t)] \ , \tag{3.29}$$

where,

$$\widetilde{V}(t) = e^{i(H_A+H_B)t/\hbar}Ve^{-i(H_A+H_B)t/\hbar} = \hbar\sum_q \widetilde{A}^q(t)\widetilde{B}^q(t) \ , \tag{3.30}$$

and $\widetilde{A}^q(t)$, $\widetilde{B}^q(t)$ are given by $\widetilde{A}^q(t) \equiv e^{iH_At/\hbar}A^qe^{-iH_At/\hbar}$ and $\widetilde{B}^q(t) \equiv e^{iH_Bt/\hbar}B^qe^{-iH_Bt/\hbar}$, respectively. Integrating Eq. (3.29), we obtain the integral relation

$$\widetilde{\rho}_{tot}(t) = \widetilde{\rho}_{tot}(0) + \frac{1}{i\hbar}\int_0^t ds\ [\widetilde{V}(s), \widetilde{\rho}_{tot}(s)] \ , \tag{3.31}$$

which then may be replaced back into the r.h.s. of Eq. (3.29), to give the integro-differential equation

$$\frac{d\widetilde{\rho}_{tot}}{dt} = \frac{1}{i\hbar}[\widetilde{V}(t), \widetilde{\rho}_{tot}(0)] - \frac{1}{\hbar^2}\int_0^t ds\ [\widetilde{V}(t), [\widetilde{V}(s), \widetilde{\rho}_{tot}(s)]] \ . \tag{3.32}$$

Using Eq. (3.27), and changing the integration variable from s to $u = t - s$, we obtain

$$\frac{d\widetilde{\rho}}{dt} = \frac{1}{i\hbar}Tr_B\ [\widetilde{V}(t), \widetilde{\rho}_{tot}(0)] + \frac{1}{\hbar^2}\int_0^t du\ Tr_B\ [[\widetilde{V}(t-u), \widetilde{\rho}_{tot}(t-u)], \widetilde{V}(t)] \ . \tag{3.33}$$

Up to now, the above expressions are exact. We now perform the so-called Markovian (or homogeneous) approximation, which concerns the limit of very short bath correlation times, i.e., $\tau_B \ll \tau_A$. An immediate consequence of this is that all bath excitations decay very rapidly during the experimentally relevant time scale τ_e. This means that at all experimental times the bath is in the stationary state $\rho_B(t) \approx \rho_B(0) = e^{-\beta H_B}/Z_B$ and moreover that the total density matrix can be decomposed as

$$\rho_{tot}(t) \approx \rho_A(t) \otimes \rho_B \ , \tag{3.34}$$

and similarly, $\widetilde{\rho}_{tot}(t) \approx \widetilde{\rho}_A(t) \otimes \rho_B$. Alternatively, this means that $d\rho/dt$ represents a coarse-grained time derivative, i.e., we are not interested in times much shorter than τ_A.

An important remark is in order here. According to Eq. (3.24), the first term of Eq. (3.33) is proportional to terms like $Tr_B(\rho_B B^q) \equiv < \widetilde{B}^q >_B$. Such static terms, without loss of generality

can be neglected (we are only interested in the fluctuating, time dependent part of V). In doing so, and for consistency reasons, one should also neglect their second order contribution to the second term of Eq. (3.24). In other words, we should replace the operators B^q with their fluctuating parts $\delta B^q = B^q - < B^q >_B$. Henceforth, for notational clarity, B^q will implicitly stand for δB^q. Following this remark, we therefore neglect the first term of Eq. (3.33) and obtain

$$\frac{d\widetilde{\rho}}{dt} = \sum_{qq'} \int_0^t du \; Tr_B \; [[\widetilde{A}^q(t-u)\widetilde{B}^q(t-u), \widetilde{\rho}(t-u) \otimes \rho_B], \widetilde{A}^{q'}(t)\widetilde{B}^{q'}(t)] \; . \tag{3.35}$$

Expanding the double commutator inside the integral, and collecting the terms related to bath degrees of freedom only, one encounters the bath correlation functions

$$J_{q'q}(u) \equiv < \widetilde{B}^{q'}(u)\widetilde{B}^q(0) >_B \; . \tag{3.36}$$

As already mentioned, these correlation functions decay in times $\tau_B \ll \tau_A$ (and thus $\tau_B \ll t, \tau_e$, as well). During this short time scale, the density matrix does not change appreciably, and thus we may replace $\widetilde{\rho}(t-u)$ by $\widetilde{\rho}(t)$, i.e., we neglect short memory effects. In addition, we may replace the upper limit t of the integral with $+\infty$, i.e.,

$$\frac{d\widetilde{\rho}}{dt} = \sum_{qq'} \int_0^\infty du \; Tr_B \; [[\widetilde{A}^q(t-u)\widetilde{B}^q(t-u), \widetilde{\rho}(t) \otimes \rho_B], \widetilde{A}^{q'}(t)\widetilde{B}^{q'}(t)] \; . \tag{3.37}$$

This is our final, generalized master equation. To express it in the energy representation, we first introduce the following "super-operator",[6]

$$\Gamma_{nm,rs} \equiv \sum_{qq'} A^q_{nm} A^{q'}_{rs} J^{(1)}_{qq'}(\omega_{sr}) \; , \tag{3.38}$$

where $J^{(1)}_{qq'}(\omega)$ denotes the one-sided Fourier tranform of $J_{qq'}(u)$, defined in chapter 2 (see Eqs. (2.35) and (2.37)). With these definitions, Eq. (3.37) in the energy representation becomes

$$\dot{\widetilde{\rho}}_{nm}(t) = \sum_{rs} e^{i(\omega_{nm}-\omega_{rs})t} \; R_{nm,rs} \; \widetilde{\rho}_{rs}(t) \; , \tag{3.39}$$

where the elements of the "super-operator" $\mathbf{R}$ are defined as

$$R_{nm,rs} = \Gamma_{sm,nr} + \Gamma^*_{rn,ms} - \sum_k \Gamma_{nk,kr}\delta_{sm} - \sum_k \Gamma^*_{mk,ks}\delta_{nr} \; . \tag{3.40}$$

Two types of elements of $\mathbf{R}$ that appear below are

$$R_{nn,nn} = -\sum_{k\neq n} \Gamma_{nk,kn} + c.c = -\sum_{k\neq n}\sum_{qq'} A^q_{nk} A^{q'}_{kn} J_{qq'}(\omega_{kn}) \equiv -\sum_{k\neq n} W_{nk} \; , \tag{3.41}$$

[6] Every operation which transforms one operator to another carries four indices, and is usually called super-operator.

and, for $n \neq r$,

$$R_{nn,rr} = \Gamma_{rn,rn} + c.c = \sum_{qq'} A^q_{rn} A^{q'}_{nr} J_{qq'}(\omega_{nr}) \equiv W_{rn} \ , \tag{3.42}$$

where we have used the definition of Appendix C for the transition rates $W_{nr} \equiv W_{n\to r}$. Another element of $\mathbf{R}$ that appears in the equation for the non-diagonal elements of $\rho(t)$ is $R_{nm,nm}$, which we discuss in Appendix D.

Now, returning to Eq. (3.39), it is very tempting to switch back to the Schrödinger equation, in order to eliminate the phase factors, i.e.,

$$\dot{\rho}_{nm}(t) = -i\omega_{nm}\rho_{nm}(t) + \sum_{rs} R_{nm,rs}\ \rho_{rs}(t) \ . \tag{3.43}$$

Importantly, however, not all $R_{nm,rs}$ in this equation, affect the dynamics in the same way. The reason for this is the following. In defining the interaction matrix $\widetilde{\rho}$, we have implicitly eliminated the internal (i.e., H_A) degrees of freedom. Hence, by definition (see Eq. (3.29)) $\widetilde{\rho}$ varies only due to the interaction term V. On the other hand, the variation of ρ contains information about the internal frequencies of H_A, as well. Now, it is very often the case that the Bohr frequencies of H_A are much larger than the relevant inverse time scale of variation due to V only, i.e., $\omega_{nm} \gg 1/\tau_A$. In other words, one has a separation of time scales into fast, intrinsic variations and, on the other hand, slow processes arising from the interaction with the bath.[7] In such cases, $\widetilde{\rho}(t)$ varies slowly, since it carries information about the slow processes only. This is the most significant advantage of defining and working in the interaction picture. Hence, one needs to go back to Eq. (3.39), and notice that the exponential factors $e^{i(\omega_{nm}-\omega_{rs})t}$ give rise to rapid oscillations, that do not appreciably contribute in the time scale τ_A of variation of $\widetilde{\rho}(t)$, unless $\omega_{nm} = \omega_{rs}$. The so-called rotating wave approximation (RWA) then consists of neglecting, in the r.h.s. of *both* Eqs. (3.39) and (3.43), terms with $\omega_{nm} - \omega_{rs} \gg 1/\tau_A$. Such terms are usually termed non-secular. Thus, Eq. (3.43) reduces to

$$\dot{\rho}_{nm}(t) = -i \sum_{rs}{}' \Omega_{nm,rs}\rho_{rs}(t) \ . \tag{3.44}$$

where

$$\Omega_{nm,rs} \equiv \omega_{nm}\delta_{rn}\delta_{sm} + iR_{nm,rs} \ , \tag{3.45}$$

and the sum extends over the secular terms (i.e., with $\omega_{nm} - \omega_{rs} \gg 1/\tau_A$) only.

3.4.1 Application: Non-degenerate spectra with non-equidistant levels

In what follows, we shall assume that $\omega_{nm} - \omega_{rs} \gg 1/\tau_A$ is true for all different pairs of coherences $\{n, m\}$ and $\{r, s\}$. This requires that (i) the energy levels of H_A are not equidistant i.e., $\omega_{nm} \neq \omega_{rs}$

[7] This is of course, a general consequence of the fact that V is a small perturbation compared to H_A, H_B.

for $\{n,m\}\neq\{r,s\}$ (as, for instance, in the case of the harmonic oscillator) and (ii) $\omega_{nm} \gg 1/\tau_A$ for all Bohr frequencies of H_A, i.e., we restrict to non-degenerate spectra. For these spectra, as explained below, the equation of motion for ρ as given in Eq. (3.44) above, gives rise to a decoupling between the evolution of populations and that of coherences. Furthermore, the different coherences decouple as well, i.e., evolve independently from each other. Let us consider these two sets of equations separately.

(i) Populations:

For the type of spectra discussed above, the sum in the r.h.s. of Eq. (3.44) reduces to terms for which either $\{n=m,\ r=s\}$ or $\{n=r,\ m=s\}$. This, for $n=m$, gives $\dot{\rho}_{nn} = R_{nn,nn}\rho_{nn} + \sum_{r\neq n} R_{nn,rr}\rho_{rr}$, or, using Eqs. (3.41) and (3.42)

$$\frac{d\rho_{nn}(t)}{dt} = \sum_{r\neq n} W_{rn}\rho_{rr}(t) - \sum_{r\neq n} W_{nr}\rho_{nn}(t)\ , \tag{3.46}$$

which are the Pauli Master equations for the populations, also discussed in Appendix C, starting from Fermi's Golden rule.

(ii) Coherences:

For $n\neq m$, Eq. (3.44) gives $\dot{\rho}_{nm} = (-i\omega_{nm} + R_{nm,nm})\rho_{nm}$, or, by splitting $R_{nm,nm}$ into its real and imaginary parts as $R_{nm,nm} \equiv -\gamma_{nm} - i\delta\omega_{nm}$,

$$\dot{\rho}_{nm} = -[i(\omega_{nm} + \delta\omega_{nm}) + \gamma_{nm}]\rho_{nm}\ . \tag{3.47}$$

We discuss the properties of the element $R_{nm,nm}$ in Appendix D. As shown there, $\gamma_{nm} > 0$ (see Ref.[2, 5] and Appendix D) and therefore gives rise to an irreversible decay of $\rho_{nm}(t)$, whereas $\delta\omega_{nm}$ may be interpreted as an average energy-level shift. The quantity γ_{nm} is further known as the decoherence rate.

3.5 Correlation functions of open systems: The quantum regression theorem

Our main interest in this section concerns the behavior of *equilibrium* time correlation functions of open systems. We have already given a definition for these quantities in the previous chapter, in terms of the stationary density matrix. However, as we mentioned there, that definition (Eq. (2.27)) does not take into account the fact that, even in equilibrium, the system $\mathcal{A}$ interacts *continuously* with the heat bath, and consequently certain irreversible effects become manifest. In particular, the $\delta-$functions appearing in Eq. (2.31) for the spectral densities are broadened (see Fig. 3.2).

When $\mathcal{A}$ is approaching its equilibrium state given by Eq. (3.22), the thermal averages of all relevant quantities approach their equilibrium values according to Eq. (3.5), i.e., in terms of the reduced density matrix $\rho(t)$. It turns out that a similar prescription, expressing the time correlation functions in terms of the reduced density matrix $\rho(t)$, is not as simple. Nevertheless, the relaxation matrix $\mathbf{R}$ must somehow contain all necessary information regarding the evolution of all physical quantities of $\mathcal{A}$, including time-correlation functions. Here, we will follow a very general theorem that gives the equation of motion of time correlation functions of an open system $\mathcal{A}$. This so-called quantum regression theorem accounts for both out of equilibrium as well as equilibrium time correlation functions. Although the first are often of interest as well, for our purposes we will finally concentrate on the latter ones only.

To this end, we first make the following two significant remarks. We begin by considering the expression for the time correlation function between two operators A and B of the system of interest $\mathcal{A}$, as given in Eq. (2.27) of chapter 2. This, for an open system, should be replaced with,

$$J_{A,B}(t+\tau,t) =< A(t+\tau)B(t) >= Tr\{\rho_{tot}(0)A(t+\tau)B(t)\} \ , \tag{3.48}$$

where all quantities are expressed in the Heisenberg picture. In particular, for the operators $A(t)$, one should use the total Hamiltonian of the closed system $\mathcal{A}\otimes\mathcal{B}$ instead of H_A alone, i.e.,

$$A(t) = e^{i(H_A+H_B+V)t/\hbar}A\ e^{-i(H_A+H_B+V)t/\hbar} \ . \tag{3.49}$$

It is the presence of the interaction term V, which does not commute with neither of H_A and H_B, that renders appropriate such a reconsideration of Eq. (2.27). Importantly, Eq. (3.48) is the correct description of time correlation functions in the equilibrium state as well. These functions are of our main interest here. Second, one should remark that, for the general out of equilibrium case, $S_{A,B}(t+\tau,t)$ depends on both time arguments separately, and not on their difference τ only, as for a stationary state.

The quantum regression theorem[1–4] can be summarized as follows. Suppose that one has a set of r independent quantities $\{X_i, i=1\ldots,r\}$, compactly written as a column vector $\mathbf{X}$. In addition, we assume that their thermal averages evolve according to the closed set of equations

$$\frac{d}{dt} < \mathbf{X}(t) >= \mathbf{Q}\cdot < \mathbf{X}(t) > \ , \tag{3.50}$$

where $\mathbf{Q}$ denotes a $r\times r$ matrix with time independent elements. Then the theorem asserts that for any chosen operator Y of $\mathcal{A}$, the set of time correlation functions $< \mathbf{X}(t+\tau)Y(t) >$ follows the same equation in τ, i.e.,

$$\frac{d}{d\tau} < \mathbf{X}(t+\tau)Y(t) >= \mathbf{Q}\cdot < \mathbf{X}(t+\tau)Y(t) > \ , \tau > 0. \tag{3.51}$$

More explicitly,

$$\frac{d}{d\tau} < X_i(t+\tau)Y(t) >= \sum_{ij} Q_{ij} < X_j(t+\tau)Y(t) > \ . \tag{3.52}$$

This theorem is particularly useful for finite systems with a discrete energy spectrum.[8] For such systems, we can easily find a set of operators whose thermal averages evolve according to an equation like Eq. (3.50). Consider the dyads $X_{nn'} \equiv |n' >< n|$ (notice the order of the indices n and n'). Since

$$< X_{nn'} >= Tr_A(\rho(t)|n' >< n|) = \rho_{nn'} \ , \tag{3.53}$$

and $\rho_{nn'}(t)$ evolves according to Eq. (3.44), we can employ the quantum regression theorem by just replacing i with the pair $\{n, n'\}$, i.e., X_i by $X_{nn'}$ and finally $Q_{ij} = Q_{nn',rr'}$ by $\Omega_{nn',rr'}$. In particular, by choosing Y to be $X_{mm'}$ we obtain

$$\frac{d}{d\tau} < X_{nn'}(t+\tau)X_{mm'}(t) >= -i\sum_{rr'} \Omega_{nn',rr'} < X_{rr'}(t+\tau)X_{mm'}(t) > \ , \tag{3.54}$$

which can be integrated to give

$$< X_{nn'}(t+\tau)X_{mm'}(t) >= \sum_{rr'} (e^{-i\Omega\tau})_{nn',rr'} < X_{rr'}(t)X_{mm'}(t) > \ . \tag{3.55}$$

Now, since the set of all dyads $X_{nn'}$ is complete (i.e., any operator Y can be written in terms of these) we can account for time correlation functions between any pair A and B of system operators by considering the above correlations between the X_{nm}'s only. Specifically, by writing $A = \sum_{nn'} A_{nn'}X_{nn'}$ and $B = \sum_{mm'} B_{mm'}X_{mm'}$ we obtain

$$< A(t+\tau)B(t) >= \sum_{nn',mm'} A_{nn'}B_{mm'} \sum_{rr'} (e^{-i\Omega\tau})_{nn',rr'} \ , < X_{rr'}(t)X_{mm'}(t) > \tag{3.56}$$

So far, we have talked about the general out-of-equilibrium correlation functions. The equilibrium time correlation functions $J_{A,B}(\tau)$ can be obtained from Eq. (3.56), by letting $t \gg \tau_A$, i.e., when the stationary equilibrium density state has been reached. Thus, omitting the time argument t , and adding the subscript "ss" to denote the stationary time correlation functions, we obtain

$$< A(\tau)B(0) >_{ss}= \sum_{nn',mm'} A_{nn'}B_{mm'} \sum_{rr'} (e^{-i\Omega\tau})_{nn',rr'} < X_{rr'}(0)X_{mm'}(0) >_{ss} \ . \tag{3.57}$$

We should draw attention to the fact that the zero time argument in $X_{rr'}(0)$ and $X_{mm'}(0)$ above, does not correspond to the $t = 0$ limit of the general, non-equilibrium correlation function, Eq. (3.48). As explained above we should think of $< A(\tau)B(0) >_{ss}$ as

$$< A(\tau)B(0) >_{ss} \equiv \lim_{t>>\tau_A} < A(t+\tau)B(t) >= Tr\left(\rho_{tot}(T)A(\tau)B(0)\right) \ , \tag{3.58}$$

[8] The quantum regression is also similar to the so-called Onsager's hypothesis[6–8] for the case of hydrodynamic fluctuations.

where $\rho_{tot}(T) = e^{-\beta(H_A+H_B+V)}/Z_{tot}$, denotes the equilibrium state of $\mathcal{A}\oplus\mathcal{B}$. Now, this can be approximated as $\rho_{tot} \approx \rho(T) \otimes \rho_B(T)$, i.e., we may neglect the interaction term V in the various Boltzmann factors. This is legitimate as long as V is much small than k_BT.[9] On the other hand, we should repeat here that we cannot neglect V from the time exponential factors $e^{iH_{tot}t/\hbar}$.

The above equation can be simplified by using the orthogonality of X_{nm} and the fact that $\rho(T)$ is diagonal. Specifically, one obtains

$$< X_{rr'}(0)X_{mm'}(0) >_{ss} = \rho_{mr'}(T)\delta_{m'r} = \rho_{mm}(T)\delta_{mr'}\delta_{m'r} \ , \tag{3.59}$$

which, when substituted back in Eq. (3.57), gives

$$< A(\tau)B(0) >_{ss} = \sum_{nn',mm'} A_{nn'}B_{mm'}(e^{-i\Omega\tau})_{nn',m'm}\rho_{mm}(T) \ . \tag{3.60}$$

This is the general form of the correlation between two observables A and B in the presence of the coupling with the bath, and should be contrasted with Eq. (2.30) of chapter 2. In what follows, the above expression will be greatly simplified and become more physically transparent, when applied to the special case of a non-degenerate spectra with non-equidistant energy levels.

We should note that all the above expressions assume $\tau > 0$ (in what follows, we shall not need the expression for negative τ).

3.5.1 Application: Non-degenerate spectra with non-equidistant levels

Let us return to the case of a non-degenerate spectrum with non-equidistant energy levels, discussed previously. We have seen that we can separate the equations of motion in two groups: (i) a set of Pauli master equations for the N populations ρ_{nn} and (ii) a set of N^2, independent equations for the coherences ρ_{nm}, $n \neq m$. We can thus apply the quantum regression theorem for both sets separately, as follows.

(i) Populations:

As already shown, the diagonal elements of ρ obey the set of equations

$$\dot{\rho}_{nn}(t) = -\sum_r \Lambda_{nr}\rho_{rr}(t) \ , \tag{3.61}$$

where $\Lambda_{nr} \equiv -W_{rn}$ when $n \neq r$, and $\Lambda_{nn} \equiv \sum_{r\neq n} W_{nr}$. Thus we can apply the quantum regression theorem for the closed set of N operators $\{X_{nn}\}$, and obtain

$$\frac{d}{d\tau} < X_{nn}(\tau)X_{mm'}(0) >_{ss} = -\sum_r \Lambda_{nr} < X_{rr}(\tau)X_{mm'}(0) >_{ss} \ , \tag{3.62}$$

[9] This is of course the reason that the interactions included in V cannot be manifested in one-time, equilibrium thermal averages.

which, according to Eq. (3.59), gives

$$< X_{nn}(\tau)X_{mm'}(0) >_{ss} = (e^{-\Lambda\tau})_{nm}\rho_{mm}\delta_{mm'} \ . \tag{3.63}$$

(ii) Coherences:

Since the coherences evolve independently from each other according to Eq. (3.47), we can apply the quantum regression theorem for each one of them independently. Thus, for each $n \neq n'$

$$\frac{d}{d\tau} < X_{nn'}(\tau)X_{mm'}(0) >_{ss} = [-\gamma_{nn'} - i(\omega_{nn'} + \delta\omega_{nn'})] < X_{nn'}(\tau)X_{mm'}(0) >_{ss} \ , \tag{3.64}$$

which, according to Eq. (3.59), gives

$$< X_{nn'}(\tau)X_{mm'}(0) >_{ss} = e^{-i(\omega_{nn'}+\delta\omega_{nn'})\tau}e^{-\gamma_{nn'}\tau}\rho_{mm}\delta_{mn'}\delta_{m'n} \ , \ n \neq n' \ . \tag{3.65}$$

Having at hand both types of correlation functions Eqs. (3.63) and (3.65), the general correlation between any pair of operators A and B can be written

$$\begin{aligned} < A(\tau)B(0) >_{ss} &= \sum_{nn'} A_{nn}B_{n'n'}(e^{-\Lambda\tau})_{nn'}\rho_{n'n'} \\ &+ \sum_{n\neq n'} A_{nn'}B_{n'n}e^{-i(\omega_{nn'}+\delta\omega_{nn'})\tau}e^{-\gamma_{nn'}\tau}\rho_{n'n'} \ , \end{aligned} \tag{3.66}$$

where we should repeat that $\tau > 0$. This expression should be contrasted with the one given in chapter 2, Eq. (2.30). In particular, the two expressions coincide only at time scales $\tau \ll \lambda_i^{-1}$, $\gamma_{nn'}^{-1}$ (and $\tau \ll \delta\omega_{nn'}^{-1}$). At long enough times τ the correlations show decaying oscillations, because of the influence of the bath.[10] Alternatively, since the time scale τ is set by the experiment at hand, one can indirectly observe the effects of the coupling to the bath by using an appropriate probe.[11] For magnetic molecule systems, such a probe consists of the nuclear spins in the sample. The corresponding analysis is performed in the following chapter, where we apply our present theoretical framework to account for the NMR data of the nuclear spin-lattice relaxation rate $1/T_1$.

Consider finally the spectral density $J_{A,B}(\omega)$. This, according to Eq. (2.40) of chapter 2, can be obtained once the one-sided Fourier transform $J_{A,B}^{(1)}(\omega)$ is known. The latter can be easily evaluated since we have the time correlation functions for positive τ. It is given by

$$J_{A,B}^{(1)}(\omega) = \sum_{nn'} \rho_{n'n'}A_{nn}B_{n'n'}(\frac{1}{\Lambda - i\omega})_{nn'} + \sum_{n\neq n'} \rho_{n'n'}\frac{A_{nn'}B_{n'n}}{\gamma_{nn'} - i(\omega - \omega_{nn'} - \delta\omega_{nn'})} \ . \tag{3.67}$$

[10] This is analogous to the damped harmonic oscillator problem.

[11] Such effects can only observed by dynamic probes, and not static ones (see also footnote in previous page).

By adding to this the quantity $(J^{(1)}_{B,A}(\omega))^*$ we obtain the spectral density

$$J_{A,B}(\omega) = \sum_{nn'} \rho_{n'n'} \{ A_{nn} B_{n'n'} (\frac{1}{\mathbf{\Lambda} - i\omega})_{nn'} + A_{n'n'} B_{nn} (\frac{1}{\mathbf{\Lambda} + i\omega})_{nn'} \}$$
$$+2 \sum_{n \neq n'} \rho_{n'n'} A_{nn'} B_{n'n} \frac{\gamma_{nn'}}{\gamma^2_{nn'} + (\omega - \omega_{nn'} - \delta\omega_{nn'})^2} \, . \tag{3.68}$$

This is the central equation of this section. The first sum involves only the diagonal matrix elements of the operators A and B and moreover it gives rise to Lorentzian peaks around $\omega = 0$. For this reason such terms are called elastic. The width of these elastic peaks are determined by the eigenvalues λ_i of the relaxation matrix $\mathbf{\Lambda}$. The second sum, on the other hand, involves only the non-diagonal matrix elements of A and B, and it gives rise to Lorentzian peaks centered around the characteristic Bohr frequencies $\omega_{nn'}$ of the system $\mathcal{A}$, but shifted by $\delta\omega_{nn'}$. Accordingly, the width of these inelastic peaks is determined by the decoherence rates $\gamma_{nn'}$. These general features of the various spectral density functions of open systems are demonstrated in Fig. 6.2 (b) and are compared with the $\delta-$function structure of the corresponding ones for ideally closed systems.

More generally, it should be noted, that the Lorentzian character of the spectral density stems from the assumption of Markovian dynamics, i.e., the decay with time independent rates. This in turn stems from the assumption of very short memory (or fast motion) $\tau_B \ll \tau_A$. In more general situations, where the Markovian approximation does not hold, the spectral density does not have a Lorentzian shape. For various treatments of such more general cases see for example Refs. [9–11]. For the particular case of the shape of NMR spectrum see for instance Ref. [12].

To summarize, the results of this chapter are based on a perturbative second order approach and the simultaneous conditions $\tau_B \ll \tau_A$ and $\omega_{nn'} \gg \tau_A^{-1}$, which allow for the Markovian and the rotating wave approximation, respectively. The characteristic relaxation time τ_A corresponds collectively to the various decay times λ_i^-1 and γ_{nm}^{-1}, defined above. It should be noted that the above expressions hold whether $\omega > \tau_B^{-1}$, or vice versa. For example, let us concentrate in one of the components, i.e., a given $\lambda_0 = \lambda^*$, of the elastic peak. This is generally temperature dependent and decreases with decreasing T. Then, if $\lambda_0(T^*)$ crosses an available probing frequency, say the proton Larmor frequency ω_N, at some temperature T^* (i.e., $\lambda_0(T^*) = \omega_N$), then the elastic portion of the various spectral densities $J_{A,B}(\omega_N)$ of the system will show a peak at $T = T^*$. Such a low frequency enhancement as a function of T, is observed for $1/T_1$ in a large number of magnetic molecule systems. This in turn signifies that the fluctuations related to relaxation (λ_i) in these zero-dimensional magnetic systems, slow down rapidly (as discussed in the next chapter, by a few orders of magnitude in a few decades of T) with decreasing

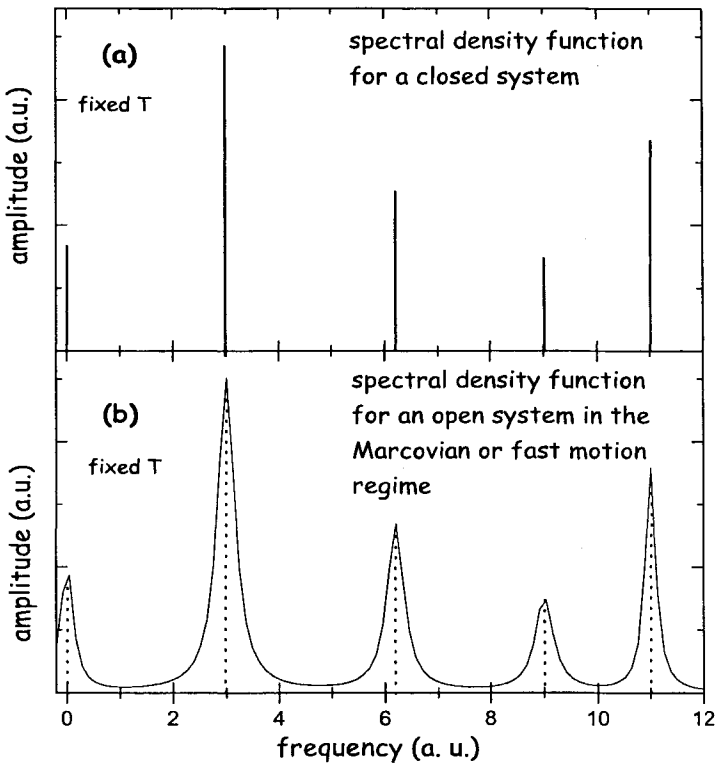

Figure 3.2 Typical structure of spectral density functions $J_{A,B}(\omega)$ of ideally closed (a) and open systems (b). Figure 6.2 (b), in particular, corresponds to the Markovian (or fast motion) limit, i.e., $\tau_B \ll \tau_A$. When interactions with a thermal bath are taken into account, the sharp $\delta-$function lines get broadened and shifted (with $\lambda_i, \gamma_{nn'}, \delta\omega_{nn'} \ll \omega_{nn'}$. The elastic peak ($\omega = 0$) corresponds to diagonal (in the energy representation) portions of the operators A and B (or whenever A and/or B is diagonal) and its width is related to the set of eigenvalues λ_i of the relaxation matrix $\mathbf{\Lambda}$ (to be more accurate, the elastic portion of the spectrum is a sum of Lorentzian peaks). On the other hand, the widths of the remaining Lorentzian peaks are related to the decoherence rates $\gamma_{nn'}$.

T, and consequently they can be seen by the low frequency NMR probes.

Finally, we should point out that there is an alternative way of deriving the results of this chapter, which makes use of the so-called projector operator technique,[7–9, 13, 14] first given by Zwanzig[15] and Mori.[16] This technique is also particularly useful for deriving the equations of motion, in the Heisenberg picture, for thermal averages of the various quantities of interest (generalized Langevin equations), rather than that of the reduced density matrix (generalized master equation).

References

[1] M. Lax, Phys. Rev. **129**, 2342 (1963); **157**, 213 (1973).

[2] C. C.-Tannoudji, J. D.-Roc, and G. Grynberg, *Atom-Photon Interactions, Basic processes and Applications* (Wiley-Interscience, New York, 1992).

[3] H. J. Carmichael, *Statistical Methods in Quantum Optics 1, Master Equations and Fokker-Planck Equations* (Springer, Berlin, 1999).

[4] H.-P. Breuer, and F. Petruccione, *The theory of Open Systems* (Oxford University Press, New York, 2002).

[5] K. Blum, *Density Matrix Theory and Applications* (Prenum Press, New York, 1996).

[6] L. Onsager, Phys. Rev. **37**, 405 (1931); **38**, 2265 (1931).

[7] D. Forster, *Hydrodynamic Fluctuations, Broken symmetry, and Correlation Functions* (W. A. Benjamin, Inc., 1975).

[8] *Microscopic Structure and Dynamics of Liquids*, edited by J. Dupuy, and A. J. Dianoux (Plenum Press, New York, 1978).

[9] E. Fick, G. Sauermann, *The Quantum Statistics of Dynamic Processes* (Springer-Verlag, Berlin, 1990).

[10] S. Dattagupta, *Relaxational Phenomena in Condensed Matter Physics* (Academic Press, Inc., 1987).

[11] R. Kubo, M. Toda, and N. Hashitsume, *Statistical Physics II, Nonequilibrium Statistical Mechanics* (Springer-Verlag, Second Edition, 1991).

[12] A. Abragam, *Principles of Nuclear Magnetism* (Clarendon Press, Oxford, 1961).

[13] H. Grabert, *Projector Operator Techniques in Nonequilibrium Statistical Mechanics*, in *Springer Tracts in Modern Physics*, vol. 95, edited by G. Hohler, and E. A. Niekisch (Springer-Verlag, Berlin, 1982).

[14] F. Haake, *Statistical Treatments of Open Systems by Generalized Master Equations*, in *Springer Tracts in Modern Physics*, vol. 66, edited by G. Hohler, and E. A. Niekisch (Springer-Verlag, Berlin, 1973).

[15] R. Zwanzig, in *Lectures in Theoretical Physics*, vol. 3 (Interscience, New York, 1961).

[16] H. Mori, Prog. Theor. Phys. (Kyoto) **34**, 423 (1965).

4. Nuclear Magnetic Resonance as a probe of spin dynamics of magnetic molecules

4.1 Introduction

Nuclear Magnetic Resonance (NMR) provides a very suitable experimental tool for probing both static and dynamic properties of magnetic systems. In particular, the measurement of the so-called nuclear spin-lattice relaxation rate $1/T_1$ gives information about the low-frequency (or long-time) behavior of the spin fluctuations.[1] For instance, the early observation[2, 3] of a strong field dependence of $1/T_1$ at high T, in one dimensional (1D) anti-ferromagnetic (AFM) linear chains has revealed a long-time persistence of the various spin-spin time correlation functions (see also Ref. [4] and references therein). In these low-dimensional, bulk systems, it has been confirmed that the characteristic decay of the above long-time "tail" of the spin correlations is related to a spin (bulk) diffusive behavior originating from various anisotropic terms present in the Hamiltonian, such as the magnetic dipolar interactions.

Since magnetic molecules are model zero-dimensional magnetic systems with a finite number of degrees of freedom and well defined discrete energy spectra, it is expected that their properties (and in particular those probed by NMR), are of distinct physical origin from those of higher dimensional systems. In particular, the long-time persistence of the spin fluctuations, which in these systems is associated with the finite number of spins and the periodic boundary conditions,[5] eventually shows a cut-off due to the interaction with the surrounding degrees of freedom, and specifically the coupling with the local deformations of the host lattice, i.e., the phonons. Remarkably, this decay is manifested in a number of experimental findings, both in the field and temperature dependence of $1/T_1$. The reason for this, as mentioned above, is that the nuclear Larmor frequency ω_L is an extremely small frequency scale, as compared with the exchange frequencies $J/\hbar$ and the electron Larmor frequency ω_e. As an example, consider $J/k_B \sim 10$ K, and $B \sim 1$ T. Taking $g_e = 2$, (and consulting the numerical values given in Appendix E) these values correspond to $J/\hbar \sim 1.3 \times 10^{12}$ s^{-1}, $\omega_e \sim 176 \times 10^9$ s^{-1}, whereas $\omega_L \sim 267 \times 10^6$ s^{-1}.

Let us discuss some of the experimental findings of $1/T_1$ in magnetic molecule systems. First, the $1/T_1$ data at high T ($k_BT \gg J$) shows a strong field dependence as in the 1D case of AFM linear chains. Since at this high-T regime the amplitude of the spin fluctuations has saturated to a constant value (corresponding to uncorrelated spins), one is able to estimate the high$-T$ limit of the cut-off frequency ω_0.

The temperature dependence of $1/T_1$ is also of great interest. Specifically, one can follow the spin dynamical behavior starting from the high-T regime, where the spins are uncorrelated, down to lower temperatures where the correlations are governed by the strong exchange interactions. Generally, and mainly for the antiferromagnetic (AFM) ring systems, it has been found that the temperature dependence of the measured $1/T_1$ resembles the behavior of the product $\chi_0 T$, where $\chi_0(T)$ denotes the zero-field magnetic susceptibility. Remarkably however, in addition to this overall behavior, and specifically for molecules consisting of ions with intrinsic spins $s > 1/2$, a systematic enhancement of $1/T_1$ at intermediate temperatures ($T \sim J/k_B$) takes place. This peak of $1/T_1$ at $T \sim J/k_B$, superimposed on the $\chi_0 T$ behavior, has been explained and reproduced[6] by using a simplified expression for $1/T_1$ in terms of a Lorentzian function which incorporates a temperature dependent cut-off frequency $\omega_0(T)$. From the fit to the data, the temperature dependence of ω_0 could be also obtained. This confirmed that $\omega_0(T)$ drops monotonically with decreasing T, intersecting ω_L at some intermediate temperature T^*. The satisfactory agreement with the data merely expresses the fact that the broadening of the magnetic energy lines is indeed of Lorentzian character, or in other words the long-time decay of the spin fluctuations is exponential. According to the previous chapter, this means that the phonon excitations of the host lattice decay in extremely short times, i.e., we are in the Markovian limit. We will use this ingredient in Sec. 4.3.

Another experimental finding, particularly for systems with a non-magnetic ground state (such as the AFM ring systems, and the $\{V_{12}\}$ studied in the following chapter), concerns the behavior of $1/T_1$ at very low T ($k_BT \ll J$), where only the lowest two states are populated. In this temperature regime, and since the contribution to the spin fluctuations from the non-magnetic ground state vanishes, $1/T_1$ becomes proportional to the population of the first excited state only. Hence, a measurement of $1/T_1$ at low enough T provides the excitation gap and thus the exchange constant J.

In addition to the above, $1/T_1$ has been a suitable tool for probing level-crossing effects,[7–10] occurring at some critical field values $B = B_c$ for which two levels of the magnetic spectrum intersect. Such a level-crossing manifests in the field dependence of $1/T_1$ at low-T, by an enhancement around $B = B_c$. Of particular experimental and theoretical interest regarding this problem is the question

of whether the crossing between the two relevant levels is a true level-crossing, or a level-anticrossing. The latter stems from the existence of small anisotropic terms in the Hamiltonian which admix the two states of interest and give rise to a level repulsion.

In this chapter, we will provide a general theoretical account of what $1/T_1$ probes in magnetic molecule systems and explain accordingly the above findings.[1] To this end, we separate our subsequent analysis in three sections. In Sec. 4.2, we discuss some general aspects of NMR in the context of magnetic molecule systems. In Sec. 4.3, we use the general results of the previous chapter, and define the quantity $1/T_1$ as the relaxation rate of the longitudinal nuclear magnetization. $1/T_1$ will be further expressed in terms of the various spectral functions of the magnetic molecule evaluated at the nuclear Larmor frequency ω_L. To this end, since $\omega_L \ll J/\hbar, \omega_e$ we will infer that to obtain a finite $1/T_1$ one needs to take into account the broadening of the various spectral lines of the spin fluctuations. The machinery for doing this has been already described in the previous chapter, for weak system-bath coupling and in the Markovian regime. Hence, in Sec. 4.4 we will apply this general formalism and express the various spectral functions of magnetic molecule systems including their interaction with the lattice degrees of freedom and specifically the phonons. We will assume that the spin-phonon coupling is weak and moreover that we are in the Markovian limit. Finally, we will further simplify the resulting expression of $1/T_1$ by using simple symmetry arguments, and then apply this expression to two different field regimes, namely for fields away from level-crossings and in the vicinity of level-crossings. Finally, we provide a summary and a general discussion in Sec. 4.5.

4.2 General aspects of NMR in the context of magnetic molecule systems

We first need to examine the various interactions relevant for NMR in the context of magnetic molecule systems. Consider the situation depicted in Fig. 4.1, with a proton ^{1}H spin ($I = 1/2$) being at a given distance from a magnetic molecule, in particular the AFM ring $\{Fe_{10}\}$. This consists of 10 Fe^{3+} (s=5/2) ions arranged in a planar geometry and interacting via AFM nearest-neighbor exchange. Furthermore, this system is very well described by the isotropic Heisenberg model with a single exchange constant J. We take the direction of the applied magnetic field as the z-axis, i.e., $\mathbf{B} = B\mathbf{z}$. For "high-field" NMR ($B \gtrsim 10^{-2}$ T), the dominant energy of the ^{1}H nuclear spin stems from the Zeeman interaction with $\mathbf{B}$, written as[2]

$$H_{NMR} = -\gamma_p \hbar \mathbf{I} \cdot \mathbf{B} = -\hbar \omega_L I_z, \tag{4.1}$$

[1] For a review of various NMR studies in a number of magnetic molecule systems, which includes apart from $1/T_1$, the NMR spectra and the spin-spin relaxation rate $1/T_2$, see Ref. [4].

[2] Here, the spin operators are taken to be dimensionless.

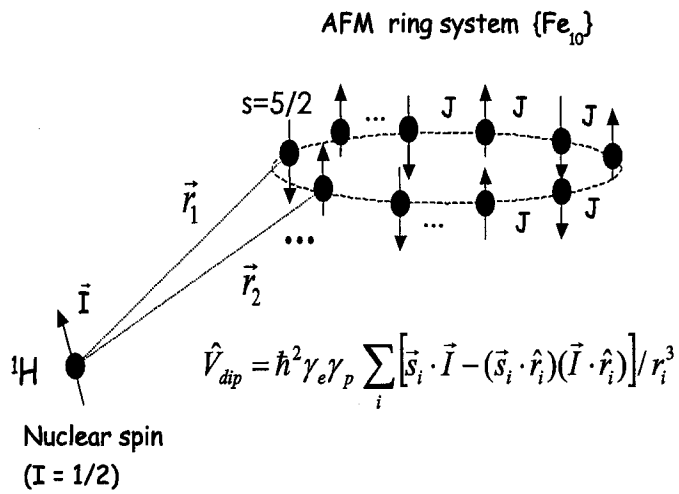

Figure 4.1 Proton (^{1}H) $1/T_1$ as a local probe of the spin dynamics of magnetic molecule systems. The figure shows the magnetic molecule $\{Fe_{10}\}$, a typical AFM ring system, comprised of 10 Fe^{3+} exchanged coupled ions, i.e., spins $s = 5/2$. The proton spin (I=1/2) interacts via the magnetic dipolar interaction with the Fe^{3+} ions.

where ω_L denotes the ^{1}H Larmor frequency $\omega_L \equiv \gamma_p B$, with γ_p denoting the corresponding gyromagnetic ratio. This is given in terms of the nuclear magneton μ_N,[3] as $\gamma_p = g_p \mu_N$, $g_p \simeq 5.586$ (see Appendix E for the numerical values of various constants). Hence, in the presence of the external field the nuclear spin states $|\pm>$ are split by $\hbar\omega_L$, with the spin-up $|+>$ state having the lowest energy (since, $\gamma_p > 0$). For a typical experimental value of $B = 1$ T, $\hbar\omega_L$ amounts to approximately 10^{-3} K (in units of Boltzmann's constant k_B). This means that, in thermal equilibrium at typical temperatures, the two spin states are almost equally populated, since

$$\frac{p_-}{p_+} = \exp(-\beta\hbar\omega_L) \approx \exp(-10^{-3}/T) \ , \tag{4.2}$$

with the temperature T taken in units of K. The equilibrium nuclear magnetization (per nuclear spin, along the z-axis), denoted M_{eq}, is given by

$$M_{eq} = \hbar\gamma_p < I_z >= \frac{1}{2}\hbar\gamma_p (p_+ - p_-) = \frac{1}{2}\hbar\gamma_p \tanh\frac{\hbar\omega_L}{2k_B T} \approx \frac{(\hbar\gamma_p)^2}{4k_B T} B \ , \tag{4.3}$$

since for nuclear spins $\beta\hbar\omega_L \ll 1$, i.e., we are always in the high temperature regime.

[3] This is defined as $\mu_N \equiv (m_e/m_p)\mu_B$, and should not be confused with the magnitude of the given, *nuclear* magnetic moment.

In addition to the external field $\mathbf{B}$, there exist, at the site of the nucleus, small fluctuating fields arising from the surrounding, lattice degrees of freedom, such as phonons, nuclear and electronic spins, etc. We shall denote these fields collectively by $\mathbf{B}_{loc}$. Hence, one should add to the Zeeman interaction, the (small) spin-bath coupling

$$H_{loc} = -\gamma_p \hbar \mathbf{I} \cdot \mathbf{B}_{loc} \ , \tag{4.4}$$

From the point of view of the nuclear spin, $\mathbf{B}_{loc}$ fluctuates in time. Its transverse components can then induce quantum-mechanical transitions between the two nuclear spin states provided energy conservation holds (see below). Without loss of generality we will assume that on the average $\mathbf{B}_{loc}$ vanishes. Importantly, the fluctuations of $\mathbf{B}_{loc}$ are equilibrium ones, since during an NMR experiment one probes the nuclear spin system only, without altering the state of its surroundings. The physical characteristics of these fluctuations are governed by the specifics of the bath Hamiltonian. For magnetic molecule systems, the dominant contribution to $\mathbf{B}_{loc}$ stems from the dipolar hyperfine interaction with the exchanged-coupled electronic spins. Hence, NMR provides information about the equilibrium fluctuations of the magnetic molecule at hand. Considering again the situation depicted in Fig. 4.1, the interaction of the proton spin with the local field created by the exchange-coupled Fe^{3+} ions can be explicitly written as

$$H_{loc} = V_{dip} = \hbar^2 \gamma_e \gamma_p \sum_i \left(\frac{\mathbf{I} \cdot \mathbf{s}_i}{r_i^3} - \frac{(\mathbf{I} \cdot \mathbf{r}_i)(\mathbf{s}_i \cdot \mathbf{r}_i)}{r_i^5} \right) \ , \tag{4.5}$$

where γ_e is the electronic gyromagnetic ratio (i.e., $\gamma_e = -g\mu_B$, with g being the electronic $g-$factor and μ_B the Bohr magneton) and $\mathbf{r}_i$ denotes the vector joining the nuclear spin with the ion at site i. Thus, by comparing Eqs. (4.4) and (4.5), one can express the various components of $\mathbf{B}_{loc}$ as

$$B_{loc}^{\alpha} = -\hbar \gamma_e \sum_i \left(\frac{1}{r_i^3} s_i^{\alpha} - \frac{\mathbf{s}_i \cdot \mathbf{r}_i}{r_i^5} r_i^{\alpha} \right) \ , \quad \alpha = \{x, y, z\}. \tag{4.6}$$

One can write the above expressions in a more compact way by introducing the second rank dipolar tensor $\mathbf{D}$, with elements

$$D_i^{\alpha\alpha'} = -\hbar \gamma_e \left(\frac{\delta^{\alpha\alpha'}}{r_i^3} - \frac{r_i^{\alpha} r_i^{\alpha'}}{r_i^5} \right) . \tag{4.7}$$

Then, one can write $\mathbf{B}_{loc} = \sum_i \mathbf{D}_i \cdot \mathbf{s}_i$, and accordingly

$$H_{loc} = -\hbar \gamma_p \sum_i \mathbf{I} \cdot \mathbf{D}_i \cdot \mathbf{s}_i \ . \tag{4.8}$$

Note that, due to the tensorial character of the hyperfine interaction, $\mathbf{B}_{loc}$ is not, in general, parallel to the electronic spins $\mathbf{s}_i$. Thus, as we show below, although only the transverse components of the fluctuations of $\mathbf{B_{loc}}$ contribute to $1/T_1$, this is not true for the fluctuations of the individual electronic moments comprising the molecule.

The hyperfine interaction Eq. (4.5) (or (4.8)) gives the dominant contribution to the NMR line width in magnetic molecule systems.[4] It also gives the dominant contribution to the relaxation rate $1/T_1$ of the longitudinal nuclear magnetization, immediately after the nuclear system has been perturbed out of equilibrium by a series of radiofrequency (rf) pulses. As we show below, $1/T_1$ is related to the relaxation of the diagonal elements of the nuclear density matrix, and is given in terms of the bath's spectral densities evaluated at the nuclear Larmor frequency. Usually, one also defines the relaxation rate (or decoherence rate) of the non-diagonal elements denoted by $1/T_2$. Although this is not of interest here (see for example Refs. [11, 12] and Appendix D) one should note that there are two distinct types of contributions to $1/T_2$. The first is, as in $1/T_1$, related to bath's spectral densities evaluated at ω_L, whereas the second is related to spectral densities evaluated at zero frequency. Then, for the analysis of $1/T_2$ one should include interactions within the nuclear spin system (which conserve the total energy of all nuclei together), such as their mutual magnetic dipolar couplings. For this reason, $1/T_2$ is usually called spin-spin relaxation rate, in contrast to $1/T_1$ which is related to exchange of energy with the lattice (spin-lattice relaxation rate). Typically, $T_2 \gtrsim 10$ μs whereas $T_1 \sim 1$ ms.

4.3 Nuclear spin-lattice relaxation rate $1/T_1$

We will now define $1/T_1$ and also derive a general expression which gives expresses quantity in terms of the various equilibrium spin-spin correlation functions of the magnetic molecule. We will again consider the simple case depicted in Fig. 4.1, but now we will include the interaction of the exchanged coupled moments with the phonons. The situation is now the one shown in Fig. 4.2. In addition, we shall restrict to the case of non-degenerate magnetic energy spectrum, for which we may apply the simple formalism presented in the previous chapter. We should keep in mind however that this is not generally the case in magnetic molecule systems, since they do have additional degeneracies other than the Zeeman one. A more careful analysis is required for the effects related to these degeneracies.

We start by applying the general results of chapter 3 for the diagonal elements of the nuclear density matrix. We only need to recognize that, as Fig. 4.2 implies, the system of interest ($\mathcal{A}$) is the nuclear spin whereas the bath consists of the magnetic molecule system together with the phonon degrees of freedom with which it interacts. Moreover, the role of the operators A^q and B^q of chapter 3 is now played by $-\gamma_p I^\alpha$ and B^α_{loc}, respectively (compare Eq. (3.21) with Eq. (4.4)). We shall only be concerned with the recovery of the longitudinal nuclear magnetization $M(t)$ at $t \geq 0$, immediately after the system has been perturbed out of equilibrium by a series of rf pulses, which result in $M(t=0) = 0$.[11, 12]

[4] The residual portion arising from nuclear-nuclear dipolar interactions is much smaller (by a factor of $\gamma_p/\gamma_e \sim 10^{-3}$).

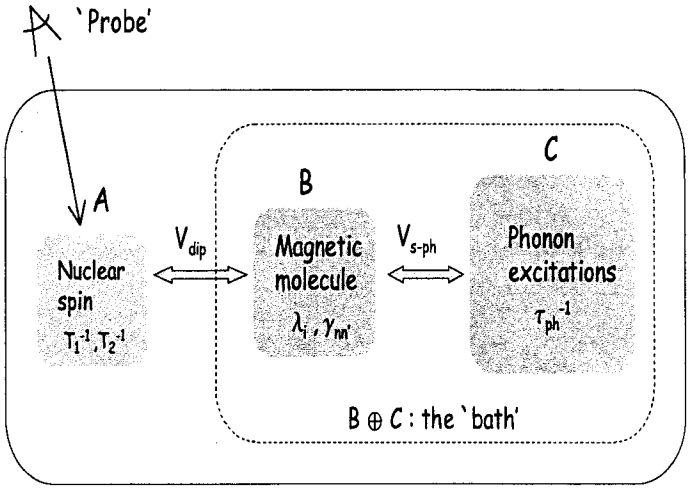

Figure 4.2 NMR applied to magnetic molecule systems. Since the molecules comprises a finite number of exchanged coupled electronic moments their spectra consist of a finite number of discrete energy states. Then, to account for the nuclear spin-lattice relaxation rate $1/T_1$ one needs to include the broadening of these levels and therefore the interaction of the electronic moments with the surroundings degrees of freedom e.g., phonons.

The recovery to M_{eq}, under certain conditions (discussed in the previous chapter and in Appendix C) proceeds with a constant rate denoted by $1/T_1$.[5] The first of these conditions (Markov approximation) requires that the characteristic relaxation times τ_s of the molecule ($\mathcal{B}$) are much shorter than T_1. As we are going to see, this condition is indeed fulfilled. The second condition (RWA) requires that $\omega_L \gg T_1^{-1}$ which is always satisfied in NMR, since typically $\omega_L \sim 10^8$ s^{-1} whereas $T_1 \sim 1$ ms.[6]

We begin with the Pauli master equations for the populations p_- and p_+ of the spin-down $|- >$ and spin-up $|+ >$ nuclear spin states, which read

$$\dot{p_-} = W_{+-}p_+ - W_{-+}p_- = -\dot{p_+} \ , \tag{4.9}$$

where $W_{-+} \equiv W_{-\rightarrow+}$ denotes the quantum-mechanical transition rate from the spin-down state $|- >$ to the spin-up state $|+ >$, and similarly for W_{+-}. Below, we shall give explicit expressions for W_{-+} and W_{+-} in terms of the various spectral densities of the magnetic molecule. Let us consider the evolution

[5] One should notice however that since there are many non-equivalent protons inside each molecular unit, the measured longitudinal magnetization is the sum of the individual ones, each of which proceeds with a different $1/T_1$, owing to the different distances, etc. Thus, the measured magnetization appears to be non-exponential. In this case, an average $1/T_1$ can be obtained by taking the initial slope of the measured $\ln(1 - M(t)/M_{eq})$.

[6] Similar conditions will be assumed below for the coupling between $\mathcal{B}$ and $\mathcal{C}$.

of the longitudinal magnetization (per nuclear spin) $M = \hbar\gamma_p(p_+ - p_-)/2$. Using Eq. (4.9) and the normalization condition, $p_- + p_+ = 1$, one obtains

$$\begin{aligned}\dot{M} &= \frac{\hbar\gamma_p}{2}(W_{-+} - W_{+-}) - (W_{-+} + W_{+-})M \\ &= (W_{-+} + W_{+-})\left(\frac{\hbar\gamma_p}{2}\frac{W_{-+} - W_{+-}}{W_{-+} + W_{+-}} - M\right) ,\end{aligned} \tag{4.10}$$

which, when using the detailed balance condition $W_{+-}/W_{-+} = e^{-\beta\hbar\omega_L}$, becomes

$$\dot{M} = \frac{1}{T_1}(M_{eq} - M) , \tag{4.11}$$

where $1/T_1 \equiv W_{-+} + W_{+-}$ and M_{eq} denotes the equilibrium magnetization at temperature T given by Eq. (4.3). Equation (4.11) is the well-known Bloch equation.[11–13] Physically, this equation says that, starting from a non-equilibrium state (i.e., $M(t=0) \neq M_{eq}$), $M(t)$ will subsequently relax back to its equilibrium value M_{eq} with a constant rate $1/T_1$. Thus, $1/T_1$ denotes the relaxation rate of the longitudinal nuclear magnetization.

Let us now give some explicit expressions for the transition rates and consequently $1/T_1$. According to Eqs. (3.42) of chapter 3, the emission rate W_{-+} is given by

$$W_{-+} = \gamma_p^2 \sum_{\alpha\alpha'} I^{\alpha}_{-+} I^{\alpha'}_{+-} J_{\alpha\alpha'}(\omega_L) , \tag{4.12}$$

with the spectral densities $J_{\alpha\alpha'}$ defined by

$$J_{\alpha\alpha'}(\omega_L) = \int_{-\infty}^{+\infty} dt\; e^{i\omega_L t} < \widetilde{B}^{\alpha}_{loc}(t)\widetilde{B}^{\alpha'}_{loc}(0) >_B \; . \tag{4.13}$$

Since the matrix element I^{α}_{-+} vanishes for $\alpha = z$, only the transverse $(\alpha, \alpha' = x, y)$ components of $\mathbf{B}_{loc}$ contribute in Eq. (4.12). This is expected since the longitudinal component of $\mathbf{B}_{loc}$ cannot induce transitions between the two nuclear spin states $|+>$ and $|->$.[7] The absorption rate W_{+-} is given in terms of W_{-+} according to the detailed balance condition, which, since $\beta\hbar\omega_L \ll 1$, reduces to

$$W_{+-} = e^{-\beta\hbar\omega_L} W_{-+} \simeq W_{-+} , \tag{4.14}$$

and consequently, $1/T_1 = (1 + e^{-\beta\hbar\omega_L})W_{-+} \simeq 2W_{-+}$. Thus, finally we arrive at

$$\frac{1}{T_1} = \sum_{ij,\alpha\alpha'} C^{\alpha\alpha'}_{ij} J_{s^{\alpha}_i s^{\alpha'}_j}(\omega_L) , \tag{4.15}$$

where $J_{s^{\alpha}_i s^{\alpha'}_j}(\omega_L)$ is the spectral density corresponding to the pair of electronic spin operators s^{α}_i and $s^{\alpha'}_j$, and $C^{\alpha\alpha'}_{ij} \equiv 2\gamma_p^2 \sum_{\zeta\zeta'} I^{\zeta}_{-+} I^{\zeta'}_{+-} D^{\zeta\alpha}_i D^{\zeta'\alpha'}_j$. The order of magnitude of the elements $C^{\alpha\alpha'}_{ij}$ is $(\hbar\gamma_e\gamma_p)^2/r^6$, with r denoting an average of r_i.

[7] Nevertheless, the longitudinal component of $\mathbf{B}_{loc}$ contributes to the spin-spin relaxation rate $1/T_2$.

Equation (4.15) is our final expression for $1/T_1$. A number of comments of physical importance are in place here, regarding this expression. First of all, written in this way, $1/T_1$ is given in terms of two quantities of distinct physical character, namely the geometrical coefficients $C_{ij}^{\alpha\alpha'}$ and the spectral functions $J_{s_i^\alpha s_j^{\alpha'}}(\omega_L)$. The first contains all detailed geometrical information about the distances and the various angles of the protons with respect to the electronic spin sites. The need for such a detailed information is, in most cases, unnecessary, since within each molecular unit, there is a large number of protons (typically of order ~ 100) that are inequivalent (i.e., with different values of $C_{ij}^{\alpha\alpha'}$ each), and as a result the measured $1/T_1$ corresponds to an average over all different $1/T_1$'s (see footnote 5). Thus one is only interested in an average $C_{ij}^{\alpha\alpha'}$. On the other hand, the most physically significant ingredient of Eq. (4.15) is the spectral functions $J_{s_i^\alpha s_j^{\alpha'}}(\omega_L)$: These contain information that is solely related to the spin dynamics of the magnetic molecule.

A second remark is that in Eq. (4.15) there are generally contributions from both auto ($i = j$) and pair ($i \neq j$) correlation functions, as well as from both longitudinal ($\alpha = \alpha' = z$) and purely transverse terms (i.e., $\alpha, \alpha' = x, y$). Terms with $\alpha = z$ and $\alpha' = \{x, y\}$ do not appear in isotropic Hamiltonians (see below).

We should also make the following technical remark. In accordance to a comment made in the previous chapter (just before Eq. (3.35)), and for consistency reasons, the various spin operators s_i^α appearing in the expression for the spectral functions $J_{s_i^\alpha s_j^{\alpha'}}(\omega_L)$ should be replaced by their fluctuating part only, i.e., $\delta s_i^\alpha \equiv s_i^\alpha - < s_i^\alpha >_B$.

Perhaps the most important ingredient of Eq. (4.15) however, is that the various spectral functions must be evaluated at the resonant frequency ω_L. This is an immediate consequence of conservation of energy for the total nuclear spin plus bath system. In other words, from the entire frequency spectrum of the local field fluctuations only the resonant part ($\omega = \omega_L$) can induce transitions among the nuclear spin states and thus contribute to $1/T_1$. This physically intuitive condition is a very significant one when applied to magnetic molecule systems. Consider for instance, a magnetic molecule which can be described by the isotropic Heisenberg model, such the AFM ring system $\{Fe_{10}\}$, shown in Fig. 4.1. The energy excitations of such a system take the typical values $0, \pm J, \pm(J \pm \hbar\omega_e), \pm\hbar\omega_e, \pm 2J$, etc. This can be schematically seen in Fig. 4.3 which shows only the lowest energy levels of $\{Fe_{10}\}$. These are a non-magnetic $S = 0$ ground state, and a magnetic $S = 1$ triplet state with energy excitation $E = J$ (for $B = 0$). In the presence of a finite magnetic field B, the 3−fold Zeeman degeneracy of the latter splits as illustrated in Fig. 4.3. In particular, the $M = -1$ component (or $|1, -1>$) of the triplet state intersects the $|0, 0>$ state at the level-crossing field $B_c \equiv J/(g\mu_B)$. Now, since typically $J \sim$ few tens

of Kelvin, i.e., much larger than $\hbar\omega_L$, the only spectral lines close to $\hbar\omega_L$ are the one at zero frequency and the ones corresponding to level-crossings, for example, when $J - \hbar\omega_e$ (assuming $J > 0$) approaches zero (see Fig. 4.4). For both cases however, in order to obtain a finite contribution to $1/T_1$ one has to take into account the broadening of these spectra lines (see Fig. 4.4). This broadening arises from the interaction of the electronic spins with the phonons. Qualitatively, one can account for this effect by simply introducing by hand a single frequency cut-off (ω_0) in the expression for the spectral functions. Such an approach is often followed in the literature, and is the one taken also in the next chapter, for the analysis of $1/T_1$ data for the magnetic molecule $\{V_{12}\}$. Nevertheless, this is only an empirical approach and does not give more in depth information regarding for instance the origin of ω_0 or the conditions under which this approach applies.

In what follows, we apply the general formalism of the previous chapter and write down the explicit form of the various spectral densities of magnetic molecule systems when considered as open systems. We will then employ a number of simple arguments (some of which have been mentioned above) and provide simplified expressions for $1/T_1$. Our analysis will provide further insight to a number of issues that are currently of interest in the literature. In particular, we shall discuss (i) why the overall temperature dependence of $1/T_1$ seems to be that of the product $\chi_0 T$; (ii) the origin of the peak of $1/T_1$ at intermediate temperatures; (iii) how the low$-T$ behavior of $1/T_1$ can provide the first excitation gap and thus the exchange constant J; (iv) how the field dependence of $1/T_1$ at low$-T$ can reveal level-crossings in the magnetic energy spectrum; and finally (v) we will discuss the field dependence of $1/T_1$ at room temperatures.

4.4 Spectral functions of magnetic molecules regarded as open systems

We consider the case of the isotropic Heisenberg model with eigenstates of well defined total spin and magnetic quantum number M. We shall denote these states by $|\kappa SM>$, where κ denotes additional quantum numbers. In addition, as mentioned before, we shall assume a non-degenerate spectrum.

We start by examining the various matrix elements appearing in the expressions for the spectral functions (see Eq. (3.68) of previous chapter), and in particular the selection rules arising from the symmetries of the spin Hamiltonian. First, since the Hamiltonian commutes with both the total $\mathbf{S}^2$ and S^z, one obtains, using the Wigner-Eckart theorem (see for instance Ref. [14]), that $< \kappa SM|s_i^z|\kappa' S'M' >= 0$, unless $\Delta S = S' - S = 0, \pm 1$ and $\Delta M = M' - M = 0$, whereas $< \kappa SM|s_i^{x,y}|\kappa' S'M' >= 0$, unless $\Delta S = 0, \pm 1$ and $\Delta M = \pm 1$. Then, one can simplify the general expression Eq. (3.68) of the previous chapter by noting that $J_{s_i^z s_j^\alpha} = 0$, for $\alpha = x, y$. The only non-vanishing spectral functions are then the

longitudinal and the purely transverse ones, i.e.,

$$J_{s_i^z s_j^z}(\omega_L) = \sum_{nn'} \rho_{n'n'} \Big\{ (s_i^z)_{nn} (s_j^z)_{n'n'} \Big(\frac{1}{\mathbf{\Lambda} - i\omega_L} \Big)_{nn'} + (s_i^z)_{n'n'} (s_j^z)_{nn} \Big(\frac{1}{\mathbf{\Lambda} + i\omega_L} \Big)_{nn'} \Big\} \ , \tag{4.16}$$

and

$$J_{s_i^\alpha s_j^{\alpha'}}(\omega_L) = 2 \sum_{n \neq n'} \rho_{n'n'} (s_i^\alpha)_{nn'} (s_j^{\alpha'})_{n'n} \ \frac{\gamma_{nn'}}{\gamma_{nn'}^2 + (\omega_L - \omega_{nn'} - \delta\omega_{nn'})^2} \ , \quad \alpha, \alpha' = x, y \ . \tag{4.17}$$

respectively. The relaxation matrix $\mathbf{\Lambda}$ as well as the various decoherence rates $\gamma_{nn'}$ and energy shifts $\delta\omega_{nn'}$ appearing in these expressions, have been defined in the previous chapter. Their origin is the interaction of the magnetic molecule with the phonon degrees of freedom. We should repeat here that the above expressions hold provided the RWA and Markov approximations are justified. This is indeed the case here, since the intrinsic relaxation rate τ_{ph}^{-1} of phonons is typically extremely fast (compared, for instance, with the eigenvalues λ_i of $\mathbf{\Lambda}$).

Apart from the spin rotations, there exist additional symmetry operations related with the arrangement of the electronic moments in space. Such a case can be found in AFM ring systems where the spin Hamiltonian is invariant with respect to all spin permutations $i \leftrightarrow j$. Using this symmetry one can show the relations $(s_i^z)_{nn} = S_{nn}^z/N$, which when replaced in Eq. (4.16) give the simplified expression

$$\begin{aligned} J_{s_i^z s_j^z}(\omega_L) = \frac{1}{N^2} J_{S^z S^z}(\omega_L) &= \frac{1}{N^2} \sum_{nn'} \rho_{n'n'} S_{nn}^z S_{n'n'}^z 2Re \Big(\frac{1}{\mathbf{\Lambda} - i\omega_L} \Big)_{nn'} \\ &= \frac{2}{N^2} Re \ < S^z \frac{1}{\mathbf{\Lambda}^T - i\omega_L} S^z > \ , \end{aligned} \tag{4.18}$$

where we have introduced the transpose matrix of $\mathbf{\Lambda}$, denoted by $\mathbf{\Lambda}^T$. Hence, for all systems with the above permutation symmetry, $1/T_1$ reduces to

$$\frac{1}{T_1} = \Big(\frac{1}{N^2} \sum_{ij} C_{ij}^{zz} \Big) J_{S^z S^z}(\omega_L) + \sum_{ij} \sum_{\alpha\alpha' \neq z} C_{ij}^{\alpha\alpha'} J_{s_i^\alpha s_j^{\alpha'}}(\omega_L) \ . \tag{4.19}$$

Let us consider this expression in the following limiting cases.

4.4.1 Away from level-crossings

We first consider the case when the external magnetic field is such that we are not close enough to any level-crossing such as the one shown in Fig. 4.3. For this situation we note that all excitation energies $\omega_{nn'}$ (such as J, ω_e, etc.) are much larger than ω_L, and moreover we expect $\gamma_{nn'}, \delta\omega_{nn'} \ll \omega_{nn'}$ (otherwise perturbation theory is not applicable). Thus the second term of Eq. (4.19) reduces to a sum of terms proportional to

$$\frac{\gamma_{nn'}}{\gamma_{nn'}^2 + \omega_{nn'}^2} \ , \tag{4.20}$$

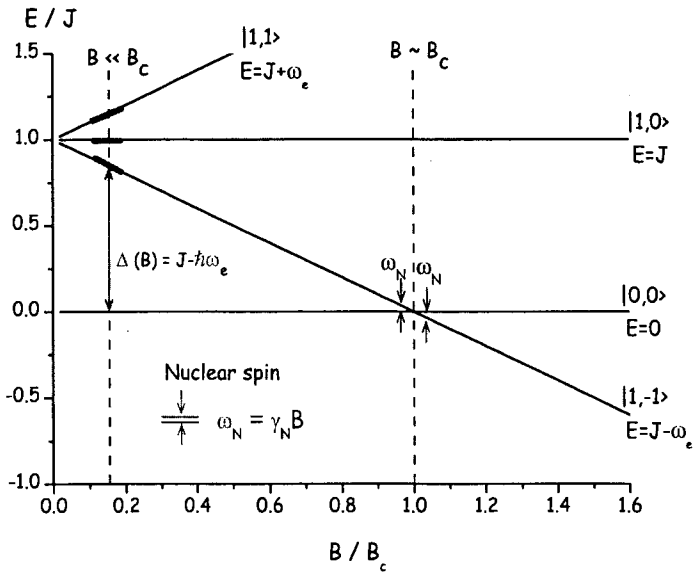

Figure 4.3 Low energy diagram for AFM ring systems and other related molecules such as $\{V_{12}\}$. The lowest states (denoted by $|S, M>$) consist of a non-magnetic $|0,0>$ ground state ($E = 0$) and a triplet $|1, M>$ with the magnetic quantum numbers $M = -1, 0, 1$ and energies $J - \hbar\omega_e$, J and $J + \hbar\omega_e$, respectively. The lowest level-crossing between $|1> \equiv |0,0>$ and $|2> \equiv |1,-1>$ takes place at $B = B_c \equiv J/(g\mu_B)$. In the figure we indicate two regimes of interest, namely (a) when $B \ll B_c$ and (b) when $B \sim B_c$. In the first case, $1/T_1$ gives information about the broadening of the excited levels according to Eq. (4.27). On the other hand, when $B \sim B_c$ a resonance condition occurs between the nuclear spin system and the magnetic molecule as a whole. This manifests in the field dependence of $1/T_1$ (as given by Eq. (4.33)) as an enhancement of $1/T_1$ at $B = B_c$. The width of this peak is determined by the decoherence rate γ_{12}, mainly determined by intra- and intermolecular dipolar as well as hyperfine interactions.

which is negligibly small, as compared to the first term of Eq. (4.19), since $\gamma_{nn'} \ll \omega_{nn'}$. Hence, in this case, $1/T_1$ is dominated by the first term of Eq. (4.19), which in turn, according to Eq. (4.18), is proportional to the spectral density of the total magnetic moment S_z, i.e.,

$$\frac{1}{T_1} = A \int_{-\infty}^{+\infty} dt\ e^{i\omega_L t} < \delta S^z(t)\delta S^z(0) > \\ = 2A\ Re < S^z \frac{1}{\mathbf{\Lambda}^T - i\omega_L} S^z > \ , \tag{4.21}$$

where $A \equiv \sum_{ij} C^{zz}_{ij}/N^2$.

The following remarks are in place here. First, the above expression gives rise to a sum of Lorentzian lines, all centered around $\omega = 0$, with their widths being equal to the various eigenvalues $\{\lambda_i\}$ of $\mathbf{\Lambda}$. For the total magnetic moment fluctuations $< \delta S^z(t)\delta S^z(0) >$ this corresponds to a sum of exponentially decaying functions of the form $e^{-\lambda_i t}$. Hence, the decay of $< \delta S^z(t)\delta S^z(0) >$ is not a single exponential, as the experiment shows.

Clearly, one possibility for the appearance of a single exponential decay is that only one of the eigenvalues of $\mathbf{\Lambda}$ is in the regime of ω_L and therefore will essentially contribute to $1/T_1$. Equivalently, in the corresponding long-time regime the fluctuations appear to decay with a single exponential. Such an explanation has been given in the numerical work reported in Ref. [15], which is based on numerically diagonalizing $\mathbf{\Lambda}$, as obtained from a specific spin-phonon coupling model and considering one-phonon processes only.

Here, we briefly comment on another possibility, which is the subject of a current investigation. In principle, Eq. (4.21) can be reduced to one Lorentzian only, if the column vector $\mathbf{y}$, whose entries y_n are given by $y_n \equiv S^z_{nn}$ is itself an eigenvector of $\mathbf{\Lambda}$. Going back to the quantum regression theorem of the previous chapter, this would be equivalent with saying that the total magnetic moment $< S^z(t) >$ relaxes independently from any other (independent) operator. Let us demonstrate this statement by writing down the equation of motion for $< S^z(t) >$,

$$\frac{d}{dt} < S^z(t) > = \sum_n (S^z)_{nn}\dot{\rho}_{nn}(t) = -\sum_n (S^z)_{nn}\Lambda_{nr}\rho_{rr}(t)\ . \tag{4.22}$$

where the second equality follows from Eq. (3.61) of the previous chapter. If the vector y (defined by $y_n \equiv (S^z)_{nn}$) is an eigenvector of Λ with eigenvalue λ^*, then

$$\frac{d}{dt} < S^z(t) > = -\lambda^* < S^z(t) > \ , \tag{4.23}$$

i.e., $< S^z(t) >$ relaxes independently from the remaining operators (modes).

For our subsequent discussion, we will put aside the above remarks and for simplicity we will replace the set of $\{\lambda_i\}$ by an average decay rate denoted by ω_0. In other words, we approximate

$$< \delta S^z(t)\delta S^z(0) > \simeq < (\delta S^z)^2 > e^{-\omega_0 t} , \tag{4.24}$$

which, according to Eq. (4.21), gives

$$\frac{1}{T_1} = 2A < (\delta S^z)^2 > \frac{\omega_0}{\omega_0^2 + \omega_L^2} . \tag{4.25}$$

The quantity $< (\delta S^z)^2 > \equiv < (S^z)^2 > - < S^z >^2$, denotes the static thermal average of the spin fluctuations in the presence of the field, and is related to the differential susceptibility $\chi(B,T)$ as we discuss in Appendix B. Specifically,

$$\chi(B,T) \equiv \frac{\partial}{\partial B} < M_z > = \frac{(g\mu_B)^2}{k_B T} < (\delta S^z)^2 > . \tag{4.26}$$

$\chi(B,T)$ reduces to $\chi_0(T)$ at low enough fields and high enough T (according to the definition of χ_0). This is a good approximation for molecules with an $S = 0$ ground state and large excitation gap J (such as the AFM rigs, and the magnetic molecule $\{V_{12}\}$ studied in the next chapter) for $B \ll B_c \equiv J/(g\mu_B)$, and not very low T. On the other hand, in molecules with a magnetic ($S \neq 0$) ground state and small energy excitations (such as $\{V_{15}\}$,[16]) replacing $\chi(B,T)$ by $\chi_0(T)$ is not generally a good approximation.

Using Eq. (4.26) and defining $\chi_{mole}(B,T) \equiv N_A \chi(B,T)$ (N_A = Avogadro's number), we finally obtain

$$\frac{1}{T_1} = \frac{2Ak_B}{N_A \hbar^2 \gamma_e^2} \left(\chi_{mole}(B,T)\ T\right) \frac{\omega_0}{\omega_0^2 + \omega_L^2} . \tag{4.27}$$

According to this relation, the temperature and field behavior of $1/T_1$ depends on whether the frequency cut-off ω_0 is temperature and/or field dependent. In what follows we discuss several situations.

(i) *T and B independent ω_0*

If the decay rate ω_0 is T and B independent, then

$$\frac{1}{T_1} \propto \chi(B,T)\ T\ \frac{B_0}{B_0^2 + B^2}, \tag{4.28}$$

where $B_0 \equiv \omega_0/\gamma_p$. Thus for a fixed field, the $T-$dependence of $1/T_1$ is solely determined by $\chi(B,T)T$ (or $\chi_0(T)T$). More specifically, since the contribution to $\chi(B,T)T$ from the ground state is zero (since it is non-magnetic ($S = 0$)), at sufficiently low T ($T \ll J/k_B$) the only contribution to $1/T_1$ arises from the first excited state $|1,-1>$, which carries a Boltzmann factor $e^{-\beta\Delta(B)}$, where $\Delta(B) \equiv J - \hbar\omega_e$, denotes the first excitation energy (see Fig. 4.3). Hence, for $T \ll J/k_B$,

$$\frac{1}{T_1} \propto \frac{B_0}{B_0^2 + B^2}\ e^{-\beta\Delta(B)} . \tag{4.29}$$

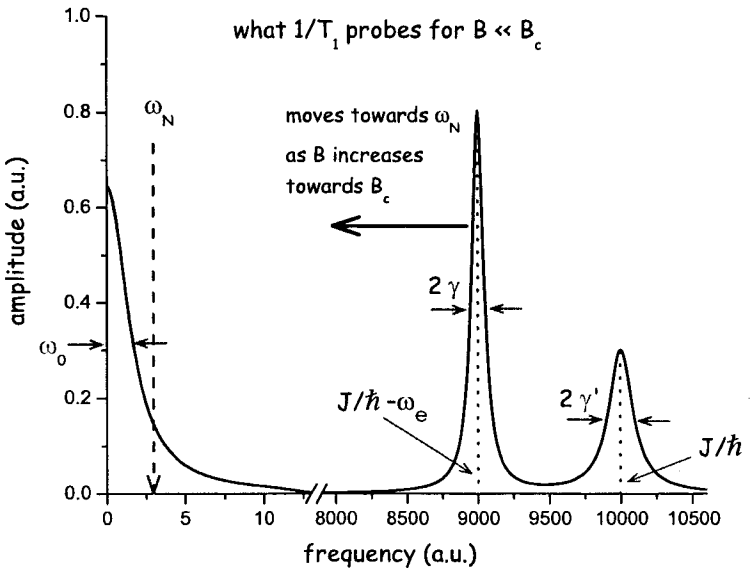

Figure 4.4 Low frequency portion of the spectral density function of magnetic molecules (such as the AFM ring systems) with the low energy spectra shown in Fig. 4.3. This consists of the elastic line centered around $\omega = 0$ and the lines at J and $J - \hbar\omega_e$. The width of the elastic line (denoted by $2\omega_0$) is related to thermal relaxation processes whereas the widths of the remaining, finite energy lines (here denoted by 2γ, $2\gamma'$) are related with the decay of the corresponding coherences. Now, the proton ^{1}H $1/T_1$ probes at $\omega = \omega_L$, i.e., at a very low frequency of the spin fluctuation spectrum. At $B \ll B_c$, only the elastic broadened line contributes to $1/T_1$, since $J - \hbar\omega_e, J \gg \hbar\omega_L$. Accordingly $1/T_1$ is given by Eq. (4.27). The height of this Lorentzian (here shown in arb. units) is proportional to $\chi(B,T)T$. As the magnetic field increases, the line at $J - \hbar\omega_e$ moves towards $\hbar\omega_L$ (which moves to the right, but very little compared to the line $J - \hbar\omega_e$, since $\gamma_p/\gamma_e \sim 10^{-3}$). Then, when B approaches B_c close enough an additional finite contribution to $1/T_1$ arises from a resonance between $J - \hbar\omega_e$ and $\hbar\omega_L$. Accordingly, for fields close to level-crossings one must add to Eq. (4.27) a term proportional to Eq. (4.33). More generally, the figure also demonstrates the significance of including the broadening effects for finite systems with discrete energy spectra.

This expression can be used to obtain the excitation gap $\Delta(B)$ for a given field B, and consequently the exchange constant J (see next chapter). On the other hand, at high enough temperatures ($k_BT \gg J$) where $\chi(B,T)T$ saturates to a constant value,[8] $1/T_1$ is determined by the Lorentzian factor only, i.e.,

$$\frac{1}{T_1} \propto \frac{B_0}{B_0^2 + B^2} , \tag{4.30}$$

which can be used to obtain the value of ω_0 (see next chapter).

(ii) *$T-$dependent, but $B-$independent ω_0*

Here we will assume that ω_0 is $T-$dependent, but $B-$independent. In addition, we assume that $\omega_0(T)$ is an increasing function of T, and specifically it crosses the value ω_L at some intermediate temperature T^*. For a fixed field, $1/T_1$ is given by

$$\frac{1}{T_1} \propto \left(\chi(B,T)\, T\right) \frac{\omega_0(T)}{\omega_0^2(T) + \omega_L^2} . \tag{4.31}$$

This expression can be conveniently rewritten in terms of the quantity R defined as

$$R(T) \equiv \frac{T_1^{-1}}{\left(\chi(B,T)\, T\right)} \propto \frac{\omega_0(T)}{\omega_0^2(T) + \omega_L^2} . \tag{4.32}$$

According to this expression, the quantity R shows a peak at $T = T^*$, since by hypothesis $\omega(T^*) = \omega_L$. The value of R at the peak position goes like $\sim 1/B$. In addition, when one increases the field the condition $\omega_0(T^*) = \omega_L = \gamma_p B$ is satisfied at higher T^*, since by hypothesis $\omega_0(T)$ is an increasing function of T. Thus, according to Eq. (4.32), when one increases the field, the height of the peak of R decreases (like $\sim 1/B$) and its position T^* shifts to higher T. Equations (4.31) and (4.32) can be used in order to determine the temperature dependence of $\omega_0(T)$ by simply comparing the experimental data for R (using the $1/T_1$ data and $\chi_0(T)$ instead of $\chi(B,T)$) with the Lorentzian appearing in the r.h.s. of Eq. (4.32). An analysis based on these lines has in fact been performed in Ref. [6] and is in excellent agreement with experimental data for a number of different AFM rings. The obtained temperature dependence of ω_0 seems to follow a power law $\omega_0 \propto T^n$, with $n \sim 3.5$. A first-principles justification of this temperature dependence is currently lacking.

4.4.2 Level-crossing effects

When B is in the vicinity of $B_c \equiv J/(g\mu_B)$, the contribution from the second term of Eq. (4.19) cannot be neglected as before (i.e., for $B \ll B_c$), since in the denominator of the Lorentzian

$$\frac{\gamma_{nn'}}{\gamma_{nn'}^2 + \left(\omega_L - (J/\hbar - \omega_e)\right)^2} , \tag{4.33}$$

[8] At high enough T ($k_BT \gg J$) all Boltzmann factors for the various populations become equal to $1/\mathcal{N}$, where $\mathcal{N}$ is the dimensionality of the Hilbert space.

(see Eq. (4.20)) the difference $\omega_L - (J/\hbar - \omega_e)$ can now be as close as possible to the small number $\gamma_{nn'}$ (see Fig. 4.4). Hence, $1/T_1$ in addition to the term of Eq. (4.27), it has also an inelastic contribution which is proportional to Eq. (4.33). The latter term, in contrast to the first, is very sensitive to field changes around the level crossing field B_c. In particular, at low T, $1/T_1$ as a function of field shows an enhancement at $J/\hbar - \omega_e = \omega_L$, i.e., at $B = J/(\hbar\gamma_e + \hbar\gamma_p) \simeq B_c$. The width of this peak is determined by the decoherence rate $\gamma_{nn'}$.[9] Such an enhancement has indeed been observed experimentally,[7–10] and is, according to the above, a direct manifestation of energy conservation. The above analysis must be corrected accordingly in order to take into account level-anticrossing effects, i.e., when small anisotropic terms in the spin Hamiltonian couple the two energy levels of interest thus giving rise to a level-repulsion (see Ref. [4], and references therein).

4.5 Summary and open issues

In this chapter we provided a general account of a number of issues associated with the behavior of the nuclear spin-lattice relaxation rate $1/T_1$ in magnetic molecule systems. One of the main physical ingredients in this study has been the understanding from the very beginning that due to the discrete character of the magnetic energy spectra of these systems one needs to take into account the broadening effects associated with the interaction of the exchanged coupled electronic moments with the phonon degrees of freedom. In addition, since $1/T_1$ probes the spin fluctuations at a very low frequency (ω_L) (as compared with the spectrum excitations), this broadening enters explicitly in the expression for $1/T_1$. On the other hand, the experiment suggests that this broadening is of Markovian character, i.e., the characteristic phonon excitations decay much faster than $1/T_1$, thus giving rise to an exponential decay of the spin fluctuations.

More specifically, we have employed the general theoretical framework developed in chapter 3 in order to include the spin-phonon interactions in deriving microscopic expressions for $1/T_1$, in terms of the relaxation matrix $\mathbf{\Lambda}$ and the various decoherence rates $\gamma_{nn'}$ and energy shifts $\delta\omega_{nn'}$ for the magnetic molecule systems. The general expression Eq. (4.15) can be further simplified by employing a number of simple symmetry arguments and considering several specific cases. In particular, we arrived at Eq. (4.27) valid for AFM ring systems at fields away from level-crossings and demonstrated both the $\chi_0 T$ factor and the Lorentzian broadening first used in Ref. [6] and subsequently discussed on a numerical basis in Ref. [15]. We also demonstrated how the measurement of $1/T_1$ can give the exchange

[9] For an analysis of the decoherence rate $\gamma_{nn'}$, one needs to take into account the various intra- and inter-molecular dipolar couplings, just like for the nuclear $1/T_2$ whose dominant contribution stems from the nuclear-nuclear dipolar interactions.

constant J, and also reveal the occurrence of level-crossing effects.

There are still a number of open theoretical questions regarding the experimental findings of $1/T_1$. The first concerns the difference that seems to exist between molecules with intrinsic spins $s = 1/2$ and molecules with $s > 1/2$. The latter show a systematic enhancement of $1/T_1$ at intermediate temperatures, whereas the available experimental data for the few existing molecules with $s = 1/2$ do not show such a behavior. This can be associated with the temperature dependence of the cut-off frequency ω_0. In other words, in molecules with $s = 1/2$ there seems to be a temperature independent ω_0 whereas in molecules with ω_0 there is a strong temperature dependence which in fact has been obtained by the experimental data as described in Ref. [6]. In particular, for the magnetic molecule $\{V_6\}$,[17] there is an indication that the origin of the cut-off is not a direct spin-phonon interaction but instead a weak intra-molecular antisymmetric interaction. This interaction is further manifested in pulsed field measurements as described in chapter 6. A similar temperature independent ω_0 seems to be the case for the magnetic molecule $\{V_{12}\}$ studied in the following chapter. A second open question concerns the explicit temperature dependence of ω_0 in AFM ring systems, and in particular whether the approximate power law can be justified from first principles. Finally, there still exists a question regarding the experimental evidence that the long-time decay of the spin fluctuations can be well described by a single exponential function, contrary to what one expects according to Eq. (4.21) which generally gives a number of exponential functions with different decay rates each.

References

[1] T. Moriya , Prog. Theor. Physics **28**, 512 (1962).

[2] F. Borsa and M. Mali, Phys. Rev. B **9**, 2215 (1974).

[3] J-P. Boucher, M. Ahmed Bakheit, M. Nechtschein, M. Villa, G. Bonera, and F. Borsa, Phys. Rev. B **13**, 4098 (1976).

[4] F. Borsa, A. Lascialfari, and Y. Furukawa, cond-mat/0404378; cond-mat/0404379.

[5] J. Luscombe, M. Luban, and F. Borsa, J. Chem. Phys. **108**, 7266 (1998).

[6] S. H. Baek, M. Luban, A. Lascialfari, E. Micotti, Y. Furukawa, F. Borsa, J. van Slageren, and A. Cornia, Phys. Rev. B **70**, 134434 (2004).

[7] M. H. Julien, Z. H. Jang, A. Lascialfari, F. Borsa, H. Horvatic, A. Caneschi, and D. Gatteschi, Phys. Rev. Lett. **83**, 227 (1999).

[8] M. Affronte, A. Cornia, A. Lascialfari, F. Borsa, D. Gatteschi, J. Hinderer, M. Horvatic, A. G. M. Jansen, and M.-H. Julien, Phys. Rev. Lett. **88**, 167201 (2001).

[9] A. Lascialfari, F. Borsa, M.-H. Julien, E. Micotti, Y. Furukawa, Z. H. Jang, A. Cornia, D. Gatteschi, M. Horvatić, and J. van Slageren, J. Mag. Mag. Mat. **272-276**, 1042 (2004).

[10] E. Micotti, A. Lascialfari, F. Borsa, M. H. Julien, C. Berthier, M. Horvatic, J. van Slageren, and D. Gatteschi, Phys. Rev. Lett. **72**, 020405(R) (2005).

[11] C. P. Slichter, *Principles of Magnetic Resonance* (Springer Verlag, Berlin, 1989).

[12] A. Abragam, *Principles of Nuclear Magnetism* (Clarendon Press, Oxford, 1961).

[13] F. Bloch, Phys. Rev. **70**, 460 (1946); **102**, 104 (1956); **105**, 1206 (1957).

[14] E. Merzbacher, *Quantum Mechanics* (John Wiley & Sons, Inc., New York), 3rd edition.

[15] P. Santini, S. Carretta, E. Liviotti, G. Amoretti, P. Carretta, M. Filibian, A. Lascialfari, and E. Micotti, Phys. Rev. Lett. **94**, 077203 (2005).

[16] D. Procissi, B. J. Suh, J. K. Jung, P. Kögerler, R. Vincent, and F. Borsa, J. Appl. Phys. **93**, 7810 (2003).

[17] M. Luban, F. Borsa, S. Bud'ko, P. Canfield, S. Jun, J. K. Jung, P. Kögerler, D. Mentrup, A. Müller, R. Modler, D. Procissi, B. J. Suh, and M. Torikachvili, Phys. Rev. B **66**, 054407 (2002).

5. Magnetic susceptibility and spin dynamics of polyoxovanadate cluster V12: a proton NMR study of a model spin tetramer

A paper published in Physical Review B[1]

D. Procissi,[2] A. Shastri,[2,3] I. Rousochatzakis,[2,4] M. Al Rifai,[2,3] P. Kögerler,[2] M. Luban,[2]
B. J. Suh,[5] and F. Borsa[2,6]

Abstract

We report susceptibility and nuclear magnetic resonance (NMR) measurements in a polyoxovanadate compound with formula $(NHEt)_3[V_8^{IV}\ V_4^V\ As_8\ O_{40}\ (H_2O)]\cdot H_2O \equiv \{V_{12}\}$. The magnetic properties can be described by considering only the central square of localized V^{4+} ions and treated by an isotropic Heisenberg Hamiltonian of four intrinsic spins 1/2 coupled by nearest-neighbor antiferromagnetic interaction with $J \approx 17.6$ K. In this simplified description the ground state is nonmagnetic with $S_T = 0$. The ^{1}H NMR line width (full width at half maximum (FWHM)) data depend on both the magnetic field and temperature, and are explained by the dipolar interaction between proton nuclei and V^{4+} ion spins. The behavior of the nuclear spin-lattice relaxation rate T_1^{-1} (NSLR) in the temperature range $(4.2 - 300$ K) is similar to that of χT vs. T and it does not show any peak at low temperatures contrary to previous observations in AFM rings with larger intrinsic spins. The results are explained by using the general features of the Moriya formula and by introducing a single $T-$independent broadening parameter for the electronic spin system. From the exponential T-dependence of T_1^{-1} at low T (2.5 K $< T <$ 4.2 K) we have obtained a field dependent gap following the linear relation $\Delta_{NMR} = \Delta_0 - g\mu_B H$, with the gap $\Delta_0 \approx 17.6$ K in agreement with the susceptibility data. Below 2.5 K, the proton T_1^{-1} deviates from the exponential decrease indicating the presence of a small, almost temperature independent, but strongly field dependent, nuclear relaxation contribution, which we will investigate in detail in the near future.

[1] Reprinted with permission of Phys. Rev. B **69**, 094436 (2004).
[2] *Dept. of Physics and Astronomy and Ames Laboratory, Iowa State University, Ames, Iowa 50011, USA*
[3] *Dept. of Physics and Astronomy, Minnesota State University, Moorhead, MN, USA*
[4] Principally involved in the theoretical analysis and interpretation of the data and the writing of the paper.
[5] *Dept. of Physics, The Catholic University of Korea, Puchon 420-743, Korea*
[6] *Dip. Fisica "A. Volta" e Unita' INFM di Pavia, Via Bassi 6, Pavia 127100, Italia*

5.1 Introduction

Magnetic polyoxovanadate clusters are a very interesting class of spin systems in which a few magnetic moments are strongly coupled by exchange interaction and are arranged in a vast variety of both geometrical and spin structures.[1] Within this class of molecules the $(NH\,Et)_3[V_8^{IV}\,V_4^{V}\,As_8\,O_{40}\,(H_2O)]\cdot H_2O \equiv \{V_{12}\}$ cluster is comprised of 12 vanadium atoms arranged in a stack of three V squares as shown in Fig. 5.1(a). The top and bottom squares form strongly antiferromagnetically (AFM) coupled singlet states at room temperature and below and thus do not contribute significantly to the magnetic properties of the cluster at $T \leq 300$ K.[2] The central square of V^{4+} ions, on the other hand, forms a square of $s = 1/2$ localized moments coupled by an almost isotropic AFM nearest-neighbor exchange interaction. Thus $\{V_{12}\}$ behaves as a prototype of a spin 1/2 Heisenberg tetramer. The investigation of the spin dynamics of this molecule over the whole temperature range and for different values of the external magnetic field is of interest because one can follow the evolution from the high temperature regime of uncorrelated paramagnetic spins ($k_BT \gg J$) to the low temperature regime with a ground state of total spin $S_T = 0$. The nuclear magnetic resonance (NMR) of protons probes the spin dynamics of the system since the protons in the molecule are coupled to the V^{4+} electron spins via nuclear-electron dipolar interactions. In particular the proton spin-lattice relaxation rate T_1^{-1} is proportional to the low frequency part of the spectral density of the electron spin fluctuations.[3] As pointed out in a preliminary report on $\{V_{12}\}$,[4] the low spin value ($s = 1/2$) of each magnetic moment makes this system a good quantum counterpart of several other investigated AFM rings with high intrinsic spin value ($s = 5/2$), i.e. nearly classical spins.[5, 6] Unfortunately, no "bonafide" AFM ring system, with $S_T = 0$ ground state, composed of spins $s = 1/2$ is presently available except for $\{Cu_8\}$ ring which, however, has an exchange interaction constant (J) so large that the spin system is in the $S_T = 0$ ground state at room temperature and below.[7] Thus $\{V_{12}\}$ appears to be the only $s = 1/2$ single quantum system whose results can be compared with the $s = 1/2$ classical AFM rings.

In the present paper we report a detailed proton NMR investigation of the spin dynamics of the model spin tetramer aimed at testing the following issues: (i) the behavior of the electronic spin correlation function in the high temperature regime ($k_BT > J$); (ii) the evolution of the spin correlations when the temperature becomes of the order of the exchange coupling J ($k_BT \sim J$); (iii) the spin fluctuations at very low temperature when the molecular magnet is mostly in its singlet ground state ($k_BT < J$). In Sec. 5.2 we describe the experimental details of the NMR measurements. In Sec. 5.3 we present the experimental results including magnetic susceptibility results which will guide us in the interpretation of the NMR data. In Sec. 5.4 we analyze the data by using the general features of the Moriya formula

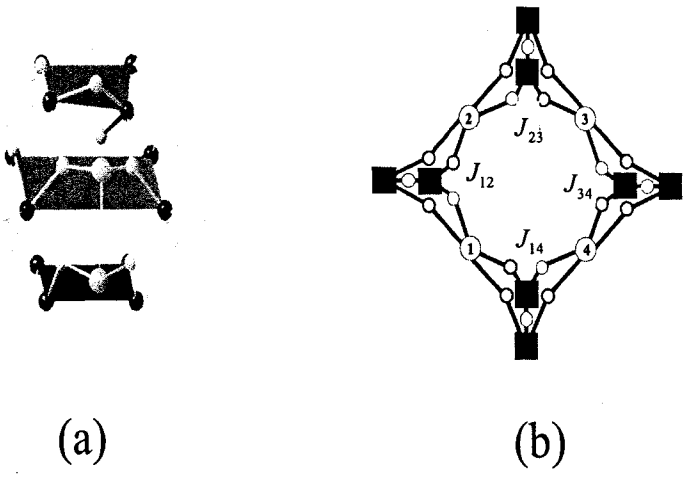

Figure 5.1 (a) Schematic representation of the $[V_8^{IV}\ V_4^{V}\ As_8\ O_{40}\ (H_2O)]^{4-}$ cluster anion. The three planes formed by the vanadium anions (black spheres) are depicted in dark gray. (b) Schematic view of the central tetramer with definition of the super-exchange and parameter pathways through the diarsenic ligands: (■) As and (○) O.[1, 2]

and exact first-principles results based on the isotropic Heisenberg model. Finally, in Sec. 5.5 we give a summary and conclusions of the paper.

5.2 Experimental details

Measurements of magnetization versus temperature were performed at 0.5 T using Quantum Design magnetic property measurement system (MPMS) superconducting quantum interference device (SQUID) magnetometers. The NMR measurements were performed on polycrystalline powder samples synthesized as described in the Ref. [2], by using a standard Fourier transform (FT) pulse spectrometer. The proton NMR line was sufficiently narrow (< 70 kHz) to be irradiated by a single radio frequency (rf) pulse of duration between $2 - 4$ μsec. The proton nuclear spin-lattice relaxation rate T_1^{-1} was measured by monitoring the recovery of the nuclear magnetization following a short sequence of saturating radio frequency pulses. The recovery of the nuclear magnetization was found to be exponential in most cases over more than one decade. Each molecule contains many non equivalent protons with different dipolar coupling to the four V^{4+} magnetic moments, namely 24×5 protons belonging to the

C_2H_5 groups that are part of the triethyl ammonium cations and the remaining four belonging to the two water molecules. Thus the observation of an exponential recovery law implies the presence of a common spin temperature.[8, 9] The common spin temperature is established if $T_1 \gg T_2$, where T_2 is the spin-spin relaxation time. Under these circumstances the measured T_1^{-1} is the weighted average of the relaxation rate for the different protons in the molecule. At high temperature and high magnetic field we observed non-exponential behavior due to the breakdown of the common spin temperature approximation and the T_1^{-1} quantity was derived from the initial part of the nuclear magnetization recovery curve (i.e. tangent to the origin). In this case also the measured T_1^{-1} is a weighted average of the different relaxation rates.[5, 6] The spin-lattice relaxation rate in the rotating frame was measured by using an initial $\pi/2$ rf pulse immediately followed by a lock-in rf pulse of intensity $H_1 \sim 0.001$ T and of variable duration τ. The $T_{1\rho}^{-1}$ parameter was obtained from monitoring the amplitude of the free precession decay as a function of the duration τ of the lock-in pulse.[9]

5.3 Experimental Results

The results for the magnetic susceptibility χ measured in our $\{V_{12}\}$ sample at 0.5 T are plotted in Fig. 5.2 as χT vs. T. The rapid drop of χT for $T \leq 100$ K is indicative of the non-magnetic ground state ($S_T = 0$). The inset in Fig. 5.2 shows χ vs. T. The proton NMR line was found to be a single symmetric line whose full width at half maximum (FWHM) is plotted in Fig. 5.3 as a function of temperature at two different external magnetic fields (0.5 T and 4.7 T). The low temperature limit (i.e., $\sim$ 50 kHz) of the low field line width $T-$dependence, can be ascribed almost entirely to the nuclear dipole-dipole interaction among the 124 protons in the molecule. The partial line narrowing from 50 kHz to 28 kHz occurring on increasing temperature is due to the averaging of the nuclear dipolar interaction by the onset of molecular hindered rotation of the C_2H_5 groups. This can be inferred by the fact that a similar line narrowing is commonly observed in the same temperature range as here in many compounds containing the same radical group.[8, 9] From a comparison of the line width data for the two fields there appears to be only a slight inhomogeneous field dependent broadening. The inhomogeneous broadening is due to the relatively small dipolar coupling of the protons with the for V^{4+} magnetic moments. The nuclear spin-lattice relaxation rate T_1^{-1} is shown as a function of temperature in Fig. 5.4 for external fields of 0.5 T and 4.7 T, respectively. In the temperature range $(4.2-300$ K) the behavior of T_1^{-1} vs. T is similar to the behavior χT vs. T. It is of particular importance to note that there is no enhancement of T_1^{-1} at temperatures close to $J/k_B \approx 17.6$ K, contrary to what has been reported in other AFM rings and clusters with intrinsic spins $s > 1/2$.[5, 6] The T_1^{-1} results in the low temperature range

(1.5 – 4.2 K) are shown separately in Figs. 5.5(a) and 5.5(b). It is noted that below 4 K the majority of the molecules are in the nonmagnetic ground state and therefore the T_1^{-1} data in this low–T regime are of particular interest and will be analyzed separately. A detailed field dependent study of T_1^{-1} was performed at 300 K and the results are shown in Fig. 5.6. We have included two points which refer to measurements at 4.7 T. In this case the relaxation rate in the rotating frame probes the spectral density at $\omega_1 = \gamma_N H_1$, and thus the points have been plotted in the graph at the magnetic field in the rotating frame $H_1 = \omega_1/\gamma_N \sim 0.001$ T. The strong field dependence of T_1^{-1} indicates that the spectral density of the magnetic fluctuations is peaked at low frequency, a characteristic feature of low dimensional Heisenberg systems.[5, 6, 10]

5.4 Analysis of experimental results

5.4.1 Magnetic susceptibility

The magnetic susceptibility data in Fig. 5.2 can be fitted well by a theoretical calculation based on the exact solution of the Heisenberg Hamiltonian. In Ref. [2] the starting Hamiltonian is an empirical anisotropic Heisenberg Hamiltonian with four exchange parameters, i.e. $J_{12}^{xy}/k_B = -9.28$ K, $J_{12}^{zz}/k_B = -9.516$ K, $J_{23}^{xy}/k_B = -7.77$ K, $J_{23}^{zz}/k_B = -8$ K (with $J_{12} = J_{34}$ and $J_{23} = J_{14}$), as shown in the schematic depiction of Fig. 5.1(b).[7] The choice of the Hamiltonian with these parameters was dictated by the need to reproduce the energy level scheme (shown in Fig. 5.7(a)) obtained directly from inelastic neutron scattering (INS) experiments.[2] However, an almost identical fit of the susceptibility can be obtained by using a far simpler isotropic Heisenberg Hamiltonian with a single exchange parameter J.[8] The eigenstates of H are of the form $|S_T M S_{13} S_{24}>$, where $\mathbf{S_{13}} \equiv \mathbf{s_1} + \mathbf{s_3}$, $\mathbf{S_{24}} \equiv \mathbf{s_2} + \mathbf{s_4}$, and $\mathbf{S_T} \equiv \mathbf{S_{13}} + \mathbf{S_{24}}$. Thus, we have a singlet $S_T = 0$ ground state ($|0011>$) with $E = 0$, a triplet $S_T = 1$ ($|1M11>$) with $E = J$, a singlet ($|0000>$) and two triplets ($|1M01>$, $|1M10>$) with $E = 2J$ and finally a quintet $S_T = 2$ state ($|2M11>$) with $E = 3J$, for a total number of $(2s+1)^N = 2^4 = 16$ states (see Fig. 5.7(b)). It is then straightforward to obtain the field-free partition function Z.[11] Moreover, the zero field molar susceptibility $\chi_0(T)$ is given by the fluctuation formula $\chi_0 = N_A(g\mu_B)^2/(3k_BT) < \mathbf{S}_T^2 >$. One then finds

$$\chi_0 T = \frac{2N_A(g\mu_B)^2}{Zk_B}(e^{-J/k_BT} + 2e^{-2J/k_BT} + 5e^{-3J/k_BT}) \,, \tag{5.1}$$

[7] In Ref.[2] the convention $H = -2J_{ij}^{\alpha\beta} s_i^\alpha s_j^\beta$ was used (α and β take on the values x, y, z).
[8] Here, we have used the convention $H = +J(\mathbf{s}_1 \cdot \mathbf{s}_2 + \mathbf{s}_2 \cdot \mathbf{s}_3 + \mathbf{s}_3 \cdot \mathbf{s}_4 + \mathbf{s}_4 \cdot \mathbf{s}_1) + 2J$.

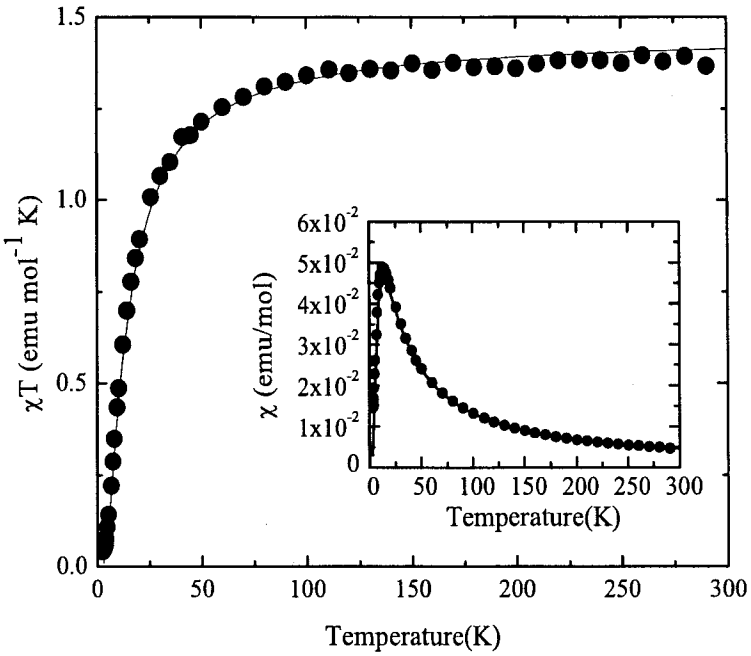

Figure 5.2 Temperature dependence of χT in $\{V_{12}\}$ at 0.5 T. The solid curve is the theoretical result (Eq. (5.1)) with $g = 1.97$ and $J = 17.6$ K. Also shown in the inset is the susceptibility χ vs T at 0.5 T.

where N_A is Avogadro's number. We found that Eq. (5.1) provides a very good fit to the experimental data upon choosing $g \approx 1.97$ and $J/k_BT \approx 17.6$ K. The theoretical susceptibility curve is given by the solid line in Fig. 5.2. This agreement is further evidence of the fact that the overall magnetic properties can be associated with the four central spins $s = 1/2$.

5.4.2 ^{1}H NMR line width (FWHM) vs T

The ^{1}H NMR line width $\Delta\nu$ (FWHM) as a function of temperature and for two different fields is shown in Fig. 5.3. The dependence of $\Delta\nu$ on both the magnetic field and the temperature is ascribed to magnetic dipolar broadening via the dipolar interaction of the ^{1}H with the V^{4+} magnetic moments. For the dipolar magnetic broadening, the inhomogeneous line width $\Delta\nu$ for a given susceptibility per spin χ, is given by

$$\frac{\Delta\nu}{\nu_N} = \frac{\Delta\nu}{\frac{\gamma_N}{2\pi}H} = A_z\chi \sim \frac{<\mu>}{r^3H}\,, \tag{5.2}$$

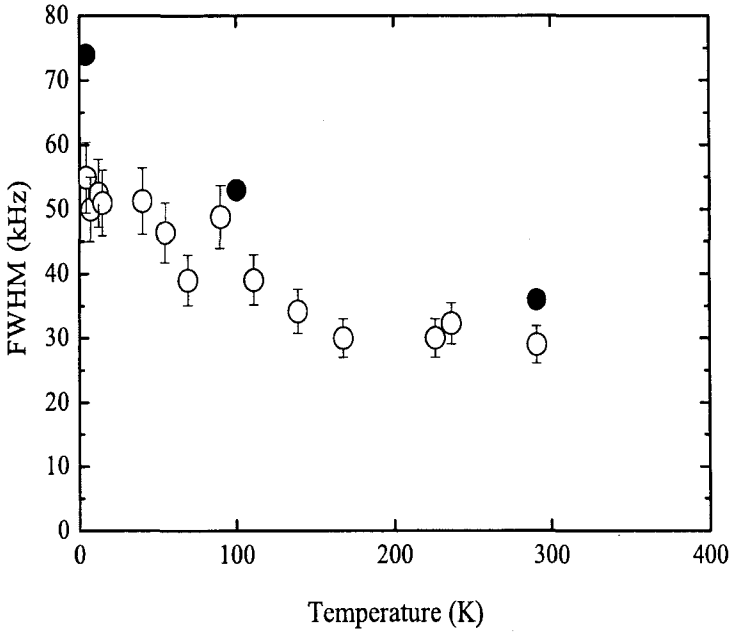

Figure 5.3 Temperature dependence of the proton linewidth (FWHM) in $\{V_{12}\}$ at two different external fields, $H_0 = 0.5$ T (open circles) and $H_0 = 4.7$ T (filled circles).

where ν_N is the proton Larmor frequency, A_z is the component of the dipolar hyperfine coupling constant along the direction of the external magnetic field H, and r is the average distance between the ^{1}H and the vanadium ions.[8] From the field dependence at room temperature (not shown here) and the susceptibility in Fig. 5.2 one can estimate the component A_z of the dipolar coupling constant by considering the slope

$$\frac{\Delta\nu(H_{02}) - \Delta\nu(H_{01})}{\frac{\gamma_N}{2\pi}(H_{02} - H_{01})} = A_z\chi \sim \frac{<\mu>}{r^3 H} \ . \tag{5.3}$$

We obtained a value of $A_z \sim 10^{22}$ cm^{-3} which corresponds to the field generated by a V^{4+} magnetic moment at an average distance of about 3 Å. This agrees with the results for $\{V_{15}\}$ and $\{V_6\}$ given in Ref.[12]. The result demonstrates that ^{1}H NMR is a direct probe of the magnetic properties of the V^{4+} ions in the $\{V_{12}\}$ compound.

5.4.3 ^{1}H spin-lattice relaxation rate T_1^{-1}

One can obtain a general expression for the spin-lattice relaxation rate T_1^{-1} through a method based on a perturbative treatment ("weak collision approach") of the dipolar coupling between nuclear and paramagnetic spins.[3, 8, 9] The major features of the spin-lattice relaxation rate can be easily seen in the following formula

$$T_1^{-1} = (\hbar^2 \gamma_N \gamma_e)^2 \sum_{ij,\alpha\alpha'} C_{ij}^{\alpha\alpha'} \int_{-\infty}^{+\infty} dt\ e^{i\omega_N t}\ < s_i^{\alpha}(t) s_j^{\alpha'}(0) > \ , \tag{5.4}$$

where the coefficients $C_{ij}^{\alpha\alpha'}$ contain all the detailed geometrical coefficients of the dipolar interactions, $\{i,j\}$ are paramagnetic spin sites and $\{\alpha,\alpha'\}$ cartesian coordinates. It can be easily seen that the difficulty in evaluating T_1^{-1} in Eq. (5.4) arises firstly from the calculation of$C_{ij}^{\alpha\alpha'}$ and secondly from the calculation of all the spin-spin correlation functions. The following simplifications have been made in order to get the major features.

(1) We use the isotropic Heisenberg Hamiltonian that we used for the susceptibility.

(2) We replace the delta functions that arise from Eq. (5.4) by Lorentzian functions with a single temperature independent broadening parameter ω_0 whose physical interpretation is in terms of a cut-off frequency of the spin-spin correlation functions due to couplings that do not commute with the Heisenberg isotropic exchange.[10]

(3) The difference in the dipolar interactions of the inequivalent protons (different $C_{ij}^{\alpha\alpha'}$ for different protons) in the molecule is treated by averaging out the geometrical details of the system, i.e. we deal with a single, average T_1^{-1}.

(4) Since the energies of the electronic spin system are of the order of $J/k_BT \approx 17.6$ K, we keep only terms that correspond to zero transition frequencies. This simplification is valid for fields far below the first level crossing (~ 13.3 T);

By using the total spin symmetries of the Hamiltonian, i.e., $[H, \mathbf{S}_T^2] = [H, S_T^z] = 0$ and the resulting selection rules, we get the following general form for the spin lattice relaxation rate[3, 13]

$$T_1^{-1} = F_L(T,H)\frac{\omega_0}{\omega_0^2 + \omega_L^2} + F_T(T,H)\frac{\omega_0}{\omega_0^2 + \omega_e^2}\ , \tag{5.5}$$

where the first term comes from the (auto and pair) longitudinal correlation functions and the second comes from the transverse terms. The temperature and field dependence of F_L and F_T arises from the various Boltzmann factors of the electronic spin levels. There is no need for a further simplification of setting F_L and F_T equal.[13]

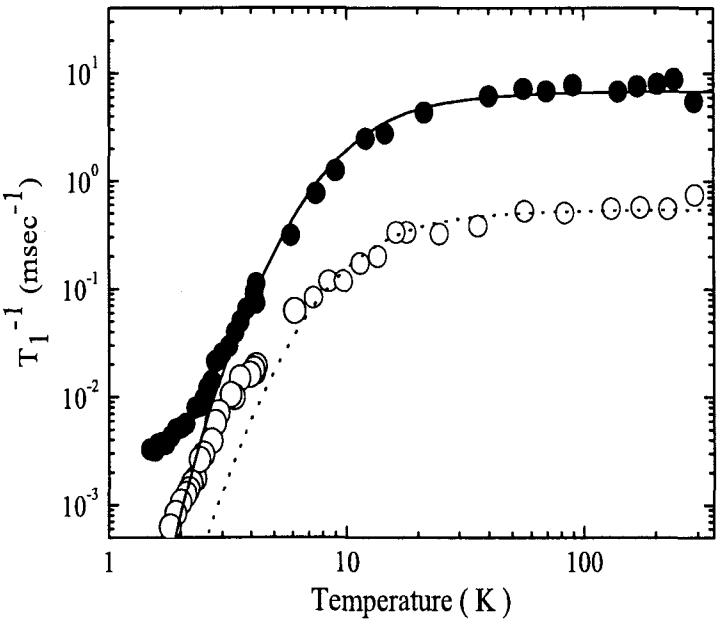

Figure 5.4 Temperature dependence of the proton spin-lattice relaxation rate in $\{V_{12}\}$: (filled circles) data at $H = 0.5$ T. The solid curve is the best fit according to Eq. (5.8), with $\alpha = 5.6$ msec^{-1}, $\beta = 76.8$ msec^{-1}, $\gamma = 28$ msec^{-1}; (open circles) data at 4.7 T. The dotted curve is the same curve as for the 0.5 T data, but with a rescaling factor which takes into account the field dependence in Eq. (5.7) with $H_0 = 1.3$ T.

In the expressions for F_L and F_T in Eq. (5.5), the contribution from the ground state vanishes since the ground state is a non-degenerate $S_T = 0$ state. We will use this additional feature in writing Eq. (5.8), and also in the low$-T$ behavior of T_1^{-1} (Eq. 5.9). We are now ready to discuss our experimental results using the above general features of T_1^{-1}.

5.4.3.1 T_1^{-1} vs. field at $T = 300$ K

In the high temperature regime ($T = 300$ K) the Boltzmann factors in F_L and F_T in Eq. (5.5) are all close to unity. Hence, one should be able to reproduce the field dependence of T_1^{-1} at $T = 300$ K with the relation

$$T_1^{-1} = P\frac{\omega_0}{\omega_0^2 + \omega_L^2} + Q\frac{\omega_0}{\omega_0^2 + \omega_e^2} , \tag{5.6}$$

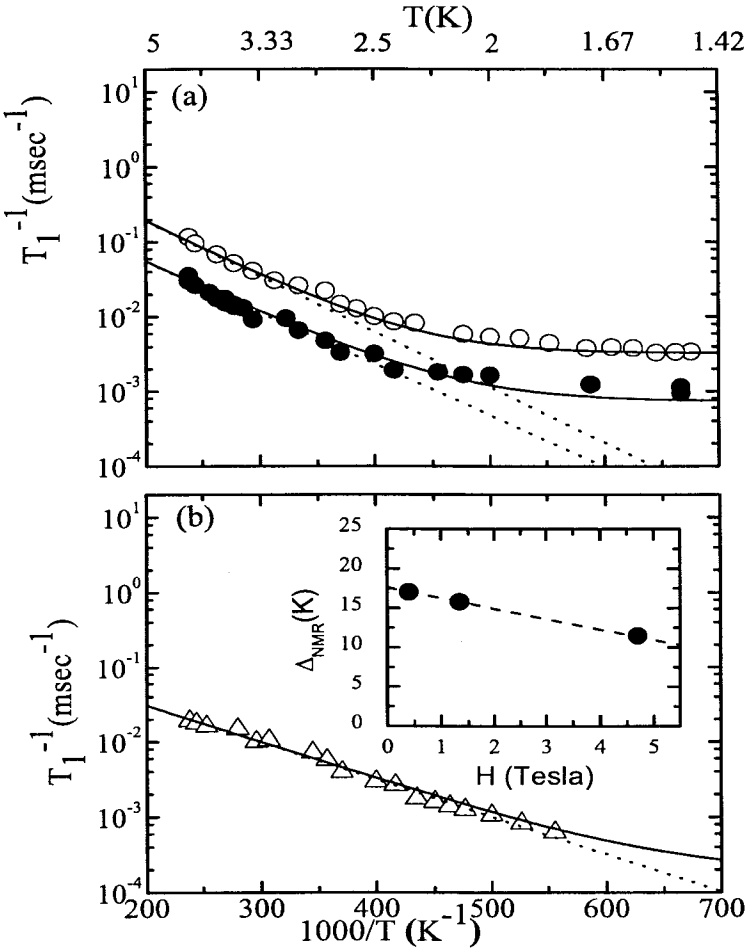

Figure 5.5 (a) Semilog plot of T_1^{-1} vs $1000/T$ for the low$-T$ range (1.5$-$4.2 K) for different magnetic fields: (open circles) 0.4 T data; (filled circles) 1.34 T data. The dotted curves are fits according to Eq. (5.9) with $Z = 1$, $A(0.4\text{ T}) = 7$ msec^{-1} , $A(1.34\text{ T}) = 1.3$ msec^{-1} and with $\Delta_{NMR}(0.4\text{ T}) = 17.1$ K, $\Delta_{NMR}(1.34\text{ T}) = 15.8$ K. The solid curve corresponds to the addition in Eq. (5.9) of a constant, field-dependent term $G(H)$, with $G(0.4\text{ T}) = 3.9 \times 10^{-3}$ msec^{-1}, and $G(1.34\text{ T}) = 7.3 \times 10^{-4}$ msec^{-1}. (b) (open squares) 4.7 T data. The dotted curve corresponds to Eq. (5.9) with $Z = 1$, $A(4.7$ T$) = 0.3$ msec^{-1}, and $\Delta_{NMR}(4.7\text{ T}) = 11.3$ K. The solid curve corresponds to the addition in Eq. (5.9) of the constant $G(H)$, with $G(4.7\text{ T}) = 1.7 \times 10^{-4}$ msec^{-1}. The inset shows the obtained values of Δ_{NMR} vs H, and the solid black line is the linear dependent expected behavior $\Delta_{NMR}(H) = \Delta_0 - g\mu_B H$ with $\Delta_0 = 17.6$ K and $g\mu_B = 1.33$ K/T.

where P and Q are constants. Indeed, the field dependence of T_1^{-1} at $T = 300$ K, can be well described by the relation

$$T_1^{-1} = K\frac{H_0^{-1}}{1+(H/H_0)^2}\ , \tag{5.7}$$

where K and H_0 are fitting parameters. From the fit in Fig. 5.6 one obtains $K/H_0 = 8.9$ msec^{-1} and $H_0 = 1.3$ T. Equation 4(b) arises from Eq. (5.6) in two limiting cases: (i) if $P \ll Q$ and $\omega_0 \sim \omega_e$, in which case one would have $\omega_0 = \gamma_e H_0 \sim 2.3 \times 10^{11}$ Hz; and (ii) if $P \sim Q$ and $\omega_0 \sim \omega_N \ll \omega_e$, in which case one would have $\omega_0 = \gamma_N H \approx 3.5 \times 10^8$ Hz. Both choices are consistent with the fact that the $T_{1\rho}^{-1}$ value is of the order of the zero field extrapolated T_1^{-1} since the spin-lattice relaxation in the rotating frame is proportional to the spectral density of the fluctuations at very low frequency, i.e., $\omega_1 \sim 250$ kHz. One could argue that there is no physical reason why $P \ll Q$ since the constants are both related to the components of dipolar coupling tensor, and therefore the second choice is the relevant one. One way to determine this experimentally would be to perform a T_1^{-1} measurement using a different (other than proton) nuclei. Unfortunately, an attempt to detect the ^{51}V NMR signal was unsuccessful most likely due to the very short T_1 and/or T_2. Furthermore ^{13}C NMR in natural abundance yields a signal which is too weak for the required low field measurements.

5.4.3.2 T_1^{-1} vs. temperature at $H = 0.5$ T for $T > 4.2$ K

For $H = 0.5$ T, we have $\hbar\omega_e \ll J$, and therefore we can neglect the field dependence in the Boltzmann factors in F_L and F_T. Hence, the temperature dependence of T_1^{-1} in Fig. 5.4 can be reproduced reasonably well by the following relation

$$T_1^{-1} = \frac{1}{Z}(\alpha(H)e^{-J/k_BT} + \beta(H)e^{-2J/k_BT} + \gamma(H)e^{-3J/k_BT})\ , \tag{5.8}$$

where the field dependence in the fitting parameters α, β and γ arises from the Lorentzian broadening as in Eq. (5.5). There is no contribution in Eq. (5.8) from the ground state, as indicated previously. The data of T_1^{-1} for $H = 0.5$ T can be fitted by Eq. (5.8), for $T > 4$ K, with the proper choice of fitting parameters α, β, and γ (solid black curve in Fig. 5.4 with $\alpha = 5.6$ msec^{-1}, $\beta = 76.8$ msec^{-1}, $\gamma = 28$ msec^{-1}). One can see a deviation from the behavior given in Eq. (5.8) below $T = 4.2$ K in Fig. 5.4 which will be treated separately.

5.4.3.3 T_1^{-1} vs. temperature at $H = 4.7$ T and for $T > 4.2$ K

If one assumes that the constants α, β and γ in Eq. (5.8) have the same field dependence as in Eq. (5.7) and that the parameter ω_0, which defines the width of the Lorentzian function, is $T-$independent,

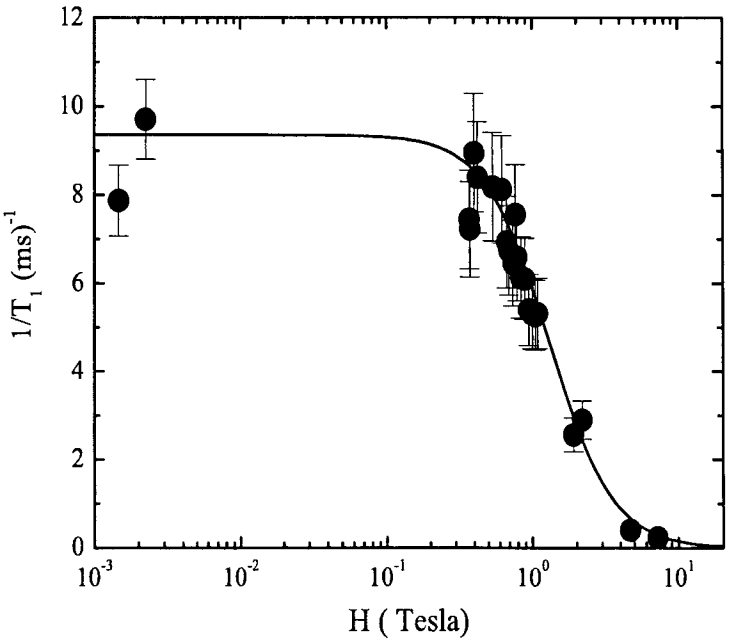

Figure 5.6 T_1^{-1} vs H at $T = 300$ K. The solid black line represents the best fit to the data according to Eq. (5.7) with $H_0 = 1.3$ T and $K/H_0 = 8.9$ msec^{-1}. The two points plotted at very low fields are $T_{1\rho}^{-1}$ measurements at 4.7 T (see the text).

one can try to fit the T_1^{-1} data at $H = 4.7$ T with the same set of parameters as for the fit at 0.5 T simply by rescaling by the field dependence given by Eq. (5.7). We would expect that at 4.7 T, which is approximately 1/3 of the first level crossing field, the Boltzmann factors that enter F_L, F_T would be affected significantly especially at low T. Indeed, there is a deviation below 10 K (see the dotted line in Fig. 5.4). It is noteworthy that one finds good qualitative agreement over a wide temperature range and this implies that the broadening parameter ω_0 is $T-$independent at these temperatures. The above result suggests that the T and H dependence of T_1^{-1} can be expressed in first approximation as the product of a temperature dependent function $f(T)$ and a field dependent function $g(H)$. This approximation obviously breaks down at high fields and low temperatures.

5.4.3.4 T_1^{-1} vs. temperature for $T < 4.2$ K

For temperatures below the ^{4}He boiling temperature only the ground state ($|0000>$) and the first excited state ($|1-111>$) are of importance. Then, for given field, the temperature dependence of T_1^{-1},

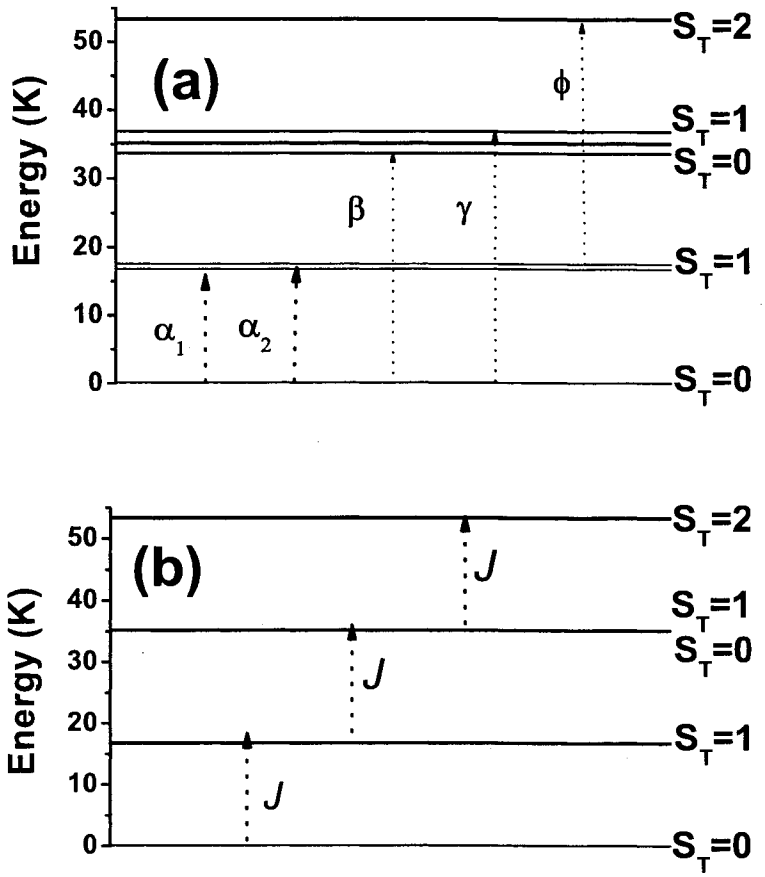

Figure 5.7 (a) Level scheme as obtained from INS (Ref.[2]) (depicted are the observed inelastic neutron scattering transitions). (b) Level scheme as obtained from isotropic Heisenberg model for four spins $s = 1/2$.

assuming again no $T-$dependence in ω_0 in Eq. (5.5), follows the relation

$$T_1^{-1} = \frac{A(H)}{Z} e^{-\Delta_{NMR}(H)/k_B T} , \tag{5.9}$$

where $\Delta_{NMR}(H) = \Delta_0 - \Delta E(H)$, with $\Delta_0 = J$, is the gap between the ground state $S_T = 0$ and $S_T = 1$ excited state and $A(H)$ is a fitting parameter for each field coming from the Lorentzian broadening. One can easily see that $A(H)e^{-\Delta_{NMR}(H)/k_B T}$ in Eq. (5.9) corresponds to $\alpha(H)$ in Eq. (5.8) when $k_B T \gg J$.

The initial part of the curve (2.5 K$< T <$ 4.2 K) in Fig. 5.5(a) and 5.5(b) can indeed be fit with Eq.(5.9) (dotted curves in Fig. 5.5(a) and 5.5(b)) with $A(0.4T) = 5.8$ msec^{-1}, $A(1.34T) = 1.3$ msec^{-1}, $A(4.7T) = 0.3$ msec^{-1}, and $\Delta_{NMR}(0.4T)/k_B = 17.1$ K, $\Delta_{NMR}(1.34T)/k_B = 15.8$ K, and finally $\Delta_{NMR}(4.7T)/k_B = 11.4$ K. The obtained gap values Δ_{NMR} vs. H are plotted in the inset of Fig. 5.5(b),

the dashed curve represents the Zeeman field dependence of the gap given by $\Delta_{NMR}(H) = \Delta_0 - g\mu_B H$, with $\Delta_0/k_B = 17.6$ K.

For the case of the low field data (0.4 T and 1.34 T) one must note the deviation from the exponential thermally activated behavior given in Eq. (5.9) with $\Delta_0/k_B \sim 17.6$ K for $T < 2.5$ K (Fig. 5.5(a)), while in the case of the high field data (4.7 T) the fit given by Eq. (5.9) reproduces the data also below 2.5 K as shown in Fig. 5.5(b). The weak temperature dependence below 2.5 K suggests that we fit the data in this regime by simply adding a $T-$independent but $H-$dependent term in Eq. (5.9) (see Fig. 5.5). It is noted that in the octanuclear $\{Cu_8\}$ antiferromagnetic ring, of $S_T = 0$ ground state, a similar deviation at low temperatures was observed.[7] In $\{Cu_8\}$ the ^{63,65}Cu NMR and nuclear quadrupole resonance (NQR) indicated the presence of nonequivalent Cu sites, suggesting a deviation from the exact isotropic Heisenberg Hamiltonian. Moreover, inelasting neutron scattering[2] in the present system, indicated the presence of anisotropic exchange. However, no contribution to T_1^{-1} can arise in Moriya's formula from a non-degenerate $S_T = 0$ ground state, whatever the form of the Hamiltonian, and in particular whether H includes anisotropic exchange and non-equivalent sites. Therefore, we are lead to conclude that the very low$-T$ contribution to T_1^{-1} is coming either from paramagnetic "defects" or from a relaxation mechanism other than proton-vanadium dipolar coupling terms of Moriya's theory.

5.5 Summary and conclusions

In this work we have presented comprehensive susceptibility and ^{1}H nuclear magnetic resonance experimental results of the polyoxovanadate cluster $\{V_{12}\}$. The susceptibility experimental data were well fitted using results from exact calculations based on an isotropic Heisenberg Hamiltonian for the spin 1/2 tetramer. From the NMR spectral measurements and the temperature and field dependence of the NMR line width we have established that the inhomogeneous broadening is due to the dipolar coupling of the protons with the localized vanadium ions. The spin dynamics of the tetramer has been characterized through the proton spin-lattice relaxation rate, T_1^{-1}, in different temperature regimes and for different fields, and we used general arguments (based on Moriya's first-principles treatment) to reproduce the results. At high temperature ($k_BT \gg J$) T_1^{-1} exhibits a strong and well defined field dependence which is well reproduced by a Lorentzian spectral density of the spin fluctuations. This field behavior is similar to that observed in one-dimensional magnetic systems.[10] In the intermediate temperature range (10 K $< T <$ 300 K) the temperature behavior of T_1^{-1} is similar to the $T-$dependence of χT indicating that the proton T_1^{-1} is dominated by the amplitude of the local spin fluctuations. Particularly relevant is the absence of an enhancement of the relaxation rate T_1^{-1} for $k_BT \sim J$ which

is found in other similar molecular magnetic rings comprised of spins with $s > 1/2$.[6] The fact that we were able to roughly reproduce the high and low field data simply by means of a rescaling factor is evidence of the fact that the T and H dependence of T_1^{-1} can be expressed in first approximation as the product of two independent functions $f(T)$ and $g(H)$ and most importantly that the broadening parameter ω_0 is weakly temperature dependent down to at least 10 K. Finally, in the low$-T$ regime (2.5K $< T <$ 4.2 K), and for both high and low fields, T_1^{-1} decreases exponentially as the temperature is lowered. The value of the gap Δ obtained from the fit of the data is consistent with the simple linear field dependence $\Delta_{NMR}(H) = \Delta_0 - g\mu_B H$ with $\Delta_0 = 17.6$ K in excellent agreement with the susceptibility results and with INS and dynamic magnetization measurements.[14] For $T < 2.5$ K the temperature dependence of T_1^{-1} deviates from the thermally activated exponential behavior and this is most evident in the low field data (0.4 T and 1.34 T). This deviation will be explored in detail in the near future.

The most remarkable conclusion of the present work is found by comparing the behavior of the present $s = 1/2$ tetramer with the $s > 1/2$ AFM rings. Although in both cases the proton T_1^{-1} can be well described by Moriya's theory, the characteristic frequency ω_0 defining the broadening of the magnetic levels of the molecule, and thus the spin fluctuations is quite different for the $s = 1/2$ quantum case and the $s > 1/2$ classical case. In $\{V_{12}\}$, ω_0 appears to be almost $T-$independent and thus it does not give rise to the peak in T_1^{-1} observed in AFM rings,[4, 6] where ω_0 is strongly $T-$dependent becoming of the order of the nuclear Larmor frequency at the peak.[15] Another important finding is the existence of a residual nuclear relaxation mechanism at very low temperatures. It will be noted that similar results were obtained in half-integer isotropic high-spin ground state molecules of different spin values.[16]

Acknowledgements

We would like to acknowledge fruitful discussion with H. Nojiri. Ames Laboratory is operated for the U.S. Department of Energy by Iowa State University under Contract No. W-7405-Eng-82.

References

[1] A. Müller, R. Sessoli, E. Krickemeyer, H. Bögge, J. Meyer, D. Gatteschi, L. Pardi, J. Westphal, K. Hovemeier, R. Rohlfing, and J. Döring, Inorg. Chem. **36**, 5239 (1997).

[2] R. Basler, G. Chaboussant, A. Sieber, A. Andres, M. Murrie, P. Kögerler, H. Bögge, D. C. Crans,

E. Krickemeyer, S. Janssen, H. Mutka, A. Müller, and H. Güdel, Inorg. Chem. **41**, 5675-5685 (2002).

[3] T. Moriya , Prog. Theor. Physics **28**, 512 (1962).

[4] B. J. Suh, D. Procissi, P. Kögerler, E. Micotti, A. Lascialfari, and F. Borsa, ICM, Rome, (2003).

[5] A. Lascialfari, Z. H. Jang, F. Borsa, D. Gatteschi, and A. Cornia, J. Appl. Phys. **83**, 6946 (1998).

[6] A. Lascialfari, D. Gatteschi, F. Borsa, and A. Cornia, Phys. Rev. B **55**, 14341 (1997).

[7] A. Lascialfari, Z. H. Jang, F. Borsa, D. Gatteschi, A. Cornia, D. Rovai, A. Caneschi, P. Carretta, Phys. Rev B **61**, 6839, (2000).

[8] A. Abragam, *Principles of Nuclear Magnetism* (Clarendon Press, Oxford, 1961).

[9] C. P. Slichter, *Principles of Magnetic Resonance* (Springer Verlag, Berlin, 1989).

[10] F. Borsa and M. Mali, Phys. Rev. B **9**, 2215 (1974).

[11] The partition function is given by $Z = 1 + 3e^{-J/k_BT} + 7e^{-2J/k_BT} + 5e^{-3J/k_BT}$.

[12] D. Procissi, B. J. Suh, K.J. Jung, P. Kögerler, R. Vincent and F. Borsa, J. Appl. Phys. **93**, 7810 (2003).

[13] M. Luban, F. Borsa, S. Bud'ko, P. Canfield, S. Jun, J. K. Jung, P. Kögerler, D. Mentrup, A. Müller, R. Modler, D. Procissi, B. J. Suh, M. Torikachvili, Phys. Rev. B **66**, 054407, (2002).

[14] H. Nojiri and M. Luban, (private communications), (2003).

[15] S. H. Baek, M. Luban, A. Lascialfari, E. Micotti, Y. Furukawa, F. Borsa, J. van Slageren, and A. Cornia (Unpublished).

[16] Z. Salman, A. Karen, P. Mendels, V. Marvaud, A. Scuiller, M.Verdaguer, J. S. Lord and C. Baines, Phys. Rev. B **65**, 132403 (2002).

6. Pulsed Fields measurements: The Landau-Zener-Stückelberg model without dissipation

6.1 Introduction

Pulsed field techniques have been a valuable tool in probing the spin dynamics of magnetic molecule systems. These experiments have shown a variety of remarkable effects, such as magnetization hysteresis and abrupt magnetization steps. The hysteretic behavior is related to (and gives information concerning) the coupling with the lattice degrees of freedom (mainly the phonons), and signify that the characteristic thermal relaxation times of the magnetic molecule systems can be low enough to be in the regime of currently available sweep rates. On the other hand, the magnetization steps are manifestations of the so-called Landau-Zener-Stückelberg (LZS) transitions,[1–4] of purely quantum-mechanical origin (see below) and can give information on the microscopic interactions present in all nanomagnetic systems. In addition to hysteresis and LZS steps, there have been observed effects related to the dissipative LZS effect, i.e., the combined thermal and quantum-mechanical transitions.

More specifically, in pulsed field experiments one measures the magnetization in time, in the presence of fast sweeping external fields of various forms. Moreover, the magnetic fields can reach very large values (a few tens of Tesla) with sweep rates as high as 1 T/ms. In addition, the value of the magnetization can be measured in very fine time intervals. Hence, in pulsed field experiments the Hamiltonian becomes explicitly time dependent. To explain the response to pulsed fields one generally needs to take into account the interaction with the lattice degrees of freedom, such as phonons.[1] The situation is the one depicted in Fig. 6.1. Let us denote by τ_s the characteristic time scale of the thermal transitions, under a static external field. When the field changes in time, the outcome of the measurement of $M(t)$ depends largely on the competition between the time scale τ_s with the experimental time scale τ_e, determined by the sweep rate. For instance, if the sweep of the field $B(t)$ is extremely slow, then the measured magnetization $M(t)$ is the instantaneous equilibrium value $M_{eq}(B(t))$, corresponding to

[1] At ultra-low T there are not enough phonon modes excited and thus the phonon system cannot be considered as a large reservoir. In this case, the role of the heat bath can be played by the spin degrees of freedom within the sample, such as the nuclear spins.[5]

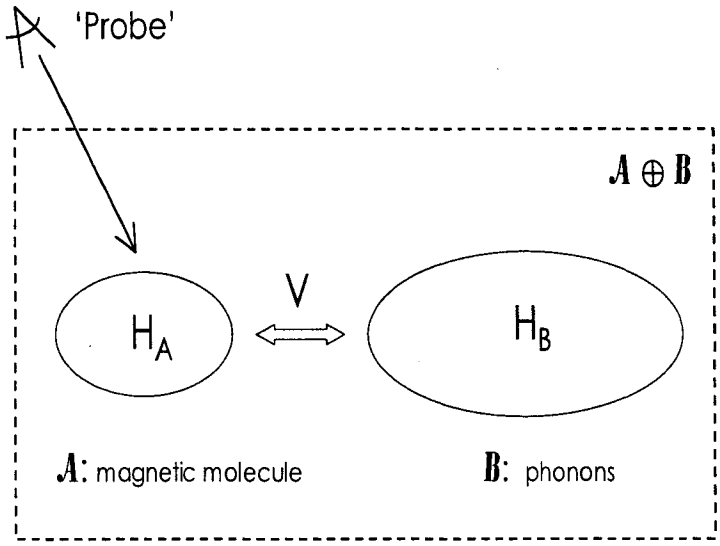

Figure 6.1 To explain hysteresis effects in pulsed field measurements one has to take into account the coupling to the lattice degrees of freedom, which consist mainly of phonons. Small intramolecular anisotropic terms (contained in H_A) are responsible for the occurrence of LZS transitions and magnetization steps.

the instantaneous $B(t)$. On the other hand, if τ_s is in the regime of the available sweep time τ_e, the measured magnetization lags behind $M_{eq}(B(t))$, i.e., it shows hysteresis. On the other hand, the occurrence of a magnetization step is not related to the coupling to the lattice but instead originates from intramolecular magnetic interactions which are so small that cannot be observed by static measurements such as susceptibility. The field values at which a magnetization step takes place corresponds to an avoided level crossing (or anticrossing) in the magnetic energy spectrum, as a function of external field. Such level anticrossings are formed if the corresponding levels are coupled by the small anisotropic term.

In Sec. 6.2, we provide an analytical derivation of the well-known LZS formula for the pure quantum-mechanical LZS model, i.e., we shall neglect the coupling to the bath in Fig. 6.1, and moreover we shall assume that the field is changing linearly with time. A general first-principles analysis of hysteresis effects in magnetic molecules as well as the dissipative LZS effect can be found in chapter 8. In Sec. 6.3, we take into account the general expressions of Sec. 6.2, and give some order of magnitude considerations in actual magnetic molecule systems. In particular, we emphasize the difference between the LZS effects occurring in systems with a small spin ground state with the corresponding ones occurring in SMMs.

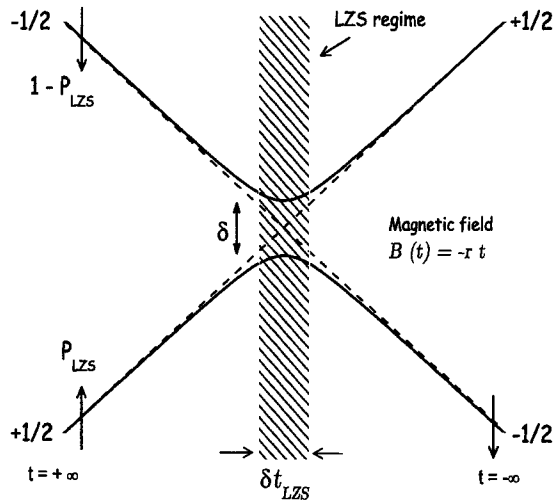

Figure 6.2 LZS transitions. The solid lines correspond to the adiabatic energy states ($|1;t>$ and $|2;t>$) of the LZS model of Eq. (6.1), whereas the dashed diagonal lines correspond to the spin-up $|->$ and spin-down $|+>$ state. The initial conditions Eqs. (6.15) is that shown on the right ($t=-\infty$). The probabilities P_{LZS} and $1-P_{LZS}$ of adiabatic and nonadiabatic transitions, respectively, are indicated. In the extreme adiabatic regime the system remains on the lower branch ($|-;t>$) at all times and therefore ends up in the spin-up $|+>$ state. In the opposite limit, of the nonadiabatic regime, the state of the system does not change at all, and therefore remains in the initial state $|->$ at all times. The shaded area in the immediate vicinity of $B=0$ indicates the LZS regime where the magnetization step takes place. Also indicated is the zero-field energy gap δ.

6.2 The LZS model without dissipation

The traditional quantum-mechanical two-level[2] LZS model[1–4] consists of a spin 1/2 system, subject to a linearly time dependent field along the $\mathbf{z}-$axis and a small static transverse field. Without loss of generality we take the latter to be directed along the $\mathbf{x}-$axis. Then, the Hamiltonian for this problem is given by

$$H_A/\hbar = -\Gamma_e^2 t\sigma_z - \Gamma_v\sigma_x \ , \tag{6.1}$$

where we have defined $\Gamma_e^2 = g\mu_B r/(2\hbar)$. Both Γ_v and Γ_e have dimensions of frequency. These provide two different time scales and therefore their ratio Γ_e/Γ_v is of particular importance, as we show below.

[2]Apart from the two-level LZS model, there also exist multilevel variations of this problem. We refer in particular to Refs. [6–8] and references therein.

Starting from the initial condition that, in the remote past $t = -\infty$, the system is in the spin-down state, i.e., $|\psi(-\infty)>=|->$, the problem consists of finding the wavefunction $|\psi(t)>$ by solving analytically the time-dependent Schrödinger equation. Of particular interest is the probability (denoted by P_{LZS}) that, in the remote future the system ends up in the spin-up $|+>$ state.

First, one can easily solve for the adiabatic eigenstates $|\alpha;t>$ (with $\alpha = 1,2$) and the corresponding eigenvalues $\epsilon_\alpha(t)$ of this Hamiltonian by taking t as a parameter, i.e., by solving for each t the equation

$$H_A(t)|\alpha;t>=\epsilon_\alpha(t)|\alpha;t> \ . \tag{6.2}$$

In particular, the eigenvalues are of the form

$$\epsilon_{1,2}(t)/\hbar = \mp((\Gamma_e^2 t)^2+\Gamma_v^2)^{1/2} \ , \tag{6.3}$$

i.e., the adiabatic energy diagram has the avoided level crossing form shown in Fig. 6.2. The zero-field energy gap δ is equal to $\delta = 2\hbar\Gamma_v$.

Suppose now, that one begins in the remote past ($t = -\infty$) with a large positive field ($B = +\infty$) with the spin system being in its ground state $|1;-\infty>=|->$. As mentioned above, Γ_v is very small and therefore its effect will become important only when the first term approaches zero, i.e., when B crosses zero. In the immediate vicinity of $B = 0$, there is an enhanced probability that the off-diagonal term induces transitions between the two states of the system. As a result, in the remote future ($t = +\infty$) there is a finite probability that the system is in its excited adiabatic state $|2;+\infty>=|->$. We denote this probability by $1 - P_{LZS}$. On the other hand, the probability that the system remains on the lowest energy branch $|1;t>$ at all times is given by P_{LZS}. According to the adiabatic theorem of quantum mechanics (Refs. [11, 12]) one expects that P_{LZS} should be larger the slower we cross the anti-crossing regime, i.e., $P_{LZS} \to 1$ when $\Gamma_e/\Gamma_v \to 0$. Let us derive the exact analytical expression giving P_{LZS} in terms of the ratio Γ_e/Γ_v. We seek the analytical solution of the time-dependent Schrödinger equation

$$i\hbar\frac{d}{dt}|\psi(t)>=H_A(t)|\psi(t)> \ . \tag{6.4}$$

Writing $|\psi(t)>$ as a linear combination of the spin-down $|->$ and spin-up $|+>$ states, i.e.,

$$|\psi(t)>=f(t)|+>+g(t)|-> \ , \tag{6.5}$$

we obtain a system of two coupled equations for the amplitudes $f(t)$ and $g(t)$

$$\begin{aligned} i\dot{f} &= -\Gamma_v g - \Gamma_e^2 t f \ , \\ i\dot{g} &= -\Gamma_v f + \Gamma_e^2 t g \ , \end{aligned} \tag{6.6}$$

which can easily be decoupled, by taking another time derivative, as

$$\ddot{f} + (\Gamma_v^2 - i\Gamma_e^2 + \Gamma_e^4 t^2) f = 0 \ ,$$
$$\ddot{f} + (\Gamma_v^2 + i\Gamma_e^2 + \Gamma_e^4 t^2) g = 0 \ . \tag{6.7}$$

Let us consider the first equation only. By introducing $F(t) = e^{-i(\Gamma_e t)^2/2} f(t)$ we obtain

$$\ddot{F} + 2i\Gamma_e^2 t\dot{F} + \Gamma_v^2 F = 0 \ . \tag{6.8}$$

Then, changing variables from t to $s = -i(\Gamma_e t)^2$ and introducing the dimensionless parameter $\gamma = (\Gamma_v/2\Gamma_e)^2$, we finally arrive at[3]

$$sF''(s) + (\frac{1}{2} - s)F'(s) + i\gamma F(s) = 0 \ , \tag{6.9}$$

which one recognizes as the differential equation satisfied by the confluent hypergeometric function $M(a, c, z)$ (see for example Refs. [9, 10]), whose general solution can be written as

$$F(s) = c_1 M(-i\gamma, 1/2, s) + c_2 \ s^{1/2} M(1/2 - i\gamma, 3/2, s) \ . \tag{6.10}$$

The integration constants c_1 and c_2 are to be determined by the initial condition. A very important remark is that the function $s^{1/2}$ appearing in the r.h.s of this expression is not well defined, unless we define a branch cut. To this end we choose the cut shown in Fig. 6.3 (b). In going from $t = -\infty$ to $t = +\infty$ along the path C_t indicated in Fig. 6.3 (a), the corresponding path C_s in the $s-$plane (Fig. 6.3 (b)) goes around the branch point $s = 0$, and as a result the function $s^{1/2}$ acquires an overall minus sign. To obtain the probability P_{LZS} we need first to find the asymptotic behavior of Eq. (6.10) at $t \to \pm\infty$. To this end we use the asymptotic expansion[9, 10] of the confluent hypergeometric function

$$\lim_{|s|\to+\infty} M(a, c, -i|s|) = \frac{\Gamma(c)}{\Gamma(a)} e^{-i|s|} |s|^{a-c} e^{i\pi(c-a)/2} + \frac{\Gamma(c)}{\Gamma(c-a)} e^{-i\pi a/2} |s|^{-a} \ , \tag{6.11}$$

where $\Gamma(z)$ denotes the Gamma function.[9] One should keep in mind that this limiting behavior holds for $|s| \gg 1$, or equivalently for $|t| \gg \Gamma_e^{-1}$.

Substituting Eq. (6.11) in each term of Eq. (6.10) and collecting terms together (and taking care of the branch cut of $s^{1/2}$) one obtains the asymptotic behavior of $f(s)$ at $t \to \pm\infty$ as

$$\lim_{t\to\pm\infty} f(s) = l_\pm(\gamma) \ e^{-i|s|/2} \ |s|^{-i\gamma-1/2} + p_\pm(\gamma) \ e^{i|s|/2} \ |s|^{i\gamma} \ , \tag{6.12}$$

with the functions $l_\pm(\gamma)$ and $p_\pm(\gamma)$ defined as

$$l_\pm(\gamma) = \left(c_1 \frac{\Gamma(1/2)}{\Gamma(-i\gamma)} \pm c_2 \frac{\Gamma(3/2)}{\Gamma(-i\gamma + 1/2)} \right) \ e^{i\pi/4} \ e^{-\pi\gamma/2} \ ,$$
$$p_\pm(\gamma) = \left(c_1 \frac{\Gamma(1/2)}{\Gamma(i\gamma + 1/2)} \mp i c_2 \frac{\Gamma(3/2)}{\Gamma(i\gamma + 1)} \right) \ e^{-\pi\gamma/2} \ . \tag{6.13}$$

[3]The prime in $F'(s)$ denotes differentiation with respect to the new variable s.

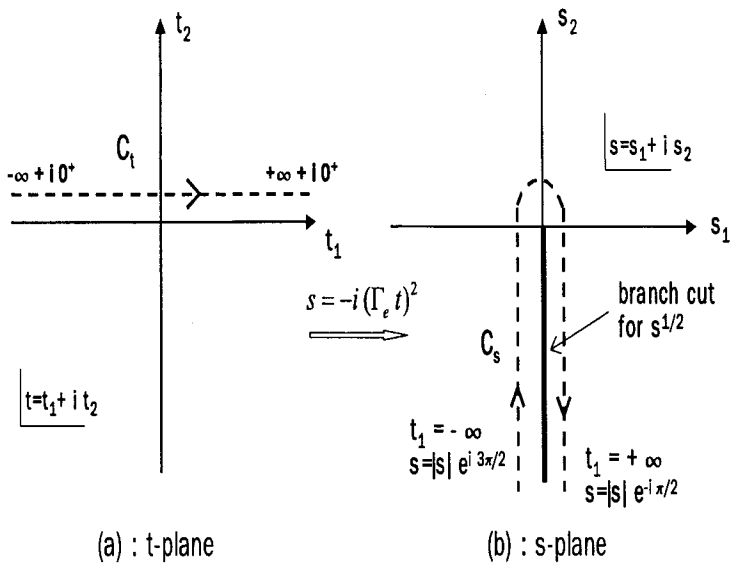

Figure 6.3 (a) The path C_t indicates the sweep of the magnetic field from $B = +\infty$ at $t = -\infty$ to $B = -\infty$ at $t = +\infty$. We choose to cross the time axis from above, i.e., we define $t = t_1 + t_2$, with $t_2 \to 0^+$. In doing so, $s = s_1 + is_2 = 2\Gamma_e^2 t_1 t_2 - i\Gamma_e^2(t_1^2 - t_2^2)$ follows the path C_s indicated in (b). Then the function $s^{1/2}$ acquires an overall minus sign since the path goes around the branch cut.

The next step is to apply the initial condition of the problem, in order to find the constants c_1 and c_2. We denote by $f_{\pm\infty}$ and $g_{\pm\infty}$ the values of $f(t)$ and $g(t)$ at $t \to \pm\infty$, respectively. We have assumed that at $t = -\infty$, the spin system is in the spin-down state $|- >$, i.e., according to Eq. (6.5),

$$f_{-\infty} = 0 \ ,$$
$$g_{-\infty} = 1 \ , \tag{6.14}$$

with an arbitrary choice of the relative phase between $f_{-\infty}$ and $g_{-\infty}$. Inspecting the r.h.s. of Eq. (6.12), as $t \to -\infty$, the magnitude of the first term drops like $|s|^{-1/2} = (\Gamma_e t)^{-1}$, whereas the second term oscillates in time. Hence, for the initial conditions Eq. (6.14) to apply, one must have identically

$$p_-(\gamma) = 0 \ , \tag{6.15}$$

which provides us with a first relation between c_1 and c_2. A second relation is obtained by taking the time derivative of f in Eq. (6.12) and carefully comparing it with Eqs. (6.6). This provides us with the

required second relation between c_1 and c_2

$$|l_-(\gamma)| = \sqrt{\gamma} \; . \tag{6.16}$$

Solving Eqs. (6.15) and (6.16) for c_1 and c_2, and after some lengthy but straightforward algebra, one obtains

$$\begin{aligned} |c_2|^2 &= \frac{4\gamma e^{\pi\gamma}}{\cosh\pi\gamma\,(1+\tanh\pi\gamma)^2} \; , \\ c_1 &= \frac{-i\,\Gamma(i\gamma+1/2)}{2\,\Gamma(i\gamma+1)}\, c_2 \; . \end{aligned} \tag{6.17}$$

To arrive at these expressions we have used the following properties of the Gamma function[9]

$$\begin{aligned} |\Gamma(i\gamma)|^2 &= \frac{\pi}{\gamma\sinh\pi\gamma} \; , \\ |\Gamma(i\gamma+1/2)|^2 &= \frac{\pi}{\cosh\pi\gamma} \; , \\ |\Gamma(i\gamma+1)|^2 &= \frac{\pi\gamma}{\sinh\pi\gamma} \; . \end{aligned} \tag{6.18}$$

Replacing the above values for c_1 and c_2 back into the expressions for $l_+(\gamma)$ and $p_+(\gamma)$ (Eq. (6.13)) one finally obtains the asymptotic values f_∞ and g_∞, and consequently the probability P_{LZS}

$$P_{LZS} \equiv |f_\infty|^2 = \frac{4\tanh\pi\gamma}{(1+\tanh\pi\gamma)^2} = 1 - e^{-4\pi\gamma} = 1 - e^{-\pi\Gamma_v^2/\Gamma_e^2} \; , \tag{6.19}$$

or equivalently, in terms of the energy gap $\delta = 2\hbar\Gamma_v$ and the sweep rate r,

$$P_{LZS} = 1 - e^{-\pi\delta^2/(2\hbar g\mu_B r)} \; . \tag{6.20}$$

This is the well-known LZS formula.[1, 3, 4] According to this, $P_{LZS} \to 1$, i.e., the system remains at all times on the lowest energy branch (see Fig. 6.2), when $\Gamma_e \ll \Gamma_v$ (adiabatic regime). This is expected from the adiabatic theorem of quantum mechanics. On the other hand, when $\Gamma_e \gg \Gamma_v$, the anti-crossing regime ($B \approx 0$) is crossed so rapidly that the wavefunction does not change at all, i.e., the system remains in the spin-down state $|- >$ (dotted diagonal line in Fig. 6.2) and by definition $P_{LZS} = 0$ (extreme non-adiabatic regime). This is in accordance with the sudden approximation of quantum mechanics which applies whenever a Hamiltonian term changes very fast (as compared to the intrinsic Bohr frequencies of the problem). For a nice account of both the adiabatic and sudden approximations in quantum mechanics see Ref. [11] (see also [12]).

We consider now the time interval δt_{LZS} during which the LZS transitions occur.[4] This is given by

$$\delta_{LZS} = 2\,\frac{\Gamma_v}{\Gamma_e^2} = 2\,\frac{\delta}{g\mu_B r} \; , \tag{6.21}$$

[4]Outside this time interval, the Zeeman term dominates and the off-diagonal term is not effective in inducing transitions between $|- >$ and $|+ >$.

which, by a simple inspection of the Hamiltonian (Eq. (6.1)), corresponds to the time interval during which the Zeeman term is smaller in magnitude than the second, off-diagonal term (For a mathematical criterion for obtaining δt_{LZS} see Ref. [3]). According to this simple relation one can indirectly obtain δ by measuring the time width of the magnetization step. This is done for the magnetic molecule $\{V_6\}$ in the following chapter.

6.3 Order of magnitude considerations in actual magnetic molecule systems

Let us now obtain some typical numerical estimates in actual magnetic molecule systems. Assuming $g \approx 2$, and denoting $\widetilde{\delta}$ and $\widetilde{r}$ as the quantities δ and r in units of K and T/ms, respectively, we have $\Gamma_e^2 \simeq 8.79 \times 10^{10}\ \widetilde{r}\ \mathrm{s}^{-2}$, whereas $\Gamma_v \simeq 6.55 \times 10^{10}\ \widetilde{\delta}\ \mathrm{s}^{-1}$.

Consider first the time width δt_{LZS} during which the LZS step occurs (This is indicated in Fig. 6.2 by the shaded area around $B \approx 0$). According to Eq. (6.21), $\delta t_{LZS} \simeq 1.489\ \widetilde{\delta}/\widetilde{r}$ s. As an example, if $\widetilde{\delta} \sim 0.1$ and $\widetilde{r} \sim 1$, then $\delta t_{LZS} \sim 15$ ms, which can easily be measured since, in pulsed field experiments, one is able to measure $M(t)$ in very fine time intervals.

Consider next the order of magnitude of the transition probability P_{LZS}. The magnitude of the exponent in the second term of Eq. (6.20) is $1.53 \times 10^{11}\ \widetilde{\delta}^{\,2}/\widetilde{r}$. This means that for a typical value $\delta \sim 0.1$ K, one must use extremely high sweep rates, i.e., of order $r \gtrsim 10^9$ T/s (not experimentally feasible), in order to reach the non-adiabatic regime $P_{LZS} < 1$. Hence for all currently available sweep rates we are in the extreme adiabatic regime ($P_{LZS} = 1$). This in turn, means that the system makes a complete transition from the initial spin-down $|- >$ state to the spin-up $|+ >$ state, i.e., a complete magnetization reversal in the immediate vicinity of $B \approx 0$.[5] This extreme adiabaticity condition is fulfilled in the large category of magnetic molecules with low spin ground states, such as $\{V_6\}$ (see Refs. [13–15] and chapter 7), and the similar compound $\{V_{15}\}$.[16]. The AFM ring systems also fall in the same category. A general analysis of pulsed field studies in this category of molecules is given in chapter 8.

On the other hand, the LZS effects taking place in the so-called single molecule magnets (SMMs) correspond to the nonadiabatic regime ($P_{LZS} < 1$). The reason is that the characteristic energy gap δ responsible for the occurrence of LZS transitions (magnetization tunneling) in these systems is extremely small ($10^{-7} - 10^{-9}$ K, see Refs. [17–19]). The origin of such a small energy scale in these molecules

[5] For the low T, pulsed field studies of the magnetic molecule $\{V_6\}$ (see the following two chapters), for which $\delta \sim 0.4$ K, a small deviation from the expected adiabatic behavior has been observed, but this is attributed to thermal transitions (dissipative LZS effect, see chapter 8).

is attributed to their large spin ground states (e.g., $S = 10$ for $\{Fe_8\}$ and $\{Mn_{12}\}$). Moreover, the corresponding $(2S+1)-$fold degeneracy at zero field is split by single-ion anisotropic terms (of the form DS_z^2) present in the spin Hamiltonian. Consider now the remaining degeneracy between the lowest states $|S, S>$ and $|S, -S>$. This degeneracy can in principle be split by small, say of order ξ, residual transverse (anisotropic) terms. However, since $|S, S>$ and $|S, -S>$ have $\Delta M = 2S$, the two states couple in a very high order k (e.g., $k = 2S$) of perturbation theory and consequently are split by an energy δ (tunnel splitting) which is proportional to ξ^{2S}. Hence, this large exponent gives an extremely small tunnel splitting. Such a small δ can give $P_{LZS} < 1$ and the resulting LZS transitions are not complete. In such a case, a measurement of the deviation of the LZS step from its adiabatic limit gives an estimate of δ. Remarkably, such an indirect measurement of such a small energy scale, by use of Eq. (6.20), has been performed (for more details see Ref. [20]).

References

[1] L. Landau, Phys. Z. Sowjetunion **2**, 46 (1932); C. Zener, Proc. R. Soc. London, Ser. A **137**, 696 (1932); E. C. G. Stückelberg, Helv. Phys. Acta **5**, 369 (1932).

[2] E. Majorana, Nuevo Cimento **9**, 43-50 (1932).

[3] V. V. Dobrovitski, and A. K. Zvezdin, EuroPhys. Lett. **38** (5), 377-382 (1997).

[4] S. Miyashita, J. Phys. Soc. Jpn. **64**, 3207 (1995).

[5] N. V. Prokof'ev, and P. C. E. Stamp, Rep. Prog. Phys. **63**, 669-726 (2000).

[6] V. N. Ostrovsky, and H. Nakamura, J. Phys. A: Math. Gen. **30**, 6939-6950 (1997).

[7] Y. N. Demkov, and V. N. Ostrovsky, Phys. Rev. A **61**, 032705 (2000).

[8] Y. N. Demkov, and V. N. Ostrovsky, J. Phys. B: At. Mol. Opt. Phys. **34**, 2419-2435 (2001).

[9] M. Abramowitz and I. Stegun, *Handbook of Mathematical Functions* (Dover Publications, Inc., New York, 1972), Chap. 13.

[10] J. B. Seaborn, *Hypergeometric Functions and Their Applications* (Springer-Verlag, New York, 1991).

[11] A. B. Migdal, *Qualitative Methods in Quantum Theory* (Advanced Book Classics, Perseus Publishing, Cambridge, 1977).

[12] A. Messiah, *Quantum Mechanics* (Interscience Publishers, New York, 1961).

[13] M. Luban *et al.*, Phys. Rev. B **66**, 054407 (2002).

[14] I. Rousochatzakis, Y. Ajiro, H. Mitamura, P. Kögerler, and M. Luban, Phys. Rev. Lett. **94**, 147204 (2005).

[15] I. Rousochatzakis and M. Luban, Phys. Rev. B **72**, 094537 (2005).

[16] I. Chiorescu *et al.*, Phys. Rev. Lett. **84**, 3454 (2000); Phys. Rev. B **67**, 020402(R) (2003).

[17] J. R. Friedman, M. P. Sarachik, J. Tejada, and R. Ziolo, Phys. Rev. Lett. **76**, 3830 (1996); L. Thomas, F. Lionti, R. Ballou, D. Gatteschi, R. Sessoli, and B. Barbara, Nature (London) **383**, 145 (1996).

[18] C. Sangregorio, T. Ohm, C. Paulsen, R. Sessoli, and D. Gatteschi, Phys. Rev. Lett. **78**, 4645 (1997).

[19] R. Schenker, M. N. Leuenberger, G. Chaboussant, H. U. Güdel, and D. Loss, Chem. Phys. Lett. **358**, 413 (2002).

[20] W. Wernsdorfer and R. Sessoli, Science **284**, 133 (1999).

7. Hysteresis Loops and Adiabatic Landau-Zener-Stückelberg transitions in the Magnetic Molecule $\{V_6\}$

A paper published in Physical Review Letters[1]

I. Rousochatzakis,[2] Y. Ajiro,[3] H. Mitamura,[4] P. Kögerler,[2] and M. Luban[2]

Abstract

We have observed hysteresis loops and abrupt magnetization steps in the magnetic molecule $\{V_6\}$, where each molecule comprises a pair of identical spin triangles, in the temperature range 1-5 K for external magnetic fields B with sweep rates of several Tesla/ms executing a variety of closed cycles. The hysteresis loops are accurately reproduced using a generalization of the Bloch equation based on direct one-phonon transitions between the instantaneous Zeeman-split levels of the ground state (an $S = 1/2$ doublet) of each spin triangle. The magnetization steps occur for $B \approx 0$ and they are explained in terms of adiabatic Landau-Zener-Stückelberg transitions between the lowest magnetic energy levels as modified by inter-triangle anisotropic exchange of order 0.4 K.

Letter

Magnetic molecules provide a very convenient platform for exploring fundamental issues in nanomagnetism. Heisenberg exchange between the magnetic-ion spins embedded in each molecule gives rise to a discrete spectrum of magnetic energy levels. Moreover, the magnetic interaction (dipole-dipole) between molecules is generally so small as compared to intra-molecular exchange interactions that a crystal sample may be regarded as a macroscopic assembly of independent identical quantum nanomagnets. One significant goal is to understand the interactions of the magnetic molecules with the environment ("heat bath"), for example via phonons. In particular, it is essential to understand the

[1]Reprinted with permission of Phys. Rev. Lett. **94**, 147204 (2005).

[2]*Dept. of Physics and Astronomy and Ames Laboratory, Iowa State University, Ames, Iowa 50011, USA*

[3]*Dept. of Chemistry, Graduate School of Science, Kyoto University, Kyoto 606-8502, Japan and CREST, Japan Science and Technology Agency, Saitama 332-0012, Japan*

[4]*Institute for Solid State Physics, University of Tokyo, Chiba 106, Japan*

nature of the thermal relaxation mechanism, the controlling factors responsible for irreversible and dissipative phenomena, and the detailed route to thermal equilibrium of these nano-size quantum spin systems. The simpler the spin system the greater the prospects for achieving a deep understanding of the underlying issues, and this opportunity is provided by the magnetic molecule $\{V_6\}$.[1] Each $\{V_6\}$ includes a pair of triangles of exchange-coupled vanadyl (VO^{2+}, spin 1/2) ions. As shown below, at low temperatures the instantaneous magnetization, $M(t)$, of this spin system, in response to pulsed magnetic fields, $B(t)$, with sweep rates of several Tesla/ms, exhibits pronounced hysteresis loops as well as abrupt magnetization steps that are due to Landau-Zener-Stückelberg (LZS) transitions[2, 3] between lowest energy levels. By explaining the details of the dynamical magnetization one establishes both the low-temperature relaxation mechanism for the individual magnetic molecules as well as microscopic information concerning the lowest energy levels, not readily accessible. Indeed, our analysis suggests the existence in this magnetic molecule of an effective inter-triangle anisotropic exchange of order 0.4 K; otherwise Kramers' theorem[4, 5] would forbid the occurrence of LZS transitions.

There are several important differences between the present work and previous studies of $M(t)$ in magnetic molecules in time-dependent magnetic fields. From our observation of hysteresis effects in $\{V_6\}$ we conclude that the thermal relaxation time τ in this molecule is of order 0.1 ms. This is many orders of magnitude shorter than those reported for "single-molecule magnets" such as $\{Mn_{12}\}$[6] and $\{Fe_8\}$[7] where a large anisotropy energy barrier is responsible for relaxation times of order $10^3 - 10^5$ sec. Also, we assume that the phonon bottleneck effect which typically occurs at low temperatures (e.g. $T < 200$ mK for $\{V_{15}As_6\}$[8]) does not arise: For the temperatures of our experiment ($T > 1.5$ K) the number of available resonant phonons per molecule is large so that they equilibrate independently from the spins (typical times $\tau_{ph} < 10^{-6}$ s, much smaller than both the experimental time scale $\tau_{exp} \sim 1$ ms and the relaxation times τ of the spins). Moreover, due to the high sweep rate of $B(t)$ in our measurements, LZS transitions are consequential only in the immediate vicinity of $B = 0$. Away from $B = 0$, we use a generalization of the standard Bloch equation for $M(t)$, where the relaxation rate depends on the instantaneous $B(t)$. The excellent agreement obtained between theory and experiment allows us to identify the dominant mechanism for thermal relaxation in terms of direct one-phonon processes. To our knowledge, this is the first time that quantitative agreement between theory and experiment has been achieved for hysteresis loops in magnetic molecules.

We first summarize the most important known features of $\{V_6\}$.[1] The magnetic molecule $[H_4\ V_6^{IV}O_8\ (PO_4)_4\ \{(OCH_2)_3CCH_2\ OH\ \}_2]^{6-}$, abbreviated as $\{V_6\}$, and isolated as $(CN_3H_6)_4Na_2\ \{V_6\} \bullet 14\ H_2O$, may be pictured (see Fig. 7.1) in terms of two identical triangular units per molecule, each unit consisting

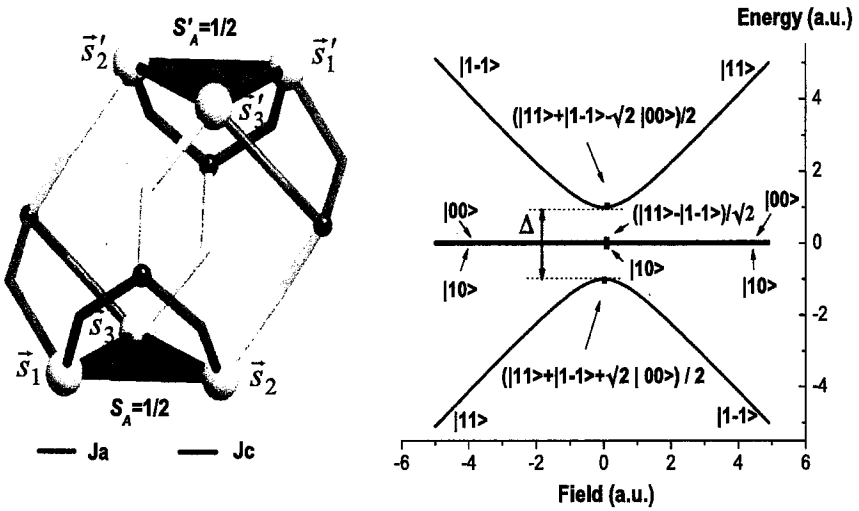

Figure 7.1 Left: Structure of the two spin triangles in the $\{V_6\}$ anion (bright grey spheres). Phosphate exchange paths (green), and other ligands not shown, mediate strong intra-triangle exchange (J_a, blue) and weak inter-triangle exchange (yellow bonds). At low temperatures each triangle behaves as a spin 1/2 entity ($S_A = S'_A = 1/2$). Right: Energy diagram for one scenario of inter-triangle exchange where a term of the form $(\Delta/2)(S_{Ax}S'_{Az} - S_{Az}S'_{Ax})$ admixes several of the states $|S, M_S; S_A = 1/2, S'_A = 1/2>$, shown as blue lines.

of three spins $s = 1/2$ (VO^{2+} ions) interacting via isotropic antiferromagnetic (AFM) exchange. Two of the 2-spin exchange constants (shown in blue) are equal ($J_a \approx 65$ K in units of k_B), and an order of magnitude larger than the third (shown in red, $J_c \approx 7$ K). Additionally, from nuclear magnetic resonance (NMR) studies and chemical structure analysis it has been argued that there exists a very weak inter-triangle exchange interaction (yellow bonds, approximately 0.3 K). In the absence of inter-triangle exchange, for $B = 0$ the ground state of each triangle consists of a 2-fold degenerate doublet with total spin $S = 1/2$, consistent with Kramers' theorem. The excited levels are a second degenerate doublet with $S = 1/2$ and excitation energy $(J_a - J_c) \approx 58$ K, and a 4-fold degenerate level with $S = 3/2$ and excitation energy (also measured from the ground state) $3J_a/2 \approx 97$ K. In the experiments described below we consider temperatures in the range 1.5-5 K and $B < 25$ Tesla, well below the field value (≈ 74 Tesla) when the $S = 3/2, M_S = -3/2$ level crosses the ground state $S = 1/2, M_S = -1/2$ level. As such, it suffices to consider only the ground state doublet of each triangular unit. A weak residual inter-triangle anisotropic exchange will lift the 4-fold degeneracy for $B = 0$ of each molecule and give

rise (in general) to four distinct energy levels (see below). As remarked above, the occurrence of these splittings can be manifest when the molecules are subject to pulsed magnetic fields, giving rise to a sudden reversal in magnetization when the field crosses $B = 0$, as a result of LZS transitions between the split levels. Apart from the vicinity of $B = 0$ the magnetic properties at low T of a $\{V_6\}$ sample may be accurately described in terms of an ensemble of independent $S = 1/2$ spin triangles.

Time-resolved magnetization measurements were performed on a powdered sample for half-cycle and full-cycle sweeps by a standard induction method using compensated pickup coils and a nondestructive long pulse magnet installed at ISSP. Utilizing fast digitizers, the inductive method provides data for dM/dt and dB/dt which are subsequently integrated to give results for M versus B. The pulsed fields have a nearly sinusoidal shape as a function of time, with a half-period about 21 ms (0-maximum-0). The sample of 36.9 mg was packed in a thin-walled cylindrical teflon capsule (inner diameter 3.0 mm) and then directly immersed in a liquid Helium bath.

In Figs. 7.2 and 7.3 we present our experimental and theoretical results for the magnetization versus applied magnetic field for two different temperatures (1.7 K and 4.2 K) and for half-cycle and full-cycle sweeps shown in the insets of Fig. 7.2(a) and Figs. 7.3(a) and 7.3(b). The two striking features of the M vs. B data are hysteresis loops and the appearance of magnetization steps (in Fig. 7.2) and near-reversals (Fig. 7.3) in the immediate vicinity of $B = 0$. The hysteresis loops (all data except in the immediate vicinity of $B = 0$) are reproduced (solid lines in Figs. 7.2 and 7.3) by numerical solution of the following generalization[10] of the familiar Bloch equation[4, 9]

$$\frac{d}{dt}M(t) = \frac{1}{\tau(T, B(t))}\big[M_{eq}(T, B(t)) - M(t)\big], \tag{7.1}$$

with the relaxation rate $1/\tau$ given by

$$\frac{1}{\tau(T, B(t))} = \frac{3(g\mu_B)^3 V_{sl}^2}{2\pi\rho v^5 \hbar^4}\, B(t)^3 \coth\Big(\frac{g\mu_B B(t)}{2k_B T}\Big) + R_0. \tag{7.2}$$

Here μ_B is the Bohr magneton, ρ denotes the mass density, v the sound velocity, V_{sl} the characteristic modulation of the spin energy under long-wavelength acoustic deformation, and $M_{eq}(T, B(t))$ is the standard two-level equilibrium magnetization for an instantaneous field $B(t)$ and for temperature T, *i.e.*, $M_{eq}(T, B(t))/M_{max} = \tanh[g\mu_B B(t)/(2k_B T)]$, where $M_{max} = 2(N_A g\mu_B/2)$. We have derived Eq. (7.1) from first principles[10] upon making the assumption that for these temperatures the phonons are in thermal equilibrium with the cryostat at all experimental times. The first term of Eq. (7.2) is the low-temperature relaxation rate of the spins due to direct one-phonon processes, where spin flips are triggered by an acoustic phonon mode meeting the resonance condition for the *instantaneous* energy separation of the two-level spin system. This term is a generalization of the standard expression for the

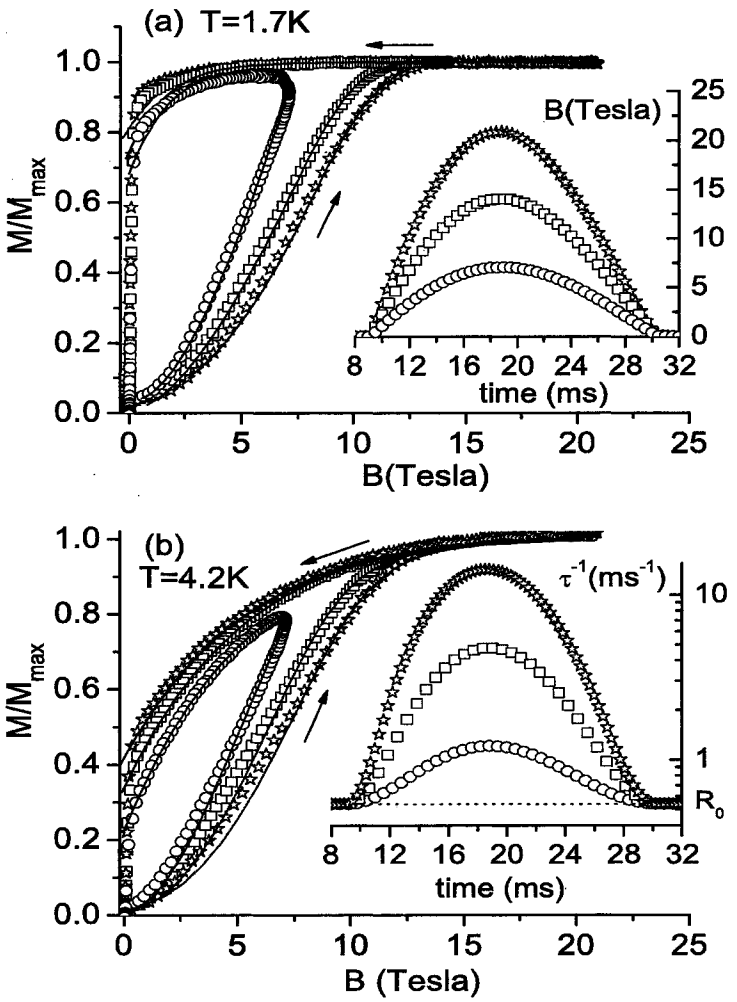

Figure 7.2 Measured magnetization vs magnetic field for $T = 1.7$ K (a) and $T = 4.2$ K (b), for the three half-cycle sweeps shown in the inset of Fig. 7.2(a). The solid red lines are obtained using Eqs. (7.1) and (7.2). The time dependence of the relaxation rate τ^{-1} according to Eq. (7.2) for $T = 4.2$ K is given in the inset of Fig. 7.2(b). The dotted line indicates the residual constant R_0 in Eq. (7.2). The sudden drop of M to zero at $B = 0$ is explained in the text in the context of LZS transitions.

relaxation rate due to one-phonon processes in a static external field.[4] Both the $B(t)^3$ factor, proportional to the phonon energy density, and the statistical mechanical factor depend on the instantaneous resonance frequency, proportional to $B(t)$. The numerical value of V_{sl} depends on the specific details of the spin-phonon coupling (see, for example, discussion for paramagnetic spins in Ref. [4]), which at present is unclear. The quantity R_0 in Eq. (7.2) represents additional relaxation processes present and it is taken as a fitting parameter. Using the measured value of $\rho = 1.93$ g/cm^3 and estimating $v = 3000$ m/s, we obtain excellent agreement with our data for the choices $R_0 = 0.2$ ms^{-1} for $T = 1.7$ K and $R_0 = 0.5$ ms^{-1} for $T = 4.2$ K and $V_{sl}/k_B = 0.35$ K. Despite the smallness of R_0 it is important to retain this term in order to achieve a good fit to the experimental data in the low-field regime (below 4 Tesla for 1.7 K and below 7 Tesla for $T = 4.2$ K); for higher fields the dominant contribution to $1/\tau$ comes from the one-phonon term. We emphasize that the solution of Eq. (7.1) is extremely sensitive to the explicit functional form of the first term of Eq. (7.2)): Adopting a different choice of functional form one cannot achieve quantitative agreement with the observed hysteresis loops, for the whole field range and for different choices of field sweeps. Achieving an excellent fit to our measured data for a variety of choices of $B(t)$ thus affirms the basic correctness of these two equations.

We now discuss the magnetization steps observed for $B \approx 0$, and in particular the interval between points A and B in Figs. 7.3(a) and 7.3(b) (the other steps seen in Figs. 7.2 and 7.3 have the same physical origin and will not be discussed separately). In this interval the external field varies approximately linearly with time, with sweep rates of order 1 Tesla/ms. We note that at point A, M_A/M_{max} is somewhat less than unity due to thermal relaxation before entering the fast-reversal regime. Equivalently, at point A we are dealing with a statistical mixture of spin-up and spin-down states. The most striking feature though is that the magnetization M_B, at point B, nearly equals $-M_A$. We find that the time-widths of the near-reversals is shorter the faster the sweep rate, and is in the range 0.5-0.8 ms. We propose that adiabatic LZS transitions are responsible for the magnetization steps observed in our system. The characteristic energy gap Δ of the LZS 2-level[5] model is related to the time-width δt_{LZS} of the magnetization step and the field sweep rate r by the relation $\delta t_{LZS} = 2\Delta/(g\mu_B r)$.[2, 3] Thus, the measured time-widths of the steps give, as a first estimate for the zero-field energy gap, $\Delta \approx 0.4$ K. Using the above estimate for Δ, we are indeed in the regime of adiabatic LZS transitions, since the transition probability $P_{LZS} = 1 - \exp\big(-\pi\Delta^2/(2\hbar g\mu_B r)\big) \approx 1$,[2, 3] thus implying that $M_B = -M_A$. The observed deviation of M/M_{max} from exact reversal is about 15% for $T = 1.7$ K. This discrepancy may be due to the role of the heat bath, i.e., the problem of dissipative LZS transitions (see, for example

[5] We anticipate that a similar relation holds for the general 4-level LZS problem.

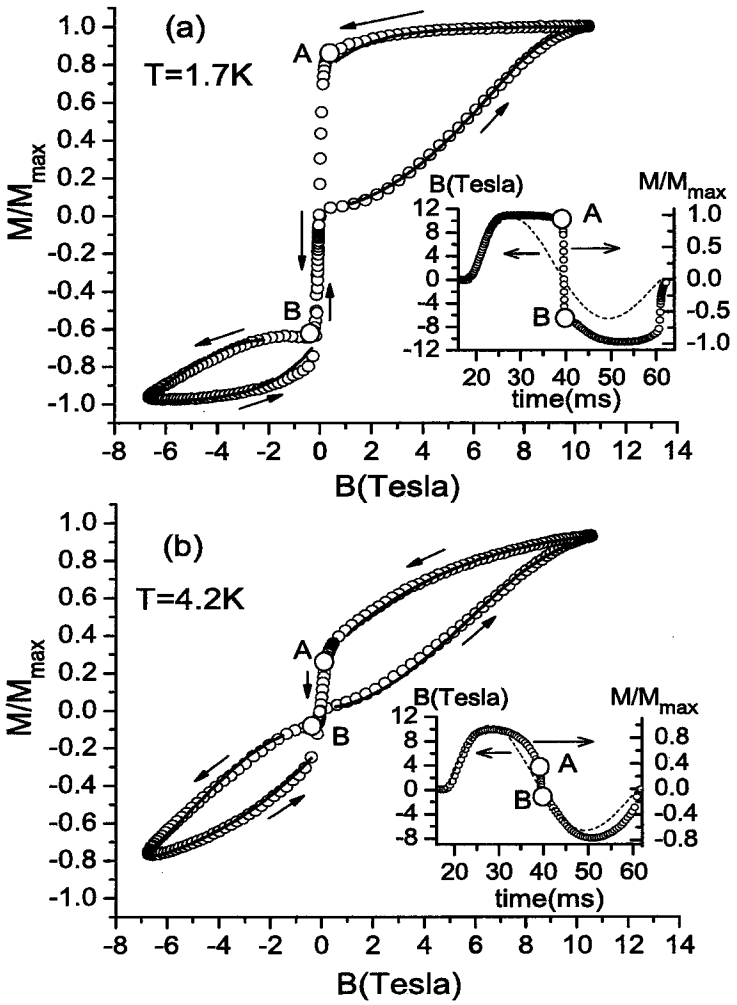

Figure 7.3 Measured magnetization vs magnetic field for $T = 1.7$ K (a) and $T = 4.2$ K (b), for the full-cycle sweep shown in the inset of Figs. 7.3(a) and 7.3(b) (dotted lines). The solid lines are obtained using Eqs. (7.1) and (7.2). The insets also show the measured magnetization (circles) vs time. The LZS transitions occur in the interval between the points A and B.

Ref. [11] and references therein); however, a systematic investigation of this issue is in progress. More generally, it should be noted that, according to the above formula for δt_{LZS}, it is the high sweep rates used in our experiment that ensure that the adiabatic LZS transitions take place over such a short time interval as to be clearly distinct from the hysteresis loops of the thermal relaxation regime.

The origin of LZS transitions in $\{V_6\}$ remains to be discussed. The relatively large estimated value (0.4 K) of the zero-field energy gap Δ for these molecules suggests that its origin cannot be due to dipolar or hyperfine fields. In addition, as explained above, the lowest energy levels of each *independent* triangle are doubly degenerate for $B = 0$ (and not four-fold degenerate as in $\{V_{15}As_6\}$,[8]) consistent with Kramers' theorem. Hence, for $B = 0$ the ground state of such a molecule would consist of four degenerate states, namely the three symmetric states of the $S = 1$ triplet and the antisymmetric $S = 0$ singlet state. Inter-triangle exchange coupling could lift this degeneracy and give rise to avoided level crossings. However, since isotropic inter-triangle exchange cannot account for admixing states of total spin, we suggest that the avoided level crossings are due to the anisotropic (symmetric or antisymmetric) portion. One scenario is given in Fig. 7.1. The behavior of the dynamical magnetization thus involves LZS transitions between (at most) four levels. A detailed theoretical treatment of these transitions will be given elsewhere.

In summary, time-resolved magnetization measurements using sweep rates of order 1 Tesla/ms show hysteresis loops and magnetization steps for $B \approx 0$ in the magnetic molecule $\{V_6\}$. The two effects are clearly distinct because of the relatively high sweep rates used in our experiment. In the absence of both an anisotropy energy barrier and the phonon bottleneck effect, the hysteresis effects exhibited by this molecule occur because the spin relaxation times are of the experimental time scale. Using a generalization of the Bloch equation we were able to reproduce our experimental data for $T = 1.7$ K and $T = 4.2$ K for a large variety of field sweeps, and thus identify direct one-phonon resonant transitions among the Zeeman-split doublet of each triangle as the dominant mechanism underlying the hysteresis behavior. The main assumption of our model, namely that the phonons are in equilibrium with the cryostat, should break down for temperatures below 1 K due to the phonon bottleneck effect. In fact, our preliminary data at $T = 0.6$ K indicate that the relaxation rate $1/\tau$ deviates from Eq. (7.2). A systematic investigation of this issue is in progress. The steps of the magnetization for $B \approx 0$ are attributed to adiabatic LZS transitions between lowest magnetic energy levels impacted by the existence of anisotropic inter-triangle exchange interaction of order 0.4 K. This estimate is consistent with that previously suggested by NMR data.[1] A more precise value of Δ could possibly be determined by specific heat measurements,[12] or by Electron Paramagnetic Resonance (EPR) techniques. The small

departures from complete magnetization reversal suggests that one cannot entirely neglect the role of the heat bath. More generally, exploring nanomagnets with pulsed magnetic fields can reveal a variety of fascinating dynamical phenomena and provide microscopic information that otherwise is not readily accessible.

Ames Laboratory is operated for the U.S. Department of Energy by Iowa State University under Contract No. W-7405-Eng-82.

References

[1] M. Luban *et al.*, Phys. Rev. B **66**, 054407 (2002).

[2] L. Landau, Phys. Z. Sowjetunion **2**, 46 (1932); C. Zener, Proc. R. Soc. London, Ser. A **137**, 696 (1932); E. C. G. Stückelberg, Helv. Phys. Acta **5**, 369 (1932).

[3] S. Miyashita, J. Phys. Soc. Jpn. **64**, 3207 (1995).

[4] A. Abragam and B. Bleaney, *Electron Paramagnetic Resonance of Transition Ions* (Clarendon Press, Oxford, 1970).

[5] S. Miyashita, N. Nagaosa, Prog. Theor. Phys. **106**, 533 (2001).

[6] R. Sessoli, D. Gatteschi, A. Caneschi, and M. A. Novak, Nature (London) **365**, 141 (1993).

[7] C. Sangregorio *et al.*, Phys. Rev. Lett. **78**, 4645 (1997).

[8] I. Chiorescu *et al.*, Phys. Rev. Lett. **84**, 3454 (2000); Phys. Rev. B **67**, 020402(R) (2003).

[9] F. Bloch, Phys. Rev. **70**, 460 (1946); **102**, 104 (1956); **105**, 1206 (1957).

[10] I. Rousochatzakis and M. Luban (unpublished)

[11] M. Nishino, K. Saito and S. Miyashita, Phys. Rev. B **65**, 014403 (2001).

[12] M. Affronte *et al.*, Phys. Rev. Lett. **88**, 167201 (2002); Phys. Rev. B **68**, 104403 (2003).

8. Master Equations for pulsed magnetic fields: Application to magnetic molecules

A paper published in Physical Review B[1]

Ioannis Rousochatzakis and Marshall Luban

Department of Physics and Astronomy and Ames Laboratory, Iowa State University, Ames, Iowa 50011, USA

Abstract

We extend spin-lattice relaxation theory to incorporate the use of pulsed magnetic fields for probing the hysteresis effects, magnetization steps (LZS effect) and magnetization plateaus exhibited, at low temperatures, by the dynamical magnetization of magnetic molecules. The main assumption made is that the lattice degrees of freedom equilibrate in times much shorter than both the experimental time scale (determined by the sweep rate) and the typical spin-lattice relaxation time. We first consider the isotropic case (a magnetic molecule with a ground state of spin S well separated from the excited levels and also the general isotropic Heisenberg Hamiltonian where all energy levels are relevant) and then we include small off-diagonal terms in the spin Hamiltonian to take into account the Landau-Zener-Stückelberg (LZS) effect. In the first case, and for an $S = 1/2$ magnetic molecule we arrive at the generalized Bloch equation, recently used for the magnetic molecule $\{V_6\}$ in Phys. Rev. Lett. **94**, 147204 (2005). An analogous equation is derived for the magnetization, at low temperatures, of antiferromagnetic ring systems. The LZS effect is discussed for magnetic molecules with a low spin ground state, for which we arrive at a very convenient set of equations that take into account the combined effects of LZS and thermal transitions. In particular, these equations explain the deviation from exact magnetization reversal at $B \approx 0$ observed in $\{V_6\}$. They also account for the small magnetization plateaus ("magnetic Foehn effect"), following the LZS steps, that have been observed in several magnetic molecules. Finally, we discuss the role of the Phonon Bottleneck effect at low temperatures and specifically we indicate how this can give rise to a pronounced Foehn effect.

[1]Reprinted with permission of Phys. Rev. B **72**, 134424 (2005)

8.1 Introduction

The subject of magnetic molecules has attracted much attention both for its scientific importance for studying fundamental issues in nanomagnetism as well as for potential applications. Within each molecular unit are embedded a finite number of magnetic ions, coupled via Heisenberg super-exchange interactions. Furthermore, the intermolecular magnetic interactions are of dipolar origin and can usually be neglected. As a result, measurements on crystalline samples reflect the magnetic properties of isolated individual molecules, with its most prominent feature, arising from the finite number of magnetic ions, being the appearance of a discrete magnetic energy level spectrum.

This feature of the spectrum is reflected in the relaxational behavior which mainly arises from the interaction with environmental degrees of freedom, i.e., a "heat bath", such as phonons: The relaxation times of the dynamical magnetization can become very long even at moderately high temperatures. Specifically, in molecules with a high spin ground state[1–3] (single molecule magnets (SMM's)) an anisotropy energy barrier is responsible for relaxation times as high as $10^3 - 10^5$ sec, whereas in some molecules with a low spin ground state, they are of the order of $10^{-3} - 10^0$ sec for $T \lesssim 4$ K.[4–9] The existence of long relaxation times becomes manifest through the appearance of dynamical hysteresis effects when using pulsed magnetic fields, and this is one of the most exciting phenomena observed in magnetic molecules. Clearly, the hysteresis behavior is observable when the experimental time scale τ_e (determined by the field sweep rate) is in the regime of the spin-lattice relaxation times (or shorter). This opportunity is available for magnetic molecules in conjunction with the current experimental capability of using strong magnetic fields with sweep rates as high as 1 Tesla/ms.[6–9]

Another effect manifested in pulsed field measurements, is the appearance of abrupt magnetization steps at given fields.[1–3, 6–9] These steps are quantum-mechanical in origin and reveal the existence of small, off-diagonal terms in the spin Hamiltonian which in turn give rise to avoided level crossings in the magnetic energy spectrum and to Landau-Zener-Stückelberg (LZS)[10, 11] transitions. The origin of these interactions may be single-ion anisotropy or anisotropic exchange. The characteristic energy splitting δ of the LZS effect varies greatly among magnetic molecules. For instance, in SMM's due to the large spin of the ground state, δ/k_B can be of order 10^{-7} K (as usual, k_B stands for Boltzmann's constant), whereas in molecules with low spin ground state, typically $\delta/k_B \sim 0.1$ K.[4, 6] This implies that for currently available sweep rates one can probe the non-adiabatic regime in SMM's,[12] whereas in molecules with low spin ground states we are already in the extreme adiabatic regime. Experimentally, and for the molecules with low spin ground states, there have been observed deviations from the pure quantum-mechanical prediction regarding the height of the steps that have been associated with the

role of dissipation within the LZS regime.

Of particular interest is also another effect induced by dynamic fields, namely the appearance of small plateaus[4, 8, 9] in $M(t)$ following each magnetization step, thus giving rise to satellite peaks in dM/dB. It has been first shown[4] for the low temperature experiments on the magnetic molecule $\{V_{15}\}$ that the origin of these plateaus is the Phonon Bottleneck (PB) effect.[4, 5, 13, 14] Numerically solving a quantum master equation that had been previously derived for static fields, Saito and Miyashita[15] provided an alternative viewpoint of this effect, which they termed "the magnetic Foehn effect": They suggested that this behavior is widespread whether or not one is in the PB regime and that it is a consequence (or an "after-effect") of the LZS transitions. As it turns out (see Sec. 8.4 below), the PB effect can give rise to an enhancement of the Foehn effect. This has been recently observed experimentally and will be reported elsewhere.[16]

At present, a first-principles account of such relaxational phenomena in magnetic molecules induced by dynamical magnetic fields is lacking. Our main goal is to show that one can generalize the conventional spin-lattice relaxation theory in the context of pulsed fields studies of magnetic molecules. The present work is devoted to (and motivated by) pulsed field studies of molecules with a low spin ground state: The simplicity of these systems, apart from providing a basis for better understanding the main physical ideas, allows one to directly compare the predictions of the generalized theory with experimental data. Hence, these systems, when subject to pulsed fields, provide a convenient means for obtaining information on the various relaxational processes and microscopic interactions present in all nanomagnetic systems.

One such system is the $(S = 1/2)$ magnetic molecule $\{V_6\}$,[6, 17] which shows both pronounced hysteresis loops as well as nearly complete reversals of the magnetization at $B \approx 0$. The hysteresis loops have been accurately reproduced[6] using a generalization of the standard[13, 18, 19] Bloch equation which in turn revealed that the one-phonon acoustic process is the dominant relaxation mechanism at low temperatures, and in addition provided an estimate of the spin-phonon coupling energy. The first-principles derivation of this equation is provided here within the more general context of our analysis. On the other hand, the abrupt magnetization reversals at $B \approx 0$ were interpreted as the result of adiabatic LZS transitions originating from the existence of a small (~ 0.4 K) intra-molecular, anisotropic exchange. The small deviation from the pure quantum-mechanical prediction of complete magnetization reversal was attributed to dissipation effects inside the LZS regime, but no quantitative account was given in Ref. [6]. This effect is also analyzed in the present work.

Another class of molecules with low spin ground state where the generalized theory can be easily

applied is that of the antiferromagnetic (AFM) ring systems at low T. These are magnetic molecules comprising an even number of uniformly spaced metal ions arranged as a planar ring (see for example Refs. [20–24]). The AFM exchange interactions give rise, to a non-magnetic $S = 0$ ground state, a first excited $S = 1$ triplet state, etc. In addition to their hysteretic behavior, these systems can show several magnetization steps and sometimes the small magnetization plateaus mentioned above.[8, 9] As we show below, the present work accounts for these dynamical effects in a general way.

The organization of this chapter is the following. In Sec. 8.2 we develop the spin-lattice relaxation theory in pulsed fields for magnetic molecules with a spin S ground state that is well separated from the excited levels. We arrive at a generalization of the standard master equations and show how these lead to the generalized Bloch equation for the case of $S = 1/2$ mentioned above. In Sec. 8.3 we extend this theory to include the general isotropic Heisenberg Hamiltonian where all energy levels are relevant. We apply this to AFM rings at low T and for fields around the first level-crossing field value, where they behave as two-level systems. We provide the treatment of dissipative LZS transitions in Sec. 8.4. This is done for the case of a level anti-crossing between two levels with different magnetic quantum numbers. We apply the resulting theory to the spin 1/2 case and that of AFM rings at low T, and demonstrate how this theory accounts for the deviation from the quantum-mechanical prediction for the magnetization steps as well as the formation of the plateaus mentioned above (Foehn effect). In this way, in particular, we provide an explanation for the deviation from exact magnetization reversal observed in $\{V_6\}$.[6] We also indicate the role of the PB effect at low T, and specifically how it can give rise to a pronounced Foehn effect. Finally, in Sec. 8.5, we provide a brief discussion and summary of the present work.

8.2 Master equations for spin S

We first consider a magnetic molecule with a ground state of definite total spin S, well separated from the excited levels.[2] We assume that the temperature is low enough and the field regime covered is well below the lowest level-crossing field, so that we only need to consider the ground state spin S level. We focus on the isotropic case i.e., we do not consider non-diagonal terms in the spin Hamiltonian.

We employ the standard[25–27] method of treating both the spin and the bath degrees of freedom quantum-mechanically. The Hamiltonian of the combined system (spin S + heat bath) is written as

$$H(t) = H_s(t) + H_B + V \ , \tag{8.1}$$

[2]The same theory can be applied to independent paramagnetic ions with total spin S (see for example Ref. [29]).

where $H_s(t) = \hbar\gamma B(t) S_z \equiv \hbar f(t) S_z$ corresponds to the Zeeman energy, H_B is the bath Hamiltonian, and V is the spin-bath coupling. As usual, $\gamma = g\mu_B/\hbar$ denotes the electronic gyromagnetic ratio. In our notation, $f(t) = \gamma B(t)$ has units of frequency and the spin operators are taken to be dimensionless. Typical sweep forms are shown in figures below; the experimental sweep time τ_e can be as short as 1 ms.

For our purposes it is unnecessary to specify the detailed form of the interaction V, however, it can always be written in the general form

$$V = \hbar \sum_q A_q \otimes R_q \ , \tag{8.2}$$

where A_q (R_q) are hermitian operators of the spin (bath) system. This coupling may, for example, originate from the modulation of the exchange coupling terms (between the individual magnetic ions of the molecule) or the modulation of the interaction of each individual ion with its local environment (e.g. the crystal field) which dynamically affects the spin degrees of freedom through the spin-orbit coupling.[14, 28, 30] In both cases, the modulation originates from lattice deformations, i.e., phonons. The terms bath and environmental degrees of freedom will be understood to mean phonons.

The equation of motion for the density matrix $\rho_{tot}(t)$ of the combined system follows the von Neumann equation[25–27]

$$\dot{\rho}_{tot}(t) = -i[H(t)/\hbar, \rho_{tot}(t)] \ . \tag{8.3}$$

We switch to the interaction picture

$$\widetilde{\rho}_{tot} = e^{i(F(t)S_z + H_B t/\hbar)} \ \rho_{tot} \ e^{-i(F(t)S_z + H_B t/\hbar)} \ , \tag{8.4}$$

where $F(t) \equiv \int_0^t f(t')\, dt'$. The equation satisfied by $\widetilde{\rho}_{tot}$ is

$$\dot{\widetilde{\rho}}_{tot}(t) = -i[\widetilde{V}(t)/\hbar, \widetilde{\rho}_{tot}(t)] \ , \tag{8.5}$$

where we have defined

$$\widetilde{V}(t) = \hbar \sum_q \widetilde{A}_q(t) \otimes \widetilde{R}_q(t), \tag{8.6}$$

with $\widetilde{A}_q(t) = e^{iF(t)S_z} \ A_q \ e^{-iF(t)S_z}$, and similarly $\widetilde{R}_q(t) = e^{iH_B t/\hbar} \ R_q \ e^{-iH_B t/\hbar}$. Now, all the relevant information about the spin system is contained in the so-called reduced density matrix $\rho(t) \equiv \mathrm{Tr}_b \ (\rho_{tot}(t))$, since for example

$$< S_z > = \mathrm{Tr}_s \mathrm{Tr}_b \{\rho_{tot}(t) S_z\} = \mathrm{Tr}_s \{\rho(t) S_z\} \ , \tag{8.7}$$

where Tr_s (Tr_b), denotes the partial trace over the spin (bath) degrees of freedom. Thus we are mainly interested in finding an equation of motion for $\rho(t)$. We first make the assumption that the spin-bath

coupling is sufficiently weak so that the Born approximation can be used. Furthermore, we consider temperatures high enough ($T > 1$ K) so that the number of available phonon modes per spin is very large and as a result the phonons equilibrate *independently* from the spins. Given this consideration and the expectation that the phonon relaxation times τ_b (typically $\tau_b < 10^{-6}$ sec) are much shorter than both the experimental time scale τ_e and the spin-lattice relaxation time τ_s, the density matrix of the combined system (spin system + bath) can be factored as $\widetilde{\rho}_{tot}(t) \approx \widetilde{\rho}(t) \otimes \rho_B$, where $\rho_B = e^{-\beta H_B}/Z_B$ describes the stationary state of the heat bath at temperature T. Here Z_B denotes the bath partition function, and $\beta \equiv 1/(k_B T)$. The above factorization of the total density matrix is expected to break down at sufficiently low temperatures (typically $T < 1$ K) where one expects the phonon bottleneck (PB) effect[4, 13, 14] to take place. Employing the above approximations, one arrives at the following integro-differential equation of motion for $\widetilde{\rho}$,[25–27]

$$\dot{\widetilde{\rho}}(t) = \frac{1}{\hbar^2} \int_0^t du \; \mathrm{Tr}_b[[\widetilde{V}(u), \widetilde{\rho}(u) \otimes \rho_B], \widetilde{V}(t)] \; . \tag{8.8}$$

We denote the adiabatic eigenvalues of $H_s(t)$ by $\epsilon_M(t) = \hbar f(t) M$, where $M = -S, \ldots, S$. The adiabatic excitation frequencies of $H_s(t)$ are of the form $\omega_\mu(t) = f(t)\mu$, where $\mu = -2S, \ldots, 2S$. Now, for a given operator A_a of the spin system it is very convenient to construct the so-called eigenoperator $A_{a,\mu}$ corresponding to a given excitation frequency $\omega_\mu(t)$ as

$$A_{q,\mu} \equiv \sum_{M,M'} (A_q)_{MM'} |M><M'| \; \delta_{M'-M,\mu} \; , \tag{8.9}$$

where δ_{ij} denotes the Kronecker delta symbol. These operators obey the equation

$$A_q = \sum_\mu A_{q,\mu} \; , \tag{8.10}$$

where the sum extends over all possible integers μ. The reason for introducing the eigenoperators $A_{q,\mu}$ is that they take a very simple form in our interaction picture, namely

$$\widetilde{A}_{q,\mu}(t) = e^{-iF(t)\mu} \; A_{q,\mu} \; . \tag{8.11}$$

We note in particular that for a static external field B_0, we have $F(t) = \omega_0 t$, where $\omega_0 \equiv \gamma B_0$ and the phase factor in Eq. (8.11) becomes the familiar form $\exp(-i\omega_0 t)$. In the present case, Eq. (8.8) along with Eqs. (8.6), (8.10) and (8.11) and the variable change $u \longrightarrow t - u$, give

$$\begin{aligned} \dot{\widetilde{\rho}}(t) = \sum_{qq',\mu\mu'} \int_0^t du e^{-iF(t)\mu'} e^{-iF(t-u)\mu} (A_{q',\mu} \widetilde{\rho}(t-u) A_{q,\mu'} \\ - A_{q,\mu'} A_{q',\mu} \widetilde{\rho}(t-u)) < \widetilde{R}_q(u) \widetilde{R}_{q'}(0) >_B + h.c., \end{aligned} \tag{8.12}$$

where the quantities in angular brackets

$$< \widetilde{R}_q(u)\widetilde{R}_{q'}(0) >_B \equiv \mathrm{Tr}_b(\rho_B \widetilde{R}_q(u)\widetilde{R}_{q'}(0)) \ , \tag{8.13}$$

are equilibrium time correlation functions of the bath, and the symbol $h.c.$ denotes hermitian conjugate. As mentioned already, $\tau_b << \tau_s, \tau_e$. This allows one to perform the following simplifications. First, we may extend the upper limit of integration in Eq. (8.12) to infinity. Second, the variation of $\widetilde{\rho}(t-u)$ in the time scale of τ_b is extremely small (since $\tau_s >> \tau_b$), so it is justified to perform the usual Markov approximation,[25–27] namely we replace $\widetilde{\rho}(t-u)$ by $\widetilde{\rho}(t)$. Similarly, the variation of $F(t-u)$ in the time scale of τ_b is also small. Therefore we may approximate $F(t-u)$ by

$$F(t-u) \approx F(t) - u \cdot \dot{F}(t) = F(t) - uf(t) \ , \tag{8.14}$$

i.e., by a Taylor expansion through first order in u. The neglect of higher order terms is valid since $u^2\dot{f}(t) << uf(t)$, is equivalent to $\tau_b << \tau_e$ (with τ_b taken as the maximum value of u, and τ_e as a typical value of $f/\dot{f}$). Substituting Eq. (8.14) into Eq. (8.12), we obtain

$$\dot{\widetilde{\rho}}(t) = \sum_{qq',\mu\mu'} e^{-iF(t)(\mu'+\mu)} \Gamma_{qq'}(\omega_\mu(t)) \times (A_{q',\mu}\widetilde{\rho}(t)A_{q,\mu'} - A_{q,\mu'}A_{q',\mu}\widetilde{\rho}(t)) + h.c. \ , \tag{8.15}$$

where we define the bath correlation functions, evaluated at the time-dependent frequency $\omega_\mu(t)$, as

$$\Gamma_{qq'}(\omega_\mu(t)) \equiv \int_0^\infty du \ e^{i\omega_\mu(t)\ u} < \widetilde{R}_q(u)\widetilde{R}_{q'}(0) >_B \ . \tag{8.16}$$

We emphasize that the 'adiabatic' $\omega_\mu(t)$ factor in Eq. (8.16) originates from the second term in the Taylor expansion of $F(t-u)$ and it has important implications in what follows. In particular, since $\omega_\mu(t)$ is proportional to the instantaneous field $B(t)$, it will lead to an equation of motion with relaxation rates that depend explicitly on $B(t)$.

We further adopt the so-called rotating wave approximation (RWA):[25–27] The relative rate of change of a typical phase factor of Eq. (8.15), with $\mu + \mu' \neq 0$ is proportional to $\gamma B(t)$ which is of order 10^{11} s^{-1} (for $B \sim 1$ Tesla). This implies that such non-secular terms "oscillate" very rapidly during the experimental time scale, and thus do not appreciably contribute to the dynamics in Eq. (8.15).[3] Thus, by retaining only the terms with $\mu' = -\mu$, we may replace Eq. (8.15) by

$$\dot{\widetilde{\rho}}(t) = \sum_{qq',\mu} \Gamma_{qq'}(\omega_\mu(t))(A_{q',\mu}\widetilde{\rho}(t)A_{q,-\mu} - A_{q,-\mu}A_{q',\mu}\widetilde{\rho}(t)) + h.c. \ . \tag{8.17}$$

[3]This holds true as long as $B(t)$ remains nonzero; in the level-crossing regime, $B(t) \approx 0$, the RWA is not strictly valid. However, the time interval δt over which the non-secular terms cannot be neglected is extremely small compared to the experimental time scale: For $\tau_e \sim 1$ ms one gets $\delta t \sim 10^{-8}$ ms and therefore, given the much slower relaxation rates τ_s, the inclusion of these terms does not change anything in such a small time interval. Hence, the RWA can be safely used for all fields, even the level-crossing regime.

This is our generalized master equation in the weak coupling and RWA limit and for slowly changing (compared to τ_b) external fields.

Before we discuss the major consequences of this generalized master equation, we go one step further and derive the equations of motion for the populations ρ_{MM} of the various states $|M>$. Using the matrix elements

$$(A_{q,\mu})_{MM'} = (A_q)_{MM'}\delta_{M'-M,\mu}, \tag{8.18}$$

and the relation $\widetilde{\rho}_{MM} = \rho_{MM}$, one finds that the populations decouple from the non-diagonal terms and evolve according to the following generalization of the standard Pauli master equation

$$\dot{\rho}_{MM} = \sum_{M'} W_{M'M}(t)\rho_{M'M'} - \sum_{M'} W_{MM'}(t)\rho_{MM} \ . \tag{8.19}$$

The transition rates $W_{M\to M'} \equiv W_{MM'}$ are defined as

$$W_{MM'} = \sum_{q,q'} \gamma_{qq'}(\omega_{MM'}(t))(A_q)_{MM'}(A_{q'})_{M'M}, \tag{8.20}$$

where $\hbar\omega_{MM'} \equiv \epsilon_M - \epsilon_{M'}$, and

$$\gamma_{qq'}(\omega) \equiv \Gamma_{qq'}(\omega) + \Gamma^*_{q'q}(\omega) = \int_{-\infty}^{+\infty} du e^{i\omega u} < \widetilde{R}_q(u)\widetilde{R}_{q'}(0) >_B \ . \tag{8.21}$$

An important property of the transition rates is the detailed balance condition that arises from the following quantum property[25–27] of the (stationary) bath correlation functions appearing in Eq. (8.21)

$$\gamma_{qq'}(-\omega) = \exp(-\beta\hbar\omega)\gamma_{q'q}(\omega) \ . \tag{8.22}$$

The detailed balance condition follows straightforwardly from Eq. (8.20) along with Eq. (8.22)

$$W_{M'M} = \exp(-\beta\hbar\omega_{MM'})W_{MM'} \ . \tag{8.23}$$

We have now arrived at the main results of this Section. A comparison with the standard relaxation theory (for static fields) shows clearly the physics underlying the generalization made here: Equation (8.20) involves transition rates that depend on the adiabatic energy excitations of the spin system, which in turn are proportional to $B(t)$. All information about specific details of relaxation mechanisms is contained in the bath correlation functions as well as the matrix elements $(A_q)_{MM'}$ (see Eq. (8.20)).

Reviewing our derivation, the key assumption made is that the bath degrees of freedom equilibrate *independently* from the spins in times $\tau_b << \tau_e, \tau_s$. The basis of this assumption is that the number of available environmental modes per spin is so large that the bath can be considered to be a large reservoir, hence allowing the neglect of any feedback from the spin dynamics. This allowed the decomposition

$\rho_{tot}(t) \approx \rho(t) \otimes \rho_B$ and also the Taylor expansion (particularly the second term) in Eq. (8.14). Despite the intuitive appeal of this assumption, it must be checked by comparing the predictions of the resulting theory with experimental data.

A simple, realistic system where the present theory is easily applicable and is in fact in excellent agreement with experimental data (for $T > 1.5$ K) is the magnetic molecule $\{V_6\}$,[6] mentioned in the Introduction. It is straightforward to show that the generalized Bloch equation used in Ref. [6], to reproduce the experimental data for this $S = 1/2$ system follows immediately from the present theoretical framework: For $S = 1/2$, the equation of motion (Eq. (8.19)) for the populations of the spin-up ($|+>$) and spin-down ($|->$) states reads

$$\dot{\rho}_{++} = W_{-+}(t)\rho_{--} - W_{+-}(t)\rho_{++} \ ,$$
$$\dot{\rho}_{--} = W_{+-}(t)\rho_{++} - W_{-+}(t)\rho_{--} \ . \tag{8.24}$$

On using the normalization condition $\rho_{++} + \rho_{--} = 1$, and the detailed balance condition $W_{+-} = \exp(\beta\hbar\Omega)W_{-+}$ (here $\Omega \equiv \gamma B$) one finds that the magnetic moment per spin, $M \equiv -\hbar\gamma < S_z >$, follows the equation

$$\dot{M}(t) = \frac{1}{\tau_s(T, B(t))} \left(M_{eq}(T, B(t)) - M(t)\right) \ , \tag{8.25}$$

where $M_{eq} = (\hbar\gamma/2)\tanh(\beta\hbar\Omega/2)$ and and $1/\tau_s = W_{-+}\left(1 + \exp(\beta\hbar\Omega)\right)$. This is the generalized Bloch equation that was used in Ref. [6]. Its physical interpretation is that $M(t)$ relaxes towards the instantaneous equilibrium value $M_{eq}(T, B(t))$ with a relaxation rate that depends explicitly on $B(t)$.

In principle one can invert Eq. (8.25) and extract $1/\tau_s$ in terms of $M(t)$ and $\dot{M}(t)$ obtained by experiment and the adiabatic equilibrium magnetization $M_{eq}(T, B(t))$. Alternatively, one can directly compare the experimental data with a numerical solution of Eq. (8.25) by choosing a physically appropriate functional form of $1/\tau_s(T, B(t))$ and adjusting the free parameters. Due to the explicit dependence of $1/\tau_s$ and M_{eq} on $B(t)$ one can obtain information on the underlying specific relaxation mechanism(s) by using different sweep forms $B(t)$. Along these lines, it was confirmed in Ref. [6] that for the magnetic molecule $\{V_6\}$ and for $1 < T < 5$ K, the dominant contribution to $1/\tau_s$ is the one-phonon processes term $1/\tau_s^*$ given by

$$1/\tau_s^* = A\Omega(t)^3 \coth\left(\beta\hbar\Omega(t)/2\right) \ , \tag{8.26}$$

with $A = 3V_{sl}^2/(2\pi\hbar\rho v^5)$, where v denotes the sound velocity, ρ the mass density, and V_{sl} the characteristic energy modulation of the given spin-phonon coupling mechanism.[13, 14] Apart from the establishment of the dominant relaxation mechanism at $1 < T < 5$ K, a first estimate of V_{sl} (~ 0.35 K) was obtained. More generally, the excellent agreement of this theory with experimental data signifies

that our starting assumptions are valid for $\{V_6\}$ for $T > 1$ K. However, our main assumption, namely that the phonons remain in equilibrium at all experimental times, can be expected to break down at lower T since the number of available resonant phonons per molecule rapidly decreases on cooling, and the phonon bottleneck (PB) effect[4, 13, 14] takes place. In fact, preliminary data[31] for $\{V_6\}$ at $T = 0.6$ K shows a significant deviation from the theory suggesting the onset of the PB effect.

We remark that the theory of this Section, which is based on the Hamiltonian of Eq. (8.1), cannot account for the magnetization steps observed in $\{V_6\}$ at the level-crossing regime $B \approx 0$. These, however, can in fact be explained in terms of adiabatic LZS transitions. The necessary extension of our theory is given in Sec. 8.4.

8.3 Master equations for the general isotropic Heisenberg model

Here we extend the previous analysis and discuss the general isotropic Heisenberg model where all the energy levels are relevant. The analysis is parallel to the above and straightforward, and thus only the main new points are emphasized.

The Hamiltonian of the combined system (magnetic molecule + heat bath) is again given by Eq. (8.1) where now $H_s(t)$ explicitly includes the Heisenberg exchange Hamiltonian

$$H_0 = \sum_{i<j} J_{ij} \mathbf{S}_i \cdot \mathbf{S}_j \ , \tag{8.27}$$

and where J_{ij} denotes the exchange constants between the spins at sites i and j. The eigenstates $|n>$ of H_s are of the form $|n>=|\nu\ S\ M>$, where ν corresponds to additional quantum numbers. Since H_0 and S_z commute one can define the interaction picture by

$$\widetilde{\rho} = e^{i(H_0 t/\hbar + F(t)S_z)}\ \rho\ e^{-i(H_0 t/\hbar + F(t)S_z)}. \tag{8.28}$$

In addition, the adiabatic energy eigenvalues have the form $\epsilon_n(t) = \epsilon_{0n} + \hbar f(t) M$, where the first term corresponds to the zero-field spectrum of the exchange Hamiltonian (Eq. (8.27)) and the second term to the Zeeman splitting energy. Hence, the adiabatic excitation frequencies are of the form $\omega(t) = \omega_0 + f(t)\mu$, where $\hbar\omega_0 \equiv \epsilon_{0n'} - \epsilon_{0n}$ and $\mu = M' - M$. Thus, any given excitation frequency $\omega(t)$ can be characterized completely by ω_0 and μ. As before, we introduce a set of eigenoperator $A_q(\omega_0, \mu)$ given by

$$A_q(\omega_0, \mu) \equiv \sum_{n,n'} (A_q)_{nn'} |n><n'| \times \delta_{M'-M,\mu}\ \delta(\epsilon_{0n'} - \epsilon_{0n}, \hbar\omega_0) \ , \tag{8.29}$$

which take the following form in the interaction picture,

$$\widetilde{A}_q(\omega_0, \mu) = e^{-i\omega_0 t} e^{-iF(t)\mu} A_q(\omega_0, \mu). \tag{8.30}$$

Employing the same steps as in Sec. 8.2, one arrives at the master equation

$$\dot{\widetilde{\rho}}(t) = \sum_{qq'} \sum_{\omega(t)} \Gamma_{qq'}(\omega(t))(A_{q'}(\omega_0,\mu)\widetilde{\rho}(t)A_q(-\omega_0,-\mu) - A_q(-\omega_0,-\mu)A_{q'}(\omega_0,\mu)\widetilde{\rho}(t)) + h.c. \tag{8.31}$$

Then, using the matrix elements

$$(A_q(\omega_0,\mu))_{nn'} = (A_q)_{nn'}\delta_{M'-M,\mu}\delta(\epsilon_{0n'} - \epsilon_{0n}, \hbar\omega_0) \ , \tag{8.32}$$

one obtains the generalized Pauli equations as before

$$\dot{\rho}_{nn} = \sum_{n'} W_{n'n}(t)\rho_{n'n'} - \sum_{n'} W_{nn'}(t)\rho_{nn} \ , \tag{8.33}$$

where $W_{nn'}$ are given by

$$W_{nn'} = \sum_{qq'} \gamma_{qq'}(\omega_{nn'}(t))(A_q)_{nn'}(A_{q'})_{n'n} \ , \tag{8.34}$$

with $\gamma_{qq'}(\omega)$ as in Eq. (8.21). According to the above analysis, the dynamics of the reduced density matrix has the same major features as in the case of Sec. 8.2, but now with the appropriate and reasonable modification for the excitation frequencies.

As discussed in the Introduction, a class of magnetic molecules where the above analysis can be easily applied is that of AFM rings at low T and for fields in the vicinity of a given level crossing value. Specifically, we will assume $T << \Delta_0/k_B$, where Δ_0 denotes the first, zero-field excitation energy and consider fields in the vicinity of the first level-crossing field ($B_c = \Delta_0/\hbar\gamma$) only, where the singlet $|0,0>$ intersects the $M = -1$ (or $|1,-1>$) level of the $S = 1$ triplet state (see Fig. 8.1(c)); a similar analysis can be employed for fields in the vicinity of higher level crossings. For these temperatures and fields, the AFM rings behave as a two-level system. Hence, we are dealing with a situation that is very similar to the spin 1/2 case, discussed in Sec. 8.2. In fact, one can arrive at the same generalized Bloch equation for $M(t)$ (Eq. (8.25)), where now $M_{eq} = \hbar\gamma \ \mathrm{sech}(\beta\Delta(t)/2)$, and $\Delta(t) \equiv \Delta_0 - \hbar\gamma B(t)$. Similarly, $1/\tau_s$ will depend explicitly on $\Delta(t)$. For instance, the contribution $1/\tau_s^*$ of the one-phonon processes to the relaxation rate is given by Eq. (8.26) with $\Omega(t)$ replaced by $\Delta(t)/\hbar$.

Similarly with the approach followed in Ref. [6] for $\{V_6\}$, finding the physically appropriate functional form for $1/\tau_s$ can be facilitated by comparing the theoretical predictions with experimental data for a variety of field sweeps. We illustrate this idea in Fig. 8.1(a) by showing typical hysteresis loops obtained by numerically solving Eq. (8.25) using two different, commonly used sweeps shown in Fig. 8.1(b). The relaxation is assumed to be driven by one-phonon processes plus a small residual term.

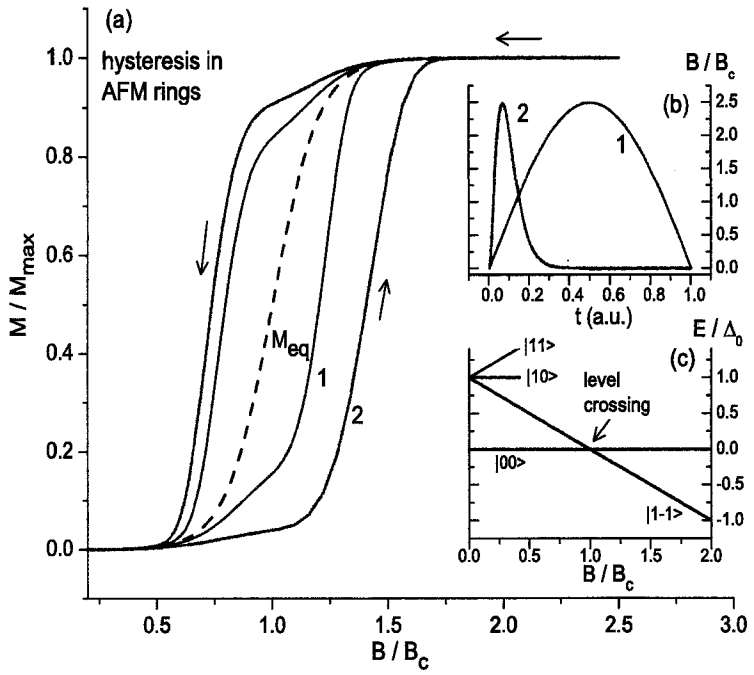

Figure 8.1 Hysteretic behavior of AFM ring systems at low T and for two commonly used sweep forms $B(t)$ shown in Fig. 8.1(b). The loops are obtained by a numerical solution of Eq. (8.25), with M_{eq} given in the text and $1/\tau_s$ taken as the sum of the one-phonon term plus a small residual contribution. All the parameters used are arbitrary. The equilibrium magnetization is denoted by the dashed line. The low-energy diagram and the true level crossing between the two relevant states $|0,0>$ and $|1,-1>$ is shown in Fig. 8.1(c).

Since we have assumed an isotropic Hamiltonian and therefore a true level-crossing at $B \approx B_c$, nothing exciting happens in that regime. Instead, our choice for $1/\tau_s$ gives rise to a plateau for $B \approx B_c$ since in that regime the one-phonon term vanishes and the relaxation is driven only by the small residual term. This is qualitatively different from observations in AFM ring systems such as the dimer $\{Fe_2\}$,[8] and dodecanuclear $\{Fe_{12}\}$,[9] which show a step-like behavior of $M(t)$ and consequently peaks in $dM(t)/dB$ at the level crossing fields. In addition, in some cases, the major peaks are accompanied with small satellite peaks; a small plateau in $M(t)$ is formed after each step (Foehn effect). As we show in the following Section, both of these features, namely the magnetization steps and plateaus can be explained by extending our theory to include small off-diagonal terms in the spin Hamiltonian.

8.4 Dissipative LZS model in the adiabatic regime

We now include small off-diagonal terms in the spin Hamiltonian in order to take into account the combined effect of LZS and thermal transitions. We will consider the adiabatic regime: As mentioned in the Introduction, this is indeed the relevant regime for a large class of molecules with low spin ground state, where the energy splittings are typically of order $\delta/k_B \sim 0.1$ K. In particular, the magnetic molecules $\{V_6\}$[6] and $\{V_{15}\}$[4] as well as the AFM rings fall in this category. Since the effect of the small non-diagonal terms becomes manifest only in the immediate vicinity of the intersection of two[4] energy levels, we are able to construct the following quite adequate theory.

8.4.1 General theory

We consider two energy eigenstates of the isotropic Heisenberg Hamiltonian (denoted as $|m_1>$ and $|m_2>$) with total spins S_1 and S_2 and magnetic quantum numbers m_1 and m_2, respectively, which are coupled by a small off-diagonal (anisotropic) term. This term gives rise to an avoided level crossing between the two energy levels with a small energy gap denoted by δ. For fields in the immediate vicinity of this level anti-crossing, one can write the Hamiltonian in the basis of $|m_1>$ and $|m_2>$, i.e.,

$$H_s(t) = \begin{pmatrix} E_0 + m_1\hbar f(t) & \delta/2 \\ \delta/2 & m_2\hbar f(t) \end{pmatrix} , \tag{8.35}$$

where E_0 denotes the zero-field energy difference between the two states for $\delta = 0$. Without loss of generality, we assume that $m_2 > m_1$, with E_0, δ being real and positive. In the absence of the off-diagonal term (i.e., $\delta = 0$) the two levels cross at the moment when $f = f_c \equiv E_0/\hbar(m_2 - m_1)$. We denote the adiabatic energy levels of $H_s(t)$ by $\epsilon_\pm(t)$ and the corresponding eigenstates by $|\epsilon_\pm; t>$, i.e., $H_s(t)|\epsilon_\pm; t> = \epsilon_\pm(t)|\epsilon_\pm; t>$. In the basis of $|m_1>$ and $|m_2>$, they can be expressed in the convenient parametric form

$$\begin{aligned} |\epsilon_+; t> &= \begin{pmatrix} \cos\theta/2 \\ \sin\theta/2 \end{pmatrix} , \\ |\epsilon_-; t> &= \begin{pmatrix} -\sin\theta/2 \\ \cos\theta/2 \end{pmatrix} , \end{aligned} \tag{8.36}$$

and $\epsilon_\pm(t) = [E_0 + \hbar f(m_1 + m_2) \pm \hbar\Omega]/2$, where

$$\Omega \equiv [(\delta/\hbar)^2 + (m_1 - m_2)^2(f - f_c)^2]^{1/2}. \tag{8.37}$$

[4]For $\{V_6\}$, as explained in Ref. [6], the number of intersecting energy levels at $B \approx 0$ is four.

The time-dependent parameter θ is given by

$$\theta = \tan^{-1} \frac{\delta/\hbar}{(m_1 - m_2)(f - f_c)} , \tag{8.38}$$

and extends from 0 to π as f goes from $-\infty$ to $+\infty$. In particular, $\theta \approx \pi/2$ when f is in the immediate vicinity of f_c.

As in Secs. 8.2 and 8.3, we switch to the interaction picture

$$\widetilde{\rho} \equiv U_s^{\dagger} \rho U_s , \tag{8.39}$$

where $U_s(t)$ is the evolution operator for the spin Hamiltonian $H_s(t)$ alone, which obeys $i\hbar \dot{U}_s = H_s(t) U_s$. Contrary to the previous isotropic cases, it is clear that due to the presence of two non-commuting terms in $H_s(t)$ the form of $U_s(t)$ cannot be written in a closed analytical form (compactly written, $U_s(t) = T\exp(-i \int_{-\infty}^{t} dt' H_s(t'))$, where T denotes the chronological operator). Thus, an analysis parallel to that of the previous sections cannot be readily employed. Nevertheless, it is possible to circumvent this difficulty by exploiting the fact that we are in the adiabatic regime. According to the adiabatic theorem one has

$$U_s(t)|\alpha; -\infty >= e^{-i\phi_\alpha(t)}|\alpha; t >, \tag{8.40}$$

where the phases $\phi_\alpha(t)$ are given by $\phi_\alpha(t) = \int_{-\infty}^{t} \epsilon_\alpha(t')dt'/\hbar$. As we mentioned before, adiabaticity holds even inside the LZS regime.

We now express the spin operators A_q appearing in the spin-phonon interaction term V (Eq. (8.2)), in the adiabatic basis as

$$A_q = \sum_{\alpha,\beta} A_q^{\alpha\beta}(t)|\alpha; t >< \beta; t|, \tag{8.41}$$

where $A_q^{\alpha\beta}(t) \equiv < \alpha; t|A_q|\beta; t >$. In the interaction picture these take the form

$$\widetilde{A}_q(t) = \sum_{\alpha,\beta} A_q^{\alpha\beta}(t) e^{i(\phi_\alpha(t) - \phi_\beta(t))}|\alpha; -\infty >< \beta; -\infty| . \tag{8.42}$$

Following the previous steps, it is straightforward to derive an expression similar to Eq. (8.12), where one encounters typical matrix elements such as $A_q^{\alpha\beta}(t-u)$ and phase factors of the form $e^{i\phi_\alpha(t-u)}$. The next step is to approximate $A_q^{\alpha\beta}(t-u) \approx A_q^{\alpha\beta}(t)$, and also to make a Taylor expansion of the phases in first order in u, as before, i.e.,

$$\phi_\alpha(t-u) \approx \phi_\alpha(t) - u\, \epsilon_\alpha(t)/\hbar. \tag{8.43}$$

It is then possible to obtain the following set of Pauli master equations by introducing the representation $\widetilde{\rho}_{\alpha\beta}(t) \equiv < \alpha; -\infty|\widetilde{\rho}(t)|\beta; -\infty >$, and then performing the RWA,

$$\dot{\widetilde{\rho}}_{\alpha\alpha} = W_{\beta\alpha}(t)\widetilde{\rho}_{\beta\beta} - W_{\alpha\beta}(t)\widetilde{\rho}_{\alpha\alpha}, \tag{8.44}$$

where the transition rates $W_{\alpha\beta}$ are now given by

$$W_{\alpha\beta}(t) = \sum_{qq'} A_q^{\alpha\beta}(t) A_{q'}^{\beta\alpha}(t) \gamma_{qq'}(\omega_{\alpha\beta}(t)), \tag{8.45}$$

and $\gamma_{qq'}(\omega)$ as in Eq. (8.21). We now compare this expression for the transition rates with the corresponding ones found previously. The new ingredient here is the extra time dependence of the transition rates carried by the matrix elements $A_q^{\alpha\beta}(t)$. Clearly this results from the explicit time dependence of the adiabatic energy states. Physically this means, for example, that longitudinal fluctuating fields (contained in V) can become effective in inducing transitions between the two levels inside the LZS regime because of the admixing of the two states. This introduces an additional complication when one attempts to quantitatively account for magnetization data inside the LZS regime.

It turns out that one can obtain a simplified Bloch type of equation for the quantity $n(t) \equiv \widetilde{\rho}_{--} - \widetilde{\rho}_{++}$, in terms of which the magnetization can be simply expressed. Using the above master equations and the normalization condition $\widetilde{\rho}_{--} + \widetilde{\rho}_{++} = 1$, one arrives at the following equation for $n(t)$

$$\dot{n}(t) = \frac{1}{\tau_s(t)} [n_{eq}(t) - n(t)] \ , \tag{8.46}$$

where $n_{eq} = \tanh(\beta\hbar\Omega/2)$, $1/\tau_s = W_{-+}\left(1 + e^{\beta\hbar\Omega}\right)$. In order to express $< S_z >= \mathrm{Tr}\{\rho S_z\}$ in terms of $n(t)$ one notes that

$$< S_z >= \sum_{\alpha,\beta} < \alpha; t|\rho|\beta; t > S_z^{\beta\alpha}(t) = \sum_{\alpha,\beta} e^{i(\phi_\beta(t) - \phi_\alpha(t))} \widetilde{\rho}_{\alpha\beta} S_z^{\beta\alpha}(t) \ . \tag{8.47}$$

Now, for the longitudinal magnetization one can safely repeat the RWA by neglecting the terms with $\alpha \neq \beta$. Then $< S_z > \approx \widetilde{\rho}_{--} S_z^{--} + \widetilde{\rho}_{++} S_z^{++}$, or for the magnetization M,

$$M \approx \frac{-\hbar\gamma}{2} [(m_1 + m_2) - (m_2 - m_1)^2 n(t) \frac{f - f_c}{\Omega}] \ . \tag{8.48}$$

Equations (8.46) and (8.48) are of central importance for describing the combined effects of LZS and thermal transitions.[5] According to Eq. (8.48), the magnetization is given in terms of two distinct quantities, namely the ratio $(f - f_c)/\Omega$ and $n(t)$. Interestingly, the factor $(f - f_c)/\Omega$, carries the physics of the purely quantum LZS effect, since it changes sign inside the LZS regime as expected in the adiabatic regime of the LZS transitions. On the other hand, the quantity $n(t)$ contains all information about thermal transitions and dissipation since its dynamics is determined by the spin-bath coupling according to Eq. (8.46).

[5]It is noted that the analysis of Ref. [15], which is based on a quantum master equation previously developed for static fields, provides an alternative set of phenomenological equations, to be contrasted to Eqs. (8.46) and (8.48) that we derived from first-principles.

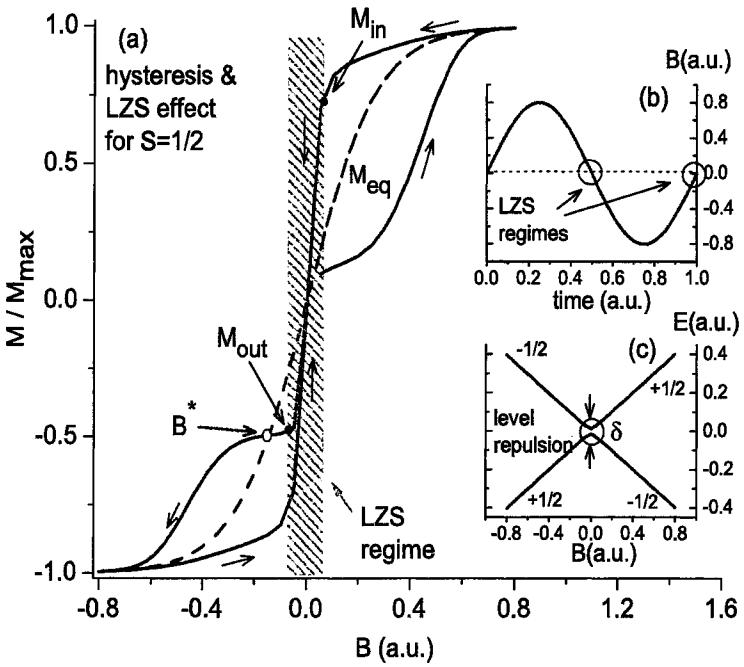

Figure 8.2 Hysteresis and LZS effect at $B \approx 0$ for the case of an S=1/2 magnetic molecule, as obtained by solving numerically our equations (see text) for the full-cycle sweep shown in Fig. 8.2(b). The shaded area indicates the LZS regime. The equilibrium magnetization is denoted by the dashed line. Note the deviation from the exact magnetization reversal at $B \approx 0$ as described in the text, and the formation of the small plateau after the step. B^* denotes the field at which M crosses M_{eq}, as discussed in the text. The low-energy diagram and the level anti-crossing between the two levels $|-1/2>$ and $|+1/2>$ is shown in Fig. 8.2(c). The small circles in Figs. 8.2(b) and 8.2(c) indicate the LZS regimes, where the magnetization steps take place.

8.4.2 Qualitative analysis

We will now give a qualitative analysis of the predictions of this theory by examining the general structure of Eqs. (8.46) and (8.48). We will also demonstrate the main ideas by providing numerical solutions for typical examples, namely the $S = 1/2$ case and that of AFM rings at low T. These are shown in Figs. 8.2, 8.4 and in Fig. 8.3, respectively. For these solutions, we have assumed that $1/\tau_s$ is the sum of the one-phonon process contribution plus a small residual term to account for the relaxation inside the LZS regime. The parameters chosen are somewhat arbitrary; the exact shape of the M vs B curves is determined by the actual parameters of a given system (magnitude of δ, spin-phonon coupling terms, etc). As explained below, Eqs. (8.46) and (8.48) account nicely for all the dynamical effects shown in pulsed field measurements, namely hysteresis loops (already discussed in Secs. 8.2 and 8.3) outside the LZS regime, the thermal deviation of the LZS steps from the pure quantum-mechanical prediction (see in particular Figs. 8.2 and 8.3), as well as the formation of magnetization plateaus (Foehn effect) immediately after exiting the LZS regime (see Figs. 8.2 and 8.3, but mostly Fig. 8.4). Furthermore, we will discuss how the PB effect, which takes place at very low T, can give rise to an enhancement of the Foehn effect.

8.4.2.1 Hysteresis loops

We begin by noting that for either $\delta = 0$ or for fields outside the LZS regime one has $(f - f_c)/\Omega \propto \mathrm{sgn}(f - f_c)$ and therefore the only time dependence of M stems from the quantity $n(t)$. In addition, all matrix elements $A_q^{\alpha\beta}$ appearing in Eq. (8.45) become time-independent. Then, by taking the time derivative of Eq. (8.48), one recovers the results for the isotropic case, and in particular the generalized Bloch equation, Eq. (8.25), derived before for the case of $S = 1/2$ and that of the AFM rings at low T. Thus, as expected, one can neglect the LZS effect for fields outside the immediate vicinity of level crossings. This justifies the use of Eq. (8.25) in Ref. [6], for fields away from $B \approx 0$. Typical hysteresis loops for fields outside the LZS regime are shown in Figs. 8.2(a) and 8.3(a) for the $S = 1/2$ case and that of AFM rings at low T, respectively. One should note that although the magnetization obeys the same generalized Bloch equation (Eq. (8.25)) for either $\delta = 0$ or for $\delta \neq 0$ but for fields outside the LZS regime, the solution is drastically different for these two cases (compare for example Figs. 8.1 and 8.3, for the case of AFM rings). This is because, when $\delta \neq 0$, the occurrence of an LZS step introduces a different (as compared to the $\delta = 0$ case) initial condition immediately after exiting the LZS regime. A direct consequence of this is the Foehn effect discussed below.

8.4.2.2 Thermal corrections to the LZS step

A deviation from the exact quantum-mechanical prediction regarding the magnetization step at $f \approx f_c$, is expected to arise from thermal transitions inside the LZS regime. This can be seen as follows. Assuming that one crosses f_c from below, and denoting by M_{in} and M_{out} the magnetization when entering and when exiting the LZS regime, respectively, (similarly for n_{in} and n_{out}), we can obtain from Eq. (8.48)

$$M_{in} + M_{out} = -\hbar\gamma[(m_1 + m_2) - (m_2 - m_1)^2 \delta n_{LZS}/2] \ , \tag{8.49}$$

where $\delta n_{LZS} \equiv n_{out} - n_{in}$, denotes the overall change of $n(t)$ inside the LZS regime, as obtained using Eq. (8.46). This quantity is negative, i.e., $n_{out} < n_{in}$ (this can be easily seen by plotting n_{eq} vs f and solving Eq. (8.46) graphically, i.e., without specifying the form of $1/\tau_s$). The first term of Eq. (8.49) gives the quantum-mechanical prediction in the adiabatic regime, since in the absence of thermal transitions inside the LZS regime (i.e., $\dot{n}(t) = 0$) the second term vanishes. To be more specific, for the spin $S = 1/2$ case ($m_2 = -m_1 = 1/2$, and $E_0 = 0$), Eq. (8.49) gives

$$M_{out} = -M_{in} - \hbar\gamma|\delta n_{LZS}|/2 \ . \tag{8.50}$$

One then obtains the expected magnetization reversal ($M_{out} = -M_{in}$) in the absence of thermal effects ($\delta n_{LZS} = 0$). Thus, the second term of Eq. (8.49) (or that of Eq. (8.50)) gives the thermal correction; its magnitude clearly depends on the competition between two time scales, namely τ_s and the time δt_{LZS} spent inside the LZS regime, given by $\delta t_{LZS} = 2\delta/(\hbar\gamma r)$, which is controlled by the sweep rate r. Hence, for a given T, the thermal correction becomes larger with decreasing sweep rates.[6] Furthermore, since $1/\tau_s$ is expected to increase with increasing T the thermal effects are more pronounced at higher T, as indeed observed for $\{V_6\}$.[6] Of course, at high enough T, the LZS effect is completely masked by the thermal transitions and the step disappears. More generally, it should be noted that it is $M_{in} + M_{out}$, rather than $M_{out} - M_{in}$ (height of the step), that is of more direct relevance in experimentally determining the extent of the thermal effects. The numerical solution for the $S = 1/2$ case shown in Fig. 8.2(a) demonstrates the deviation from exact magnetization reversal at $B \approx 0$, as a result of thermal transitions inside the LZS regime. This is consistent with the experimental data for $\{V_6\}$.

[6]This behavior should be contrasted with the sweep rate dependence of the magnetization steps for the pure quantum-mechanical LZS model but in the non-adiabatic regime, which is the relevant case for SMM's. According to the well known formula $P_{LZS} = 1 - \exp[-\pi\delta^2/(2\hbar^2\gamma r)]$ for the transition probability P_{LZS}, when lowering r one increases P_{LZS} i.e., reduces the effect of non-adiabatic transitions, thus giving rise to a larger height of the magnetization step.

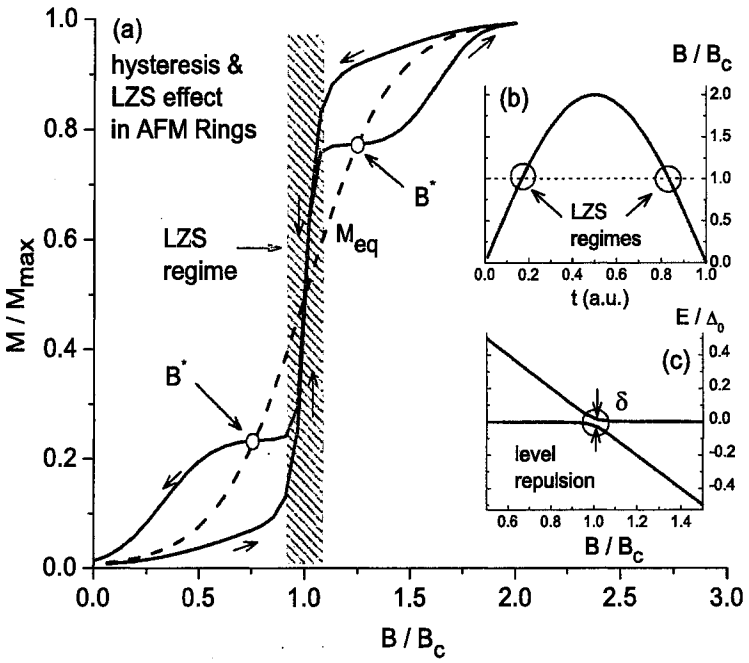

Figure 8.3 Hysteresis and LZS effect at $B \approx B_c$ for AFM ring systems at low T and for fields around the first level-crossing value B_c, as obtained by solving numerically our equations (see text) for the half-cycle sweep shown in Fig. 8.3(b). The shaded area indicates the LZS regime. The equilibrium magnetization is denoted by the dotted line. Note the deviation from the pure quantum mechanical prediction regarding the step (see text) and the formation of small plateaus after each step. B^* denotes the fields at which M crosses M_{eq}, as discussed in the text. The low-energy diagram and the level anti-crossing between the levels $|0,0>$ and $|1,-1>$ is shown in Fig. 8.3(c). The small circles in Figs. 8.3(b) and 8.3(c) indicate the LZS regimes, where the magnetization steps take place. This typical behavior of $M(t)$ in the case of $\delta \neq 0$ should be contrasted with that of $\delta = 0$ shown in Fig. 8.1.

8.4.2.3 The magnetic Foehn effect

Another effect which is also of particular interest is the "magnetic Foehn effect"[15] mentioned in the Introduction, which concerns the formation of plateaus shortly after exiting the LZS regime. Although these plateaus occur outside the LZS regime, they are a direct consequence of the LZS effect, as can easily be explained by considering the particular example shown in Fig. 8.4 (the analysis for the other cases shown in Figs. 8.2(a) and 8.3(a) is analogous). Immediately after exiting the LZS regime, $M_{out} > M_{eq}$ in contrast to the typical hysteretic behavior where M lags behind M_{eq}. Then, outside the LZS regime where, as explained above, M tends towards M_{eq}, M will decrease even though the field is swept towards larger values. This drop of M eventually stops at a field B^*, at the moment when M equals M_{eq}. Thus, B^* corresponds to a local minimum in M(since then $\dot{M} = 0$). Generally, this minimum will be observable if τ_s, in that regime, is much shorter than the sweep time τ_e. If this is not the case, a broad plateau around B^* is formed instead. In fact, this seems (see below) to be the typical behavior in all experimental data reported so far. This behavior is shown in Fig. 8.4(a), where for a fixed T and with increasing sweep rate r, the minimum broadens with B^* departing from $B_c = 0$. One can exploit this feature experimentally, in order to obtain an estimate for δ, since all B^* corresponding to different sweep rates must lie on the equilibrium curve $M_{eq}(B(t))$.

The curves shown in Fig. 8.4 also suggest why a very steep minimum at B^* (pronounced Foehn effect) has not been reported so far in realistic situations. In principle, as mentioned above, the minimum at B^* should become more steep at lower sweep rates. On the other hand, on decreasing the sweep rate, one indirectly reduces the value of M_{out},[7] thus being closer to M_{eq} when exiting the LZS regime, and therefore compensating the effect of slowing down the sweep rate.

Ideally, for the realization of a very steep minimum at B^* one needs (for a fixed sweep rate), a relaxation process that is slow enough at negative fields (i.e., large $|M_{in}|$ and consequently large M_{out}) but becomes faster at positive fields, after exiting the LZS regime. Such an "asymmetry" in the field dependence of $1/\tau_s$ cannot exist unless we abandon our main assumption that the phonons are in equilibrium at all experimental times. This is because, according to our analysis, with the phonons being in equilibrium, $1/\tau_s$ depends on $|B(t)|$, and thus must be symmetric around $B_c = 0$. This raises the question whether the PB effect, which takes place at very low T, could give rise to a pronounced Foehn effect. This is indeed supported by the analysis of the PB effect described in Ref. [4], for the magnetic molecule $\{ V_{15}\}$, which shows an asymmetry in the number of resonant phonons before

[7]The reduction of M_{out} is due to thermal dissipation before entering the LZS regime (which determines the value of $|M_{in}|$ and consequently M_{out} through Eq. (8.49)) as well as inside the LZS regime (shaded area in Fig. 8.4).

entering and after exiting the LZS regime (see, in particular, the inset of Fig. 8.2(b) of Ref. [4]), as a result of the strong coupling of the phonons to the spin degrees of freedom. In short, the physical origin of this asymmetry is that $B_c = 0$ is a level-crossing field for the energy spectrum of the spin system, whereas it corresponds to a "reflection" point for that of the resonant phonons: Although, in general, when sweeping an external field one progressively brings the spin system into resonance with different phonon modes (instantaneous resonance condition) this is not true in the vicinity of a level anti-crossing, since when exiting the LZS regime the relaxation is driven by the same phonons that were in thermal contact with the spins while entering the LZS regime (for more details, see Refs. [4, 5]). The above enhancement of the Foehn effect due to the PB effect has been in fact recently observed experimentally and will be reported elsewhere.[16]

8.5 Summary

We have extended the standard spin-lattice relaxation theory, in the context of pulsed field studies of magnetic molecules. Being easily applied to simple systems, this generalized theory can give important information on the underlying relaxation mechanisms and the microscopic interactions present in magnetic molecules in general. All the dynamical magnetization effects, including hysteresis loops, LZS transitions with or without dissipation and magnetization plateaus (Foehn effect), which are manifested in pulsed fields measurements, are accounted for by the comprehensive theory presented above.

We first developed the theory for the isotropic case of molecules with a spin S ground state well separated from the excited levels but also the general Heisenberg model where all energy levels are relevant. We have shown, for two such simple cases, namely the spin $S = 1/2$ case and that of AFM ring systems at low T, that the dynamical magnetization obeys a generalization of the standard Bloch equation. In particular, this equation has been recently used[6] for the magnetic molecule $\{V_6\}$, and was found to provide results in excellent agreement with experimental data at $T > 1$ K, confirming that the dominant mechanism driving the relaxation is the one-phonon processes, and in addition providing an estimate of the spin-phonon coupling energy. Obtaining this information was greatly facilitated by using a variety of field sweep forms.

We also extended the theory to include small off-diagonal terms in the spin Hamiltonian and thus take into account the combined effects of LZS and thermal transitions. This was done here for the large class of magnetic molecules with a low spin ground state. For these molecules, and for the currently available sweep rates, one is in the extreme adiabatic regime. Our main interest in these systems, has been the role of dissipation on the LZS steps, as well as the formation of small plateaus (Foehn

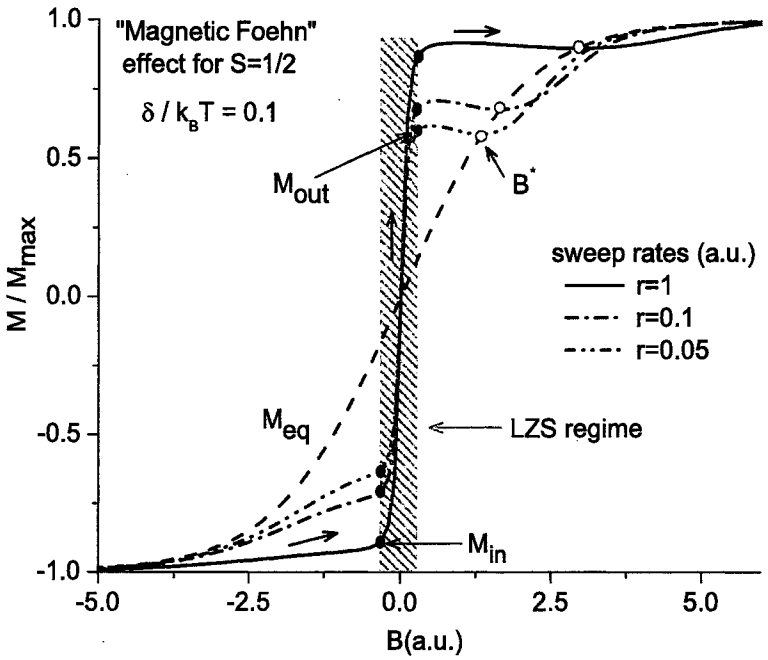

Figure 8.4 Magnetic Foehn effect for a magnetic molecule with a spin $S = 1/2$ ground state, for fixed T and for three different fields sweeps with constant sweep rates r (in arbitrary units). The shaded area denotes the LZS regime. Because of the LZS effect, immediately after exiting the LZS regime (shaded area) $M_{out} > M_{eq}$, as opposed to a usual hysteresis situation. Then, outside the LZS regime, where M tends towards M_{eq} (see text), M drops even though the field increases; a local minimum of M is formed at a field B^* at which $M = M_{eq}$. Note that this minimum is departing from the LZS regime of the magnetization step and broadens (eventually giving rise to a plateau) with increasing sweep rates.

effect) formed after each step, observed in several magnetic molecules. Interestingly enough, we arrived at a convenient set of equations where the effects of dissipation and LZS transitions can be treated separately. These equations account nicely for the description of both the magnetization steps and the plateaus. Moreover, the role of temperature and the field sweep rate on these effects becomes transparent. Finally, although our analysis is limited to high enough temperatures ($T \gtrsim 1$ K) so that one can assume that the phonons are in equilibrium at all experimental times, it nevertheless indicates how an enhanced Foehn effect could arise at lower T, where the PB effect takes place. In such a case, steep extrema in the M vs B curves could be observed.

The present theoretical work provides a first step towards exploiting the possibilities that are offered by probing magnetic molecules using external magnetic fields with high sweep rates. These probes, apart for providing information specific to magnetic molecules, offer the possibility of conducting a detailed study of the relaxational behavior of interacting spin systems as a result of their coupling with a "heat bath" and in particular the excitations of the host lattice. Development of a broad theoretical framework for dealing with relaxational phenomena induced by dynamical magnetic fields is indeed a worthy goal.

Acknowledgements

We thank Prof. Yoshitami Ajiro (Kyoto University) for very helpful comments that have greatly improved our manuscript. Ames Laboratory is operated for the U.S. Department of Energy by Iowa State University under contract No. W-7405-Eng-82.

References

[1] J. R. Friedman, M. P. Sarachik, J. Tejada, and R. Ziolo, Phys. Rev. Lett. **76**, 3830 (1996); L. Thomas, F. Lionti, R. Ballou, D. Gatteschi, R. Sessoli, and B. Barbara, Nature (London) **383**, 145 (1996).

[2] C. Sangregorio, T. Ohm, C. Paulsen, R. Sessoli, and D. Gatteschi, Phys. Rev. Lett. **78**, 4645 (1997).

[3] R. Schenker, M. N. Leuenberger, G. Chaboussant, H. U. Güdel, and D. Loss, Chem. Phys. Lett. **358**, 413 (2002).

[4] I. Chiorescu, W. Wernsdorfer, A. Müller, H. Bogge, and B. Barbara, Phys. Rev. Lett. **84**, 3454

(2000); I. Chiorescu, W. Wernsdorfer, A. Müller, S. Miyashita, and B. Barbara, Phys. Rev. B **67**, 020402(R) (20003).

[5] O. Waldmann, R. Koch, S. Schromm, P. Müller, I. Bernt, and R. W. Saalfrank, Phys. Rev. Lett. **89**, 246401 (2002).

[6] I. Rousochatzakis, Y. Ajiro, H. Mitamura, P. Kögerler, and M. Luban, Phys. Rev. Lett. **94**, 147204 (2005).

[7] H. Nojiri (private communication).

[8] Y. Shapira, M. T. Liu, S. Foner, C. E. Dube, and P. J. Bonitatebus, Jr., Phys. Rev. B **59**, 1046 (1999).

[9] Y. Inagaki, T. Asano, Y. Ajiro, Y. Narumi, K. Kindo, A. Cornia, and D. Gatteschi, J. Phys. Soc. Jpn. **72**, 1178 (2003).

[10] L. Landau, Phys. Z. Sowjetunion **2**, 46 (1932); C. Zener, Proc. R. Soc. London, Ser. A **137**, 696 (1932); E. C. G. Stückelberg, Helv. Phys. Acta **5**, 369 (1932).

[11] S. Miyashita, J. Phys. Soc. Jpn. **64**, 3207 (1995).

[12] W. Wernsdorfer and R. Sessoli, Science **284**, 133 (1999).

[13] A. Abragam and B. Bleaney, *Electron Paramagnetic Resonance of Transition Ions* (Clarendon Press, Oxford, 1970), Chap. 10.

[14] K. W. H. Stevens, Rep. Prog. Phys. **30**, 189 (1967).

[15] K. Saito and S. Miyashita, J. Phys. Soc. Jpn. **70**, 3385 (2001).

[16] W. Wernsdorfer and R. E. P. Winnpenny (private communication).

[17] M. Luban, F. Borsa, S. Bud'ko, P. Canfield, S. Jun, J. K. Jung, P. Kögerler, D. Mentrup, A. Müller, R. Modler, D. Procissi, B. J. Suh, and M. Torikachvili, Phys. Rev. B, **66**, 054407 (2002).

[18] F. Bloch, Phys. Rev. **70**, 460 (1946); **102**, 104 (1956); **105**, 1206 (1957).

[19] C. P. Slichter, *Principles of Magnetic Resonance* (Springer-Verlag, Berlin, 1992), Chap. 5.

[20] A. Caneschi, A. Cornia, A. C. Fabretti, S. Foner, D. Gatteschi, R. Grandi, L. Schenetti, Chem. Eur. J. **2**, 1379 (1996); A. Cornia, A. G. M. Jansen, M. Affronte, G. L. Abbati, and D. Gatteschi, Angew. Chem. Int. Ed. **38**, 2264 (1999).

[21] M. Gerloch, and F. E. Mabbs, J. Chem. Soc. A, 1900-1906, (1967).

[22] K. L. Taft, C. D. Delfs, G. C. Papaefthymiou, S. Foner, D. Gatteschi, and S. J. Lippard, J. Am. Chem. Soc. **116**, 823 (1994).

[23] A. Caneschi, A. Cornia, A. C. Fabretti, and D. Gatteschi, Angew. Chem. Int. Ed. Engl. **38**, 1295 (1999).

[24] J. van Slageren, R. Sessoli, D. Gatteschi, A. A. Smith, M. Helliwell, R. E. P. Winpenny, A. Cornia, A. L. Barra, A. G. M. Jansen, E. Rentschler, and G. A. Timco, Chem. Eur. J. **8**, 277 (2001).

[25] K. Blum, *Density Matrix Theory and Applications* (Prenum Press, New York, 1996), Chap. 8.

[26] H-P. Breuer and F. Petruccione, *The theory of Open Quantum Systems* (Oxford University Press, 2002), Chap. 3.

[27] H. J. Carmichael, *Statistical Methods in Quantum Optics 1, Master Equations and Fokker-Planck Equations* (Springer-Verlag, New York, 1999), Chap. 1.

[28] R. D. Mattuck, and M. W. P. Strandberg, Phys. Rev. **119**, 1204 (1960).

[29] Y. Ajiro, T. Asano, H. Aruga-Katori, T. Goto, K. Koui, K. Kamishima, and H. Ikeda, Physica B, **246**, 222 (1998).

[30] P. L. Scott and C. D. Jeffries, Phys. Rev. **127**, 32 (1962).

[31] Y. Ajiro (private communication).

9. Summary and open issues

As described in this dissertation, we have theoretically investigated a number of issues pertinent to static and, especially, dynamical properties of magnetic molecule systems. In particular, we have analyzed and explained a variety of phenomena that have been manifested in both Nuclear Magnetic Resonance and pulsed field experiments.

In chapter 2, we provided the general background on several theoretical and experimental aspects of magnetic molecule systems. To this end, we first reviewed the various energy terms appearing in the spin Hamiltonian, including exchange (both isotropic and anisotropic) interactions, single-ion anisotropy terms, as well as the spin-phonon (magnetoelastic) interactions. We then discussed the physical quantities which are of both experimental and theoretical interest, such as the zero-field static susceptibility, magnetization, specific heat and the spin-spin correlation functions, both in time and frequency domain (spectral density functions). The electronic spin correlations were treated by first neglecting the interactions with environmental bath degrees of freedom.

In chapter 3, we considered a number of basic issues relevant to the theory of open systems. Specifically, we defined the reduced density matrix and provided the derivation of its equation of motion (generalized master equation), for static external fields and in the Markovian limit. Furthermore, we made use of the quantum regression theorem and arrived at explicit expressions for the spectral density functions, as modified by the interaction with the lattice degrees of freedom, thus generalizing the corresponding discussion of chapter 2 for thermally isolated systems.

In what follows we give a brief summary of our investigations for both NMR and pulsed fields, in conjunction with a discussion of the important remaining open issues.

(i) Nuclear spin-lattice relaxation rate $1/T_1$

Chapter 4 was mainly devoted to a theoretical investigation of the long-time behavior of the electronic spin fluctuations, as probed by the nuclear spin-lattice relaxation rate $1/T_1$.[1] Applying the general results of chapter 3 to the spectral functions of magnetic molecules, we were able to arrive at a first-

[1]The results of chapter 4 together with further analysis, currently underway, will be the basis of a future publication.

principles expression for $1/T_1$, which takes into account the interaction of the electronic moments with phonons, in the Markovian limit. Utilizing symmetry properties of the spin Hamiltonian, we further simplified this expression and provided accordingly a thorough analysis of the temperature and field dependence of $1/T_1$ for a number of different situations.

Special emphasis was given to AFM ring systems and other magnetic molecules with a similar magnetic energy spectrum. In particular, for fields away from level-crossing fields, we were able to show that $1/T_1$ is proportional to the spectral density of the total magnetic moment of the molecule. Moreover, we indicated that the observation of only one peak in the $1/T_1$ vs T measurements can arise from a "decoupling" approximation, which is based on the assumption that the total magnetic moment relaxes independently from other physical quantities. Apart from the analysis of this peak, we also noted that the overall behavior of $1/T_1$ vs T should be proportional to the product $\chi(B,T)\ T$, with $\chi(B,T)$ being the differential susceptibility, which can markedly differ from the zero-field susceptibility $\chi_0(T)$. On the other hand, for fields in the immediate vicinity of a given level-crossing field B_c, our analysis accounts for the observation of a corresponding peak at $B = B_c$ in $1/T_1$ vs B data. Further theoretical analysis of $1/T_1$ is required regarding the related issue of the existence of a true level-crossing or a level-anticrossing at $B \approx B_c$.

Chapter 5, which consists of a paper published in Phys. Rev. B **69**, 094436 (2004), was concerned with the theoretical and experimental investigation of a model spin 1/2 tetramer, namely the magnetic molecule $\{V_{12}\}$. The analysis included experimental data from (i) zero-field susceptibility, (ii) NMR line-width and (iii) proton spin-lattice relaxation rate $1/T_1$, as well as a theoretical analysis of all the above. The main results were summarized as follows. The theoretical fit to the various experimental data confirmed the picture of a spin 1/2 tetramer with isotropic Heisenberg exchange interactions and with one exchange constant, $J \simeq 17.6$ K, only. In addition, no peak in $1/T_1$ at intermediate temperatures was observed for this system. This feature, seems to be common in molecules with intrinsic spins $s = 1/2$, in contrast to those with $s > 1/2$. This was further associated with the existence of a $T-$independent frequency cut-off ω_0, in contrast to the strong temperature dependence of the corresponding ω_0 in the AFM ring systems with $s > 1/2$. The origin of ω_0 in $\{V_{12}\}$ can be associated with couplings that do not commute with the isotropic Heisenberg exchange, such as anisotropic exchange, similar to the corresponding case for the magnetic molecule $\{V_6\}$. Of particular interest was also the experimental observation of a deviation of $1/T_1$ at very low T, from the predicted thermally activated behavior, an experimental finding which was also evident in the $s = 1/2$, $\{Cu_8\}$ system. The origin of this deviation has not been clarified yet.

We should note that many of the arguments presented in chapter 5 can be revisited taking into account the first-principles analysis presented in chapter 4. In particular, the discussion regarding the two Lorentzian terms of Eq. (5.5), i.e., whether ω_0 is in the regime of ω_L or ω_e, is redundant: According to chapter 4, and Eq. (4.27) in particular, the second term of Eq. (5.5) should be dropped. In addition, the fit to the $1/T_1$ vs temperature data with the sum of the Boltzmann factors in Eq. (5.8) is not needed since, as it turns out, an equally successful fit (not shown here) is provided by the product $\chi_0 T$, in agreement with the general results of chapter 4.

Generally, there are a number of issues with regards to the long-time behavior of spin fluctuations in magnetic molecule systems, that have not been clarified yet. One of these is connected with the systematic appearance of a peak in $1/T_1$ at intermediate temperatures for molecules with intrinsic spins $s > 1/2$, as opposed to molecules with $s = 1/2$. Since ions with $s > 1/2$ can have single-ion anisotropy (in contrast to $s = 1/2$), we are inclined to accept that the temperature dependence of the cut-off frequency ω_0 and consequently the peak in $1/T_1$ in these systems is attributed to spin-phonon interactions originating from the modulation of the crystal field anisotropy.[2] Nevertheless, a first-principles explanation of the temperature dependence of the corresponding cut-off frequency in AFM ring systems (with $s > 1/2$) as obtained from $1/T_1$ data is still lacking. On the other hand, in molecules with $s = 1/2$ the existence of a $T-$independent ω_0 has been associated with intra-molecular couplings that do not commute with the isotropic Heisenberg exchange (such as anisotropic exchange),[3] an issue that also requires a closer theoretical investigation.

We should note here that a similar to the AFM ring systems overall enhancement of $1/T_1$ at intermediate T, is also found in SMMs (see Ref. [1], and references therein), as well as in the diluted rare-earth ion system $LiY_{1-x}Ho_xF_4$, $x = 0.002$ (see Ref. [2]). Hence, the observation of a fast drop of the associated cut-off frequencies with decreasing temperature seems to be a characteristic feature of magnetic systems with discrete energy spectra and intrinsic spins $s > 1/2$. Accordingly, further theoretical and experimental investigation is required in order to obtain more specific and detailed information regarding the microscopics of the various spin-phonon interactions, present in all nanomagnetic systems.

(ii) Pulsed field measurements of $M(t)$

The remaining part of the dissertation, i.e., chapters 6, 7 and 8, was devoted to pulsed field studies of

[2]More generally, we also make the following remark. Since, for an ion with spin s all multipole moments of order higher than $2s$ vanish, an ion with $s = 1/2$ can only interact with a local magnetic field, whereas ions with $s > 1/2$ can couple to (or "feel") electric quadrupole fields etc. In other words, ions with higher than 1/2 spin can relax through more "channels", and consequently one generally expects faster relaxation rates in magnetic molecules with intrinsic spins $s > 1/2$ than $s = 1/2$.

[3]This does not imply that spin-phonon interactions are absent in magnetic molecules with $s = 1/2$; the pulsed field measurements in $\{V_6\}$ (chapter 7) have in fact revealed the presence of this interaction.

magnetic molecules. To this end, we began, in chapter 6, by giving an analytical account of the well-known quantum-mechanical problem of Landau-Zener-Stückelberg (LZS) transitions. In particular, we defined the major quantities of interest and considered two opposite limiting cases, with respect to the field sweep rate, namely the adiabatic and non-adiabatic regimes. As emphasized there, the non-adiabatic regime is relevant only to SMMs, since in magnetic molecules with a low spin ground state the corresponding energy splittings (responsible for the LZS effect) are large enough so that one is always in the extreme adiabatic regime.

Chapter 7, which is a paper published in Phys. Rev. Lett. **94**, 147204 (2005), was devoted to a low$-T$ ($1 < T < 5$ K) pulsed fields study of the magnetic molecule $\{V_6\}$. A significant simplification regarding this system, is that at for $T \ll 60$ K, each molecular unit behaves like a spin 1/2 entity. The main experimental and theoretical results were summarized as follows. The measurement of the dynamical magnetization in the presence of strong, fast varying fields (sweep rates ~ 1 T/ms) of well defined sweep forms $B(t)$, shows two striking features, namely pronounced hysteretic behavior and abrupt magnetization steps and reversals in the immediate vicinity of $B = 0$. In addition, a small $T-$dependent deviation from exact magnetization reversal was observed.

The hysteresis effects were attributed to the fact that the corresponding thermal relaxation time of this system is in the regime of the experimental time scale, i.e., of order 1 ms. In addition, the hysteresis loops were successfully reproduced by using a generalization of the standard Bloch equation which expresses that the dynamical magnetization $M(t)$ relaxes towards the instantaneous equilibrium magnetization $M_{eq}(T, B(t))$, with a relaxation rate that depends explicitly on the instantaneous energy separation of the Zeeman split doublet, and therefore $B(t)$. Using this equation, and fitting the data for a variety of hysteresis loops corresponding to different sweep forms, we were able to identify the dominant relaxation mechanism being that of one-phonon acoustic processes. We could also provide an estimate for the spin-phonon coupling energy ($V_{sl} \sim 0.35$ K). The specific origin of the spin-phonon coupling remains unclear.

The main assumption underlying the use of the above generalized Bloch equation was that the phonons equilibrate in times that are much shorter than both the experimental time scale (determined by the sweep rate) and the spin-lattice relaxation time. This assumption is expected to beak down for very low T (typically $T \lesssim 1$ K), since then the number of the available (resonant) phonon modes excited per spin becomes much smaller than unity. As a result, the phonons are not in equilibrium and the phonon bottleneck (PB) effect takes place. In fact, preliminary experimental data for $\{V_6\}$ at $T = 0.6$ K show a significant deviation from the above theory suggesting the onset of the PB effect.

A first-principles account for the PB effect, requires one to first write down and then solve, a system of coupled equations of motion for the spin and the phonon degrees of freedom, both being out of equilibrium. A microscopic analysis along these lines is currently lacking.[4]

Regarding the magnetization steps and reversals observed in $\{V_6\}$, these were attributed to LZS transitions between the lowest energy levels as modified by the existence of a weak (~ 0.4 K) intramolecular (between the pair of spin triangles comprising $\{V_6\}$) anisotropic exchange, which had been indicated previously by NMR measurements of $1/T_1$. The small deviation from the quantum-mechanical prediction of exact magnetization reversal at $B \approx 0$, was associated with the interactions with the lattice (dissipative LZS effect).

In chapter 8, which appears in Phys. Rev. B **72**, 134424 (2005), we provided an analytical, first-principles account on the various effects manifested in pulsed field experiments. In particular, this chapter is a generalization of the standard spin-lattice relaxation theory for static fields, to include the presence of explicit time-dependent magnetic fields in the Hamiltonian. This theory includes the analysis of hysteresis effects, LZS transitions with or without dissipation and magnetization plateaus (Foehn effect). The main underlying assumption adopted is that the phonons are in equilibrium at all experimental times. This restricts the applicability of this theory to high enough temperatures (typically $T \gtrsim 1$ K) in order to avoid the PB effect.

More specifically, we first considered the isotropic case of molecules with a spin S ground state well separated from the excited levels, but also the general Heisenberg model where all energy levels are relevant. We have shown, for two simple cases, namely the spin $S = 1/2$ case and that of AFM ring systems at low T, that the dynamical magnetization $M(t)$ obeys the generalized Bloch equation, used in chapter 7. We then extended the theory to include small off-diagonal terms in the spin Hamiltonian and thus take into account the combined effects of LZS and thermal transitions. This was done for magnetic molecules with a low spin ground state, for which we are in the extreme adiabatic regime. Our main interest in these systems, has been the role of dissipation on the LZS steps, as well as the formation of small plateaus (Foehn effect) formed after each step, as observed in several magnetic molecules. Interestingly enough, we arrived at a convenient set of equations where the effects of dissipation and LZS transitions can be treated separately. These equations account nicely for the description of both the magnetization steps and the plateaus. Moreover, the role of temperature and the field sweep rate on these effects becomes transparent. Finally, as mentioned above, although our analysis was limited to high enough temperatures (typically $T \gtrsim 1$ K) so that one can assume that the phonons are in

[4] Nevertheless, there exist a phenomenological approach which accounts for the main physical ideas of the PB effect (see for example Ref.[3]).

equilibrium at all experimental times, it nevertheless indicates how an enhanced Foehn effect could arise at lower T, where the PB effect takes place. In such a case, pronounced extrema in the M vs B curves could be observed.

More generally, the use of pulsed fields is very suitable for studying the dynamical properties of magnetic molecule systems. In particular, the above "slowing-down" of the spin fluctuations as probed by $1/T_1$ measurements is also manifested in pulsed fields: The mere observation of hysteretic behavior at low T, signifies that the corresponding spin-lattice relaxation times become long enough so that they can be probed by the currently available sweep rates ($\sim$ several T/ms). In particular, this effect is very dramatic in SMMs, where the existence of a large uniaxial anisotropy gives rise to relaxation times which can be of order of several months.[4–6]

In addition, very small ($\sim$ 0.1 K or less) intra-molecular magnetic interactions (such as the anti-symmetric Dzyaloshinskii-Moriya interaction (see chapter 2)) present in these nanomagnetic systems can be manifested in pulsed field experiments, since they give rise to LZS steps; such small interactions cannot be manifested in static experiments, such as the magnetic susceptibility. Remarkably, similar LZS steps in the magnetization have been observed for (diluted) single-ion systems as well, such as the $LiY_{1-x}Ho_xF_4$, ($x = 0.002$) system mentioned above,[7] and a spin-glass system with lone Cu2+ ions[8]. In these cases, the LZS effect involves energy levels of the combined electronic and (on-cite) nuclear spin system, as split by their mutual hyperfine interaction.

References

[1] M. Belesi, A. Lascialfari, D. Procissi, Z. H. Jang, and F. Borsa, Phys. Rev. B **72**, 014440 (2005).

[2] M. J. Graf, A. Lascialfari, F. Borsa, A. M. Tkachuk, and B. Barbara, cond-mat/0508406.

[3] A. Abragam, and B. Bleaney, *Electron Paramagnetic Resonance of Transition Metal Ions* (Dover Publications Inc., New York, 1986).

[4] J. R. Friedman, M. P. Sarachik, J. Tejada, and R. Ziolo, Phys. Rev. Lett. **76**, 3830 (1996); L. Thomas, F. Lionti, R. Ballou, D. Gatteschi, R. Sessoli, and B. Barbara, Nature (London) **383**, 145 (1996).

[5] C. Sangregorio, T. Ohm, C. Paulsen, R. Sessoli, and D. Gatteschi, Phys. Rev. Lett. **78**, 4645 (1997).

[6] R. Schenker, M. N. Leuenberger, G. Chaboussant, H. U. Güdel, and D. Loss, Chem. Phys. Lett. **358**, 413 (2002).

[7] R. Giraud, W. Wernsdorfer, A. M. Tkachuk, D. Mailly, and B. Barbara, Phys. Rev. Lett. **87**, 057203 (2001).

[8] H. Nojiri, private communication.

APPENDIX A. Single-ion anisotropy and the $g-$tensor in transition-metal ions

Here we give a general account of the origin of the various single-ion anisotropic terms present in the spin Hamiltonian of magnetic molecule systems. We also discuss the anisotropy of the $g-$factor. In transition metal ($3d$) ions, the unpaired electrons lie in the outermost shell and as a result they may be greatly influenced by the crystal field produced by neighboring ions. In fact the crystal field is typically larger than the LS-coupling and the Zeeman energies, and therefore should be taken into account before the latter, in a perturbative calculation of the energy scheme.

As we know, the intra-ionic Hamiltonian gives rise to spectroscopic energy terms, the lowest of which is determined by the Hund's rules. The crystal electric field splits the orbital degeneracy of the lowest term, with the remaining degeneracy of the ground state depending on the symmetry of the crystal field. Here we will consider an ion with an orbitally singlet ground state denoted by $|A>$; this is the case for ions comprising a magnetic molecule, for the low symmetry of the ligand fields results in lifting completely any orbital degeneracy of the ground state. Thus, the only remaining degeneracy is that of the spin (i.e., $2s+1$). A direct consequence of this is that the orbital angular momentum is "quenched" inside the ground spin-manifold, i.e., $< A|\mathbf{L}|A >= 0$ (Refs. [1–4]).

This $(2s+1)-$fold degeneracy of $|A>$ is lifted when the remaining intra-ionic energy terms are finally included: Both the orbital Zeeman term $\mu_B \mathbf{L}\cdot\mathbf{B}$ and the LS-coupling may couple the ground state $|A>$ to excited orbital states $|A'>$. The resulting energy splittings inside the ground spin-manifold can be conveniently accounted for by constructing an effective spin Hamiltonian. There are several ways of doing this(Refs.[5, 6]), based on the assumption that the energy excitations between the ground manifold $|A>$ and the excited orbital states $|A'>$ are much larger than the perturbing energy terms. Here we will give only the final expression. Denoting by

$$V = \lambda \mathbf{L}\cdot\mathbf{S} + \mu_B(\mathbf{L}+2\mathbf{S})\cdot\mathbf{B}\ , \tag{A.1}$$

the perturbing energy terms, the effective Hamiltonian H^A_{eff} describing the energies inside the ground

spin-manifold, is given, up to second order in V, by

$$H^A_{eff} =< A|V|A > + \sum_{A'} \frac{| < A|V|A' > |^2}{E_A - E_{A'}} =$$
$$= \mu_B \mathbf{B} \cdot \mathbf{g} \cdot \mathbf{s} - \lambda^2 \mathbf{s} \cdot \mathbf{\Lambda} \cdot \mathbf{s} - \mu_B^2 \mathbf{B} \cdot \mathbf{\Lambda} \cdot \mathbf{B} =$$
$$= \mu_B g^{\mu\nu} B^\mu s^\nu - \lambda^2 \Lambda^{\mu\nu} s^\mu s^\nu - \mu_B^2 \Lambda^{\mu\nu} B^\mu B^\nu \ , \tag{A.2}$$

where, in the last expression we have used the convention of summing over repeated indices and we have defined the second rank tensors $\mathbf{g}$ and $\mathbf{\Lambda}$ by

$$g^{\mu\nu} \equiv 2\delta^{\mu\nu} - \lambda(\Lambda^{\mu\nu} + \Lambda^{\nu\mu}) \ , \tag{A.3}$$

and

$$\Lambda^{\mu\nu} \equiv \sum_{A'} \frac{< A|L^\mu|A' >< A'|L^\nu|A >}{E_{A'} - E_A} \ , \tag{A.4}$$

respectively. We should note that, since $\vec{L} = \vec{L}^\dagger$ is a hermitian operator, it follows that $(\Lambda^{\mu\nu})^* = \Lambda^{\nu\mu}$. In fact, as it turns out (see below), $\Lambda^{\mu\nu}$ is real, i.e., $(\Lambda^{\mu\nu})^* = \Lambda^{\mu\nu}$.

Equation (A.2) describes the effect of the admixing of higher orbital states back to the ground manifold. The first term gives rise to an anisotropy of the $g-$factor, whereas the second term is the anisotropy energy which gives rise to a splitting of the $(2s+1)-$fold spin degeneracy even at zero field. The last term which is spin independent, as we are going to see in Appendix B, gives rise to a temperature independent paramagnetic contribution to the susceptibility, responsible for the so-called Van Vleck paramagnetism.

Let us discuss in some detail the single-ion anisotropic terms. In general, the second-rank tensor $\mathbf{\Lambda}$ has nine independent elements. From these, only two are physically relevant. This can be shown as follows. First, we know that any second-rank tensor can be split in a zero-rank scalar, a first-rank vector, and a second rank symmetric and traceless tensor, according to

$$\Lambda^{\mu\nu} = \frac{1}{3} Tr(\mathbf{\Lambda}) \delta^{\mu\nu} + \{(\Lambda^{\mu\nu} + \Lambda^{\nu\mu})/2 - \frac{1}{3} Tr(\mathbf{\Lambda}) \delta^{\mu\nu}\} + (\Lambda^{\mu\nu} - \Lambda^{\nu\mu})/2 \ . \tag{A.5}$$

Since, $(\Lambda^{\mu\nu})^* = \Lambda^{\nu\mu}$ it follows that $\Lambda^{\mu\nu} - \Lambda^{\nu\mu}$ is purely imaginary and therefore it must vanish identically. Moreover, this implies that $(\Lambda^{\mu\nu})^* = \Lambda^{\mu\nu}$. Then,

$$-\lambda^2 \mathbf{s} \cdot \mathbf{\Lambda} \cdot \mathbf{s} = l_0 \mathbf{s}^2 + \mathbf{s} \cdot \mathbf{D} \cdot \mathbf{s} \ , \tag{A.6}$$

where we have defined

$$l_o \equiv -\frac{\lambda^2}{3} Tr(\mathbf{\Lambda}) \ ,$$
$$D^{\mu\nu} \equiv -\lambda^2 [(\Lambda^{\mu\nu} + \Lambda^{\nu\mu})/2 - \frac{1}{3} Tr(\mathbf{\Lambda}) \delta^{\mu\nu}] \ . \tag{A.7}$$

The first term gives a constant, since $\mathbf{s}_i^2 = s_i(s_i+1)$ and can be omitted. Thus we are left with the second-rank, symmetric and traceless tensor. This can be diagonalized giving three eigenvalues denoted by D^{xx}, D^{yy} and D^{zz} with the corresponding principal axes {x,y,z}. However, only two of the eigenvalues are independent, since $Tr(\mathbf{D}) = D^{xx} + D^{yy} + D^{zz} = 0$. Generally then, the anisotropy energy can be conveniently written as

$$H_{ani} = Ds_z^2 + E(s_x^2 - s_y^2) + (\text{constant terms}) \ , \tag{A.8}$$

where $D \equiv D^{zz} - (D^{xx} + D^{yy})/2$ and $E \equiv (D^{xx} - D^{yy})/2$.

Two comments are in place here. First, for an ion with $s = 1/2$, there is no spin anisotropy since $s_x^2 = s_y^2 = s_z^2 = 1/4$. Thus anisotropy effects are only expected for ions with $s > 1/2$. Second, the number of independent parameters may be further reduced by taking into account the symmetry of the crystal field: According to its definition, the tensor $\mathbf{\Lambda}$ carries the symmetry of the crystal field, since the orbital states $|A>$, $|A'>$ are the different representations of this symmetry. For example, in a cubic environment one expects $\Lambda_{xx} = \Lambda_{yy} = \Lambda_{zz}$ and the anisotropy energy reduces to a constant. On the other hand, in an axially symmetric case one has $\Lambda_{xx} = \Lambda_{yy} \equiv \Lambda_\perp$, in general different from $\Lambda_{zz} \equiv \Lambda_\parallel$. Consequently, $D = \lambda^2(\Lambda_\perp - \Lambda_\parallel)$, whereas $E = 0$. Hence, for cases of axial symmetry and for an external magnetic field along the axial (easy) z-axis, the effective Hamiltonian can be written as

$$H_{eff}^A = g_\parallel \mu_B B s_z + Ds_z^2 - \mu_B^2 \Lambda_\parallel B^2 \ . \tag{A.9}$$

It should be noted that in the above generic form of V (Eq. (A.1)) one should add the diamagnetic orbital contribution, which is second order in B and spin independent, similarly with the last term of Eq. (A.2), above. Although they are spin independent, these terms must be kept when calculating the susceptibility, for they give rise to a temperature independent diamagnetic and paramagnetic contributions (see Appendix B).

References

[1] R. M. White, *Quantum Theory of Magnetism* (Springer-Verlag, Berlin, 1983), Ch. 2.

[2] A. Abragam and B. Bleaney, *Electron Paramagnetic Resonance of Transition Ions* (Clarendon Press, Oxford, 1970), Ch. 7.

[3] C. P. Slichter, *Principles of Magnetic Resonance* (Springer Verlag, Berlin, 1989).

[4] A. Abragam, *Principles of Nuclear Magnetism* (Clarendon Press, Oxford, 1961), Ch. VI.

[5] C. C.-Tannoudji, J. D.-Roc, and G. Grynberg, *Atom-Photon Interactions, Basic processes and Applications* (Wiley-Interscience, New york, 1992), pg. 38.

[6] A. Messiah, *Quantum Mechanics* (Dover Publications, New York, 1999), Ch. XVI.

APPENDIX B. Van Vleck formula for the susceptibility

Here we provide a very general and useful expression for the zero-field susceptibility. This, so-called Van Vleck formula, can be applied to exchange coupled systems (magnetic molecules) but also to other systems as well, such as single magnetic ions, with or without contributions from the orbital degrees of freedom and anisotropic terms. We start with the Hamiltonian in the presence of a small magnetic field B, as

$$H = H_0 + H_{int}(B) \ , \tag{B.1}$$

where H_0 denotes the energy in the absence of the field and H_{int} the interaction with the field, which is dominated by the Zeeman term $-\mathbf{M}\cdot\mathbf{B}$, where $\mathbf{M}$ denotes the total magnetic moment of the system; a typical second order term is the diamagnetic one (see below). Assuming that the energy spectrum of H_0 is known, a first task is to find via perturbation theory the energy spectrum $E_n(B)$, up to second order in B. For our purposes, we shall assume that this has been done already, and write explicitly the first three terms of the series expansion of $E_n(B)$, as

$$E_n(B) \approx E_n^0 + \sum_{\alpha} c_n^{\alpha} B^{\alpha} + \sum_{\alpha\alpha'} d_n^{\alpha\alpha'} B^{\alpha} B^{\alpha'} \ . \tag{B.2}$$

Now, the magnetization M^{α} along the $\alpha-$axis is given by

$$< M^{\alpha} >= -\frac{\partial F}{\partial B^{\alpha}} = k_B T \frac{1}{Z} \frac{\partial Z}{\partial B^{\alpha}} \ , \tag{B.3}$$

where F denotes the Helmhold's free energy given by $F \equiv U - T\ S = -k_B T \ln Z$, with $U =< H >$, being the total internal energy and S the entropy. Without loss of generality, we will assume that the field is along the z-axis. In this case, only the coefficients c_n^z and d_n^{zz} of Eq. (B.2) matter. In addition, for small fields the z-component of the magnetization,[1] denoted as M, is given by

$$M \approx \chi_0^{zz} B \ . \tag{B.4}$$

[1] The susceptibility is generally a second rank tensor; for example, the elements χ_0^{xz}, χ_0^{yz} give the x- and y-components, respectively, of the magnetization in the presence of a small field $\mathbf{B} = B\mathbf{z}$. These are generally non-zero whenever a Hamiltonian contains anisotropic terms.

In the above expansion, the zero-th order term is taken to be zero, since in the absence of a magnetic field M must vanish. According to Eq. (B.3) then one obtains

$$\chi_0^{zz} = \lim_{B\to 0} \frac{\partial M}{\partial B} = k_B T \lim_{B\to 0} \Big(\frac{1}{Z} \frac{\partial^2 Z}{\partial B^2} - \big(\frac{1}{Z} \frac{\partial Z}{\partial B}\big)^2 \Big) , \tag{B.5}$$

By expanding the partition function up to second order one finally obtains

$$\chi_0^{zz} = -\frac{2}{Z_0} \sum_n e^{-\beta E_n^0} \, d_n^{zz} + \frac{1}{k_B T} \Big(\frac{1}{Z_0} \sum_n e^{-\beta E_n^0} \, (c_n^z)^2 - \big[\frac{1}{Z_0} \sum_n e^{-\beta E_n^0} \, c_n^z \big]^2 \Big) , \tag{B.6}$$

where Z_0 denotes the zero-field partition function. The above expression can be written in the following, more compact, way

$$\chi_0^{zz} = -2 < d^{zz} >_0 + < (\delta c^z)^2 >_0 \, / (k_B T) , \tag{B.7}$$

where we have defined the diagonal operators d^{zz} and c^z by $< n|c^z|m >= \delta_{nm} c_n^z$, and similarly $< n|d^{zz}|m >= \delta_{nm} d_n^{zz}$. Here the symbol $<>_0$ denotes the thermal average taken with H_0 alone, and $\delta c^z \equiv c^z - < c^z >_0$. Note also that the above two terms contribute with opposite sign (see below).

Equation (B.6) or (B.7) is a very general expression. Depending on the particular system at hand, we can evaluate the susceptibility provided we know the energy eigenvalues up to second order in B. The importance of the above formula resides in the fact that one needs only to calculate some thermal averages in the absence of the external field. This is the essence of the linear response theory, which is a very general one. Let us then apply this general expression to two cases relevant in magnetic systems.

B.1 Isotropic Heisenberg model and fluctuation formula

Consider a magnetic molecule which is described by the isotropic Heisenberg Hamiltonian H_0. Let us consider the Zeeman interaction $H_{int} = -\mathbf{M} \cdot \mathbf{B} = g\mu_B B S_z$, in the field $\mathbf{B} = B\mathbf{z}$. Since H_0 and S_z commute, finding the eigenvalues in the presence of the field is a trivial task. We easily obtain $c^z = g\mu_B S_z$, whereas $d^{zz} = 0$. Then the Van Vleck formula (Eq. (B.7)) reduces to

$$\chi_0^{zz} = \frac{(g\mu_B)^2}{k_B T} < \delta S_z^2 >_0 \ , \tag{B.8}$$

which in turn can be simplified to give the fluctuation formula

$$\chi_0^{zz} = \frac{(g\mu_B)^2}{3 k_B T} < \mathbf{S}^2 >_0 \ , \tag{B.9}$$

since $< \mathbf{S} >_0 = 0$ and $< S_x^2 >_0 = < S_y^2 >_0 = < S_z^2 >_0 = < \mathbf{S}^2 >_0 / 3$.

Of course, the fluctuation formula is valid also for the case of a system with one ionic spin s only. In this particular case the fluctuation formula reduces to the Curie law

$$\chi_0^{zz} = \frac{(g\mu_B)^2}{3 k_B T} s(s+1) \ . \tag{B.10}$$

A comment related to this expression is the following. Consider a given magnetic molecule system comprising N spins s. At high T (specifically, for $T \gg J/k_B$, where J is the largest exchange constant present) the spins are become uncorrelated and therefore the thermal average of $\mathbf{S}^2$ appearing in Eq. (B.9) reduces to $N < \mathbf{s}^2 >= Ns(s+1)$. Hence, for this magnetic molecule at high T

$$\chi_0^{zz} \rightarrow \frac{N(g\mu_B)^2}{3k_BT}\, s(s+1)\ . \tag{B.11}$$

B.2 Magnetic ion with a non-degenerate ground state and total spin 1/2

Our second example comes from the magnetism of single ions. Consider the simplest case of an ion with a non-degenerate orbital ground state $|A>$, well separated from the excited levels (lowest energy excitation $\Delta >> k_BT$). In addition, we will assume that the total spin of this state is 1/2, so that there are single-ion anisotropic terms. It is known that for an orbitally non-degenerate ground state the orbital angular momentum is quenched, i.e., $< A|\mathbf{L}|A >= 0$. Apart from the ground state's spin contribution to the magnetic susceptibility we will show that there exist two more contributions, which are temperature independent. These are (i) the Van Vleck paramagnetic term and (ii) the Larmor diamagnetic contribution. Let us explain the origin of these contributions by using the effective spin Hamiltonian method described in Appendix A.

The following general comments are in place here. First, in the interaction energy of a magnetic ion with a magnetic field given in Appendix A, one should add the generic, orbital term

$$H_{dia} = \frac{eB^2}{8mc^2}\sum_i (x_i^2 + y_i^2)\ , \tag{B.12}$$

where the sum runs over all electrons i inside the magnetic ion. Second, since $S = 1/2$ there are no anisotropic energy terms in the effective spin Hamiltonian. Finally, since $\Delta >> k_BT$, one should first replace the thermal averages in Eq. (B.6), with the ground state contribution only.

The effective spin Hamiltonian for our example then is written as

$$H_{eff}^A = g_{\|}\mu_B B S_z + [-\mu_B^2 \Lambda_{\|} + \frac{e^2}{8mc^2}\sum_i (x_i^2 + y_i^2)]B^2\ , \tag{B.13}$$

where

$$\Lambda_{\|} \equiv \sum_{A'} \frac{|< A|L_z|A' >|^2}{E_{A'} - E_A}\ , \tag{B.14}$$

which is always positive. Since the second order in B terms are spin independent (i.e., the same whether $M_s = -1/2$ or $+1/2$) they give rise to a temperature independent contribution to the susceptibility.

The diagonalization of the above Hamiltonian in the 2×2 spin subspace is straightforward. It gives

$$E_{M_s} = g_{\|}\mu_B B M_s + \left[-\mu_B^2 \Lambda_{\|} + \frac{e^2}{8mc^2} \sum_i (x_i^2 + y_i^2) \right] B^2 \ . \tag{B.15}$$

Therefore, according to our general conventions, $c^z = g_{\|}\mu_B S_z$, whereas $d^{zz} = [-\mu_B^2 \Lambda_{\|} + \frac{e^2}{8mc^2} \sum_i (x_i^2 + y_i^2)]$ =constant. In addition $< S_z >_0 = 0$ whereas $< S_z^2 >_0 = < \mathbf{S}^2 >_0 /3 = S(S+1)/3 = 1/4$. Thus, the zero-field magnetic susceptibility is finally given by

$$\chi_0^{zz} = \frac{(g_{\|}\mu_B)^2}{3k_B T} S(S+1) + 2\mu_B^2 \Lambda_{\|} - \frac{e^2}{4mc^2} \sum_i (x_i^2 + y_i^2) \ . \tag{B.16}$$

The first term corresponds to the usual Curie law, and is the only temperature dependent term. The second term gives the so-called Van Vleck paramagnetism, whereas the third term, which is always present, gives the Larmor diamagnetism. In magnetic molecules, the dominant contribution to the susceptibility comes from the exchange couplings between magnetic ions, and this also follows a Curie law at high T as already shown in the previous example. Since the last two terms of Eq. (B.16) are temperature independent, they manifest themselves in the χT behavior at high enough T.

B.3 Remark: Differential susceptibility

In chapter 4, we have shown that, for magnetic molecule systems with an isotropic Heisenberg Hamiltonian and under certain symmetry conditions, the nuclear spin-lattice relaxation rate $1/T_1$ is proportional to the equilibrium fluctuation of the operator S_z, i.e., the total magnetic moment of the molecule. The purpose of this section is to indicate a simple formula that expresses these fluctuations in terms of the so-called differential susceptibility $\chi(B,T) \equiv \partial M/\partial B$, at the given finite measuring field B. This quantity is generally distinct from the zero-field susceptibility discussed above; they become equal at low fields.

We shall take $H_{int}(B) = -\mathbf{M} \cdot \mathbf{B}$ in Eq. (B.1), and assume again that $\mathbf{B} = B\mathbf{z}$. Using Eq. (B.3) above it is straightforward to obtain

$$\chi(B,T) \equiv \frac{\partial M}{\partial B} = \frac{1}{k_B T} \left(< M^2 > - < M >^2 \right) = \frac{(g\mu_B)^2}{k_B T} < (\delta S_z)^2 > \ , \tag{B.17}$$

where the thermal averages are taken with the total Hamiltonian including the Zeeman term H_{int}. This is the relevant quantity for $1/T_1$ as discussed in chapter 4, instead of χ_0. Clearly, for the AFM ring systems the two quantities are almost equal since the lowest energy gap and the peak temperature of $1/T_1$ are much larger than the Zeeman energy splittings. In systems with small energy gaps (or J) and very large magnetic fields one must use the differential susceptibility.

APPENDIX C. Pauli Master equations from Fermi's Golden rule

C.1 General treatment

The small interactions between an open system ($\mathcal{A}$) and a heat bath ($\mathcal{B}$) result in quantum-mechanical transitions between the states of $\mathcal{A}$. Under certain conditions, these transitions proceed with constant rates, which in turn, are related to certain spectral functions of $\mathcal{B}$.

There are two ways to arrive at this general result. In the first semi-classical treatment,[1, 2] one concentrates on the system $\mathcal{A}$ alone and writes down an explicitly time-dependent (i.e., classical) term $V_c(t)$ to account for the interactions with $\mathcal{B}$. Such an approach is taken when the time evolution of $V_c(t)$ is unknown and complicated, and hence it is usually treated statistically by taking appropriate averages over some physically reasonable stochastic processes. This approach however neglects the quantum nature of $\mathcal{B}$ and gives rise to transition rates without the detailed-balance property (see below), and eventually to an equilibrium state of infinite T. The second, first-principles, approach is fully quantum-mechanical,[2, 3] for one starts with the full Hamiltonian of the combined $\mathcal{A} \oplus \mathcal{B}$ system, and then obtains the equations of motion of $\mathcal{A}$ alone, at a subsequent stage. This is what we shall follow here.

We start by writing the full Hamiltonian of the closed $\mathcal{A} \oplus \mathcal{B}$ system

$$H_{tot} = H_A + H_B + V \ , \tag{C.1}$$

where H_A, H_B denote the energy of $\mathcal{A}$ and $\mathcal{B}$, respectively, when considered as closed and V accounts for their interaction. This can always be written in the general form

$$V = \hbar \sum_q A^q \ B^q \ , \tag{C.2}$$

where A^q and B^q are hermitian operators of the system $\mathcal{A}$ and $\mathcal{B}$, respectively. One then usually assumes that $\mathcal{B}$ is in equilibrium at temperature T, i.e., it can be described by the stationary state

$$\rho_B(T) = e^{-\beta H_B}/Z_B \ , \tag{C.3}$$

where $Z_B \equiv Tr(e^{-\beta H_B})$.

We shall use indices with latin letters ($|n>$) and greek letters ($|\alpha>$) for the eigenstates of $\mathcal{A}$ and $\mathcal{B}$, respectively. We further denote by E_n (E_α) and $|n>$ ($|\alpha>$) the eigenvalues and eigenstates of H_A (H_B). The combined states $\{\ |n>\otimes|\alpha>\equiv|n\alpha>\ \}$ then provide a basis set inside the Hilbert space of $\mathcal{A}\oplus\mathcal{B}$. According to Fermi's Golden rule, under certain conditions (see below), the transitions among these states, will proceed with constant rates $W_{n\alpha\to n'\alpha'}\equiv W_{n\alpha,n'\alpha'}$ given by

$$W_{n\alpha,n'\alpha'}=\frac{2\pi}{\hbar}\ |<n\alpha|V|n'\alpha'>|^2\ \delta(E_{n\alpha}-E_{n'\alpha'})\ , \tag{C.4}$$

where $E_{n\alpha}\equiv E_n+E_\alpha$. The presence of the energy conserving δ-function accounts for the fact that our system $\mathcal{A}\oplus\mathcal{B}$ is thermally isolated.

Now, since we are observing the system $\mathcal{A}$ only, the central quantities of interest are the transition rates $W_{n\to n'}\equiv W_{nn'}$, between states of the system $\mathcal{A}$. These can be obtained from $W_{n\alpha,n'\alpha'}$ by averaging over all the initial states $|\alpha>$ (probability $p_\alpha=\exp(-\beta E_\alpha)/Z_B$) of $\mathcal{B}$, and summing over all possible final states $|\alpha'>$, i.e.,

$$W_{nn'}=\frac{2\pi}{\hbar}\sum_{\alpha\alpha'}\frac{e^{-\beta E_\alpha}}{Z_B}\ |<n\alpha|V|n'\alpha'>|^2\ \delta(E_n-E_{n'}+E_\alpha-E_{\alpha'})\ . \tag{C.5}$$

The above expression can be transformed to a more physically transparent form as follows. First, we notice that

$$<n\alpha|V|n'\alpha'>=\hbar\sum_q A^q_{nn'}B^q_{\alpha\alpha'}\ . \tag{C.6}$$

In addition, we replace the above delta function $\delta(E_n-E_{n'}+E_\alpha-E_{\alpha'})=\delta(\omega_{nn'}+\omega_{\alpha\alpha'})/\hbar$, with its integral representation

$$\delta(\omega_{nn'}+\omega_{\alpha\alpha'})=\frac{1}{2\pi}\int_{-\infty}^{+\infty}e^{i\ (\omega_{nn'}+\omega_{\alpha\alpha'})\ t}\ dt\ . \tag{C.7}$$

Then, by introducing the interaction picture bath operators $\widetilde{B}^q(t)\equiv e^{iH_Bt/\hbar}B^qe^{-iH_Bt/\hbar}$, and noticing that

$$(\widetilde{B}^q(t))_{\alpha\alpha'}=B^q_{\alpha\alpha'}\ e^{i\omega_{\alpha\alpha'}t}\ , \tag{C.8}$$

we finally arrive at

$$W_{nn'}=\sum_{qq'}A^q_{nn'}A^{q'}_{n'n}J_{qq'}(\omega_{nn'})\ , \tag{C.9}$$

where

$$J_{qq'}(\omega_{nn'})\equiv\int_{-\infty}^{+\infty}dt\ e^{i\omega_{nn'}t}\ <\widetilde{B}^q(t)\widetilde{B}^{q'}(0)>_B\ , \tag{C.10}$$

are spectral functions of the bath $\mathcal{B}$, with

$$<\widetilde{B}^q(t)\widetilde{B}^{q'}(0)>_B\equiv Tr_B(\rho_B\widetilde{B}^q(t)\widetilde{B}^{q'}(0))\ , \tag{C.11}$$

denoting the equilibrium time correlation functions of $\mathcal{B}$.

Equation (C.9) is the central equation of this section. According to this expression, the transition rates between two states $|n>$ and $|n'>$ of the system $\mathcal{A}$ are proportional to the Fourier transform of appropriate time correlation functions of the bath system $\mathcal{B}$, evaluated at the frequency $\omega_{nn'}$. In physical terms, from the whole spectrum of the relevant bath fluctuations only the resonant part can induce transitions between the states of $\mathcal{A}$.

Furthermore, it is clear from the above general expression for $W_{nn'}$, that if there are two terms in V that are uncorrelated, i.e., $J_{qq'} = 0$, then, as expected, $W_{nn'}$ is given by the sum of the two separate contributions. This is for example the case when the bath consists of two separate, non-interacting (uncorrelated) systems $\mathcal{B}_1$ and $\mathcal{B}_2$. Another possibility appears whenever several $J_{qq'}$ vanish due to certain symmetries. For instance, as we show in chapter 4, one can separate the nuclear spin-lattice relaxation rate $1/T_1$, in two terms, the first being related to transverse spin correlation functions and the second to the longitudinal ones.

The following additional remarks follow from the properties of the spectral function. First, as expected, the rates $W_{nn'}$ are real quantities since, according to Eq. (2.34) of chapter 2,

$$(J_{qq'}(\omega))^* = J_{q'q}(\omega) \ , \tag{C.12}$$

since the operators B^q are chosen to be hermitian.[1] Second, a direct consequence of Eq. (2.32) of chapter 2,

$$J_{qq'}(-\omega) = e^{-\beta\omega} J_{q'q}(\omega) \ , \tag{C.13}$$

is the detailed-balance condition written as

$$W_{n'n} = e^{-\beta\hbar\omega_{nn'}} W_{nn'} \ . \tag{C.14}$$

This condition is of central importance, since it forces the system to reach an equilibrium state with temperature equal to that of the bath (see below why). Notice that $W_{nn'}$ is in general different than $W_{n'n}$ although for the combined system $\mathcal{A} \oplus \mathcal{B}$, a microscopic reversibility holds, i.e.,

$$W_{n\alpha,n'\alpha'} = W_{n'\alpha',n\alpha} \ . \tag{C.15}$$

Let us now discuss what happens when we treat the bath classically, i.e., when we replace the bath operators B^q appearing in V in Eq. (C.2), by some c-numbers $f^q(t)$. It follows that the thermal average

[1] In some cases, it is convenient to choose a set of generally, non-hermitian operators A^q and B^q, but in such a way that the total V is a hermitian operator. This of course, does not alter the reality of $W_{nn'}$.

appearing in the expression for the correlation functions $< B^q(t)B^{q'}(0) >_B$, should be replaced by a statistical average, over some physically appropriate and stationary stochastic process, i.e.,

$$< \widetilde{B}^q(t)\widetilde{B}^{q'}(0) >_B \;\; \rightarrow \;\; \overline{f^q(t)f^{q'}(0)} = \overline{f^{q'}(0)f^q(t)} = \overline{f^{q'}(-t)f^q(0)} \; . \tag{C.16}$$

The last two equalities follow from the commutativity of the c-numbers $f^q(t)$ and $f^{q'}(0)$ and the stationarity of the stochastic process. Consequently, Eq. (2.32) of chapter 2 should be replaced by $J_{qq'}(-\omega) = J_{q'q}(\omega)$, which in turn gives $W_{nn'} = W_{n'n}$, or equivalently, according to Eq. (C.14), to an equilibrium state with infinity temperature ($\beta = 0$).

Going back to our general relation Eq. (C.9), one can write down the so-called Pauli master equations for the populations p_n

$$\dot{p}_n(t) = \sum_{n' \neq n} W_{n'n} \; p_{n'}(t) - (\sum_{n' \neq n} W_{nn'}) \; p_n(t) \; , \tag{C.17}$$

which physically express that the rate of change of p_n is the additive result of a gain term (transitions *from* other states $|n' >$) and a loss term (transitions *to* other states $|n' >$). The most important feature of these rate equations is that they are of Markovian character, i.e., they neglect certain memory effects: $\dot{p}_n$(t) depends only on the populations $p_n(t)$ at the same instant t, and not on the values $p_n(t')$ at previous times $t' < t$. Moreover, the transition rates are constant. Both features follow from the Fermi's Golden rule whose use can only be justified under certain conditions. These are discussed separately, in the following section.

Finally, from the structure of the Pauli master equations Eq. (C.17), one infers that $\mathcal{A}$ eventually comes to thermal equilibrium with $\mathcal{B}$, i.e., with the same temperature T. This is because, the stationary, equilibrium state $\{p_n^s\}$ is reached when $\dot{p}_n^s = 0$ for all n's, or equivalently when a detailed-balance is attained, i.e.,

$$p_n^s W_{nn'} = p_{n'}^s W_{n'n} \; , \tag{C.18}$$

for all mutual transitions between n and n'. This condition, according to Eq. (C.14), is equivalent to

$$\frac{p_n^s}{p_{n'}^s} = \frac{W_{n'n}}{W_{nn'}} = e^{-\beta(E_n - E_{n'})} \; , \tag{C.19}$$

i.e., finally the system comes in thermal equilibrium (same temperature) with the bath.

C.2 Order of magnitude considerations: Applicability of Fermi's Golden rule

We now discuss the conditions of applicability of Fermi's golden rule, which consists in the appearance of constant transition rates. For the formal proof of Fermi's golden rule one may consult several

books on Quantum Mechanics (see for example Refs. [4, 5]). Here, we provide the general underlying physical ideas, to be found also in Chapter 2 within the more appropriate framework of the generalized master equations for the reduced density matrix of system $\mathcal{A}$. To this end, we first take into account some order of magnitude considerations, given the results of Fermi's golden rule.

First, we shall need to consider two different cases, namely when the final state belongs to a continuum or consists of one discrete energy level.

(I) Transitions to a continuum of final states

Consider first, the case of quantum-mechanical transitions from a given state towards a band of $\mathcal{N}$ energy levels (denoted by $\{n'\}$) forming a (quasi-)continuous spectrum of width ΔE. One can define an average density of states given by $\rho_f = \mathcal{N}/\Delta E \equiv 1/\delta E$. In such cases, the quantity of interest is the transition rate $W_{n\to\Delta E}$ towards the entire energy band, i.e.,

$$W_{n\to\Delta E} = \sum_{n'\epsilon\Delta E} W_{n\to n'} = \sum_{qq'} \sum_{n'\epsilon\Delta E} A^{q}_{nn'} A^{q'}_{n'n} \, J_{qq'}(\omega_{nn'}) \ , \tag{C.20}$$

according to Eq. (C.9). Expanding $J_{qq'}(\omega_{nn'})$ according to Eq. (C.10), one encounters the function

$$g_{qq'}(t) \equiv \sum_{n'\epsilon\Delta E} \{A^{q}_{nn'} A^{q'}_{n'n}\} \, e^{i\omega_{nn'}t} \ . \tag{C.21}$$

This frequency superposition has a time width τ_c' of order $\hbar/\Delta E$. Furthermore, we assume that the bath time correlation functions $J_{qq'}(t)$ decay in times τ_B ("the bath correlation time") much longer than $\hbar/\Delta E$.[2] Under these assumptions, we may approximate

$$\int_{-\infty}^{+\infty} dt \ g_{qq'}(t) \ J_{qq'}(t) \approx J_{qq'}(0) \int_{-\infty}^{+\infty} dt \ g_{qq'}(t) \ , \tag{C.22}$$

whose order of magnitude is $\mathcal{N}v^2\tau_c'/\hbar^2$, with v denoting an average estimate for $V_{nn'}$. Thus, the order of magnitude of $W_{n\to\Delta E}$ is

$$W_{n\to\Delta E} \sim \mathcal{N}\frac{v^2}{\hbar^2} \, \tau_c' \sim \frac{v^2}{\hbar}\rho_f \ . \tag{C.23}$$

This estimate is in agreement with the usual integrated form of Fermi's Golden rule. According to the above, one can define a correlation time $\tau_c \equiv \mathcal{N}\tau_c' = \mathcal{N}\hbar/\Delta E \equiv \hbar\rho_f$. We shall see below, that for the discrete spectrum case, one can still use Eq. (C.23), i.e., define an appropriate density of states ρ_f, by introducing the broadening of the discrete line.

(II) Transitions to a discrete final state

For a quantum-mechanical transition towards a discrete energy level, we cannot define a density of states

[2] Equivalently, this means that the frequency width of the bath spectral density is much shorter than ΔE. In other words, the bath spectral density is so narrow that it "sees" the band ΔE as a continuum. This requirement is satisfied when the bath $\mathcal{B}$ corresponds to an external radiation pulse like in typical spectroscopic experiments. The correlation time τ_B then is determined by the duration of the pulse: A longer τ_B corresponds to a shorter frequency width (towards monochromatic) and consequently the band ΔE appears to be "more continuous".

in analogy with the previous continuous spectra case (the superposition of exponentials in Eq. (C.21) is absent). On the other hand, the bath correlation functions appearing in Eq. (C.21) can give rise to a finite $W_{n\to n'}$, when the decay of $J_{qq'}(t)$ is taken into account. More specifically, assuming that $J_{qq'}(t) \approx J_{qq'}(0)e^{-t/\tau_B}$ then, according to Eq. (C.9), $W_{nn'}$ becomes of order

$$W_{nn'} \sim \frac{v^2}{\hbar^2} \frac{\tau_B^{-1}}{\tau_B^{-2} + \omega_{nn'}^2} \,. \tag{C.24}$$

This is of the same form as Eq. (C.23) of the continuous case, if we loosely take ρ_f to be equal to the second, Lorentzian factor. In particular, when $\tau_B \ll 1/\omega_{nn'}$, Eq. (C.24) reduces to $W_{n\to n'} \sim \frac{v^2}{\hbar^2}\tau_B$, i.e., the role of $\tau_c = \mathcal{N}\tau_c'$ of Eq. (C.23), is now played by τ_B. Generally however, the Lorentzian function should be kept.[3] The origin of the decay of $J_{qq'}(t)$ lies in terms in the Hamiltonian of the bath, that are not included in H_B. Such terms, may for example arise from the interaction between $\mathcal{B}$ and a third system $\mathcal{C}$ (e.g., spin-phonon coupling, when $\mathcal{B}$ consists of electronic spins and $\mathcal{C}$ consists of the phonons), or interactions within $\mathcal{B}$ (e.g., phonon-phonon interactions when the bath $\mathcal{B}$ consists of the phonons).

Taking into account the above considerations regarding the order of magnitude of $W_{nn'}$, let us return to the question of the applicability of Fermi's Golden rule, for both the continuum and the discrete spectrum cases. First, one needs to point out the various independent time scales of the problem. These are: (i) the observation time t, (ii) the transition rate as given by Fermi's golden rule, and finally (iii) the correlation time τ_c whose origin depends on the particular problem at hand. Generally then, Fermi's golden rule applies when $W\, t \ll 1$ and for $t \gg \tau_c$.[4] The first condition assures that perturbation theory up to second order is adequate, whereas the second is the so-called Markovian approximation. This consists of neglecting certain memory effects that take place in time scales much shorter than t. Combining these conditions we obtain the requirement $\tau_c \ll \hbar/v$. In particular, in the continuum spectrum case, this means that the perturbation energy v must be very small compared to the width δE, i.e., $v \ll \delta E$.[5]

References

[1] C. P. Slichter, *Principles of Magnetic Resonance* (Springer Verlag, Berlin, 1989).

[2] A. Abragam, *Principles of Nuclear Magnetism* (Clarendon Press, Oxford, 1961).

[3] See chapter 2 for more details; see also chapter 4 for an application in NMR, where this Lorentzian factor is actually observed.

[4] To arrive at Fermi's Golden rule, one encounters a third condition, which is called secular approximation and reads $\omega_{nm} \gg 1/t$, where ω_{nm} are the various characteristic Bohr frequencies of $\mathcal{A}$. For more details see chapter 2.

[5] Such a condition does not hold when e.g., one uses intense monochromatic fields (Laser Physics), in cases that the bath $\mathcal{B}$ consists of the external radiation pulse.

[3] F. Volino, in *Microscopic Structure and Dynamics of Liquids*, edited by J. Dupuy, and A. J. Dianoux (Plenum Press, New York, 1978), Ch. 2.

[4] A. Messiah, *Quantum Mechanics* (Dover Publications, New York, 1999), Ch. XVII.

[5] E. Merzbacher, *Quantum Mechanics* (John Wiley & Sons, Inc., New York, 1998), 3nd Ed., Ch. 19.

APPENDIX D. Decay of coherences: The element $R_{nm,nm}$

We seek an expression for $R_{nm,nm}$ in terms of spectral functions of the heat bath. To this end, we first denote its real and imaginary part as $-\gamma_{nm}$ and $-\delta\omega_{nm}$, respectively, i.e.,

$$R_{nm,nm} \equiv -\big(\gamma_{nm} + i\ \delta\omega_{nm}\big)\ . \tag{D.1}$$

According to Eq. (3.40) of chapter 3, $R_{nm,nm}$ is given by

$$R_{nm,nm} = \Gamma_{mm,nn} + \Gamma^*_{nn,mm} - \Gamma_{nn,nn} - \Gamma^*_{mm,mm} - \sum_{k\neq n}\Gamma_{nk,kn} - \sum_{k\neq m}\Gamma^*_{mk,km}\ . \tag{D.2}$$

where

$$\Gamma_{nm,rs} \equiv \sum_{qq'} A^q_{nm}A^{q'}_{rs}J^{(1)}_{qq'}(\omega_{sr})$$
$$= \sum_{qq'} A^q_{nm}A^{q'}_{rs}\Big(\frac{1}{2}J_{qq'}(\omega_{sr}) + i\Pi_{qq'}(\omega_{sr})\Big)\ . \tag{D.3}$$

Now, we note that the role of the various operators O^q appearing in the expressions of chapter 2 for the quantities $J_{qq'}(\omega)$ and $\Pi_{qq'}(\omega)$, is now played by the operators B^q appearing in the interaction energy $V = \hbar\sum_{qq'} A^q \otimes B^q$. Defining $p_\alpha \equiv e^{-\beta E_\alpha}/Z_B$, one obtains

$$\sum_{qq'} A^q_{nm}A^{q'}_{rs}J_{qq'}(\omega_{sr}) = \frac{2\pi}{\hbar^2}\sum_{\alpha\alpha'} p_\alpha V_{n\alpha,m\alpha'}V_{r\alpha,s\alpha'}\delta(\omega_{sr}+\omega_{\alpha\alpha'})\ , \tag{D.4}$$

and similarly

$$\sum_{qq'} A^q_{nm}A^{q'}_{rs}\Pi_{qq'}(\omega_{sr}) = \hbar^{-2}\mathcal{P}\sum_{\alpha\alpha'} p_\alpha\ \frac{V_{n\alpha,m\alpha'}V_{r\alpha',s\alpha}}{\omega_{sr}+\omega_{\alpha\alpha'}}\ , \tag{D.5}$$

where $V_{n\alpha,m\alpha'} \equiv < n,\alpha|V|m,\alpha' >$, and the symbol $\mathcal{P}$ denotes the Cauchy principal value. Then, by appropriately combining all terms resulting from Eq. (D.2), one can obtain the following physically transparent expressions for the real and imaginary parts of $-R_{nmnm}$.

(i) The real part of $-R_{nm,nm}$, which is denoted by γ_{nm}, may be written as the sum of two terms of different physical origin

$$\gamma_{nm} = \gamma^{\rm nonad}_{nm} + \gamma^{\rm ad}_{nm}\ . \tag{D.6}$$

The first, so-called "non-adiabatic" contribution is related to the various transition rates W_{kn} (with $\omega_{nk} \neq 0$) as

$$\gamma_{nn'}^{\rm nonad} \equiv \frac{1}{2}\Big(\sum_{k\neq n} W_{nk} + \sum_{k\neq m} W_{mk}\Big) \ , \tag{D.7}$$

where $W_{nk} \equiv W_{n\rightarrow k}$ has been defined previously (see chapter 3 and Appendix C) as

$$W_{nk} \equiv \frac{2\pi}{\hbar} \sum_{\alpha\alpha'} |V_{n\alpha,k\alpha'}|^2 \ \delta(E_{nk} + E_{\alpha\alpha'}) \ . \tag{D.8}$$

The second contribution is called "adiabatic" and is related to bath spectral density functions evaluated at zero frequency. It is given by

$$\gamma_{nm}^{\rm ad} \equiv \frac{\pi}{\hbar} \sum_{\alpha\alpha'} p_\alpha \ |V_{m\alpha,m\alpha'} - V_{n\alpha',n\alpha}|^2 \ \delta(E_\alpha - E_{\alpha'}) \ . \tag{D.9}$$

According to these relations, both $\gamma_{nm}^{\rm nonad}$ and $\gamma_{nm}^{\rm ad}$ are positive, as expected. A remark regarding the physics associated with $\gamma_{nm}^{\rm ad}$ follows by inspecting the matrix elements appearing in Eq. (D.9). Specifically, since $V_{m\alpha,m\alpha'}$ and $V_{n\alpha',n\alpha}$ are given in terms of the matrix elements A_{mm}^q and A_{nn}^q, respectively, we infer that the adiabatic contribution $\gamma_{nm}^{\rm ad}$ is related to the elements of V that are diagonal in the energy representation of the system $\mathcal{A}$.

(ii) The energy shift $\hbar\delta\omega_{nm}$ of the excitation energy $\hbar\omega_{nm}$ can be written as the difference $\delta E_n - \delta E_m$, where

$$\delta E_n \equiv \sum_\alpha p_\alpha \ \Big(\mathcal{P}\sum_{k,\alpha'} \frac{|V_{n\alpha,k\alpha'}|^2}{(E_n + E_\alpha) - (E_k + E_{\alpha'})}\Big) \ . \tag{D.10}$$

The physical meaning of this expression is very transparent. Indeed, δE_n represents the shift of the state $|n,\alpha>$ of the global system $\mathcal{A}\oplus\mathcal{B}$, as given by second order perturbation theory, but weighted with the occupation probability $p_\alpha = e^{-\beta E_\alpha}/Z_B$ of the level $|\alpha>$ of $\mathcal{B}$.

APPENDIX E. Some physical constants, and the CGS system of units

(i) Useful constants and conversion of Units

$$1 \text{ eV} = 1.602177 \times 10^{-12} \text{ erg}$$
$$= 1.519267 \times 10^{15} \text{ s}^{-1} \quad (\omega = E/\hbar)$$
$$= 11604.45 \text{ K} \quad (T = E/k_B)$$

$$\hbar = 6.582122 \times 10^{-16} \text{ eV s}$$
$$e = 4.803203 \times 10^{-10} \text{ esu}$$
$$m_e = 9.109389 \times 10^{-28}\text{g}$$
$$m_p = 1.672623 \times 10^{-24}\text{g}$$
$$c = 2.99792458 \times 10^{10}\text{cm/s}$$
$$\mu_B \equiv \frac{e\hbar}{2m_e} = 5.788382 \times 10^{-9} \text{ eV G}^{-1}$$
$$\mu_N \equiv \frac{e\hbar}{2m_p} = 3.152451 \times 10^{-12}\text{eV G}^{-1}$$
$$g_e \simeq 2$$
$$g_p = 5.58556$$
$$g_n = -3.82628$$
$$k_B = 8.61739 \times 10^{-5} \text{ eV K}^{-1}$$
$$N_A = 6.022137 \times 10^{23} \text{ mol}^{-1}$$

Electron Larmor frequency

$$\omega_e \equiv g_e \mu_B B/\hbar = [175.88\ B(T)] \text{ GHz}$$
$$= [1.3376\ B(T)] \text{ K}$$

Proton Larmor frequency

$$\omega_L \equiv g_p \mu_N B/\hbar = [267.52\ B(T)]\ \text{MHz}$$
$$= [2.04 \times 10^{-3}\ B(T)]\ \text{K}$$

(ii) The CGS system of Units

It is very convenient to always work in one system of units, preferably in the CGS. The main reason is that in SI there is a large number of unnecessary units mainly because of the introduction of the constants μ_0 and ϵ_0. For instance, the electric and magnetic fields have different units in SI. On the other hand, in the CGS, the electric field $\mathbf{E}$, the electric polarization (density) $\mathbf{P} \equiv \sum_i \mathbf{p}_i/V$ (V = volume), the electric displacement $\mathbf{D}$, the magnetic fields $\mathbf{B}$ and $\mathbf{H}$, and finally the magnetization (density) $\mathbf{M} \equiv \sum_i \mu_i/V$, are all in units of Gauss (although they are called with different names). This unit is nothing else than

$$1\ \text{Gauss} = 1\ \sqrt{\frac{\text{g}}{\text{cm s}^2}} = 1\ \sqrt{\frac{\text{erg}}{\text{cm}^3}}\ . \tag{E.1}$$

The Gauss (CGS) and the Tesla (SI) do not correspond to the same unit. But the following equivalence holds

$$1\ \text{Tesla} \leftrightarrow 10^4\ \text{Gauss}\ .$$

Also, the unit of the electric charge e denoted by 1 cb in SI, and by 1 esu (or statcoulomb) in CGS, do not correspond to the same unit. In particular

$$1\ \text{esu} = 1\ \sqrt{\frac{\text{g cm}^3}{\text{s}^2}} = 1\ \sqrt{\text{erg cm}} = 1\ \text{Gauss cm}^2. \tag{E.2}$$

and the following equivalence holds

$$1\ \text{cb} \leftrightarrow 2.9979 \times 10^9\ \text{esu}\ . \tag{E.3}$$

The following table is a helpful summary of the units of some common physical quantities in the CGS system.

Table E.1 Common physical quantities in the CGS system of units

Quantity	Symbol	Example	Unit (CGS)
El. charge	q	$E \sim q^2/r$	1 esu = 1 G cm^2
El. dipole moment	$\mathbf{p}$ (or $\mathbf{d}$)	$\mathbf{p} \equiv q\mathbf{r}$, $U = -\mathbf{p} \cdot \mathbf{E}$	1 esu cm = 1 erg/G
Magn. dipole moment	μ	$U = -\boldsymbol{\mu} \cdot \mathbf{B}$	1 erg/G
El. potential	V	$V \sim e^2/r$	1 statvolt ($= 1\sqrt{\text{erg/cm}}$)
Vector potential	$\mathbf{A}$	$\mathbf{B} = \nabla \times \mathbf{A}$	1 G/cm
El. field	$\mathbf{E}$	$E \sim e^2/r^2$	1 statvolt/cm (= 1 G)
El. Pol. density	$\mathbf{P}$	$\mathbf{P} \equiv \sum_i \mathbf{p}_i/V = q_i\mathbf{r}_i/V$	1 esu/cm^2 (= 1 G)
El. Displacement	$\mathbf{D}$	$\mathbf{D} = \mathbf{E} + 4\pi\mathbf{P}$	1 G
Magn. induction	$\mathbf{B}$	$\mathbf{B} \sim \boldsymbol{\mu}/r^3$	1 G
Magnetization dens.	$\mathbf{M}$	$\mathbf{M} = \sum_i \boldsymbol{\mu}_i/V$	1 G
Magn. field	$\mathbf{H}$	$\mathbf{H} \equiv \mathbf{B} - 4\pi\mathbf{M}$	1 G
Current density	$\mathbf{j}$	$j = q/(\text{area time})$	1 G / s
Conductivity	σ	$j = \sigma E$	s^{-1}
El. suscept.	χ	$P = \chi E$	1
Magn. Suscept.	χ	$M = \chi H$	cm^3

ACKNOWLEDGEMENTS

I would like to take this opportunity to express my gratitude to those who helped me in various ways in conducting my research and completing my graduate studies. First and foremost, my major advisor Prof. Marshall Luban for his guidance and support and for being so kind and patient throughout my research studies. Our numerous discussions on Physics have been highly enjoyable and profitable.

Next, I would like to thank Prof. F. Borsa for fruitful and stimulating discussions on NMR related issues. Also, I would like to acknowledge a number of people that have contributed to my research in various ways: D. Procissi, A. Shastri, M. Al Rifai and B. J. Suh for performing the NMR experiments on $\{V_{12}\}$; H. Mitamura and Y. Ajiro for performing the pulsed fields measurements on $\{V_6\}$; P. Kögerler for the chemical synthesis of $\{V_{12}\}$ and $\{V_6\}$; Profs. C. Stassis, J. Schmalian, J. Evans, V. V. Dobrovitski, H. Nojiri, C. Schröder, Dr. M. Belesi, and L. Engelhardt for a number of fruitful discussions.

Special thanks to Profs. J. Schmalian, D. Carter-Lewis, J. Evans and D. Vaknin for being so kind to be in my program of study committee.

I would also like to express my deep appreciation and gratitude to *all* my teachers, both in Ames and those in Heraklion of Crete, to whom I owe so much.

Finally, I am very grateful to Mrs. I. Foustanaki for her lifelong assistance, as well as M. Belesi, my parents, my sister and my brothers for their love and support.